UNIVERSITÀ DEGLI STUDI DI VERONA
DIPARTIMENTO DI BIOTECNOLOGIE

DOTTORATO DI RICERCA IN
BIOTECNOLOGIE MOLECOLARI INDUSTRIALI ED AMBIENTALI

CICLO XXIX

Analysis of Moss Light-Harvesting Complex Stress-Related (LHCSR1) Protein Function Upon Heterologous Expression in *Arabidopsis thaliana*

S.S.D. BIO / 04

Coordinatore: Ch.mo Prof. Roberto Bassi

Supervisore: Ch.mo Prof. Roberto Bassi

Dottorando: Dott. Ioannis Dikaios

Analysis of Moss Light-Harvesting Complex Stress-Related (LHCSR1) Protein Function Upon Heterologous Expression in *Arabidopsis thaliana* – Ioannis Dikaios
PhD thesis
Verona, 12 June 2017

Στην οικογένειά μου
To my family

ABSTRACT

Non-photochemical quenching (NPQ) of chlorophyll fluorescence is a process essential for the regulation of photosynthesis and plant protection from light stress. In vascular plants this process is triggered by a luminal pH sensor, the PSBS protein, which transduces chloroplast lumen acidification, induced by excess light, into a quenching reaction occurring within specific interacting chromophore-bound lightharvesting proteins (LHC). In algae, such as *Chlamydomonas reinhardtii*, stress-related light-harvesting proteins (LHCSR) fulfill both pH sensing and quenching reactions, due to their capacity of binding chlorophylls and xanthophylls. The moss *Physcomitrella patens*, an evolutionary intermediate between algae and plants, has both PSBS and LHCSR active in quenching with LHCSR working in a direct zeaxanthin-dependent manner. Plants and mosses have a very similar organization of thylakoid membranes thus suggesting LHCSR might be active in plants. To verify this hypothesis, we overexpressed *lhcsr1* gene into *Arabidopsis thaliana* PSBS mutant, *npq4*, and screened transformants by fluorescence video-imaging, resulting to the isolation of *A. thaliana* plants, which accumulate a pigment-binding, NPQ-active LHCSR1 in thylakoid membranes. In the context of functional and structural analysis of LHCSR1 protein, a series of *in vivo* transformations was performed using *A. thaliana* mutants altered in xanthophyll content or lacking specific LHC subunits. For this reason the double mutant *npq1npq4* - unable to convert violaxathin into zeaxanthin - was complemented in order to verify the direct dependence of LHCSR1 on zeaxanthin, mutant *lut2npq4* was used due to its complete lack of lutein and antenna mutants *NoMnpq4* and *ch1lhcb5* were used due to their lack of either minor antennas or the complete antenna system respectively; all of them overexpressing LHCSR1 in different levels. Finally, a first approach for the in vivo mutational analysis of *P. patens* LHCSR1 has been initiated, using *A. thaliana* as a tool for heterologous protein expression.

Contents

Chapter 1
Expression of *Pp*LHCSR1 in *Arabidopsis thaliana npq4* mutant

Chapter 2
An *in vivo* analysis of factors controlling LHCSR1 activity through heterologous expression in *Arabidopsis thaliana*

Chapter 3
Towards LHCSR1 mutational analysis *in vivo*

Aknowledgements

SUMMARY

Coming from the greek words *φώς* (light) and *σύνθεση* (synthesis), photosynthesis is undoubtedly one of the most important processes on earth since it converts light energy into readily used chemical energy, providing at the same time oxygen, an element essential for life. In order to perform this highly important task, algae, mosses and vascular plants are equipped with four multi-subunit protein complexes, Photosystems I and II (PSI, PSII), Cytochrome b_6f (Cyt-b_6f) and ATPase, all localized in the thylakoid membranes of the chloroplasts. Photosynthesis is driven by the light energy absorbed by the environment. This energy capture is achieved by arrays of proteinic complexes called light-harvesting complexes (LHCs), which coordinate chlorophylls (Chls) and carotenoids (Cars), chromophore molecules able to absorb part of the visible light. However, apart from light harvest LHCs have an additional equally important role in photoprotection.

Photosynthetic organisms are subjected to a wide range of variable environmental conditions such as fluctuating light levels during daylight, which leads to plant stress. What is dangerous for the photosynthetic apparatus and thus for the cell, is that in these conditions the amount of energy harvested could exceed the actual needs. Excess energy can lead Chl molecules to a type of excited state called triplets, which react with oxygen and produce reactive oxygen species (ROS) thus causing inhibition of photosynthesis. For this reason, photosynthetic organisms have developed a photoprotection mechanism called Non-Photochemical Quenching (NPQ) that thermally dissipates energy in excess. In higher plants, the four-transmembrane PSBS protein is responsible for the activation of NPQ upon changes in the luminal pH while in green algae the stress-related light-harvesting proteins (LHCSR) fulfill both pH sensing and quenching reactions due to their capacity of binding chlorophylls and xanthophylls. In the case of the moss *Physcomitrella patens*, an evolutionary intermediate between algae and plants, both PSBS and LHCSR proteins are active in quenching.

The high NPQ efficiency which is observed in this moss (with respect to *A. thaliana*, the model organism for higher plants) and which is mainly attributed to LHCSR1 makes this protein a central point in trying to understand NPQ and the way that this mechanism is activated.

In my PhD, I studied the complex role of LHCSR1 in Non-Photochemical Quenching through its expression in the heterologous system of *Arabidospis thaliana*.

In **Chapter 1**, LHCSR1 responsible for NPQ in *P.patens* is inserted via an heterologous expression approach, in the PSBS-less *Arabidopsis thaliana npq4* in order to observe if the protein can complement NPQ activity while being accumulated in thylakoid membranes. In fact, LHCSR could be successfully expressed in the form of a native chlorophyll a/b–xanthophyll-binding protein exhibiting partial quenching activity after induction of NPQ with high actinic light.

The possible limiting factors of LHCSR quenching activity *in planta* are investigated in **Chapter 2**, where LHCSR is introduced in *A. thaliana* mutants altered either in the carotenoid biosynthesis or the composition of LHCII antenna system. The xanthophyll requirements of LHCSR are shown using *Arabidopsis* mutants unable to accumulate zeaxanthin (*npq1*) or deficient in lutein (*lut2*) while the effect of minor antennas (*NoM*) and complete antenna system absence (*ch1*) in LHCSR expression and activity are also presented.

In **Chapter 3** an attempt to introduce mutations on LHCSR Chl-binding sites *in vivo* is described. Many studies are focused in the *in vitro* refolding of proteins, however the electrostatic environment between *in vitro* and *in vivo* is different. Performing mutational analysis *in vivo* could provide different results since the protein is found in its natural environment, favoring its structural stability. Preliminary results for Chl A2, Chl A3, Chl A5, Chl B5 and Chl B6 are reported for the heterologous expression system of *A. thaliana npq4*.

Finally, in the **Appendix** all the methods and techniques used during this work are described in detail.

Introduction

1 Oxygenic photosynthesis

Life on earth is connected directly to the presence of oxygen, a compound deriving from photosynthesis. Photosynthesis is a process, which enables plants and other organisms such as algae, mosses and even some bacteria to convert light energy into chemical energy. This energy together with the use of carbon dioxide (CO_2) and water (H_2O) can be used immediately or stored in carbohydrate molecules (biomass) hence photosynthesis is the most important process of energy conversion, providing all heterotrophic organisms with the necessary amounts of food and energy in order to survive.

In oxygenic photosynthesis water is used as an electron donor in the reduction of atmospheric carbon dioxide into organic carbon, releasing oxygen as a secondary product:

$$nH_2O + nCO_2 + \text{light} \longrightarrow (CH_2O)_n + nO_2$$

This process, taking place into specific organelles of all photosynthetic organisms called **chloroplasts**, can be divided in two phases: the **light phase**, during which the main reactions taking place regard the conversion of the received light energy into reducing power (NADPH) and the generation of an electrochemical gradient. This gradient is further used for the production of ATP, most known as the energy carrier in all living beings. This reducing power - together with ATP - is used during the **light-independent phase** of photosynthesis (usually referred to as 'dark phase') in a series of CO_2 fixation reactions, leading to the production of other more complex organic compounds.

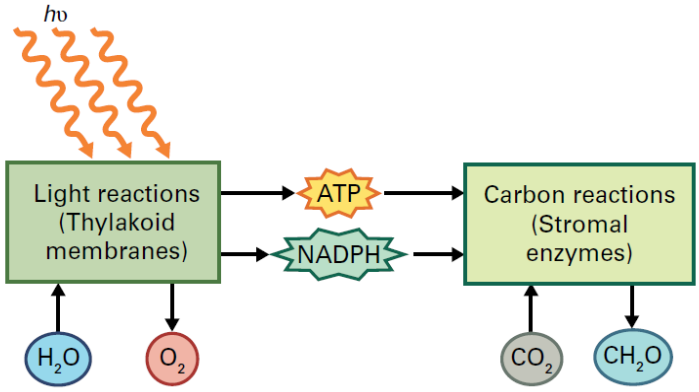

Figure 1. The light and carbon (formerly "dark") reactions of photosynthesis occur in separate chloroplast compartments. *Light is required for the synthesis of ATP and NADPH substrates in a series of reactions that occur in thylakoid membranes of the chloroplast. These products of the light reactions are then used by a series of stromal enzymes that fix CO_2 into carbohydrates during the carbon reactions.*

1.1 The chloroplast

In eukaryotes, the biophysical and biochemical reactions of photosynthesis occur in a specialized plastid, the chloroplast. All the reactions required for the process of photosynthesis take place in this organelle, which arose from the endosymbiotic association of a protoeukaryotic cell and a photosynthetic bacterium related to modern cyanobacteria. The chloroplast has a complex structure which reflects its diverse biochemical functions: It is surrounded by a double membrane system, called 'envelope' with the first membrane being highly permeable and the second one containing specific transporters able to control the flux of metabolites into the cytoplasm. The envelope membranes separate a compartment called stroma, which contains all the enzymes catalyzing the reactions during the dark phase of photosynthesis but also plastidial DNA, RNA and ribosomes. A third membrane system - the thylakoids – can be found within the stroma forming a physically continuous three-dimensional network, which encloses an aqueous space, the thylakoid lumen. In land plants some thylakoids are organized into stacks of membranes (grana thylakoids) whereas others (stromal thylakoids) are unstacked, thus exposed to the surrounding fluid medium (the chloroplast stroma). These two regions differ mainly in shape and in the composition of protein complexes that they hold. The thylakoid membranes carry a negative charge but the presence of cations, especially divalent cations like magnesium (Mg^{2+}), keeps the thylakoid membranes stacked (Barber, 1980).

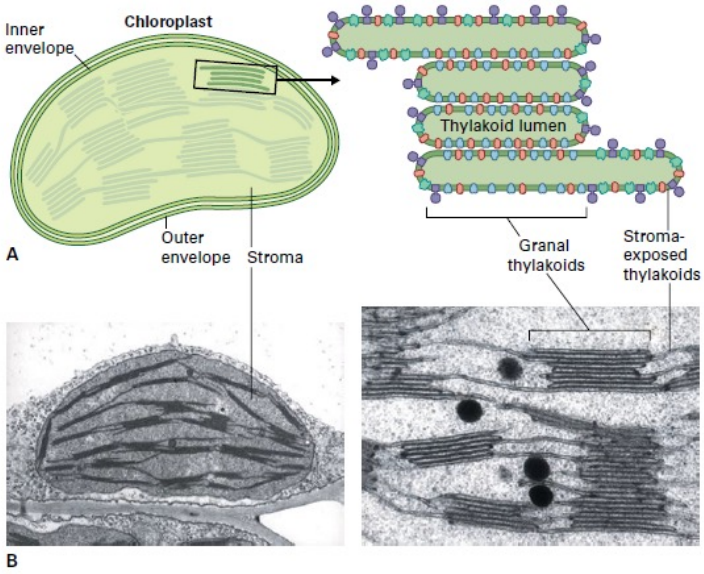

Figure 2. Plant chloroplast. *A) Schematic diagram showing compartmentalization of the organelle. In a typical plant chloroplast, the internal membranes (thylakoids) include stacked membrane regions (granal thylakoids) and unstacked membrane regions (stromal thylakoids). B) Transmission electron micrographs reveal plant chloroplast ultrastructure. The higher magnification emphasizes the membrane stacking and includes electron-dense lipid bodies known as plastoglobuli (Staehelin & Van der Staay, 1996).*

1.2 Light phase of photosynthesis and energy transfer

Four major complexes are composing the photosynthetic machinery of the light reactions: Photosystem I (PSI), Photosystem II (PSII), ATP-synthase (ATPase) and Cytochrome-b_6f (Cyt-b_6f). These complexes are not evenly distributed throughout thylakoid membranes: PSI and ATPase can be found in the stroma lamellae, PSII is almost exclusively localized in the grana and Cyt-b_6f preferably populates grana margins. These complexes catalyze the reaction of light harvesting, electron transport but also the process of phosphorylation leading to the conversion of light energy (photons) into chemical (ATP, NADPH).

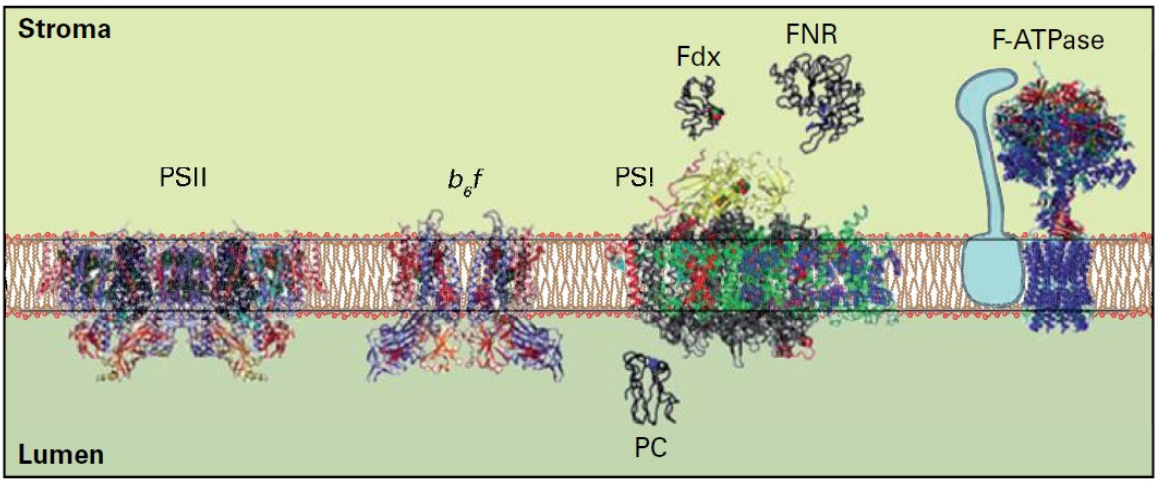

Figure 3. A structural view of the Z-scheme *showing structures of the major thylakoid membrane complexes (PSII, cytochrome b6 f complex, PSI, and ATP synthase) involved in the light reactions of oxygenic photosynthesis. Also shown are the structures of the soluble proteins Fdx and FNR on the stromal side of PSI, as well as PC in the lumen."*

The two photosystems - co-operating in series as described in the so-called Z-scheme (Hill and Bendall, 1960) - are equipped with pigments, molecules able to harvest light and channel this energy towards a reaction center (RC). Energy captured by the reaction center can then induce the excitation level of specialized chlorophylls located within the center, having as a result the translocation of an electron across the membrane through a series of co-factors. Both photosystems are evolved to operate with a very high quantum yield: PSI works with an almost perfect quantum yield of 1.0 while PSII operates with a lower efficiency of around 0.85.

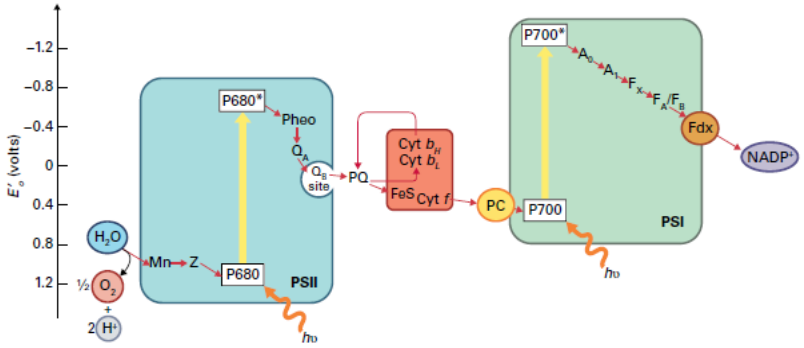

Figure 4. The current Z-scheme, *showing Em values of electron carriers. The vertical placement of each electron carrier of the non-cyclic electron transfer chain corresponds to the midpoint of its redox potential. These voltage values have been verified experimentally. P680, a special pair of Chls in the PSII-RC; P680*, excited Chl P680; PQ, plastoquinone; PC, plastocyanin; P700, a special pair of Chls in the PSI-RC; P700*, excited Chl P700. Three major protein complexes are involved in running the Z-scheme: Photosystem II, Cytochrome-b_6f and Photosystem I.*

So photosynthesis starts with the capturing of light. By definition, pigments absorb light within the visible region. This energy is transferred between individual pigment molecules in the light-harvesting antenna in an ordered way, probably through a mechanism called 'Forster transfer'. The energy transfer requires that pigments molecules are located close to each other and since from an energetic point of view it is a down-hill reaction, energy is preferentially transferred from Chlb (λ_{max} = 647nm) to Chla (λ_{max} = 663nm). After absorbing photons from the PSII antenna system, the excitation energy is channeled to a special pair of chlorophylls of the PSII-RC (P680, primary electron donor absorbing at 680nm).

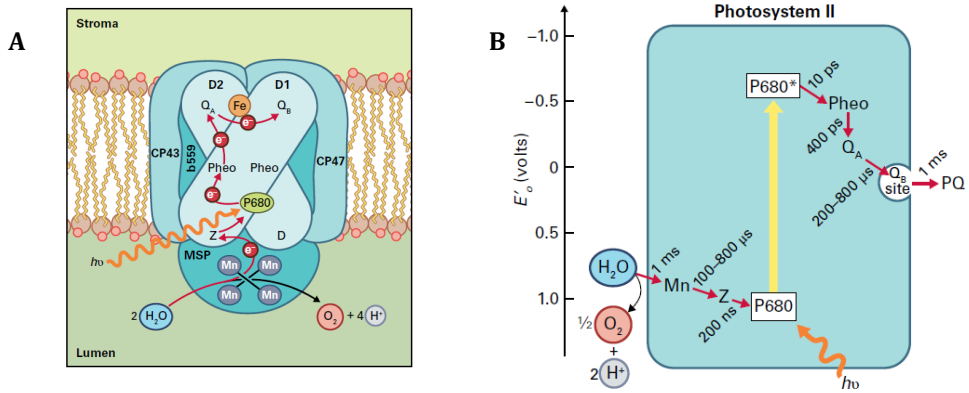

Figure 5. A) Schematic diagram of the reaction center core of monomeric PSII. *The D1 and D2 proteins bind most of the co-factors involved in charge separation and electron transport. Electrons are transferred from P680 to pheophytin (Pheo) and subsequently to two plastoquinone molecules, QA and QB. The non-heme iron (Fe) does not have a direct role in electron transfer. P680+ is reduced by Z, a tyrosine residue in the D1 subunit. Also indicated is the oxidation of water by the Mn cluster, which is bound to the luminal side of the complex and stabilized by a peripheral protein, PsbO (labeled as MSP). CP43 and CP47 are chlorophyll a-binding core antenna proteins.* **B) PSII electron carriers and the kinetics of electron transfer.** *Pheophytin receives an electron from P680 and transfers it to the first of two plastoquinones (QA), which is bound tightly to the complex; the second plastoquinone, being mobile, is able to bind the QB site when oxidized (PQ), but not when fully reduced (PQH2). Transfer of a single electron to QA occurs in approximately 400 ps. Reduction of PQ bound in the QB site to form the semiquinone PQ– occurs in approximately 200–400 µs, whereas the second reduction to form PQH2 takes place in 800 µs. Overall, within 1 ms, the oxygenevolving complex is oxidized by one electron and the quinone is reduced by one electron for each charge separation in PSII.*

Upon receiving the first energy quantum, an electron is released from P680 through an accessory chlorophyll and a pheophytin (Pheo) molecule to the tightly bound quinone Q_A, followed by the reduction of a mobile quinone PQ at the Q_B site. $P680^+$, which has a high redox potential, oxidizes a nearby tyrosine (Tyrz); Tyrz extracts an electron from a cluster of four manganese ions (OEC, oxygen-evolving complex or water-splitting complex), which binds two substrate water molecules (Zouni et al. 2001). After another photochemical cycle, the doubly reduced plastoquinone (PQ2-) takes up two protons from the stromal space to form plastoquinol (PQH2), which diffuses into the membrane toward the Cyt-b_6f complex being replaced by an oxidized quinone from the pool. After two more photochemical cycles, the manganese cluster accumulates a total of four oxidizing equivalents, which are used to oxidize two water molecules leading to the formation of O_2, the release of protons in the inner thylakoid space and the return of manganese cluster to the reduced state (Ferreira et al. 2004).

As in PSII, in PSI a special pair of chlorophylls is present in the PSI-RC (P700, primary electron absorbing at 700nm). In the case of PSI, electrons will be donated from the P700 and transferred over a couple of electrons to ferredoxin (Fd). The electrons of two molecules of reduced Fd are used by $NADP^+$ oxidoreductase (FNR) in order to convert $NADP^+$ to NADPH, which is then released into the stroma. P700+ produced by this charge separation is then re-reduced by the electrons carried from PSII via the electron transport chain. In the situation where ATP demand is higher of that for NADPH electrons can circulate around PSI in a cyclic electron flow, used for the production of ATP.

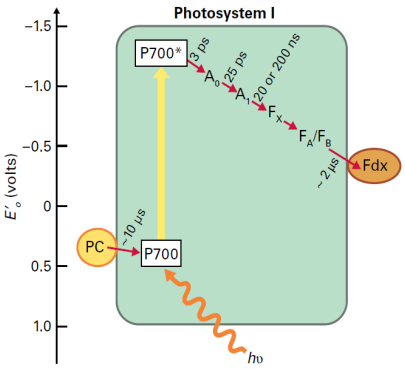

Figure 6. PSI electron carriers and the kinetics of electron transfer. *The pathway of electron transfer through the PSI complex is shown to involve P700, a monomeric chlorophyll* a *(A0), a phylloquinone (A1), and a series of additional electron carriers that include three different Fe–S centers (FX, FA, and FB). Electron transfers through these carriers occur in the time range of picoseconds to nanoseconds, with the terminal electron acceptor, ferredoxin (Fd), being reduced in approximately 2 µs.*

The result of all these charge separation reactions in between PSII and PSI, together with the electron transfer through Cyt-b_6f has as a result the formation of an electrochemical gradient between the stroma and the luminal side of the membrane, supplying ATP synthase enough to produce ATP. The ATPase enzyme is a multimeric complex with a stromal (CF1) and transmembrane regions (CF0). Proton transport through CF0 is coupled to

ATP synthesis/hydrolysis in the β-subunits of CF1. The whole CF0-CF1 complex is thought to function as a rotary proton-driven motor, in which the stationary subunits are I, II, IV, δ, α and β, and the rotary subunits are III (c), γ and ε (McCarty et al. 2000).

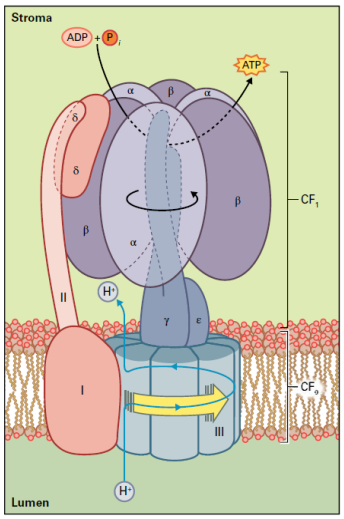

Figure 7. Model for the chloroplast ATP synthase complex. *The subunit structure of the ATP synthase indicates two major regions in the protein: an integral membrane protein portion (CF0), which functions as a channel for protons passing through the membrane, and an extrinsic portion (CF1), which contains the catalytic sites involved in ATP synthesis. CF1 consists of five different subunits (α, β, γ, δ, and ε), whereas CF0 contains four different subunits (I, II, III, and IV, of which three are shown), including 14 copies of subunit III in the membrane.*

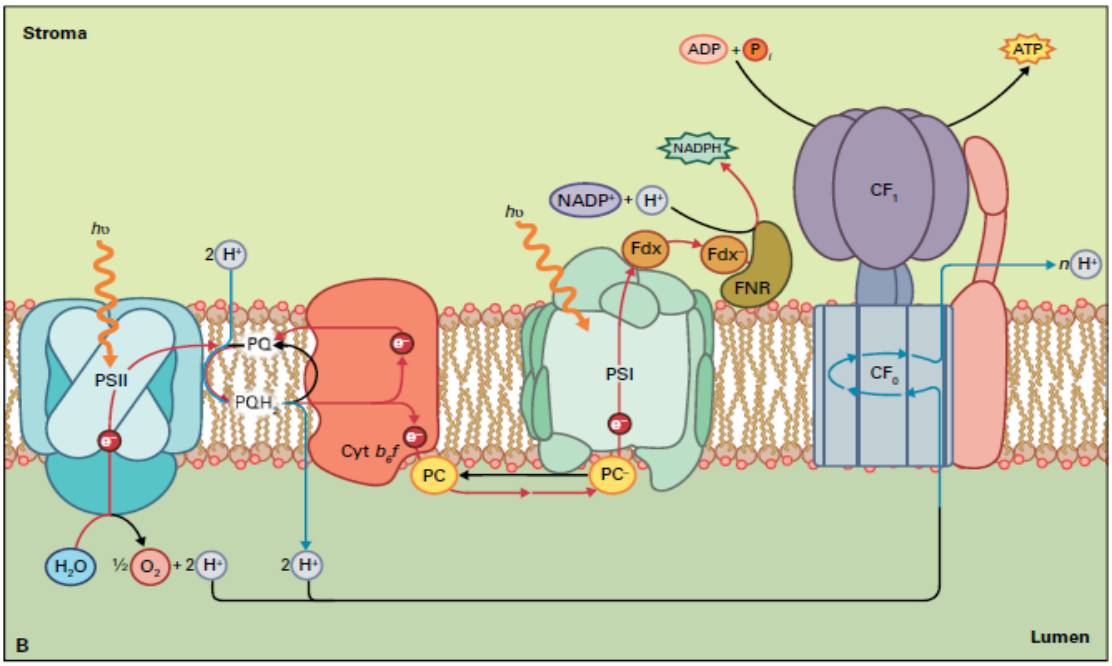

Figure 8. The supramolecular complexes of the thylakoid membrane. *The components of the chloroplast electron transport chain and the ATP-synthesizing apparatus are illustrated in the thylakoid membrane. Four membrane complexes (PSII, PSI, the cytochrome b6f complex, and the ATP synthase) are shown. Electrons are transferred from water to NADP+; accompanying this electron transfer, a proton gradient is established across the membrane. This electrochemical gradient is ultimately utilized for the synthesis of ATP by the ATP synthase. Fdx, ferredoxin; FNR, ferredoxin-NADP+ reductase.*

1.4 Light-independent phase

The light-independent phase (or 'dark phase') of photosynthesis includes a series of reactions in which atmospheric CO_2 is converted into carbohydrates or in other words the

fixation of CO_2 into biomass. The pathway, by which this conversion occurs, the Calvin–Benson cycle discovered in 1950, is crucial for sustaining most life forms. The Calvin–Benson cycle proceeds through 13 biochemical reactions that can be analyzed separately in three highly coordinated phases: carboxylation, reduction, and regeneration.

In the **carboxylation phase**, three molecules of CO_2 and three molecules of H_2O react with three molecules of ribulose 1,5-bisphosphate (RuBP; five-carbon acceptor molecule) to produce six molecules of 3-PGA. The enzyme ribulose-1,5-bisphosphate carboxylase/oxygenase (Rubisco) catalyzes these reactions. The **reductive phase** of the Calvin–Benson cycle converts the six molecules of 3-PGA coming from the carboxylation stage into six molecules of GAP. This two-step process employs ATP and NADPH, the products of the light reactions. First, the enzyme 3-phosphoglycerate kinase catalyzes the reaction of ATP with the carboxyl group of 3-PGA, yielding the mixed anhydride 1,3-bisphosphoglycerate (1,3-bis-PGA). Next, NADPH converts 1,3-bis-PGA to GAP and inorganic phosphate (Pi) in a reaction catalyzed by the chloroplast enzyme NADP–glyceraldehyde-3-phosphate dehydrogenase. One of the six molecules of GAP accounts for the net fixation of three molecules of CO_2 and represents the newly formed photosynthetic product. The other five molecules of GAP enter the last and largest set of reactions to **regenerate** three molecules of RuBP and allow continuous uptake of atmospheric CO_2. Ten of the 13 enzymes of the Calvin–Benson cycle catalyze the reshuffling of the carbons from five molecules of GAP to form three molecules of RuBP.

$$\mathbf{3\ CO_2 + 3\ Ru5P + 9\ ATP + 6\ NADPH \longrightarrow 6\ GAP + 9\ ADP + 6\ NADP^+ + 8\ Pi}$$

$$\mathbf{5\ GAP \longrightarrow 3\ Ru5P}$$

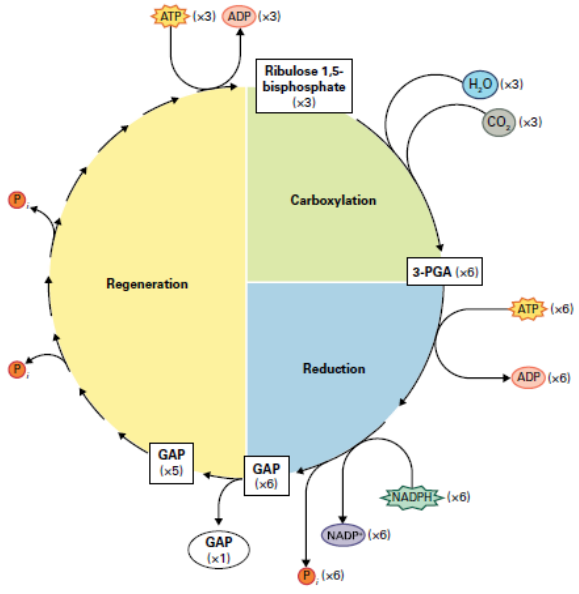

Figure 9. Three phases of the Calvin–Benson cycle: carboxylation, reduction, and regeneration. *Overall, the fixation of three molecules of CO2 into one molecule of triose phosphate requires six molecules of NADPH and nine of ATP (3 CO_2: 6 NADPH: 9 ATP ≡ CO_2: 2 NADPH: 3 ATP). The net glyceraldehydes 3-phosphate (GAP) formed is utilized either for immediate metabolic needs or converted to a storage form of carbohydrate-starch in the chloroplast or sucrose in the cytosol.3-PGA,3-phosphoglycerate.*

2 Light absorption

In the case of molecules (and in contrast to atoms) the ground state and the excited states have many closely spaced sub-states, the result of molecular vibration and rotations. These are shown in Figure 10, along with the first and second excited **singlet states** for a molecule that has two major absorption bands, such as chlorophyll, which has one absorption band in the blue spectral region and one in the red. Excitation causes transitions from the lowest sub-state of the ground state to any one of these higher energy sub-states, depending on the energy relationship. The existence of this series of sub-states in molecules yields broad absorption bands rather than the sharp absorption bands found with atoms. In molecules, two types of excited states can exist. The singlet state is relatively short-lived and contains electrons with opposite (antiparallel) spins; the more long-lived **triplet state** has electron spins that are aligned (parallel). Triplet states generally have much longer lives (take longer to de-excite) than singlet states and are at a lower energy level.

Transitions from the singlet state to the triplet state can occur, but with a low-probability. Once excited, an electron can return to the more stable ground state by one of several paths, and in each, the energy released may take several forms. In the simplest case, the energy is released as heat during a non-radiative decay (**relaxation**).

A second mechanism involves the emission of a photon in a process known as **fluorescence**. The emitted light has a longer wavelength than the absorbed light because fluorescence always arises from decay from the first excited state to the ground state and is preceded by de-excitation from higher sub-states to the first excited state via vibrational relaxations. Measurements of chlorophyll fluorescence are used to investigate the efficiency and regulation of photosynthesis. A third mechanism, **energy transfer**, involves the transfer of energy to another molecule, usually one in close proximity to the excited molecule. This process is an important vehicle for the movement of absorbed light energy through an array of pigment molecules.

Finally, the excited molecule may lose an electron to an electron-acceptor molecule through a **charge separation** event, in which the excited pigment reduces an acceptor molecule. This last mechanism, called **photochemistry**, converts light energy into chemical products and is central to the process of photosynthesis.

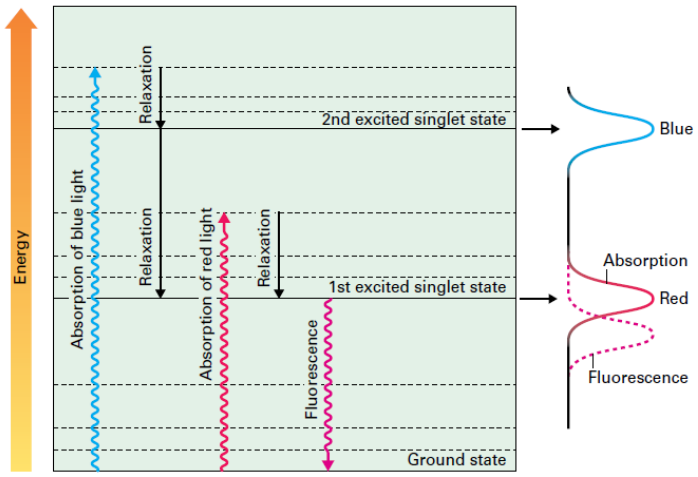

Figure 10. Energy levels in the chlorophyll molecule. *Absorption of blue or red light causes the chlorophyll molecule to convert into an excited state, with blue light absorption resulting in a higher excited state because of the greater energy of blue light relative to red light. Internal conversions or relaxations convert higher excited states to the lowest excited state, with a concomitant loss of energy as heat. Light may be reemitted from the lowest excited state through fluorescence. The spectra for fluorescence and absorption are shown at the right of the figure. The short-wavelength absorption band corresponds to a transition to the higher excited state, and the long wavelength absorption band corresponds to a transition to the lower excited state.*

2.1 Light-harvesting pigments

For light energy to be used by any system, the light must first be absorbed. This is a significant problem for photosynthetic organisms since shading and reflection can result in large losses of available light. Molecules that absorb light are called **pigments**. The absorption of a photon by a pigment molecule converts the pigment from its lowest energy (ground) state to an excited state (pigment*). Chlorophylls and carotenoids are the two main classes of pigments responsible for light absorption, charge separation but also energy transfer from the antenna system towards the photosystems reaction center of all photosynthetic organisms.

2.1.1 Chlorophylls

The most prominent dye is the one that makes leaves green, the chlorophyll (Chl). All photoautotrophic organisms contain some form of the light-absorbing pigment **chlorophyll**. Plants, algae, and cyanobacteria synthesize chlorophyll, whereas anaerobic photosynthetic bacteria produce a molecular variant called bacterio-chlorophyll. There are few forms of chlorophyll that occur naturally, all of them giving peculiar spectral features. The most widely distributed chlorophyll forms are chlorophyll a (Chl a) and chlorophyll b (Chl b). However, there are also other Chl forms such as Chl c1 and Chl c2,

Chl d (cyanobacteria, red algae) and Chl f (cyanobacteria) (Larkum et al., 2003; Chen et al., 2010).

Several steps in the biosynthesis of chlorophyll are shared; however, chlorophyll binds a magnesium (Mg) atom in the center of its tetrapyrrole ring. In addition, a long (C_{20}) hydrophobic side chain, known as a phytol tail, is attached to the tetrapyrrole ring structure of chlorophyll and renders the molecule extremely nonpolar. The distinct forms of chlorophyll have different side chains on the ring or different degrees of saturation of the ring system. For example, chlorophyll *b* is synthesized through the action of an oxygenase enzyme that converts a methyl to a formyl side group. These small changes in chemical structure substantially alter the absorption properties of the different chlorophyll species. The characteristic ability of chlorophylls to absorb light in the visible region is due to the high number of conjugated double bonds that these molecules possess. Absorption is also affected by excitonic interactions with neighboring pigments and the non-covalent interaction of the molecule with chlorophyll-binding proteins found in the photosynthetic membrane.

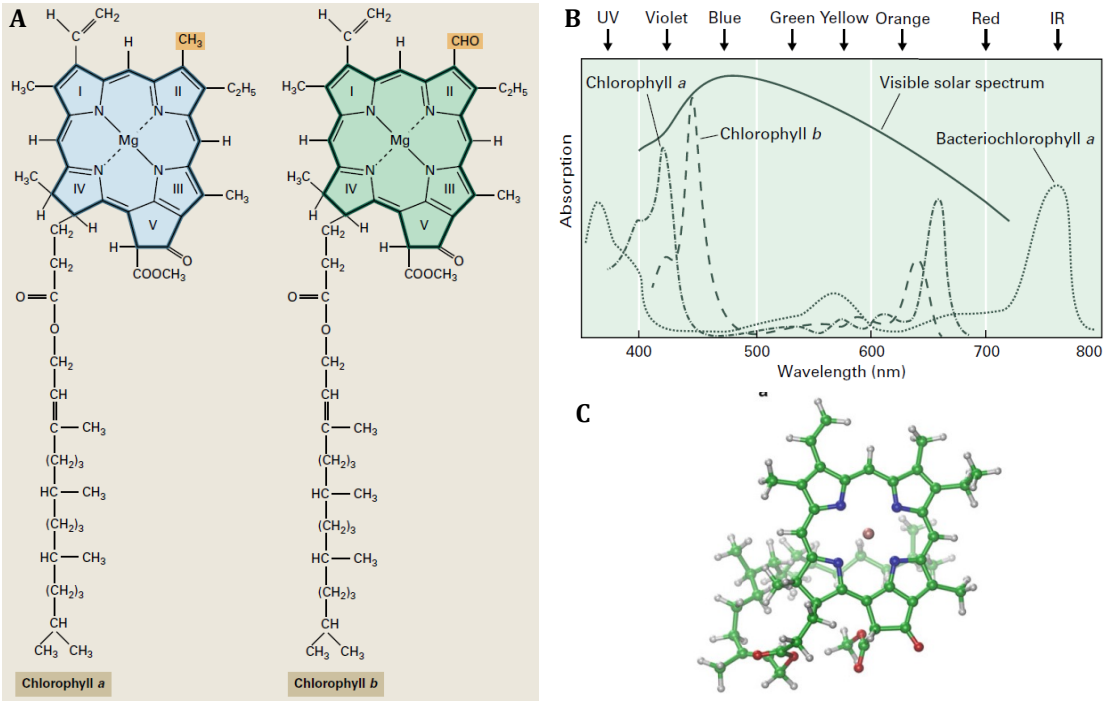

Figure 11. A) Structures of chlorophylls. *Chlorophyll molecules have a porphyrin-like ring structure that contains a central magnesium (Mg) atom coordinated to the four modified pyrrole rings. Chlorophylls also contain a long hydrocarbon tail that makes the molecules hydrophobic. Various chlorophylls differ in their substituents around the ring structure. In chlorophyll a, a methyl group is present, whereas in chlorophyll b, a formyl group is present at the same position.* **B) Absorption spectra of chlorophylls.** *The absorbance spectra of pigments dissolved in nonpolar solvents are shown for chlorophylls a and b and bacteriochlorophyll a. The visible region of the solar spectrum is also diagrammed. Note the spectra of these pigments show substantial shifts in absorption in vivo, where they are associated with specific proteins.* **C) Molecular structure of chlorophyll a** *(taken from LHCII, PDB entry 1rwt.*

Chla and Chlb exhibit two absorption bands in the visible spectrum. The Qy transition (red region) is the red-most band, which peaks around 640-670nm in Chlb and Chla. On the other hand, the Soret band (blue region) corresponds to transitions to higher states: its maximum is around 430nm for Chla and 460nm for Chlb. This is the reason why almost the entity of plants appears green: Chl is green because it absorbs the 430nm (blue) and 670nm (red) wavelengths of the visible spectrum more effectively than it absorbs green light. The green light not absorbed is reflected, which makes it visible.

2.1.2 Carotenoids

A second group of pigment molecules found in all photosynthetic organisms is the **carotenoids**. In plants, they contribute to the photosynthetic machinery and protect them against photo-damage. They are naturally occurring in plants, algae and some types of bacteria. Carotenoids are present as micro-components in fruits and vegetables and are responsible for their yellow, orange and red colors. They are thought to be responsible for the beneficial properties of fruits and vegetables in preventing human diseases including cardiovascular diseases, cancer and other chronic disease. In recent years the antioxidant properties of carotenoids has been the major focus of research.

Carotenoids are tetraterpenoids (C_{40}) molecules derived from eight isoprene units, the products of the non-mevalonate pathway located in the chloroplast (equipped with a long chain of conjugated double bonds in the central part and terminated by variable groups (Straub and Pfander, 1987). This class of molecules can be divided in two main categories: the carotenes, which contain a conjugated double-bond system of carbon and hydrogen (i.e. a-carotene, β-carotene) and the xanthophylls, which in addition contain oxygen atoms in their terminal rings (i.e. lutein, zeaxanthin).

They are bound to the protein complexes in the thylakoid membranes by hydrophobic interactions (Gastaldelli et al., 2003). In vascular plants the most widely represented forms of carotenoids are a-carotene and β-carotene bound to the core complex of both photosystem I and photosystem II (Yamamoto and Bassi, 1996) but also the xanthophylls lutein, zeaxanthin, violaxanthin and neoxanthin which can be found in the antenna system (Bassi et al, 1993; Ruban et al, 1999; Caffarri et al, 2001; Formaggio et al, 2001).

The conjugated double bond system of carotenoids gives them specific photochemical properties. The π-electrons delocalization leads to the light absorption in the visible range 400-500nm. When carotenoids absorb light, ground electrons are raised directly to the

second excited singlet state ($S_0 \longrightarrow S_2$), without populating the first excited singlet state (S_1) due to symmetry reasons. This strong dipole-dipole transition is responsible for the characteristic absorption of the carotenoids.

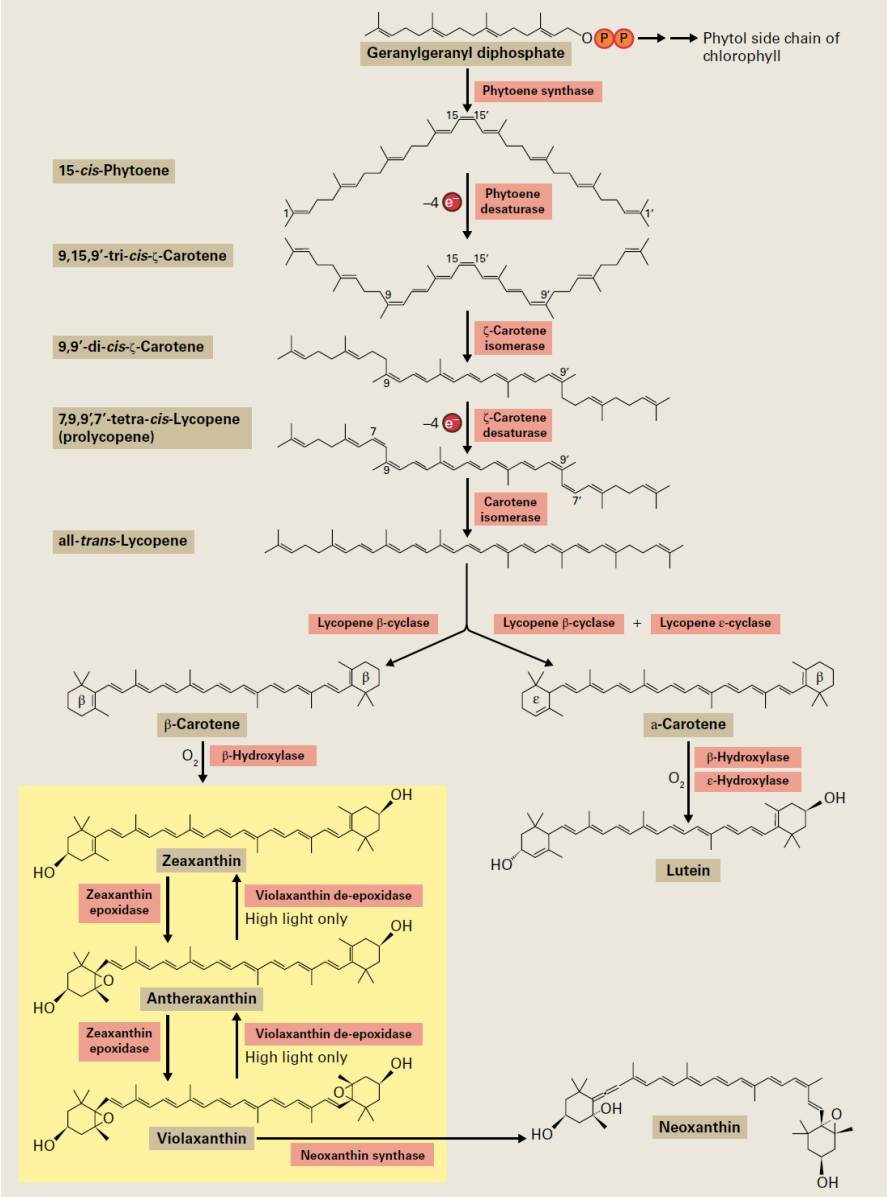

Figure 12. Biosynthesis of carotenoids and xanthophylls in plants. *The pathway for conversion of geranylgeranyl diphosphate to lycopene, shown in the upper half of the figure, involves desaturation and isomerization reactions. Two desaturases, phytoene desaturase (PDS) and zeta-carotene desaturase (ZDS), and two isomerases, zeta-carotene isomerase (Z-ISO) and carotene isomerase (CRTISO), participate in these reactions. The conversion of lycopene to carotenoids and xanthophylls is illustrated in the lower half. The Greek letters βand ε designate the ring structures of the two-carotene species. The xanthophyll cycle (lower left) protects plants from high light intensities by converting violaxanthin into zeaxanthin, which participates in thermal dissipation of excess absorbed light energy.*

Apart from their spectroscopic properties, carotenoids are also essential in photosynthesis and photoprotection. They play a major role in structure stabilization and assembly of protein complexes in the thylakoid membrane (Paulsen et al, 1993), they protect against photo-oxidative damage (Havaux and Niyogi, 1999), they have a crucial role in the transfer of excited state energy to chlorophylls (Mimuro and Katoh, 1991) but they also act as accessory pigments extending the light-harvesting capacity of Chl-complexes to the blue region.

2.2 The xanthophyll cycle

While hydroxylation of α-Car produces lutein, a carotenoid end-product that accumulates at high levels, hydroxylation of β-Car produce zeaxanthin that, under light conditions that do not saturate photosynthesis or in the dark, is readily converted to violaxanthin via antheraxanthin in a two-step reaction catalyzed by the enzyme zeaxanthin epoxidase (ZE). When light is strong and exceeds the photosynthetic capacity, Viola is de-epoxidated back into zeaxanthin by the activity of the enzyme violaxanthin de-epoxidase (VDE) (Yamamoto and Kamite 1972, Demmig-Adams et al. 1996) (fig. 14). The inter-conversion of zeaxanthin and violaxanthin is known as the xanthophyll cycle and has a key role in the adaptation of plants to different light intensities (Dall'Osto et al. 2005). When the light-driven proton translocation across the thylakoid membrane exceeds the dissipation rate of the proton gradient by ATPase, VDE is activated leading to a decrease in pH in the thylakoid lumen while ZE is always active.

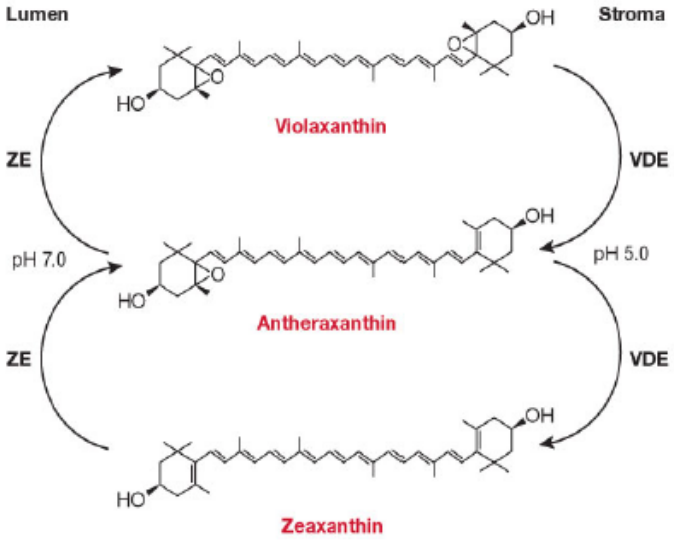

Figure 13. The xanthophyll cycle. *VDE, violaxanthin de-epoxidase; ZE, zeaxanthin epoxidase*

Upon return to light-limiting conditions of photosynthesis zeaxanthin is converted back to violaxanthin by a stromal enzyme zeaxanthin epoxidase (ZE) (Bugos et al., 1998; Jahns et al., 2009). At neutral pH, VDE is a monomeric enzyme and adopts a typical lipocalin fold with an eight-stranded antiparallel b-barrel, confirming its classification as a member of the lipocalin protein family (Arnoux et al., 2009). Instead, at acidic pH, VDE is very different from observed at neutral pH; in fact the protein adopts a stable dimeric conformation. In the dimeric state, the barrel adopts an open conformation that facilitates ligand access to the active site (Arnoux et al., 2009). The xanthophyll cycle is uniquely separated on opposite sides of the thylakoid membrane; VDE activity takes place on the thylakoid lumen side of the membrane, whereas ZE occurs on the chloroplast stromal side (Hieber et al. 2000). Xanthophyll cycle is a key component of several photo-protective mechanisms as scavenging of ROS, thermal dissipation of excitation energy in excess or Chl triplets excited state quenching (Niyogi 1999, Holt et al. 2004).

2.3 Light-harvesting complexes

In photosynthesis, light energy is absorbed and converted into stable chemical products by integral membrane pigment-protein complexes called **photosystems**. Both photosystem I (a plastocyanin-ferrodoxin oxidoreductase) and photosystem II (a light-driven water-plastoquinone oxidoreductase) are composed by an array of light-harvesting pigments that are bound by proteins called **light-harvesting complexes** (LHC) or antennas as well as the **core complex**, where photosynthetic electron transfer begins with a charge separation. The antennae absorb light energy and channel it towards the reaction center, where excitation of specially bound chlorophyll molecules results in transfer of an electron to an acceptor. LHC bind chlorophyll a, chlorophyll b and carotenoids, which increase the light absorbance and its transfer towards the reaction, center but also play an important role in photoprotection against excessive light.

PSa and PSb gene products compose the core complexes for PSI and PSII respectively. The polypeptides composing the two photosystems are encoded by the nuclear and chloroplastic genomes. Although the genes encoding the core subunits are well conserved between bacteria and eukaryotic photosynthetic organisms, the ones responsible for the antenna system are more variable and differ from organism to organism. In higher plants antenna system is composed by polypeptides, which belong to the LHC family (Durnford et al., 1996; Kozior et al., 2007). All the products coming from the LHC family are

encoded by the nuclear genome and are denominated Lhca and Lhcb for the antennae of PSI and PSII respectively (Jansson et al., 1999).

Up to now, six (6) classes of antenna proteins (Lhca 1-6) for PSI and 6 proteins (Lhcb 1-6) for PSII have been identified. In addition, two more isoforms (Lhcb7 and Lhcb8), have been identified from gene sequences (Klimmek et al., 2006). Depending on the species, these proteins can be composed by one or more genes. Lhcb1 is the largest protein class encoded by 5 different genes in *Arabidopsis thaliana* and at least 14 genes in barley (Caffarri et al., 2004).

2.3.1 Photosystem II

Photosystem II (or water-plastoquinone oxidoreductase) is the first protein complex in the light-dependent reactions of oxygenic photosynthesis. It is located in the thylakoid membrane of plants, algae, and cyanobacteria. Information on the PSII architecture is mostly derived from the high-resolution structure of the PSII oxygen-evolving center from the cyanobacterium *Thermosynechoccus elongates* (Ferreira et al., 2004). PSII is a dimeric multi-subunit complex with 19 subunits in each monomer and co-ordinates with 250-300 chlorophyll molecules depending on the species and the environmental conditions (Anderson and Andersson, 1988; Melis, 1991; Ballottari et al., 2007).

The largest supercomplex observed by electron microscopy contains a dimeric core complex (C2), two strongly bound 'major' LHCII trimers (S2), two moderately bound LHCII (M2), two CP29, two CP24 and two CP26 forming a C2S2M2 supercomplex (Dekker and Boekema, 2005). Besides the S2 and M2 LHCII trimers, there are loosely bound LHCII trimers (L) at peripheral region which can migrate between PSII and PSI to balance the excitation level of two photosystems in response to light fluctuations (Galka et al., 2012). Recent studies on the C2S2M2 supercomplex reveal the position and orientation of the antenna complexes allowing suggestions for the excitation energy pathways from the antenna system to the core complex (Caffarri et al., 2009; Pan et al., 2013).

2.3.1.a Photosystem II core

Core complex of PSII is composed by the polypeptides denominated PSB encoded from both nuclear and plastidial genes. The core of PSII is a multi-subunit complex composed of about 25-30 subunits; it contains four large membrane-intrinsic subunits

(PSBA-D), three membrane-extrinsic subunits (PSBO–Q) and a large number of small subunits (fig. 15), most of which span the membrane once and are involved in the dimerization or in chlorophylls and carotenoids binding stabilization, but they do not all have a well-clarified function (Shi et al. 2012). PSBA (D1) and PSBD (D2) bind six Chla and two Pheo-a molecules and constitute the photochemical reaction center in which the charge separation and primary electron transfer reactions take place. PSBB (CP47) and PSBC (CP43) bind 16 and 14 Chla molecules respectively and have a light-harvesting function: they absorb light and transfer the excitation energy to the reaction center and also accept excitation energy from the peripheral antenna and transfer this to the reaction center (Barber et al. 2000).

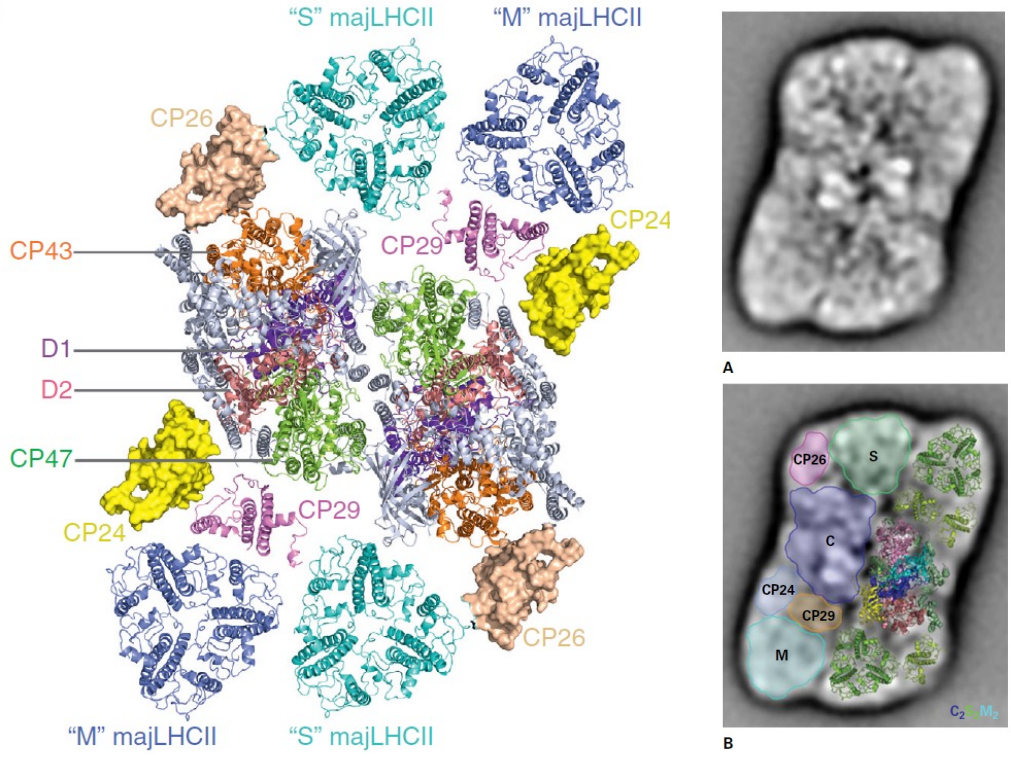

Figure 14. A structural model of C2S2M2-type PSII–LHCII supercomplex. *The model was constructed based on the electron microscopy map and the crystal structures of PSII, majLHCII and CP29. Subunits D1, D2, CP43 and CP47 of PSII core ('C-') are colored in purple, salmon, orange and green, respectively. 'S'-, 'M'-type of majLHCII trimers and the minor antenna CP29 are shown as cyan, blue and magenta ribbons. The homologous structures of CP26 and CP24, whose crystal structures are not available yet, are shown as wheat and yellow surface models, respectively* A) *Top view of the projection map determined by single particle cryoelectron microscopy.* B) *Assignment of subunits by fitting of high-resolution structures. The dimer of PSII cores (C) is in the center of the supercomplex, with monomeric LHCs (CP29, CP26, and CP24) connecting the strongly bound (S) and moderately bound (M) peripheral LHCII trimers to the core.*

2.3.1.b Antenna complexes of photosystem II

The antenna system associated with plant photosystem II (PSII) comprises a series of light-harvesting complexes II (LHCIIs) or antennae, which are supramolecular assemblies of chlorophylls, carotenoids, lipids and integral membrane proteins. These complexes not only function in capturing and transmitting light energy, but also have pivotal roles in photoprotection in high light conditions. These two processes need to be balanced on a constant mode in order to optimize photosynthesis (Niyogi, 1999). Seven peripheral antennae exist in *A. thaliana* derived as products of seven different genes: *lhcb1-7*.

Light harvesting complexes bind both Chla and Chlb (Thornber, 1969; Jansson, 1994; Caffarri et al., 2004). Analysis of LHC proteins reveals a three-transmembrane structure consisted of α-helices, with the presence of two highly conserved regions (LHC-like domains). This homology suggests the existence of a common four-helix ancestral protein that has evolved through internal gene duplication events (Engelken et al., 2010). Two major categories of light-harvesting complexes form the peripheral antenna system of PSII: the major light-harvesting complex of PSII, called LHCII (Thornber, 1969) and the minor antennae (Bassi, 1987)

b.1 The major antenna (LHCII)

Estimated to represent about half of total protein in thylakoid membrane, LHCII is the most abundant membrane protein on Earth. It is composed in vivo by homologous Lhcb1, Lhcb2 and Lhcb3 gene products, forming hetero-trimers.

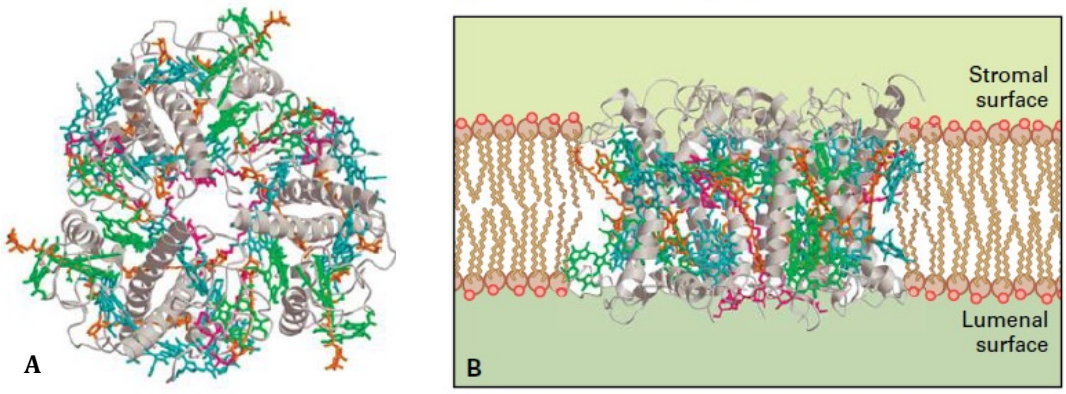

Figure 15. Trimeric structure of LHCII. *Each monomer in the complex contains three transmembrane-spanning helices and binds 14 molecules of chlorophyll* a *and* b*, as well as four xanthophyll molecules. A) View from the stromal side of the membrane. B) Side view within the plane of the membrane.*

Every monomeric LHCII is composed by three membrane-spanning α-helices (helix A, B and C) and two short amphipathic helices (D and E) located at their luminal surfaces. The amino termini are located at the stromal side and the carboxy termini are on the luminal side. Helices A and B intertwine in the middle of membrane and form a left-handed supercoil. Two conserved inter-helix ionic pairs (Glu65- Arg185 and Arg70-Glu180) contribute to the stability of the central supercoil (helices A and B). A pseudo-C2 axis runs through the core region of each monomer and relates helices A–D to helices B–E. The helix C runs nearly perpendicular to the membrane plane and does not abide to the internal pseudo-C2 axis (Pan et al., 2013). The trimerization domain covers: the amino-terminal domain, the carboxyl terminus, the stromal end of helix B, several hydrophobic residues from helix C and also pigments and lipid as phosphatidylglycerol (PG), bound to these parts of the polypeptide chain. Six Chla (two from each monomer), constitute the core of the trimer (Liu et al. 2004).

Each 25kDa monomeric subunit binds 14 chlorophylls (8 Chla, 6 Chlb) and 4 carotenoid molecules: 2.2 lutein molecules in the first and third helices, 0.8 violaxanthin and 1 neoxanthin molecules bound more peripherally (Liu et al, 2004). The chlorophylls are vertically distributed into two layers within the membrane: the layer closer to the stromal surface and one more layer close to the luminal side. The stromal surface layer contains 8 chlorophyll molecules in three separate clusters (Chl a602-a603, a610-a611-a612 and b6010-b608-b609), which surround helices A and B forming an elliptical ring. The layer close to the luminal surface contains the remaining 6 chlorophylls, which form two different clusters: one cluster with 4 chlorophylls and another one with a Chla – Chla dimer (Chl b606-b607-b605-a604 and a613-a614). In *A. thaliana* the amount of LHCII linked to the reaction center varies on environmental conditions, showing a lower LHCII content when plants grow in high light and a higher accumulation of LHCII when plants grow under low light conditions (Ballottari et al, 2007).

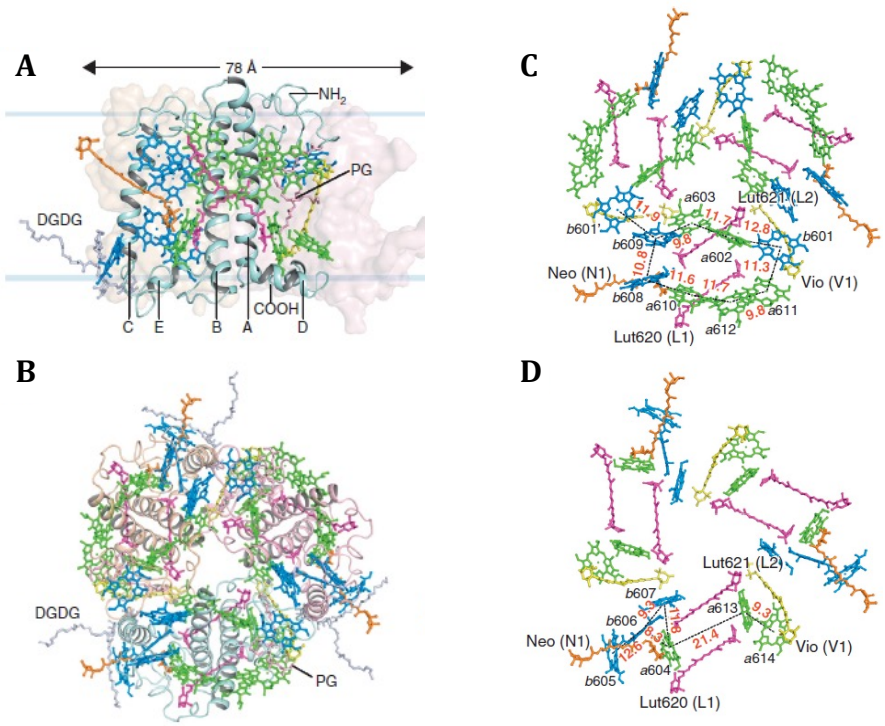

Figure 16. The overall structures of LHCII and arrangement of pigment molecules within LHCII trimer. *A) The overall structure of LHCII viewed in parallel with the membrane plane, B) LHCII viewed from the stromal side along the three-fold axis. The pigment molecules within majLHCII trimer in the layers close to C) the stromal and D) the luminal surfaces respectively. The adjacent Chls within each layer of majLHCII monomer are connected with dark dashed lines and the distances (A°) between their central Mg atoms are labeled with red digital numbers.*

There are four carotenoid binding sites observed in major LHCII named as L1, L2, N1 and V1 sites. Two central lutein molecules are bound in the grooves of both sides of helices A and B (site L1 and L2). A third xanthophyll (9'-cis-neoxanthin) is located in the Chl b-rich region around helix C stabilized by a hydrogen bond between its epoxidated cyclohexane ring and the side chain of a conserved Tyr residue (site N1) (Croce et al., 1999; Pan et al., 2013). Finally, LHCII contains a fourth carotenoid-binding site V1 occupied by a violaxanthin molecule. This site is located at the monomer-monomer interface and contributes to the LHCII trimerization and it is believed to serve as a reservoir site storing and provide violaxanthin molecules for the operation of xanthophyll cycle (Caffarri et al., 2001).

Depending on environmental conditions, a subpopulation of LHCII trimers can be phosphorylated and migrate from PSII, docking to PSI. This process is called state transition (Allen, 1992; Andersson and Anderson, 1980): when electron transport between the two photosystems is impaired due to an insufficient light absorption by PSI, state transitions provide a mechanism for the equilibration of the excitation energy between photosystems, thus increasing the efficiency of the whole process. In higher

plants this mechanism was demonstrated to depend from the presence of the specific kinase STN7 (Bellafiore et al., 2005).

b.2 The minor antennae

The minor antenna system consists of three Chl a/b and xanthophyll-binding proteins: Lhcb4 (CP29), Lhcb5 (CP26) and Lhcb6 (CP24), named according to the molecular weight of their apo-proteins in non-denaturating SDS-PAGE (Bassi, 1987; Peter and Thornber, 1991). These proteins are encoded by nuclear the genes *lhcb4*, *lhcb5* and *lhcb6* respectively, which are highly homologous to the other members of the LHC superfamily. Minor antennae have a regulatory role not only in the energy transfer from the antenna system to the reaction center but also in thermal dissipation of excess energy (Kovacs et al., 2006; de Bianchi et al., 2008; de Bianchi et al., 2011).

Lhcb4 (CP29) is composed of 258 amino acids (256-258 amino acids in its mature form). In *A. thaliana* Lhcb4, 6 Chla, 2 Chlb, 1 lutein molecule and 2 other carotenoids (violaxanthin and neoxanthin) are detected in the structure in a sub-stoichiometry amount (Dainese and Bassi, 1991). From a structural point of view Lhcb4 is important for the organization of photosystem II and plays a key role for the stability of the PSII-LHCII supercomplex (van Oort et al. 2010). The overall sequence identity between Lhcb4 and LHCII is 34% but most of the substitutions are conservative, especially in the helix regions.

As in LHCII, most of the chlorophyll binding sites overlap also in Lhcb4, except that Chls b601 and b605 in LHCII are absent in Lhcb4. The conserved Chl 609 and Chl 614 sites are, respectively by Chla and Chlb in Lhcb4 (but by Chlb and Chla in LHCII). The selective binding of Chl b/a on these sites is mainly due to the presence/absence of hydrogen-bond donor for the binding of C7-formyl group of Chlb molecule.

Lhcb5 (CP26) is composed of 243 amino acids and in *A. thaliana* co-ordinates 6 Chla, 3 Chls b and 2-3 xanthophylls (lutein, violaxanthin and neoxanthin) showing a 48% identity with LHCII (Bassi and Dainese, 1992).

Lhcb6 (CP24) is the smallest of LHC proteins, composed by 211 amino acids due to the lack of the major part of the C-terminal region of the protein. In the structure of Lhcb6, 5 Chla, 5 Chlb and 2 xanthophylls (violaxanthin and lutein) are detected (Pagano et al., 1998). Lhcb6 is associated with the moderately bound LHCII to form band 4 PSII supercomplex (Koziol et al., 2007; Betterle et al., 2009).

2.3.2 Photosystem I

High-resolution crystal structures are available for PSI from both cyanobacteria and plants (Krauss et al., 1996; Ben-Shem et al., 2003; Boekema et al., 2001). Cyanobacterial PSI is a trimer of reaction centers, with 96 chlorophylls, 22 carotenoids, two phylloquinones, and three 4Fe–4S clusters per reaction center. This structure revealed the detailed structure of the core antenna, the symmetrical cofactor branches, and their interactions with the protein subunits. By contrast, the plant PSI structure shows a supercomplex with a monomeric reaction center core and a peripheral antenna composed of four LHCI proteins. The isolation of these two complexes was performed using a detergent treatment, which separates PSI core from the antenna system without causing protein denaturation (Croce et al., 1998).

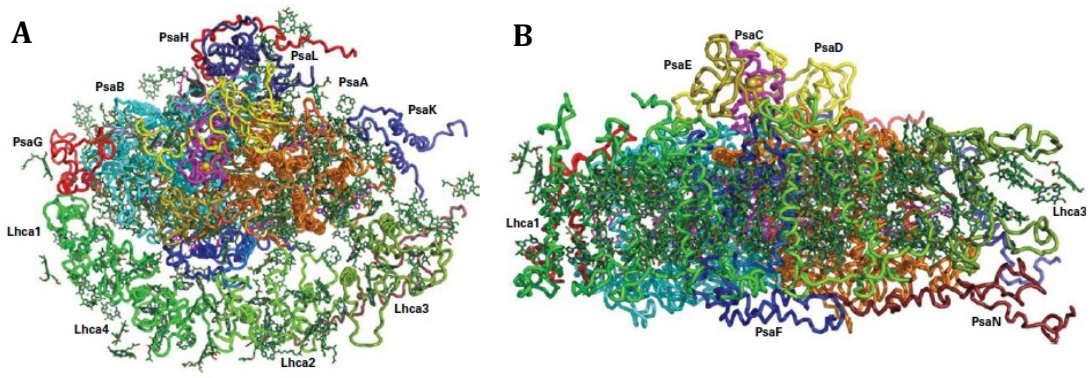

Figure 17. Structure of plant PSI. *A) View from the stromal side of the membrane. The peripheral antenna composed of Lhca1-4 proteins is shown on the lower side of the monomeric reaction center core. "Gap chlorophylls" that connect peripheral antenna to the core antenna are evident in the space between the Lhca proteins and the reaction center. B) Side view within the plane of the membrane. The PsaC, PsaD, and PsaE subunits protrude into the stroma and facilitate electron transfer to the soluble terminal acceptor, ferredoxin.*

The peripheral LHCI antenna array is located on one side of the reaction center in a crescent shape. The locations of 12 core protein subunits have been determined, ten of which are also found in cyanobacterial PSI. The positions of the electron transfer components and core antenna chlorophylls are conserved between plant and cyanobacterial PSI.

2.3.2.a Antenna complex of photosystem I

Light-harvesting complex I (LHCI) in *A. thaliana* is composed of 4 major proteins (Lhca1, Lhca2, Lhca3, Lhca4), which are encoded by nuclear genes (Croce et al., 2002; Ben-Shem et al., 2003; Amunts et al., 2007). These polypeptides are bound to one side of photosystem I core complex and are responsible for the transfer of the absorbed light energy towards the reaction center. Each antenna is present as a single copy with the entire complex being organized in two adjacent dimers: Lhca1-Lhca4 and Lhca2-Lhca3 (Croce et al., 2002; Amunts et al., 2007). Recent studies on the structure of PSI-LHCII supercomplex provide new details on the organization of the antenna system around PSI core. Lhca has the same general structure as LHCII: two inclined α-helices that interconnect, a smaller helix stretching perpendicularly to the membrane and an amphipathic helix (around 10-12 amino acids) in a position parallel to the membrane (Ben-Shem et al., 2003).

A unique characteristic of the antenna system of PSI is having a pronounced long-wavelength absorbance in the red region. This ability of chlorophylls to absorb at a lower energy with respect to the reaction center P700 is due to the presence of red forms (Gobets and van Grondelle, 2001). While they are still red forms in the core complex, the red-most Chls are found in the antenna complex LHCI (Mullet et al. 1980). *In vitro* reconstitution, together with biochemical and spectroscopic analysis of Lhca proteins, has shown that the 'red forms' are mainly associated to Lhca3 and Lhca4 and derived from the binding site, via an asparagine, for the Chl A5 (Castelletti et al. 2003). Mutagenesis but also recombinant protein experiments have demonstrated that red forms are derived from the binding site of ChlA5. More specifically, Lhca3 and Lhca4 bind to the ChlA5 binding site via an asparagine, while Lhca2 and Lhca1 through a histidine (Castelletti et al., 2003). The function of red forms is not yet fully understood, however there are suggestions regarding their role in photoprotection against light-stress and their ability to absorb light efficiently in a dense vegetation system (where light is enriched in wavelengths above 690nm). Preferential degradation of LHCI upon illumination of isolated PSI-LHCI is effective in protecting the catalytic activity of the complex (Alboresi et al. 2009).

Protein	Gene	Location of gene	Mol. mass (kDa)	Function
Hydrophobic subunits				
PsaA	*psaA*	Chloroplast	83	Reaction center protein
PsaB	*psaB*	Chloroplast	82	Reaction center protein
PsaF	*psaF*	Nucleus	17	PC docking
PsaG	*psaG*	Nucleus	11	LHCI binding
PsaH	*psaH*	Nucleus	10	LHCII-P docking
PsaI	*psaI*	Chloroplast	4	Unknown
PsaJ	*psaJ*	Chloroplast	5	Interaction with PsaF
PsaK	*psaK*	Nucleus	9	LHCI binding
PsaL	*psaL*	Nucleus	18	LHCII-P docking
PsaO	*psaO*	Nucleus	10	LHCII-P docking
PsaP	*psaP*	Nucleus	14	LHCII-P docking
Hydrophilic subunits				
Stromal orientation				
PsaC	*psaC*	Chloroplast	9	Fe–S apoprotein
PsaD	*psaD*	Nucleus	18	Ferredoxin docking
PsaE	*psaE*	Nucleus	10	Ferredoxin docking
Luminal orientation				
PsaN	*psaN*	Nucleus	10	PC docking

Table 1. Protein subunits of the plant PSI core complex.

2.3.2.b Core complex of photosystem I

Core complex of PSI is composed by the polypeptides denominated 'Psa' encoded from both nuclear and plastidial genes. PSI core is responsible for light-driven charge separation and electron transfer. It coordinates around 100 Chls and 20 β-Car molecules. Its primary and tertiary structures are highly conserved among green algae and plants; 14 subunits are present in both types of organisms (PsaA-PsaL and PsaN-PsaO), whereas PsaP is present in plants but so far seems to be absent in algae (Jensen et al. 2007). PsaA and PsaB (each ≈80 kDa) form the central heterodimer of the reaction center and are involved in binding the major electron transfer carriers, such as P700 and accessory chlorophylls, the chlorophyll *a* acceptor molecule (A0), phylloquinone (vitamin K1, the A1 acceptor), and the bound Fe–S center FX.

In particular, the PsaA-PsaB heterodimer forms the inner core of PSI, binding the P700 special Chl pair where the light-driven charge separation occurs. They bind all of the cofactors of the electron transfer chain (Jordan et al. 2001), except for the last 2 Fe_4S_4

clusters (F_A and F_B). These are bound to the peripheral subunit PsaC, which together with PsaD and PsaE forms the docking site for F_D on the stromal side of the membrane (Scheller et al. 2001). PsaF and PsaN are important for electron transfer from PC to P700 (Haldrup et al. 1999). PsaJ is a hydrophobic protein located close to PsaF and plays a role in the 32 stabilization of this subunit conformation (Fischer et al. 1999). PsaH, PsaI, PsaL, and PsaO form a cluster of integral membrane proteins, placed on one side of the core, where they are involved in interactions with LHCII during state transitions (Lunde et al. 2000, Zhang and Scheller 2004). PsaG and PsaK are located near PsaA and PsaB respectively and have been proposed to be important for the association of the outer antenna with the core (Ben Shem et al. 2004).

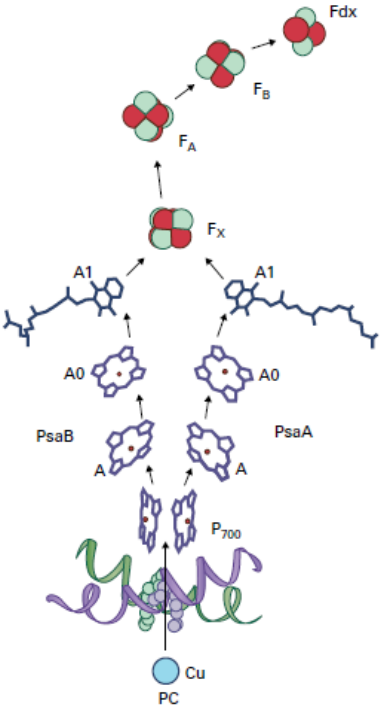

Figure 18. PSI organization of electron carriers and electron transfer pathways in the PSI reaction center complex. *The P700 dimer is located on the luminal side of the structure and two symmetrical co-factor branches radiate out from P700. Each includes an accessory chlorophyll a molecule (A), a monomeric chlorophyll a molecule identified as A0, and a phylloquinone (A1). The two branches converge at the Fe–S center FX. On the stromal side of the complex, two additional Fe–S centers (FA and FB) have been identified on the path to the soluble acceptor ferredoxin (Fd). The electron donor on the luminal side of PSI is the soluble copper protein plastocyanin (PC).*

3 Photoprotection

3.1 Generation of Reactive-Oxygen Species (ROS)

Under the high light intensities found in nature, plants may absorb more light energy than they can use for photosynthesis, something that can be dangerous for the photosynthetic apparatus. Light intensity can be variable in space and time according to time of day, season, geography, climate, and the position of leaf within canopy and cell within leaf. Under these conditions, the excessive excitation of chlorophylls can increase formation of the triplet state of chlorophyll and the formation of singlet state of oxygen

(reactive oxygen species, ROS) (Prasil et al., 1992; Tjus et al., 1998, 2001). Damage caused to the photosynthetic apparatus by singlet oxygen and its reactive products can decrease the efficiency of photosynthesis in a process known as photoinhibition (Aro et al., 1993; Hideg et al., 1998; Powles and Björkman, 1982). Oxidizing, dangerous molecules can be above all generated at three major sites in the photosynthetic apparatus: LHC of PSII, PSII reaction center and PSI acceptor side.

In the LHC upon absorption of blue light, an electron from the ground state is raised to a higher energy state and the energy is rapidly dissipated non-radiatively as heat mainly by internal conversion, and the electron rapidly relaxes to the first excited state. Absorption of a red photon causes Chl to enter directly the singlet excited state ($_1$Chl*). From there the $_1$Chl* can relax to the ground state via different pathways: the excitation energy can be emitted as fluorescence, it can be transferred to the reaction center for photosynthetic reactions or it can dissipate non-radiatively as thermal emission (Non-Photochemical Quenching). Before $_1$Chl* is relaxed back to its ground state by one of these mechanism, triplet Chl ($_3$Chl*) can be formed from $_1$Chl* through intersystem crossing. The yield of $_3$Chl* formation depends on the average lifetime of $_1$Chl*. In excess light conditions there is an accumulation of excitation energy in the antennae; photochemical reaction are saturated and thermal dissipation processes is not able to deal with all the energy absorbed, thereby increasing the lifetime of $_1$Chl* and the probability to conversion into $_3$Chl*. In contrast to $_1$Chl*, $_3$Chl* is relatively long-lived and can interact with O_2 to produce singlet oxygen.

In the case of PSII reaction center, after primary charge transfer $P680^+$ and $Pheo^-$ species are formed; $Pheo^-$ is reconverted to Pheo after electron transfer to QA, while $P680^+$ is reconverted to P680 through Tyr oxidation. However if QA is already reduced and electron transport is blocked, which is the case of excess light absorption, a charge recombination can occur between $P680^+$ and $Pheo^-$, producing a triplet P680 ($_3$P680*). $_3$P680* can generate $_1O_2$* (Melis, 1999) inducing photo-inhibition, and photo-damage in particular on the D1 subunit of PSII (Aro et al., 1993).

The potential for generation of $_1O_2$ is greater in the PSII-LHCII due to the fact that the average lifetime of $_1$Chl* in PSII-LHCII is several times longer than in the PSI-LHCI. In contrast to $P680^+$ of PSII, $P700^+$ is a very efficient excitation energy quencher from the PSI-LHCI (Dau 1994). Nevertheless, at the acceptor side of PSI, Fd can reduce molecular oxygen to the superoxide anion (O_2-) (Mehler 1951). This short-living specie can be metabolized to hydrogen peroxide (H_2O_2) or hydroxyl radical (OH•), the latter being an

extremely aggressive ROS. Reactive oxygen species produced on the acceptor side of PSI are able to damage key enzymes of photosynthetic carbon metabolism such as phosphoribulokinase and NADP glyceraldehyde-3-phosphate dehydrogenase, as well as subunits of PSI reaction center. There are evidences that also PSII can be photo-inhibited by PSI-produced ROS *in vivo* (Tjus et al., 2001).

3.2 Fates of the excited-state Chl

As mentioned previously, when the electron reaches the excited state tends to return to its ground state (S_0) through a series of de-excitation mechanisms. Which mechanism will be followed depends on the required time to dissipate energy with the fastest mechanism being favored.

Briefly, the energy can be dissipated as heat and excited molecules relax to lower vibrational states in S_1. It occurs with time around 10^{-11}-10^{-14} s, in a mechanism called **internal conversion**. In the case of **fluorescence** excitation energy is emitted from a molecule in the form of light. The energy of the emitted photon corresponds to the energy difference between the energy levels S_1 and S_0. The emitting and final states must have similar electronic spin states and the process occurs in around 10^{-7}-10^{-9} s. Although population of triplet states by direct absorption from the ground state is insignificant, a more efficient process exists for population of triplet states from the lowest excited singlet state in many molecules. This process is referred to as **intersystem crossing**, and is a spin-dependent internal conversion process (timescale 10^{-6}-10^{-11}s). Finally, once arrived in the excited state triplet (T_1) the electron must undergo a new spin inversion in order to return again to the state S_0, and then emit a photon energy corresponding to the difference between the energy levels T_1 and S_0. This emission is called **phosphorescence**.

3.3 State transitions

Balanced excitation of both photosystems is required for maximum electron transport efficiency, so it is critical that one photosystem does not receive preferential photon delivery. In addition, chloroplasts are able to adjust LHCII association with PSII to regulate distribution of quanta between the photosystems. An important short-term photoprotective mechanism, which controls the energy balance, is the "state1-state2 transitions" (Rochaix 2007). This phenomenon consists in the redistribution of excitation

energy between PSI and PSII depending on the association of LHCII with PSII (State I) or PSI (State II). When PSII is preferably excited, LHCII is phosphorylated and moves towards the unstacked region of thylakoids where PSI is located. On the contrary, when PSI is preferentially excited, LHCII is dephosphorylated and migrates back to PSII (Allen 1992). State transitions are principally observed under non saturating light conditions, where the redistribution of the antenna cross-section between the two photosystem can have a significant effect in increasing the overall thylakoid electron transport rate (Jennings and Zucchelli 1986). In higher plants the size of the mobile LHCII has been quantified in about 20-25% of the total LHCII pool. In *A. thaliana*, the STN7 kinase is responsible for the phosphorylation of LHCII (Bellafiore et al. 2005). In State II, the plastoquinone pool becomes more reduced (because of the light-limited turnover of PSI) and the reduced PQ is bound to the Q0 site of the Cyt-b_6f, this leads to a conformational change in this complex that activates STN7 (Zito et al. 1999).

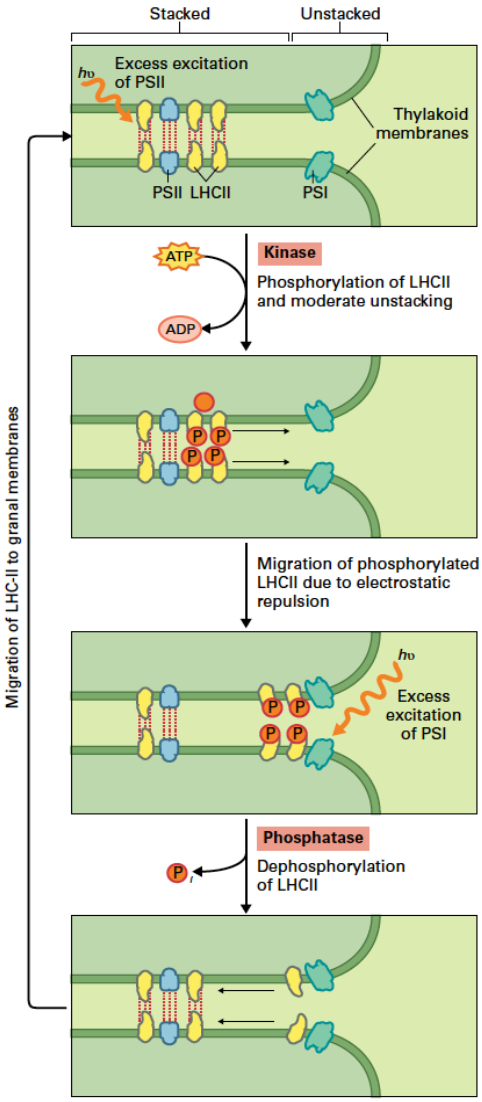

Figure 19. State1-State2 transitions. *Phosphorylation of LHCII controls energy distribution. Excess excitation of PSII relative to PSI increases the level of reduced plastoquinone, which activates a kinase that phosphorylates LHCII. This, results in a partial unstacking of the membranes because of electrostatic repulsion of negatively charged LHCII molecules and a migration of some phosphorylated LHCII from the stacked membrane region to the unstacked membrane region, where it can associate with PSI. This effectively reduces the PSII antenna size and favors absorption of quanta by PSI. Excessive PSI activation results in plastoquinol oxidation and kinase de-activation. A phosphatase is able to hydrolyze the phosphate group of LHCII, allowing it to migrate back to the more hydrophobic environment of the stacked membrane region. This mechanism allows for adjustment of the relative excitation of PSI and PSII.*

It has been suggested that the phosphorylation at the N-terminus of LHCII causes a conformational change that lowers the affinity of LHCII for PSII and at the same time increase the affinity for PSI (Nilsson et al. 1997). In State I instead, a thylakoid peripheral protein (TAP38/PPH1) dephosphorylates LHCII upon which it migrates back to PSII (Shapiguzov et al. 2010). Analyses of different PSI mutants showed that the PSAH subunit is essential for the docking of LHCII, but also other subunits are important (for instance PSAL, PSAO and PSAP) for the formation of the interaction (Lunde et al. 2000).

3.4 Non-Photochemical Quenching (NPQ)

Under the high light intensities found in nature, plants may absorb more light energy than they can use for photosynthesis. This excessive excitation of chlorophylls can increase formation of the triplet state of chlorophyll and the singlet state of oxygen. All oxygenic photoautotrophs regulate light harvesting to protect against photo-inhibition when light is in excess. Higher plants are able to regulate photosynthesis via the non-photochemical quenching (NPQ), a process that acts as a safety valve for photosynthesis and dissipates excess absorbed light energy harmlessly as heat. NPQ results in de-excitation of the singlet state of chlorophyll in the antenna of PSII, and it is routinely measured using chlorophyll fluorescence. In addition to their photoprotective roles in quenching triplet chlorophyll and singlet oxygen, specific carotenoids (e.g., zeaxanthin and lutein) have been implicated in NPQ.

NPQ is a multi-pathway process that consists of several components occur with different induction and relaxation kinetics: **qE** (Energy-dependent quenching) a flexible, rapidly reversible type of NPQ which is induced by the buildup of a high thylakoid ΔpH in the presence of excess light, **qT** which is the phosphorylation-related migration of major LHCII between PSI and PSII known as state transition, and **qI** which is the photo-inhibitory quenching caused by the slow and reversible inactivation of PSII reaction centers.

3.4.1 qE: the fast recovery component

The activation of qE mechanism is dependent of three factors: proton gradient across thylakoid membranes, PSBS protein and it is modulated in amplitude by zeaxanthin (Niyogi 1999). Absorption of sunlight that saturates plant capacity for photochemistry results in the build-up of a proton gradient across thylakoid membranes by photosynthetic electron transport and inhibition of ATPase for lack of Phosphate and ADP. The decrease in pH within the thylakoid lumen is an immediate signal of excess light that triggers NPQ. The control by lumen pH allows induction or reversal of qE within seconds of a change in light intensity, which is fast enough to cope with natural fluctuations in light intensity that are due to, for example, passing clouds on a partly sunny day (Muller et al. 2001). The requirement for low lumen pH is evidenced by the inhibition of qE by uncouplers such as nigericin. This ionophore collapses ΔpH and prevents the activation of NPQ otherwise activated within a few seconds of exposure to high light (Shikanai et al. 1999). Signal transduction of lumen over-acidification involves the PSII subunit PSBS that is essential for qE induction, as demonstrated by the phenotype of the *npq4*, the mutant lacking PSBS, that show no fast component of NPQ (Li et al. 2000).

3.4.2 The PSBS protein

Discovered almost 30 years ago as a 22 kDa protein in isolated PSII preparations (Berthold et al., 1981), PSBS belongs to the LHC protein superfamily but differs from other members for having four transmembrane helices rather than the three generally found in most LHC proteins and for the absence of most conserved Chl-binding residues in its sequence (Dominici et al. 2002). PSBS contains four transmembrane helices (TM1-4), which together form a highly compact structure (Fig. 1a). Two long intertwined helices, namely TM1 and TM3, form a supercoil in the middle and are flanked by two short helices named TM2 and TM4. The four transmembrane helices of PSBS are connected by an elongated stromal loop (partly disordered in the crystal structure due to its high flexibility) and two short luminal loops. Two amphiphilic helices, namely H1 and H2, are located in the luminal loops (Fan et al., 2015). Previous studies showed that PSBS exists as a dimer at neutral pH and may undergo dimer-to-monomer conversion upon pH decrease, which was proposed to relate to the mechanism of activation by low pH of PSBS during qE initiation.

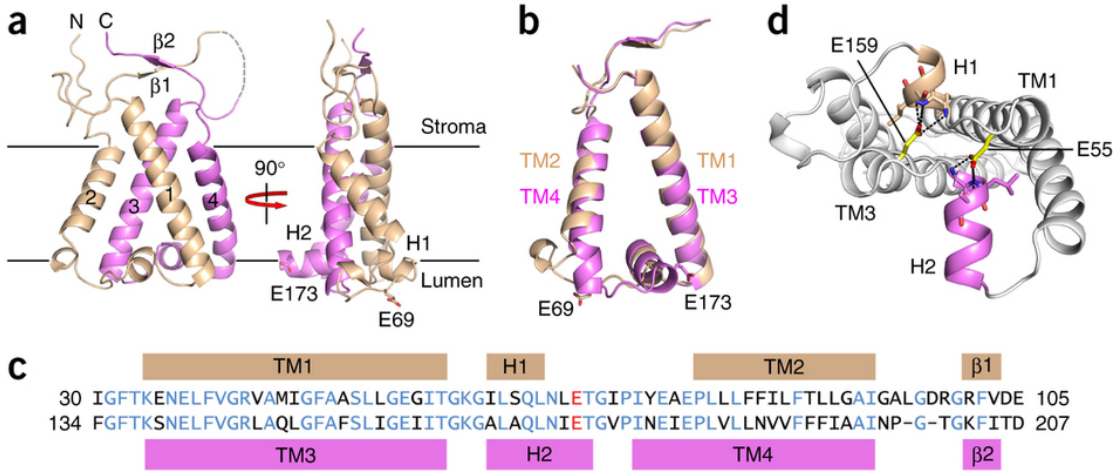

Figure 20. Overall structure of PSBS. *A) Ribbon representation of PSBS viewed from the membrane plane. The elongated stromal loop is partly disordered in the crystal structure, owing to its high flexibility, and is shown as a dashed line. B) Structural superposition of the two halves of PSBS. C) Sequence alignment between the two halves of PSBS with corresponding secondary structures indicated. The two pH-sensing Glu residues are marked with red circle. D) Structural superposition of PSBS and LHCII without bound pigments, viewed from the membrane plane. The first and second half of PSBS are coloured wheat and magenta, respectively. LHCII is coloured white.*

Typical of this protein is the presence of two lumen-exposed glutamate residues, Glu122 and Glu226, that bind DCCD (N, N'-dicyclohexylcarbodiimide), a protein-modifying agent which covalently binds to protonatable residues in hydrophobic environments (Jahns et al. 1988). In *A. thaliana*, mutations of each glutamate to non-protonatable residues, i.e. E122Q and E226Q, decreased by 50% both qE and DCCD binding capacity, whereas the double mutant has a qE-null phenotype like *npq4* (Li et al. 2004). These results suggest that these two glutamate residues are the target of protonation upon thylakoid lumen acidification and mediate the activation of PSBS-dependent qE (Bergantino et al., 2013).

The exact localization of PSBS within PSII complexes is still not defined. Based on previous data, it was initially proposed that it could be localized at the interface between the reaction center and the peripheral light harvesting antenna system.. However, other studies highlight that PSBS cannot be purified with C2S2M2 supercomplexes (Caffarri et al. 2009). As a consequence, PSBS must have a peripheral localization, although this has never been experimentally proven. Immuno-affinity and immune-precipitation experiments showed that PSBS interacts with many different photosynthetic complexes (as CP29, LHCII, PSI, or Cyt-b_6f complexes), leading to the model suggesting that PSBS might be mobile in thylakoid membranes (Teardo et al. 2007). More recent studies have shown the presence of PSBS subunit in PSII monomers isolated from *N. tabacum* plants (Haniewicz et al., 2013) supporting a possible role of PSII monomers in higher plants.

3.4.3 qE and zeaxanthin

The third factor needed for qE activation is zeaxanthin synthesis. The amount of zeaxanthin synthesized via the xanthophyll cycle is highly correlated with the level of qE (Demmig-Adams 1990). The requirement for zeaxanthin in qE has been investigated in vivo by using inhibitors and mutants. Dithiothreitol blocks zeaxanthin synthesis in leaves and results in inhibition of qE (Demmig-Adams et al. 1990). Mutants that are unable to convert violaxanthin to zeaxanthin have been isolated and show a lower level of qE. Although is generally necessary for maximal qE in vivo, zeaxanthin is not sufficient. In mutants that accumulate it constitutively, qE must still be induced by a low pH (Niyogi, 1999). This demonstrates that the low pH has an additional role in qE, besides activation of the xanthophylls cycle. In addition to zeaxanthin another xanthophyll, lutein, has also been implicated in qE. In *A. thaliana*, the mutant *lut2*, which is defective in the lycopene e-cyclase and therefore lacks lutein, has less qE with respect to wild type (Pogson et al. 1998). Double mutants of *A. thaliana* that lack lutein and zeaxanthin are totally devoid of any qE (Niyogi et al. 2001). The detailed molecular mechanisms that give rise to qE are still a matter of intense debate. PSBS is able to sense the transmembrane pH induced by electron transport, through protonation of the two glutamic acids. Thus, protonation of PSBS leads to activation of a lutein and zeaxanthin-dependent quenching. Nevertheless, the mode of interaction is still obscure. Most of the experimental evidences and proposed models suggest that qE occurs at the level of Lhcb proteins. In order for PSBS protonation to yield dissipation of $_1$Chl* and fluorescence quenching, this event must affect a Chl-binding protein. Such a protein should also bind lutein and zeaxanthin as mentioned above or, at least, should interact tightly with a xanthophyll-binding protein, thus providing a quenching effect. Early work proposed that PSBS might bind both chlorophylls and xanthophylls or zeaxanthin alone (Funk et al. 1995, Aspinall-O'Dea et al. 2002), making it a candidate for the role of quencher. Nevertheless, later analysis pointed to the non-conservation of Chl-binding residues in PSBS, while its properties both in vivo and in vitro are not consistent with binding of xanthophylls (Bonente et al. 2007) although coordination to new sites, different from those conserved in LHCs, cannot be excluded in principle. Lhcb proteins appear to be ideal candidates for the role of quenching sites; the *ch1* mutant of *A. thaliana* that lacks Chlb, thus leading to degradation of LHC proteins, exhibits a strongly reduced capacity of NPQ in the presence of both lutein and zeaxanthin, suggesting that LHCs are needed for the quenching events

(Andrews et al. 1995).

The role of individual LHCs has been investigated using reverse genetics. Down-regulation of Lhcb1 showed a decrease in qE while down-regulation Lhcb2 and knockout of Lhcb3 did not significantly decrease NPQ amplitude or slow down its kinetics (Andersson et al. 2003, Damkjaer et al. 2009, Pietrzykowska et al. 2014). CP26 knockout plants retained qE (de Bianchi et al. 2008), whereas the qI component of NPQ was down regulated (Dall'Osto et al. 2005). qE was affected in CP24 and CP29 knockout plants (Andersson et al. 2001, de Bianchi et al. 2008). In summary, depletion of a single monomeric LhcB protein could not completely abolish NPQ, implying redundancy within the subfamily members. The making of a mutant lacking all three monomeric proteins or alternatively LHCII is awaited in order to verify whether NPQ can be sustained in the absence of these gene products.

3.4.4 Possible quenching mechanisms

In LHCII the quenching was proposed as originating also from aggregation (Pascal et al. 2005, Ruban et al. 2007). This suggestion was supported by the evidence that low energy states emitting at ~700 nm can be induced in isolated Lhcb complexes upon induction of aggregation in vitro (Ruban et al. 1994, Muller et al. 2010) and that similar fluorescence changes can be observed also in vivo at low temperature (Ruban et al. 2007).

Aggregation was shown to be instrumental in catalyzing conformational change(s) within the LHCII protein, and the spectral signatures associated to this event were interpreted to indicate the formation of a tight interaction between Lute bound into the site L1 and terminal emitter Chla. In this hypothesis PSBS would promote LHCII aggregation thought membrane reorganization (Miloslavina et al. 2008). Recently a significant Chl fluorescence quenching was observed in vitro when LHCII was reconstituted in proteoliposomes in the presence of PSBS and zeaxanthin, although neither zeaxanthin nor PSBS alone could induce the same quenching (Wilk et al. 2013).

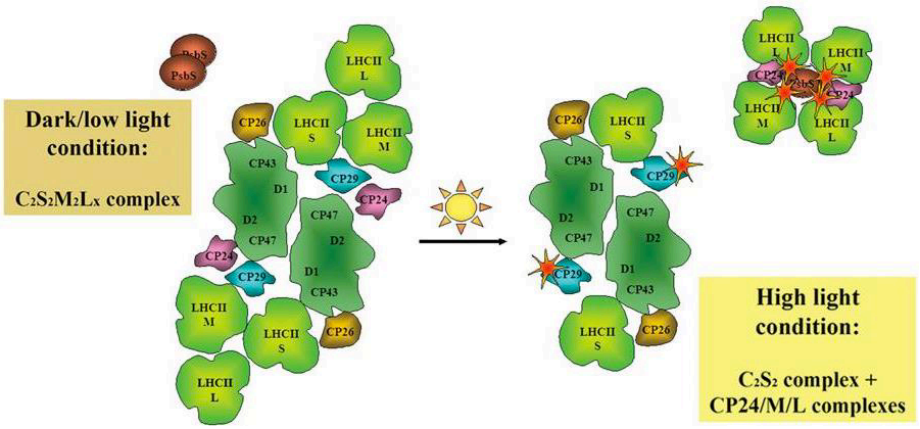

Figure 21. Reorganization of PSII–LHCII supercomplexes. *Upon two triggering events: activated PSBS induces the dissociation of a pentameric complex composed of CP24, CP29 and LHCII trimer M. CP29 remains bound to the PSII core together with CP26 and LHCII trimer S, whereas CP24 and trimers M plus L segregates into different domains with respect to PSII reaction centre-containing complexes towards grana margins. Quenching of PSII supercomplex is provided by CP29 and CP26, whereas quenching of LHCII M+L is provided by CP24 (Betterle et al., 2009). Image from de Bianchi et al., 2010.*

The role of zeaxanthin has been much debated. Zeaxanthin binding to minor Lhcb results in a conformational change (Niyogi et al. 2001) and in a decrease in the fluorescence lifetime (Joliot et al. 1973, Butler and Kitajima 1975). The presence of a zeaxanthin-binding site effective in providing enhancement of NPQ is not a property of a specific LHC protein since enhancement of the quenching amplitude has been observed in plants depleted of different antennae (de Bianchi et al. 2008, de Bianchi et al. 2011). Although it is clear that the concentration of zeaxanthin increases at the expenses of violaxanthin when leaves are illuminated by high light (Demmig-Adams 1990), qE was shown to develop in thylakoid in the absence of the xanthophyll cycle albeit with reduced value and different kinetics of formation and relaxation kinetics (Niyogi et al. 1998). It was therefore proposed that zeaxanthin acts indirectly as an allosteric modulator of qE (Horton 1996, Bassi and Caffarri 2000, Dall'Osto et al. 2005), probably controlling the organization of the antenna complexes and stabilizing a "dissipative" conformational state of the complexes.

Zeaxanthin was also proposed to have a direct role in the quenching of chlorophyll excitation through the formation of a charge-transfer state with Chl a (Holt et al. 2005). In this model, qE activation involves a charge separation between a Chl-Zea heterodimer that produce a transient zeaxanthin radical cation ($Zea^{\cdot+}$) with a short relaxation time (50–200 ps). Interestingly, it was also shown that singlet excited state quenching can occur by the formation of $Chl^{-}/Lute^{+}$ state, although probably occurring at different sites within the LHC complexes (Avenson et al. 2009). Irrespective of the location of the

quenching centers and the exact molecular mechanisms by which excited state quenching occurs all models propose a change in interactions between the bound pigments, being either Chl-Chl or Chl-Car, which would promote the formation of a quenching center. Such modification in the pigment-pigment interactions is thought to be associated with conformation of the protein structure, leading to alteration of either the inter-chromophore distances or mutual orientations.

A third observation about the triggering of qE is that PSBS action is able to affects the rigidity of grana membranes and the readjustment of the antenna organization that might result in the formation of quenching sites. High light induce dissociation of antenna from PSII core and the formation of two different quenching site; the Q1 site reflecting the functional detachment of part of the antenna of the PSII super-complex, and the Q2 quenching site that is located in the antenna that remains attached to the PSII core under HL conditions (Miloslavina et al. 2011). This has been proposed on the basis of the observation that PSBS is needed for light induced dissociation of a pentameric complex, including CP29 and CP24, together with an LHCII. Thus the unquenched conformation of Lhcb proteins is stabilized by their inclusion in this large complex, while its dissociation by PSBS would allow transition to the quenching state, also promoted by Zea binding (Betterle et al. 2009). Indeed, mutations inducing constitutive dissociation of the pentameric complex (designated as 'B4 complex' from its order of migration in sucrose gradients) show formation of two-dimensional arrays of C2S2 particles in the centre of grana discs, whereas LHCII is segregated out towards grana margins (Kovacs et al. 2006, de Bianchi et al. 2008).

Another PSBS-mediated quenching mechanism is proposed on the basis of structural analysis and biochemical data of PSBS (Fan et al., 2015). Under low light conditions, PSBS at neutral pH exists as a relatively loose dimer that has an open conformation at the luminal side. While under excess light conditions, the thylakoid lumen pH decreases and induces protonation of the two glutamate residues of PSBS. This protonation event will activate PSBS by inducing conformational changes of its luminal loops, switching the PSBS dimer from a loose to a compact conformation, which is stabilized by hydrogen bond interactions at the luminal side. Following activation, the compact PSBS dimer may trigger qE by interacting with neighboring LHC proteins to promote their conformational changes and subsequent quenching (Ruban et al., 2007; Ahn et al., 2008; Kiss et al., 2008; Betterle et al., 2009).

However, recent evidence confirming the absolute requirement of PSBS in qE lends support to its direct role in the quenching process (Dall'Osto et al., 2014). Given that PSBS can bind zeaxanthin *in vitro* (Aspinall-O'Dea, M. *et al*., 2002) together with the proposed quenching mechanism involving charge transfer within a chlorophyll-zeaxanthin heterodimer depends on PSBS *in vivo* (Holt, N. E. *et al*. 2005), it is also possible that PSBS functions in qE through such a quenching mechanism. This is supported by a recent report showing that the quenching can be reconstituted using a proteoliposome system containing PSBS, LHCII, and zeaxanthin (Wilk et al., 2013).

3.4.5 Other NPQ components: qI, qT and qZ

Photoinhibitory quenching, or qI, has been associated to a kinetic component whose relaxation is far slower than the decay of trans-thylakoid pH gradient upon light to dark transition and was attributed to processes involving damage of PSII, implying a reduction of the quantum yield of photosynthetic electron transport (Krause, 1988).

The intermediate kinetic component of NPQ, qT, Despite its name, is unlikely to be related to state1-state2 transitions since the *A. thaliana stn7* mutant blocked in state transitions showed an unaltered amplitude of the three kinetic components of NPQ (Bellafiore et al. 2005, Nilkens et al. 2010) and these state transitions occur only under low light only while they are inhibited at the excess light in which NPQ mechanism is active (Rintamaki et al. 1997).

More recently this component has been defined as qZ, for the Chl–/Zea+ depending quenching, since results showed that Zea accumulation and its binding to LHC modulate the amplitude of the intermediate kinetic component of NPQ relaxation (Nilkens et al. 2010). Even if it is true that Zea accumulation and its binding to LHC modulate the amplitude of NPQ and influence qE, it is not easy to associate Zea with the intermediate component of NPQ. This component has half-relaxation time of 10-20 minutes while the Zea decrease in the dark is much more slower with a half-time higher than 1 hour. Thus further studies are needed to fully comprehend this component.

Recently, studies performed in KO line lacking blue light photoreceptors phototropins (*phot2* mutant) in *A. thaliana* antenna show that the intermediate phase of NPQ kinetics strongly depends on the chloroplast avoidance movement (Cazzaniga et al., 2013). In fact, the slow phase of NPQ induction is lacking in *phot2* plants: it suggests that chloroplast photo-relocation, rather than xanthophyll cycle, is the main process

contributing to the quenching component previously described as qZ (Nilkens et al., 2010). Moreover, the avoidance-dependent fluorescence decay component is related neither to the qE activity nor to photoinhibition processes nor to alter state transitions. This new component has been named qM (Cazzaniga et al., 2013).

3.5 Long-term response

Long-term response is activated when photosynthetic organisms are grown in different light intensities for a prolonged period of time. These adaptation mechanisms involve a series of events such as the regulation of the expression of specific proteins, the movement of chloroplasts and modification in plant architecture.

One of the mechanisms involves regulation of the LHC gene expression or LHC protein degradation (Escoubas et al. 1995; Maxwell et al., 1995) having as a result the reduction of light-harvesting antenna size. The number of antenna complexes bound to PSI is not modified during growth of *Arabidopsis thaliana*, in contrast to the antenna complexes of PSII which is largely regulated following environmental conditions: growth in high light causes a reduction in the amount of antenna complexes bound to PSII, instead PSI antennae are more stable upon long-term exposure (Ballottari et al., 2007).

Another long-term mechanism involves the accumulation of anti-oxidant molecules during acclimation to excess light conditions. For example, in over-wintering evergreen plants and in conditions of high light stress, zeaxanthin induces a reversible excess energy quenching (Gilmore and Ball, 2000).

4 The moss *Physcomitrella patens*

4.1 Bryophytes: An introduction

Coming from the Greek words *βρύον* (bryon, meaning tree-moss) and *φυτό* (phyto, meaning plant) the word bryophyte comes as a generic term for plants which are mainly characterized for their altering life cycle, from haploid to diploid generations with a dominant gametophyte haploid (1n). Bryophytes are indeed the only land plants having a dominant branched gametophyte, which exhibits diversity of morphologies unparalleled in tracheophytes (Crim, 2001)**.** Different genres belong in the family of bryophytes, including liverworts (*Marchantiophyta*), mosses (*Bryophyta* in the strict sense) or hornworts (*Anthocerotophyta*). These lineages share several characteristics some of which passed to land plants (i.e. the origins of the naming embryophytes for land plants, coming from 'embryo') and other characteristics that are unique such as an unbranched and parasitic sporophyte with a single spore-producing tissue or sporangium (Vanderpoorten and Goffinet, 2009). During evolution of vascular plants the gametophyte structures became progressively smaller with present dicots being characterized by the dominant sporophytic generation like the case of *Arabidopsis thaliana* (Glime, 2007).

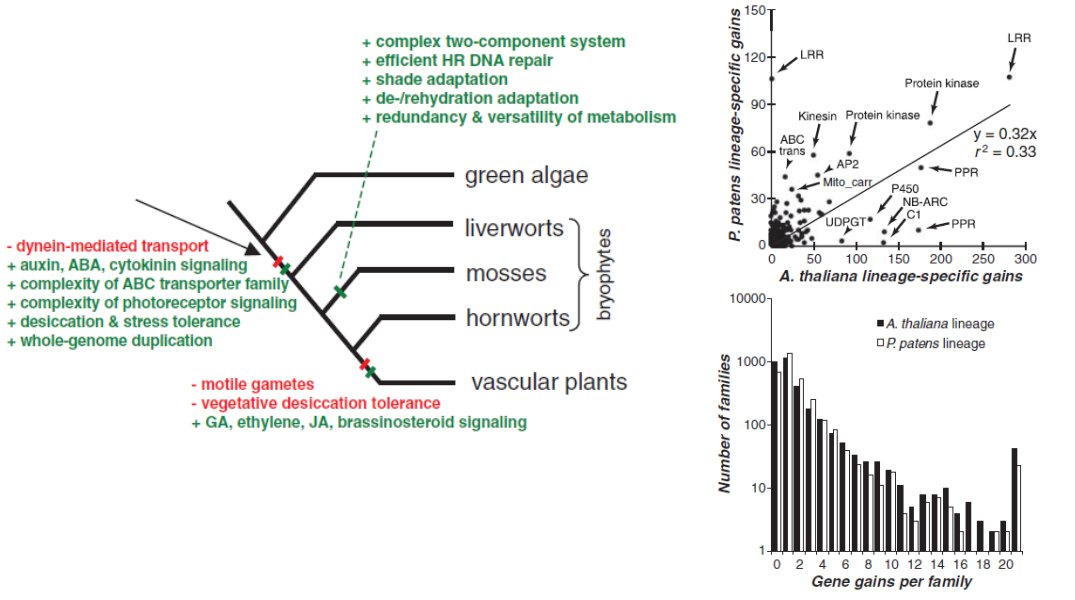

Figure 22. Land plant evolution. *A) Bryophytes comprise three separate lineages, which, together with the vascular plants (including the flowering plants), make up the embryophytes (land plants). (B,C) Domain family expansion patterns in P. patens. B) Gain is defined as the presence of paralogous gene copies uniquely arising in one lineage based on the results of reconciliation between gene family and species trees. Large gene families are labeled on the basis of the predominant Pfam domain names. Some domain names occur more than once since they are the predominant domains in multiple gene families. C) Relations between lineage-specific gains per family and the number of families in the A. thaliana and P. patens lineage.*

Bryophytes are small organisms, with dimensions from a few millimeters to 1 meter size, thus are forced to be simpler compared to vascular plants (in the case of plants different cell types have a specialized function). One major difference between bryophytes and higher plants is that the first lack lignin, having as result a great reduction in size. As a further sequence, bryophytes do not own a vascular system even though many bryophytes have hydroids and leptoids, molecules with similar functions to xylem and phloem. Finally, bryophytes lack 'true' leaves and roots having one-cell thick phyllids and rhizoids instead.

As mentioned above, the three different bryophyte lineages share common characteristic but differ as well from one another in a variety of attributes, mainly in the gametophyte body architecture but also the sporophyte. Approximately 12,000 species of mosses are currently recognized reflecting a broad morphological diversity. Taking into account that weather and ground conditions limit plant growth in different regions of the world, mosses may dominate vegetation. The success of mosses in colonizing almost all available habitats is mainly due to a high turnover of specialist species. This specificity already appears at a high taxonomic level, coming to the conclusion that the descendants of a common ancestor tend to occupy similar ecological niches – a phenomenon known as niche conservatism (Vitt and Wieder, 2009).

4.2 Evolutionary interest in mosses

Mosses are evolutionary intermediates between green algae and higher plants. They were the first colonizer in the conquest of land environment and they faced new challenges because of the different physico-chemical conditions as cycles of flooding/desiccation, extreme temperatures, water availability, exposure to UV radiations, different light intensities and higher oxygen concentration. Adaptation implied changes in morphology and in cellular, physiological and regulatory processes (Waters, 2003; Becker and Marin, 2009; Scott and Glasspool, 2006; Gerotto and Morosinotto, 2013).

In *P. patens*, both organellar genomes, the mitochondrial (Terasawa et al., 2007) and the chloroplast (Sugiura et al., 2003) genomes, are fully sequenced and have already revealed valuable information about plant evolution. In particular, analyses of complete chloroplast DNA have shown that algal chloroplast genomes vary across a broad range, from 89 kbp to over 1500 kbp (Sugiura et al., 2003). In contrast, chloroplast DNAs of

land plant are relatively uniform in size, from 120 to 160 kbp, and their gene content and organization are well conserved. Within the bryophytes, the ~123 kbp chloroplast genome of *P. patens* is situated between the ~121 kbp of the liverwort *Marchantia polymorpha* plastome and the hornwort *Anthoceros formosae* (~160 kbp).

In 2008 the draft genome sequence of the moss *P. patens* was published. It was the first bryophyte genome to be sequenced by Rensing and collaborators (Rensing et al., 2008). This allowed the comparison of genome sequences among green algae, mosses and higher plant and reconstruct the events of genome evolution that occurred in the colonization of land (Rensing et al., 2008).

In particular, compared to algae, the last common ancestor of all land plants lost genes associated with aquatic environment, while gaining key capacities for surviving on land. This leads, as examples, to signaling capacities (auxin, abscissic acid, cytokinin and more complex photoreception), tolerance for abiotic stress such as desiccation and freezing tolerance, heat resistance, synthesis and accumulation of protective "sunscreens" (as the presence of flavonoids), more elaborate transport capabilities, enhanced DNA repair mechanisms, an overall increase in gene family complexity and the development of an embryo within a multicellular reproductive organ (Waters, 2003; Glime, 2007; Rensing et al., 2008).

Genomes comparison also allowed the reconstruction of genomic events that occurred after the separation between vascular plants and mosses ancestors. In fact, they evolved and expanded with different strategies: while bryophytes developed a dominant gametophyte that still combined sexual reproduction with the availability of free water, vascular plants with their dominant sporophyte became more independent. Compared to mosses, vascular plants acquired even more complicated signaling (e.g. gibberellic acid, jasmonic acid, ethylene, brassinosteroids), but lost vegetative dehydration tolerance and mobile gametes (Rensing et al., 2008).

4.3 Life cycle of *Physcomitrella patens*

Physcomitrella patens is a monoecious (i.e. both sex organs are present on the same individual), self-fertile, annual opportunist growing in late summer to autumn in open, unshaded, moist and nutrient-rich habitats often close to the waterline. Like other mosses, it is heavily dependent on water (flooding) for its reproduction but can survive to desiccation (Schaefer and Zrÿd, 2001; Cove, 2005; Lang et al., 2008). In natural

conditions, the heterophasic lifecycle is reported as 'completed' in about four weeks, usually requiring six to eight weeks in the laboratory (Lang et al., 2008).

P. patens, like ferns and seed plants, shows alternation of generations: a haploid phase that produces gametes (the gametophyte generation) and a diploid phase that produces haploid spores by meiosis (the sporophyte generation). Unlike ferns and seed plants, the gametophyte is the dominant phase and this generation comprises most of what is familiar to us as moss plants (Cove, 2005; Bezanilla et al., 2003).

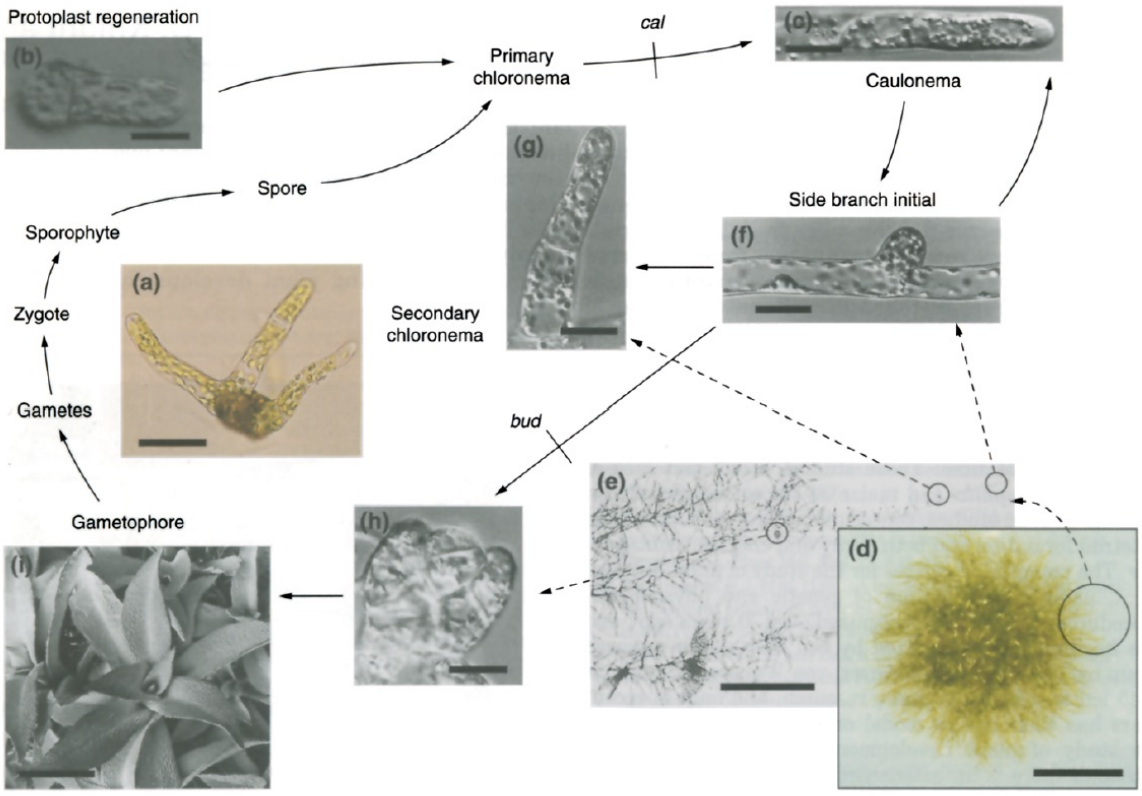

Figure 23. Life cycle of *Physcomitrella patens*. *(a) Sporeling, 3 d after spore germination; the filaments that develop are chloronemal, with apical cells that extend at about 2 ~m h -1 and divide every 24 h (scale bar represents 50 ~m). (b) Regenerating protoplast; development proceeds in a similar way to that following spore germination (scale bar represents 25 ~m). (c) Caulonemal apical cell; such cells extend at about 40 ~m h 1 and divide every 5-6 h (scale bar represents 25 ~m). (d) 28 day-old gametophyte (scale bar represents 10 mm). (e) Detail of peripheral growth of 28 d old gametophyte, showing the caulonemal filament and the various fates of its side branches (scale bar represents 1 mm). (f) Side branch initial on a caulonemal subapical cell (scale bar represents 25 ~m). (g) Secondary chloronemal side branch developing from a caulonemal subapical cell (scale bar represents 25 ~m). (h) Young bud (scale bar represents 25 ~m). (i) Scanning electron micrograph of mature gametophore (scale bar represents 1 mm).*

Life cycle of *P. patens* is characterized by a photoautotrophic haploid gametophytic generation, supporting a relatively simple and mainly heterotrophic diploid sporophyte (Schaefer and Zrÿd, 2001). Briefly, spores germinate to produce the protonemal tissue. It is composed by chloronemal and caulonemal cells which develop by apical growth and

cell division of apical and sub-apical cells. Chloronemal cells are densely packed with large chloroplasts, while caulonemal cells contain fewer, less well-developed chloroplasts. Caulonemal filaments gave rise to bud production, which involves a transition from two dimensional filament growth to three dimensional shoot development: the second gametophyte stage, called gametophore or leafy shoot, in fact, differentiates by caulinary growth from a simple apical meristem (the bud). Analysis of cell division patterns within the gametophore initial has indicated that a single stem cell resides at the apex. This cell divides to produce the cells that go on to form leaflets in a characteristic pattern (Harrison et al., 2009).

At the top of a single gametophore, both male (antheridia) and female (archegonia) sexual organs form. Flagellate sperm, known as spermatozoids, are produced in the antheridia and swim to fertilize the egg cell within an archegonium (Prigge and Bezanilla, 2010). Moist conditions are required to allow spermatozoid motility. The fertilized zygote develops into a diploid generation, the sporophyte, consisting of a short seta bearing a spore capsule, which, when mature, contains about 4000 spores (Cove, 2005; Prigge and Bezanilla, 2010).

4.4 *Physcomitrella patens* as a model organism

The first report of successful isolation of biochemical and developmental mutant in *P. patens* was in 1968 (Engel, 1968). Since then, it has been used as model genetic organism for physiological and developmental studies and, in the last 15 years, its use to explore plant functions has increased enormously. As mentioned, *P. patens* is evolutionary an intermediate between algae and vascular plants. It shares many biological features with them, in terms of gene conservation, physiology and development (Rensing et al., 2008). Some experiments show a similar response to plant growth factors and environmental stimuli as those observed in other land plants (Cove et al., 1997; Schipper et al., 2002). The dominance of the haploid gametophyte in the life cycle of this moss facilitates genetic analysis (Schaefer, 2001). In fact, in haploids recessive loss of function traits can be observed directly without further backcrossing to obtain homozygous diploids. This is directly opposite to the life cycle of higher plants, where the diploid is dominant.

In the 1990s, a principal reason which made *P. patens* a “strategic organism” with respect to other species was its capacity to perform homologous recombination: it is the only land plant known to date with highly efficient homologous recombination in its

nuclear DNA, making it a unique model for plant functional genomics approaches. *P. patens* shows levels of gene targeting comparable to those shown by the yeast *Saccharomyces cerevisiae* (Kammerer and Cove, 1996; Schaefer and Zrÿd, 1997; Hofmann et al., 1999; Schaefer and Zrÿd, 2001; Hohe et al., 2004). Such ability makes *P. patens* a very powerful tool for plant functional and physiological studies since the generation of knock-out (KO) plants depleted in specific proteins, or the gene replacement with a mutated one to study proteins function, are highly facilitated. *P. patens* has been widely used, for example, for metabolism and developmental studies (Cove, 2005; Cove et al., 2006).

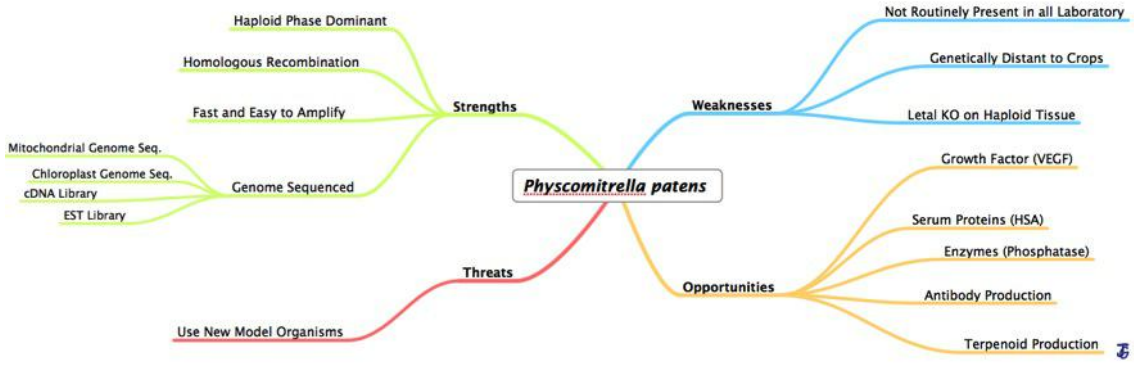

Figure 24. SWOT Analysis of a novel model organism, *Physcomitrella patens*. *Strengths, Weaknesses, Opportunities, and Threats are the four evaluation start from the centre of the graph, that describe the internal (S and W) and external (O and T) factors that are favourable and unfavourable to explain why Pp has been considered as a model organism.*

Due to the very interesting peculiarity of *P. patens* to perform homologous recombination, in the recent years also many molecular genetics and genomics tools were developed for *P. patens* (Cove, 2005). Among them, the transformation methods have been further developed and optimized, allowing, for examples, the generation of multiple targeted gene KO (Hohe et al., 2004) or the use of Cre/Lox system to excide undesired integrated sequences (Schaefer and Zrÿd, 2001). In addition, constitutive and inducible promoters (Schaefer and Zrÿd, 2001; Cove, 2005; Quatrano et al., 2007) are available for this moss, allowing the over-expression of homologous and heterologous proteins (Quatrano et al., 2007). Also RNA interference (RNAi) systems for a knockdown of gene expression (Bezanilla et al., 2003) have been developed. Moreover, many full-length cDNA, EST libraries and BAC-end sequencing are available (Rensing et al., 2002; Quatrano et al., 2007), which led to the completion of the first draft of the complete genome sequence (Rensing et al., 2008) and later of the first physical linkage map of *P. patens* (Kamisugi et al., 2008).

4.5 Photosynthesis and photoprotection in mosses

In general, mosses photosynthetic apparatus is similar to green algae and vascular plants ones, with the presence of Chl *a* and *b*, xanthophylls and carotene as photosynthetic pigments and LHC proteins for light harvesting (Glime, 2007; Alboresi et al., 2008). Mosses often live in shade habitats, and thus they have to efficiently use the light, which filter from the surrounding trees canopy. Consistently mosses are characterized by a "shade-adapted" photosynthetic apparatus, with Chl *a/b* ratio of about 1-2.5 depending on the species. Chl *b* is specifically bound to antenna complexes and these Chl *a/b* value are typically values found in shade-adapted plants (Glime, 2007).

Another main difference with higher plants is the simpler leaf morphology: it is usually one-cell-thick thus mosses are not able to respond to different light conditions by modifying leaf thickness, as seed plants do. In addition, despite the lack of stomata is a disadvantage in term of the inability to control their internal hydric status, this leads to the advantage of direct availability of water and CO_2 from the environment. Consistently, bryophytes, which are C3 plants, are characterized by a higher CO_2 compensation point than tracheophytes, and are thus able to exploit the higher CO_2 concentration near the soil due to decomposition. This capacity allow mosses to take advantages from energy coming from "sun flecks", burst of bright light which filters from the canopy, to perform their photosynthesis (Glime, 2007).

Moreover, also mosses ability of protective energy dissipation has been studied, with particular attention to their response to desiccation. Besides the presence of efficient zeaxanthin-dependent energy dissipation, as in vascular plants, desiccation-tolerant bryophytes possess also specific dissipation mechanisms induced by structural alteration in chlorophyll proteins induced by desiccation or based on stabilization of radicals within the reaction center (these radicals are stable as long as water is absent). These mechanisms allow a rapid recovery of photosynthesis capacity upon rehydration (Heber et al., 2006, 2007) through a drought-induced non-photochemical quenching (designated d-NPQ) which is fully reversed by rehydration (Yamakawa and Itoh, 2013).

4.6 *P. patens:* A tool for studying the evolution of photosynthesis

In silico and biochemical analysis of *P. patens* antenna polypeptides showed many interesting peculiarities of *P. patens* photosynthetic apparatus (Alboresi et al., 2008). In this work they found the presence of a "functional core" of antenna proteins conserved

within the whole green lineage (Lhca1, Lhca2, Lhca3, Lhcb4, Lhcb5). On the contrary, additional antenna subunits such as Lhcb3 and Lhcb6 are only present in land plants suggesting their role in adaptation of terrestrial environment. In addition, one PSI antenna protein, Lhca4, is absent in *P. patens* but present in seed plants. The absence of this protein is confirmed not only by western blot analysis but also by Low Temperature fluorescence measurements: the absence of this protein determines a shift toward blue of PSI-LHCI purified from *P. patens* respect to PSI-LHCI purified from *A. thaliana.* They also identified a new LHC protein specific to *P. patens*, called Lhcb9.

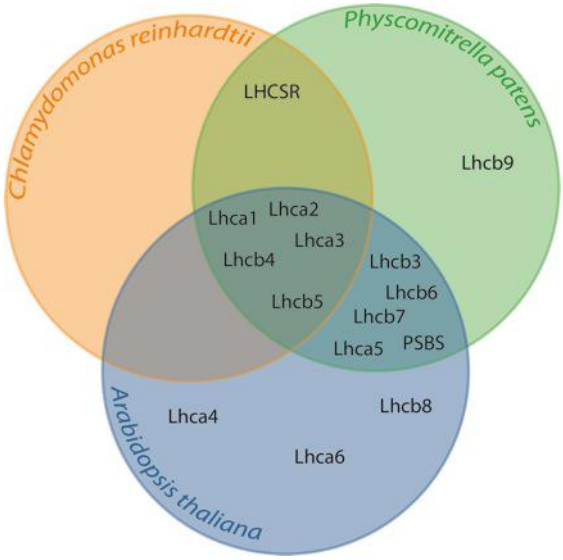

Figure 25. Distribution of Lhc subunits proteins express in different green lineage organisms. *Lhca/b polypeptides were grouped according to the presence of a genuine homologue in the different fully sequenced organisms included in the article of Alboresi et al., 2008. Chlamydomonas reinhardtii for green algae, Physcomitrella patens for mosses and Arabidopsis thaliana for the seed plant. The crossings between rings indicate proteins commonly shared between organisms. Image adapted from (Alboresi et al., 2008).*

Because of its similarity to Lhcb polypeptides, it was tentatively attributed to the PSII antenna system. This is the first report of red-shifted spectral forms in a PSII antenna system, suggesting that this biophysical feature might have a special role either in optimization of light use efficiency or in photoprotection in the specific environmental conditions (Alboresi et al., 2008, 2011b). There is still little information concerning supramolecular organization of photosystems in *P. patens*. A recent work (Busch et al., 2013) showed two projection maps of *P. patens* PSI-LHCI isolated in state 1; thus, PSI-LHCI is present in two forms differing in size, with larger complex as the dominant form with a ratio of ~3:1. They analyzed PSI–LHCI particles isolated from state 2 plants and showed that an additional density in the PSI–LHCI complex became evident: this

projection looks somewhat similar to PSI–LHCI–LHCII complexes isolated from higher plants under state 2 even though further investigations should be done in order to confirm that they have been dealing with the same kind of complex (Kouril et al., 2005; Wientjes et al., 2009). Together with this microscopy analysis, a study of *P. patens* state transition capacities was carried on. *P. patens* performs state transition; however, it has a slightly smaller capability to do so than *A. thaliana*. In agreement with that, *P. patens* shows a lower degree of LHCII phosphorylation compared with *A. thaliana* (Busch et al., 2013). In state 1 conditions, the larger particles projected (Figure 32A), represent a PSI with four LHCA proteins at the PsaF/PsaJ side of the PSI core, as seen in higher plants (Boekema et al., 2001; Ben-Shem et al., 2003). As mentioned *P. patens* does not encode an LHCA4-like subunit (Alboresi et al., 2008) and this raises the question of which LHCA protein is replacing LHCa4 in the complex (Busch et al., 2013).

P. patens contains a large number of isoforms for the different PSI subunits. In particular, for the chloroplast-encoded subunits PsaA, -B, -C, -I, and –J, only one copy was found in the chloroplast genome; however, the nuclear-encoded subunits showed a large number of isoforms ranging from two copies of PsaG, -H, and -O up to four different gene entries for PsaD and PsaF. *P. patens* underwent whole-genome duplication approximately 45 million years ago, leading to a wealth of multiple genes (Rensing et al., 2007). One effect of gene duplication is that it alleviates the pressure to maintain a single important gene, introducing the potential for development of new genes. Moreover the chloroplast genome of *P. patens* also encoded the cyanobacterial PsaM subunit, which is not present in vascular plants. In contrast, no PsaN homologue could be identified in the *P. patens* genome (Busch et al., 2013). The different isoforms are also identified at the protein level; in fact using mass spectrometry some PSI core subunits were identified: PsaA, -B, -C, -D, -E, -F, -G, -H, -K, -L, and –O (Busch et al., 2013). Regarding the members of the light-harvesting complex of PSI, LHCA1, -2, -3, and -5 and most of their different isoforms were identified. For LHCA1 (three isoforms) and LHCA2 (four isoforms), all isoforms except LHCA2.1 were detected by unique peptides upon proteomic analysis. For LHCA3, two out of four isoforms were detected, and for LHCA5 was found only in one isoform (Busch et al., 2013).

4.7 Photoprotection and NPQ triggering system in *P. patens*

Sequence analysis highlighted the presence of both *PSBS* and *LHCSR* genes in *P.*

patens genome (Alboresi et al., 2008). NPQ is present in both plants and green algae and its activation relies on PSBS protein in plants and LHCSR in the green alga *C. reinhardtii* (Li et al., 2000; Peers et al., 2009). *P. patens* is the first organism in which both proteins have been shown to be present and active in triggering NPQ. Two LHCSR isoforms exist in *P. patens*, called LHCSR1 and LHCSR2, they share 91% sequence identity. LHCSR1 encodes for the largest fraction of LHCSR pool and its deletion causes the strongest effect on NPQ amplitude, whereas *lhcsr2* KO has an NPQ phenotype closer to that of WT (Alboresi et al., 2010).

Since the great advantage in using *P. patens* relies in its capacity to make homologous recombination at high efficiency, a range of *P. patens* genotypes such as *psbs* KO, *lhcsr* KO, *psbs lhcsr* KO and genotypes differing in PSBS and LHCSR content (OE) (Alboresi et al., 2010; Gerotto et al., 2012). That makes this organism particularly interesting to study NPQ activation and the evolution of photoprotection from algae to land colonization.

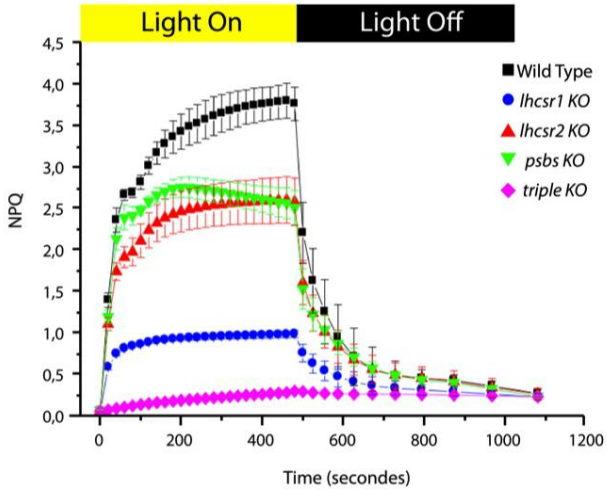

Figure 26. Non-photochemical quenching (NPQ) kinetics in high light acclimated *P. Patens* plants *(Alboresi et al., 2010).*

Analysis of various KO and OE lines clearly demonstrates that PSBS and both LHCSR isoforms are fully able to induce NPQ in *P. patens*, independently of the presence of each other, supporting the idea that they rely on different activation mechanisms (Alboresi et al., 2010; Gerotto et al., 2012). In plants, PSBS triggers quenching by inducing reorganization of protein domains within the thylakoid membrane, triggering the formation of quenching sites located in the antenna complexes (Betterle et al., 2009; Johnson et al., 2011). In the case of algae, instead, LHCSR itself is a pigment-binding protein with an intrinsic capacity for heat dissipation, which is conserved in the isolated complex (Bonente et al., 2011). Also in the case of *P. patens*, LHCSR by itself acts as a

light harvesting and/or heat dissipation complex without the need to induce any reorganization of other antenna complexes (Gerotto et al., 2012).

Moreover a positive correlation exists between the accumulation of PSBS and/or LHCSR proteins and NPQ amplitude. In this way, mosses can directly modulate their ability to dissipate energy simply by altering the accumulation level of one or both of these proteins (Gerotto et al., 2012). NPQ is also an important mechanism involved in long-term acclimation either in low light or high light conditions. High light acclimated plants show an increase of NPQ which is positively correlated to overexpression of both LHCSR1 and PSBS proteins. *P. patens* acclimated to low temperature has an increase of NPQ due to the increase of PSBS and LHCSR2 levels. These data suggest that the two functional *lhcsr* genes are differentially regulated by environmental factors (Gerotto et al., 2012).

Briefly, depending on the organism, different components for NPQ machinery are known: Lhcb monomeric antenna proteins, zeaxanthin and lutein, PSBS and LHCSR proteins. The membrane dynamic is the triggering process, which summarize the function of these three components (Betterle et al., 2009; Johnson et al., 2011). Through the evolution the involvement of these different components changed.

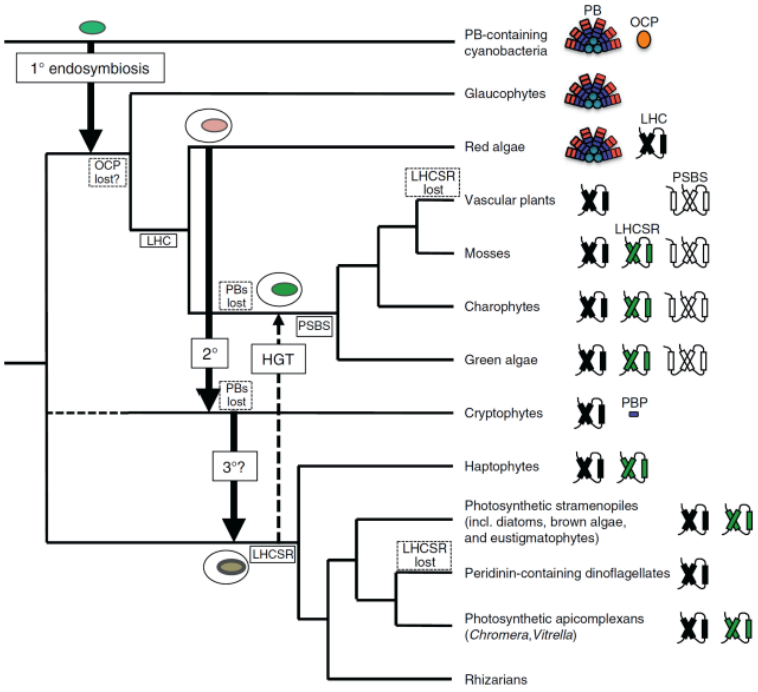

Figure 27. Non-photochemical quenching (NPQ) components through green lineage evolution. *Schematic depiction of the relationships between major groups of oxygenic photosynthetic organisms and the possible evolutionary steps relevant to flexible NPQ. Branch lengths are drawn for convenience and are not meant to imply specific lengths of time. Hypothetical endosymbioses, horizontal gene transfer (HGT) events, and acquisition events are shown in solid boxes; loss events are shown in dashed boxes. Not shown are algae derived from secondary endosymbiosis of green algae; one of these groups (Chlorarachniophytes) is part of the Rhizarian taxon. Cryptophytes have an unusual phycobiliprotein (PBP) antenna that is not part of a phycobilisome (PB) complex.*

4.8 The LHCSR protein: An effective pH sensor and energy quencher

As discussed in the previous paragraphs, many data support the importance of PSBS for NPQ activation in *A. thaliana* and evidences for its role are also found for several other vascular plants (Hieber et al., 2004; Bajkán et al., 2010). However, the presence of PSBS protein is not ubiquitous in *Viridiplantae*. Among algae, in *C. reinhardtii* (Peers et al., 2009), conserved PSBS genes are present in all sequenced green algae so far, and PSBS mRNA expression in *C. reinhardtii* is induced by light stress (Niyogi and Truong, 2013) and nutrient stress (Miller et al., 2010). However, there is presently no evidence that these genes function in flexible NPQ in *C. reinhardtii*, and the PSBS protein was not found in unicellular green algae (Bonente et al., 2008b). Although it cannot be fully excluded that PSBS gene product has not been tested under the right conditions or in the right species, the deep analysis performed suggests that PSBS in green algae might have other function than in plants consistent with the finding of the overexpressed gene products in compartments other than thylakoids (Bonente et al., 2008b).

A different LHC protein, called LHCSR (previously known as Li818), was recently found to be necessary for qE in *C. reinhardtii* (Peers et al., 2009). In fact, *C. reinhardtii* mutants depleted in LHCSR (*npq4* mutants) show a qE-deficient phenotype, as *A. thaliana* plants depleted in PSBS (Peers et al., 2009). These results demonstrated the key role of LHCSR in NPQ induction, which was further confirmed by the analysis of *C. reinhardtii* lines over-expressing LHCSR, which showed enhanced qE capacity (Peers et al., 2009). *C. reinhardtii npq4* mutants also showed reduced fitness in variable light conditions, demonstrating that LHCSR is required for survival in a dynamic light environment (Peers et al., 2009).

LHCSR, as PSBS, is a member of the LHC superfamily. Orthologues of LHCSR are found in many photosynthetic taxa and in particular in many different algal groups. Remarkably, however, it is missing in vascular plants genomes (Richard et al., 2000; Koziol et al., 2007; Alboresi et al., 2008; Peers et al., 2009; Engelken et al., 2010). Consistent with a role in photoprotection, LHCSR transcripts accumulate in conditions which are known to induce photo-oxidative stress and it was originally identified as a light-induced transcript (Richard et al., 2000) and thus it exhibits an expression regulation pattern different from the other LHCs involved in light harvesting (Richard et al., 2000; Peers et al., 2009).

More recent data also suggest that LHCSR-dependent NPQ mechanism is likely widespread among algae, as it has been recently demonstrated to be involved in NPQ also in some diatoms (Zhu and Green, 2010; Bailleul et al., 2010). Differently from C. reinhardtii, these organisms also completely lack the psbs gene in their genomes (Koziol et al., 2007; Engelken et al., 2010).

Biochemical characterization of *C. reinhardtii* LHCSR showed some similarities but also some interesting differences with respect to PSBS (Bonente et al., 2011). Alike PSBS, LHCSR binds DCCD suggesting the presence of protonable residues and thus the ability of sensing the acidification of thylakoid lumen. LHCSR does binds Chl *a*, Chl *b* and xanthophylls similar to LHC antenna complexes, unlike PSBS, which cannot form pigment proteins in *vitro* or in *vivo* (Bonente et al., 2008a; Dominici et al., 2002).

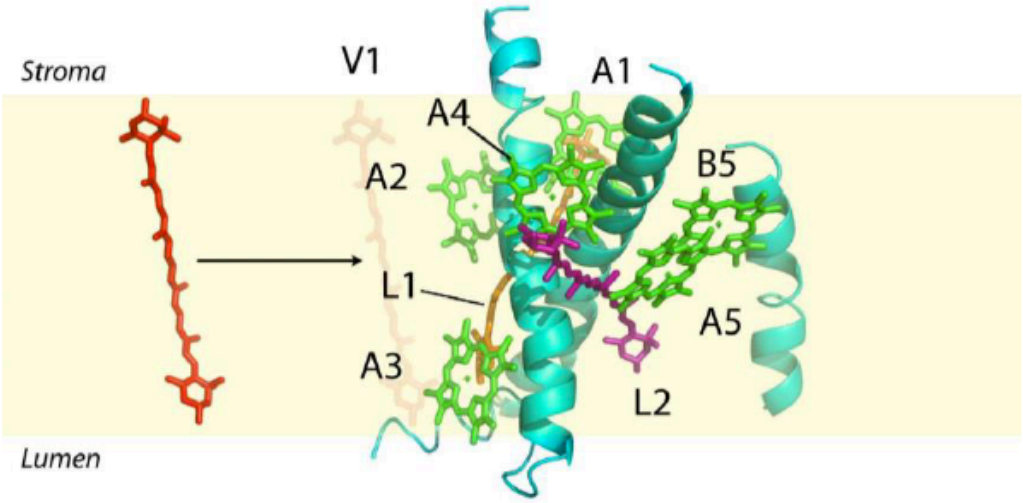

Figure 28. Model showing chlorophyll and xanthophyll chromophores bound to different sites in LHCSR3. *Model was built by homology based on crystal structure of LHCII by (Liu et al., 2004). Image from (Bonente et al., 2011).*

In vitro refolding experiments show that LHCSR is characterized by a high *Chl a*/*b* ratio, contains six/seven Chls per polypeptide, two binding sites with strong affinity for Lut and Viola, probably sites L1 and L2; the absence of Neo in the refolded complex indicates that site N1 is absent. A third Car binding site is of V1 type (Figure 28). LHCSR can also bind Zea likely in site L2 or V1. In addition spectroscopic analyses showed that LHCSR in detergent solution has very short fluorescence lifetimes (<100 ps) compared to other members of LHC family. This implies that an energy dissipation channel is constitutively active in recombinant LHCSR. Quenching activity is further enhanced upon acidification (Bonente et al., 2011).

An hypothesis proposes that LHCSR regulates energy dissipation by establishing reversible interactions with other Lhcb antenna proteins, in particular Lhcbm1 (Elrad et

al., 2002; Tokutsu and Minagawa, 2013) (Tokutsu and Minagawa, 2013) and that these interactions are induced by low lumenal pH through protonatable DCCD-binding sites present in both Lhcb proteins and LHCSR (Bonente et al., 2011). Thus, LHCSR has the properties of both an energy quencher, a function catalyzed by Lhcb proteins in vascular plants (Ahn et al., 2008; Avenson et al., 2008; Ruban et al., 2007), and a sensor for lumenal pH, which is a function covered by PSBS in plants (Li et al., 2004; Betterle et al., 2009; Bonente et al., 2008a).

A recent study (Tokutsu and Minagawa, 2013) proposes the following molecular steps for the induction of qE in *C. reinhardtii*:

- LHCSR3 is accumulated during excess light; in fact, LHCSR3 was found in the PSII supercomplex from the high light grown WT, but not in the supercomplex from the low light grown WT or *npq4* mutant.
- LHCSR3 is bound to the PSII-LHCII supercomplex to form a PSII-LHCII-LHCSR3 supercomplex in the membranes.
- LHCSR3 could bind the periphery of the supercomplex: examination of the photosynthetic supercomplexes in the high light grown *npq4* mutant revealed stable formation of the PSII-LHCII supercomplex in the absence of LHCSR3;
- Protonation of LHCSR3, which occurs upon lumenal acidification by excess light, directly modifies the antenna conformation within the supercomplex to form a quenching center (Tokutsu and Minagawa, 2013).

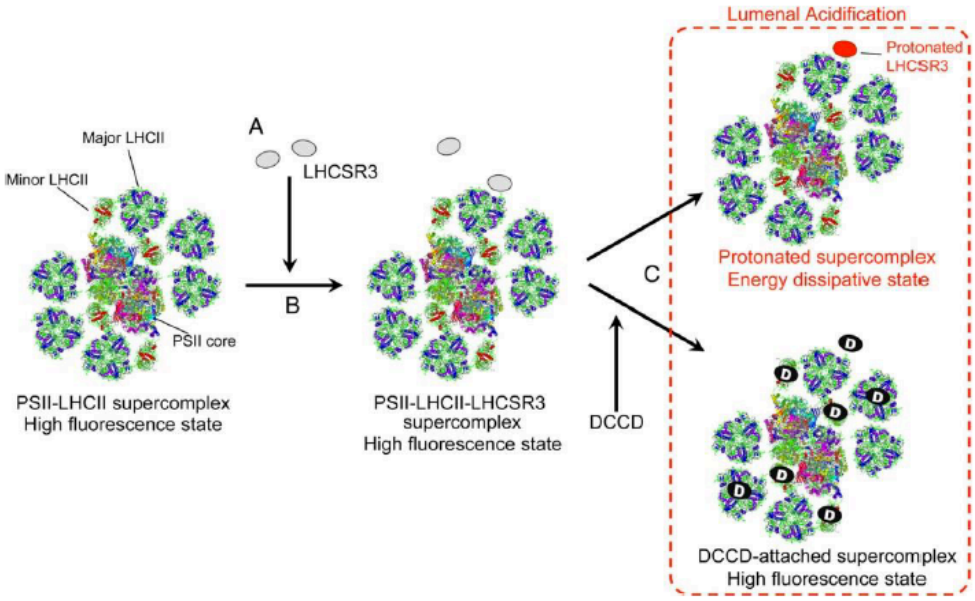

Figure 29. A model for the induction of qE in C. reinhardtii. *A) LHCSR3 expression under high light conditions. B) Binding of LHCSR3 to the PSII-LHCII supercomplex (Tokutsu et al., 2012). C) Acidification of the thylakoid lumen; energy dissipation inhibited by DCCD-binding to the PSII-LHCII-LHCSR3 supercomplex (Tokutsu and Minagawa, 2013).*

In fact, the purified PSII supercomplex containing LHCSR3 exhibited a long fluorescence lifetime at a neutral pH (7.5) by single-photon counting analysis, but a significantly shorter lifetime at pH 5.5, which mimics the acidified lumen of the thylakoid membranes in high light exposed chloroplasts. Moreover, the switch from light-harvesting mode to energy-dissipating mode observed in the LHCSR3-containing PSII supercomplex was sensitive to DCCD. It indicates that protonation of the PSII-LHCII-LHCSR3 supercomplex is necessary for qE activation (Tokutsu and Minagawa, 2013).

Bibliography

Abrahams, J.P., Leslie, A.G., Lutter, R., and Walker, J.E. (1994). Structure at 2.8 A resolution of F1-ATPase from bovine heart mitochondria. Nature 370: 621–8.

Adams, W.W., Demmig-Adams, B., Rosenstiel, T.N., and Ebbert, V. (2001). Dependence of photosynthesis and energy dissipation activity upon growth form and light environment during the winter. Photosynthesis research 67: 51–62.

Ahn, T.K., Avenson, T.J., Ballottari, M., Cheng, Y.-C., Niyogi, K.K., Bassi, R., and Fleming, G.R. (2008). Architecture of a charge-transfer state regulating light harvesting in a plant antenna protein. Science (New York, N.Y.) 320: 794–7.

Alboresi, A., Caffarri, S., Nogue, F., Bassi, R., and Morosinotto, T. (2008). In silico and biochemical analysis of Physcomitrella patens photosynthetic antenna: identification of subunits which evolved upon land adaptation. PloS one 3: e2033.

Alboresi, A., Dall'Osto, L., Aprile, A., Carillo, P., Roncaglia, E., Cattivelli, L., and Bassi, R. (2011a). Reactive oxygen species and transcript analysis upon excess light treatment in wild-type Arabidopsis thaliana vs a photosensitive mutant lacking zeaxanthin and lutein. BMC plant biology 11: 62.

Alboresi, A., Gerotto, C., Cazzaniga, S., Bassi, R., and Morosinotto, T. (2011b). A red-shifted antenna protein associated with photosystem II in Physcomitrella patens. The Journal of biological chemistry 286: 28978–87.

Alboresi, A., Gerotto, C., Giacometti, G.M., Bassi, R., and Morosinotto, T. (2010). Physcomitrella patens mutants affected on heat dissipation clarify the evolution of photoprotection mechanisms upon land colonization. Proceedings of the National Academy of Sciences of the United States of America 107: 11128–33.

Allen, J.F. (1992). Protein phosphorylation in regulation of photosynthesis. Biochimica et biophysica acta 1098: 275–335.

Allen, J.F. and Forsberg, J. (2001). Molecular recognition in thylakoid structure and function. Trends in plant science 6: 317–26.

Amunts, A., Drory, O., and Nelson, N. (2007). The structure of a plant photosystem I supercomplex at 3.4 A resolution. Nature 447: 58–63.

Amunts, A. and Nelson, N. (2008). Functional organization of a plant Photosystem I: evolution of a highly efficient photochemical machine. Plant physiology and biochemistry : PPB / Société française de physiologie végétale 46: 228–37.

Amunts, A. and Nelson, N. (2009). Plant photosystem I design in the light of evolution. Structure (London, England : 1993) 17: 637–50.

Andersson, B. and Anderson, J.M. (1980). Lateral heterogeneity in the distribution of chlorophyll-protein complexes of the thylakoid membranes of spinach chloroplasts. Biochimica et biophysica acta 593: 427–40.

Andersson, P.O., Gillbro, T., Ferguson, L., and Cogdell, R.J. (1991). Absorption Spectral Shifts of Carotenoids Related to Medium Polarizability. Photochem. Photobiol: 353–360.

Arnoux, P., Morosinotto, T., Saga, G., Bassi, R., and Pignol, D. (2009). A structural basis for the pH-dependent xanthophyll cycle in Arabidopsis thaliana. The Plant cell 21: 2036–44.

Aro, E.M., Virgin, I., and Andersson, B. (1993). Photoinhibition of Photosystem II. Inactivation, protein damage and turnover. Biochimica et biophysica acta 1143: 113–34.

Asada, K. (1999). THE WATER-WATER CYCLE IN CHLOROPLASTS: Scavenging of Active Oxygens and Dissipation of Excess Photons. Annual review of plant physiology and plant molecular biology 50: 601–639.

Aspinall-O'Dea, M., Wentworth, M., Pascal, A., Robert, B., Ruban, A., and Horton, P. (2002). In vitro reconstitution of the activated zeaxanthin state associated with energy dissipation in plants. Proceedings of the National Academy of Sciences of the United States of America 99: 16331–5.

Avenson, T.J., Ahn, T.K., Zigmantas, D., Niyogi, K.K., Li, Z., Ballottari, M., Bassi, R., and Fleming, G.R. (2008). Zeaxanthin radical cation formation in minor light-harvesting complexes of higher plant antenna. The Journal of biological chemistry 283: 3550–8.

Bailleul, B., Rogato, A., de Martino, A., Coesel, S., Cardol, P., Bowler, C., Falciatore, A., and Finazzi, G. (2010). An atypical member of the light-harvesting complex stress-related protein family modulates diatom responses to light. Proceedings of the National Academy of Sciences of the United States of America 107: 18214–9.

Bajkán, S., Váradi, G., Balogh, M., Domonkos, A., Kiss, G.B., Kovács, L., and Lehoczki, E. (2010). Conserved structure of the chloroplast-DNA encoded D1 protein is essential for effective photoprotection via non-photochemical thermal dissipation in higher plants. Molecular genetics and genomics : MGG 284: 55–63.

Ballottari, M., Dall'Osto, L., Morosinotto, T., and Bassi, R. (2007). Contrasting behavior of higher plant photosystem I and II antenna systems during acclimation. The Journal of biological chemistry 282: 8947–58.

Ballottari, M., Girardon, J., Dall'Osto, L., and Bassi, R. (2012). Evolution and functional properties of photosystem II light harvesting complexes in eukaryotes. Biochimica et biophysica acta 1817: 143–57.

Barber, J. (1980). Membrane surface charges and potentials in relation to photosynthesis. Biochimica et biophysica acta 594: 253–308.

Baroli, I., Do, A.D., Yamane, T., and Niyogi, K.K. (2003). Zeaxanthin accumulation in the absence of a functional xanthophyll cycle protects Chlamydomonas reinhardtii from photooxidative stress. The Plant cell 15: 992–1008.

Bassi, R., Giuffra, E., Croce, R., Dainese, P., and Bergantino, E. (1996). Biochemistry

and molecular biology of pigment binding proteins and C. . Jennings, R. C., Zucchelli, G., Ghetti, F., ed (New York, Plenum Press. Life Science.).

Bassi, R., Høyer-Hansen, G., Barbato, R., Giacometti, G.M., and Simpson, D.J. (1987). Chlorophyll-proteins of the photosystem II antenna system. The Journal of biological chemistry 262: 13333–41.

Bassi, R., Pineau, B., Dainese, P., and Marquardt, J. (1993). Carotenoid-binding proteins of photosystem II. European journal of biochemistry / FEBS 212: 297–303.

Bateman, R.M., Crane, P.R., DiMichele, W.A., Kenrick, P.R., Rowe, N.P., Speck, T., and Stein, W.E. (1998). EARLY EVOLUTION OF LAND PLANTS: Phylogeny, Physiology, and Ecology of the Primary Terrestrial Radiation. Annual Review of Ecology and Systematics 29: 263–292.

Becker, B. and Marin, B. (2009). Streptophyte algae and the origin of embryophytes. Annals of botany 103: 999–1004.

Bellafiore, S., Barneche, F., Peltier, G., and Rochaix, J.-D.(2005). State transitions and light adaptation require chloroplast thylakoid protein kinase STN7. Nature 433: 892–5.
Ben-Shem, A., Frolow, F., and Nelson, N. (2003). Crystal structure of plant photosystem I. Nature 426: 630–5.

Ben-Shem, A., Frolow, F., and Nelson, N. (2004). Light-harvesting features revealed by the structure of plant photosystem I. Photosynthesis research 81: 239–50.

Benson, A.A. and Calvin, M. (1950). Carbon Dioxide Fixation by Green Plants. Annual Review of Plant Physiology and Plant Molecular Biology: 25–42.

Bergantino, E., Dainese, P., Cerovic, Z., Sechi, S., and Bassi, R. (1995). A post-translational modification of the photosystem II subunit CP29 protects maize from cold stress. The Journal of biological chemistry 270: 8474–81.

Bergantino, E., Segalla, A., Brunetta, A., Teardo, E., Rigoni, F., Giacometti, G.M.,and Szabò, I. (2003). Light- and pH-dependent structural changes in the PsbS subunit of photosystem II. Proceedings of the National Academy of Sciences of the United States of America 100: 15265–70.

Berner, R.A. (1999). Atmospheric oxygen over Phanerozoic time. Proceedings of the National Academy of Sciences of the United States of America 96: 10955–7.

Berthold, D., Babcock, G., and Yocum, C (1981). A highly resolved, oxygen-evolving photosystem II preparation from spinach thylakoid membranes. FEBS Letters 134: 231–234.

Betterle, N., Ballottari, M., Zorzan, S., de Bianchi, S., Cazzaniga, S, Dall'osto, L., Morosinotto, T., and Bassi R. (2009). Light-induced dissociation of an antenna hetero-oligomer is needed for non-photochemical quenching induction. The Journal of biological chemistry 284: 15255–66.

Bezanilla, M., Pan, A., and Quatrano, R.S. (2003). RNA interference in the moss Physcomitrella patens. Plant physiology 133: 470–4.

Boekema, E., Dekker, J., van Heel, M., Rögner, M., Saenger, W., Witt, I., and Witt, H. (1987). Evidence for a trimeric organization of photosystem I complexes from the thermophilic cyanobacterium Synechococcus sp. FEBS Lett: 283–286.

Boekema, E.J., Jensen, P.E., Schlodder, E., van Breemen, J.F., van Roon, H., Scheller, H.V., and Dekker, J.P. (2001). Green plant photosystem I binds light-harvesting complex I on one side of the complex. Biochemistry 40: 1029–36.

Boekema, E.J., Van Roon, H., Van Breemen, J.F., and Dekker, J.P. (1999a). Supramolecular organization of photosystem II and its light-harvesting antenna in partially solubilized photosystem II membranes. European journal of biochemistry / FEBS 266: 444–52.

Boekema, E.J., van Roon, H., Calkoen, F., Bassi, R., and Dekker, J.P. (1999b). Multiple types of association of photosystem II and its light-harvesting antenna in partially solubilized photosystem II membranes. Biochemistry 38: 2233–9.

Bonardi, V., Pesaresi, P., Becker, T., Schleiff, E., Wagner, R., Pfannschmidt, T., Jahns, P., and Leister, D. (2005). Photosystem II core phosphorylation and photosynthetic acclimation require two different protein kinases. Nature 437: 1179–82.

Bonaventura, C. and Myers, J. (1969). Fluorescence and oxygen evolution from Chlorella pyrenoidosa. Biochimica et biophysica acta 189: 366–83.

Bonente, G., Ballottari, M., Truong, T.B., Morosinotto, T., Ahn, T.K., Fleming, G.R., Niyogi, K.K., and Bassi, R. (2011). Analysis of LhcSR3, a protein essential for feedback de-excitation in the green alga Chlamydomonas reinhardtii. PLoS biology 9: e1000577.

Bonente, G., Howes, B.D., Caffarri, S., Smulevich, G., and Bassi, R. (2008a). Interactions between the photosystem II subunit PsbS and xanthophylls studied in vivo and in vitro. The Journal of biological chemistry 283: 8434–45.

Bonente, G., Passarini, F., Cazzaniga, S., Mancone, C., Buia, M.C., Tripodi, M., Bassi, R., and Caffarri, S. (2008b). The occurrence of the psbS gene product in Chlamydomonas reinhardtii and in other photosynthetic organisms and its correlation with energy quenching. Photochemistry and photobiology 84: 1359–70.

Bowman, J.L., Floyd, S.K., and Sakakibara, K. (2007). Green genes-comparative genomics of the green branch of life. Cell 129: 229–34.

Buchanan, B.B. (1991). Regulation of CO2 assimilation in oxygenic photosynthesis: the ferredoxin/thioredoxin system. Perspective on its discovery, present status, and future development. Archives of biochemistry and biophysics 288: 1–9.

Bugos, R.C., Hieber, A.D., and Yamamoto, H.Y. (1998). Xanthophyll cycle enzymes are members of the lipocalin family, the first identified from plants. The Journal of biological chemistry 273: 15321–4.

Busch, A., Petersen, J., Webber-Birungi, M.T., Powikrowska, M., Lassen, L.M.M., Naumann-Busch, B., Nielsen, A.Z., Ye, J., Boekema, E.J., Jensen, O.N., Lunde, C., and Jensen, P.E. (2013). Composition and structure of photosystem I in the moss Physcomitrella patens. Journal of experimental botany 64: 2689–99.

Caffarri, S., Croce, R., Breton, J., and Bassi, R. (2001). The major antenna complex of photosystem II has a xanthophyll binding site not involved in light harvesting. The Journal of biological chemistry 276: 35924–33.

Caffarri, S., Croce, R., Cattivelli, L., and Bassi, R. (2004). A look within LHCII: differential analysis of the Lhcb1-3 complexes building the major trimeric antenna complex of higher-plant photosynthesis. Biochemistry 43: 9467–76.

Caffarri, S., Kouril, R., Kereïche, S., Boekema, E.J., and Croce, R. (2009). Functional architecture of higher plant photosystem II supercomplexes. The EMBO journal 28: 3052–63.

Caffarri, S., Passarini, F., Bassi, R., and Croce, R. (2007). A specific binding site for neoxanthin in the monomeric antenna proteins CP26 and CP29 of Photosystem II. FEBS letters 581: 4704–10.

Camm, E.L. and Green, B.R. (2004). How the Chlorophyll-Proteins got their Names. Photosynthesis research 80: 189–96.

Castelletti, S., Morosinotto, T., Robert, B., Caffarri, S., Bassi, R., and Croce, R. (2003). Recombinant Lhca2 and Lhca3 subunits of the photosystem I antenna system. Biochemistry 42: 4226–34.

Cazzaniga, S., Dall' Osto, L., Kong, S.-G., Wada, M., and Bassi, R. (2013). Interaction between avoidance of photon absorption, excess energy dissipation and zeaxanthin synthesis against photooxidative stress in *Arabidopsis*. The Plant journal : for cell and molecular biology 76: 568–79.

Chen, M., Schliep, M., Willows, R.D., Cai, Z.-L., Neilan, B.A., and Scheer, H. (2010). A red-shifted chlorophyll. Science (New York, N.Y.) 329: 1318–9.

Cheng, Y.-C., Ahn, T.K., Avenson, T.J., Zigmantas, D., Niyogi, K.K., Ballottari, M., Bassi, R., and Fleming, G.R. (2008). Kinetic modeling of charge-transferquenching in the CP29 minor complex. The journal of physical chemistry. B 112: 13418–23.

Cogdell, R.J., Andersson, P.O., and Gillbro, T. (1992). Carotenoid Singlet States and Their Involvement in Photosynthetic Light-Harvesting Pigments. J. Photochem. Photobiol. 15: 105–112.

Cormann, K.U., Bangert, J.-A., Ikeuchi, M., Rögner, M., Stoll, R., and Nowaczyk, M.M. (2009). Structure of Psb27 in solution: implications for transient binding to photosystem II during biogenesis and repair. Biochemistry 48: 8768–70.

Cove, D. (2005). The moss Physcomitrella patens. Annual review of genetics 39: 339–58.

Cove, D., Bezanilla, M., Harries, P., and Quatrano, R. (2006). Mosses as model systems for the study of metabolism and development. Annual review of plant biology 57: 497–520.

Cove, D.J., Knight, C.D., and Lamparter, T. (1997). Mosses as model systems. Trends in Plant Science 2: 99–105.

Croce, R. and van Amerongen, H. (2013). Light-harvesting in photosystem I. Photosynthesis research 116: 153–66.

Croce, R., Breton, J., and Bassi, R. (1996). Conformational changes induced by phosphorylation in the CP29 subunit of photosystem II. Biochemistry 35: 11142–8.

Croce, R., Canino, G., Ros, F., and Bassi, R. (2002a). Chromophore organization in the higher-plant photosystem II antenna protein CP26. Biochemistry 41: 7334–43.

Croce, R., Morosinotto, T., Castelletti, S., Breton, J., and Bassi, R. (2002b). The Lhca antenna complexes of higher plants photosystem I. Biochimica et biophysica acta 1556: 29–40.

Croce, R., Remelli, R., Varotto, C., Breton, J., and Bassi, R. (1999). The neoxanthin binding site of the major light harvesting complex (LHCII) from higher plants. FEBS letters 456: 1–6.

Dall'Osto, L., Caffarri, S., and Bassi, R. (2005). A mechanism of nonphotochemical energy dissipation, independent from PsbS, revealed by a conformational change in the antenna protein CP26. The Plant cell 17: 1217–32.

Dall'Osto, L., Cazzaniga, S., Havaux, M., and Bassi, R. (2010). Enhanced photoprotection by protein-bound vs free xanthophyll pools: a comparative analysis of chlorophyll b and xanthophyll biosynthesis mutants. Molecular plant 3: 576–93.

Dall'Osto, L., Fiore, A., Cazzaniga, S., Giuliano, G., and Bassi, R. (2007). Different roles of alpha- and beta-branch xanthophylls in photosystem assembly and photoprotection. The Journal of biological chemistry 282: 35056–68.

Dall'Osto, L., Holt, N.E., Kaligotla, S., Fuciman, M., Cazzaniga, S., Carbonera, D., Frank, H.A., Alric, J., and Bassi, R. (2012). Zeaxanthin protects plant photosynthesis by modulating chlorophyll triplet yield in specific light-harvesting antenna subunits. The Journal of biological chemistry.

Damkjaer, J.T., Kereïche, S., Johnson, M.P., Kovacs, L., Kiss, A.Z., Boekema, E.J., Ruban, A.V., Horton, P., and Jansson, S. (2009). The photosystem II light-harvesting protein Lhcb3 affects the macrostructure of photosystem II and the rate of state transitions in *Arabidopsis*. The Plant cell 21: 3245–56.

Dau, H. (1994). Molecular mechanisms and quantitative models of variable Photsystem II fluorescence. Photochemistry and Photobiology 60: 1–23.

De Bianchi, S., Ballottari, M., Dall'Osto, L., and Bassi, R. (2010). Regulation of plant light harvesting by thermal dissipation of excess energy. Biochemical Society transactions 38: 651–60.

De Bianchi, S., Betterle, N., Kouril, R., Cazzaniga, S., Boekema, E., Bassi, R., and Dall'Osto, L. (2011). *Arabidopsis* mutants deleted in the light-harvesting protein Lhcb4 have a disrupted photosystem II macrostructure and are defective in photoprotection. The Plant cell 23: 2659–79.

De Bianchi, S., Dall'Osto, L., Tognon, G., Morosinotto, T., and Bassi, R. (2008). Minor antenna proteins CP24 and CP26 affect the interactions between photosystem II subunits and the electron transport rate in grana membranes of *Arabidopsis*. The Plant cell 20: 1012–28.

Dekker, J.P. and Boekema, E.J. (2005). Supramolecular organization of thylakoid membrane proteins in green plants. Biochimica et biophysica acta 1706: 12–39.

Delosme, R., Olive, J., and Wollman, F.-A. (1996). Changes in light energy distribution upon state transitions: an in vivo photoacoustic study of the wildtype and photosynthesis mutants from Chlamydomonas reinhardtii. Biochimica et Biophysica Acta (BBA) - Bioenergetics 1273: 150–158.

Demmig-Adams, B. Carotenoids and photoprotection in plants: a role for the xanthophyll zeaxanthin. *Biochim. Biophys. Acta* **1020**, 1-24 (1990).

Depège, N., Bellafiore, S., and Rochaix, J.-D. (2003). Role of chloroplast protein kinase Stt7 in LHCII phosphorylation and state transition in Chlamydomonas. Science (New York, N.Y.) 299: 1572–5.

Dominici, P., Caffarri, S., Armenante, F., Ceoldo, S., Crimi, M., and Bassi, R. (2002). Biochemical properties of the PsbS subunit of photosystem II either purified from chloroplast or recombinant. The Journal of biological chemistry 277: 22750–8.

Drop, B., Webber-Birungi, M., Fusetti, F., Kouřil, R., Redding, K.E., Boekema, E.J., and Croce, R. (2011). Photosystem I of Chlamydomonas reinhardtii contains nine light-harvesting complexes (Lhca) located on one side of the core. The Journal of biological chemistry 286: 44878–87.

Drop, B., Webber-Birungi, M., Yadav, S.K.N., Filipowicz-Szymanska, A., Fusetti, F., Boekema, E.J., and Croce, R. (2014). Light-harvesting complex II and its supramolecular organization in Chlamydomonas reinhardtii. Bioch. et biophys acta 1837: 63–72.

Durnford, D.G., Deane, J.A., Tan, S., McFadden, G.I., Gantt, E., and Green, B.R. (1999). A phylogenetic assessment of the eukaryotic light-harvesting antenna proteins, with implications for plastid evolution. Journal of molecular evolution 48: 59–68.

Eberhard, S., Finazzi, G., and Wollman, F.-A. (2008). The dynamics of photosynthesis. Annual review of genetics 42: 463–515.

Elrad, D. and Grossman, A.R. (2004). A genome's-eye view of the light-harvesting polypeptides of Chlamydomonas reinhardtii. Current genetics 45: 61–75.

Elrad, D., Niyogi, K.K., and Grossman, A.R. (2002). A major light-harvesting polypeptide of photosystem II functions in thermal dissipation. The Plant cell 14: 1801–16.

Engel, P. (1968). The induction of biochemical and morphological mutants in the moss Physcomitrella patens. Am. J. Bot.: 438–46.

Engelken, J., Brinkmann, H., and Adamska, I. (2010). Taxonomic distribution and origins of the extended LHC (light-harvesting complex) antenna protein superfamily. BMC evolutionary biology 10: 233.

Escoubas, J.M., Lomas, M., LaRoche, J., and Falkowski, P.G. (1995). Light intensity regulation of cab gene transcription is signaled by the redox state of the plastoquinone pool. Proceedings of the National Academy of Sciences of the United States of America 92: 10237–41.

Fan M., Li M., Liu Z., Cao P., Pan X., Zhang H., Zhao X., Zhang J. and Chang W. Crystal structures of the PsbS protein essential for photoprotection in plants. *Nature Structural & Molecular Biology* 22, 729–735 (2015)

Farah, J., Rappaport, F., Choquet, Y., Joliot, P., and Rochaix, J.D. (1995). Isolation of a psaF-deficient mutant of Chlamydomonas reinhardtii: efficient interaction of plastocyanin with the photosystem I reaction center is mediated by the PsaF subunit. The EMBO journal 14: 4976–84.

Ferrante, P., Ballottari, M., Bonente, G., Giuliano, G., and Bassi, R. (2012a). LHCBM1 and LHCBM2/7 polypeptides, components of major LHCII complex, have distinct functional roles in photosynthetic antenna system of Chlamydomonas reinhardtii. The Journal of biological chemistry 287: 16276–88.

Ferrante, P., Ballottari, M., Bonente, G., Giuliano, G., and Bassi, R. (2012b). LHCBM1 and LHCBM2/7 polypeptides, components of major LHCII complex, have distinct functional roles in photosynthetic antenna system of Chlamydomonas reinhardtii. The Journal of biological chemistry 287: 16276–88.

Ferreira, K.N., Iverson, T.M., Maghlaoui, K., Barber, J., and Iwata, S. (2004). Architecture of the photosynthetic oxygen-evolving center. Science (New York, N.Y.) 303: 1831–8.

Fiore, A., Dall'Osto, L., Cazzaniga, S., Diretto, G., Giuliano, G., and Bassi, R. (2012). A quadruple mutant of *Arabidopsis* reveals a β-carotene hydroxylation activity for LUT1/CYP97C1 and a regulatory role of xanthophylls on determination of the PSI/PSII ratio. BMC plant biology 12: 50.

Fiore, A., Dall'Osto, L., Fraser, P.D., Bassi, R., and Giuliano, G. (2006). Elucidation of the beta-carotene hydroxylation pathway in *Arabidopsis thaliana*. FEBS letters 580: 4718–22.

Fischer, N., Boudreau, E., Hippler, M., Drepper, F., Haehnel, W., and Rochaix, J.D. (1999). A large fraction of PsaF is nonfunctional in photosystem I complexes lacking the PsaJ subunit. Biochemistry 38: 5546–52.

Formaggio, E., Cinque, G., and Bassi, R. (2001). Functional architecture of the major light-harvesting complex from higher plants. Journal of molecular biology 314: 1157–66.
Foyer, C.H., Descourvieres, P., and Kunert, K.J. (1994). Protection against oxygen radicals: an important defence mechanism studied in transgenic plants. Plant, Cell and Environment 17: 507–523.

Frank, H.A., Bautista, J.A., Josue, J.S., and Young, A.J. (2000). Mechanism of nonphotochemical quenching in green plants: energies of the lowest excited singlet states of violaxanthin and zeaxanthin. Biochemistry 39: 2831–7.

Fryer, M.J. (1992). The antioxidant effects of thylakoid Vitamin E (alpha-tocopherol). Plant, Cell and Environment 15: 381–392.

Galka, P., Santabarbara, S., Khuong, T.T.H., Degand, H., Morsomme, P., Jennings, R.C., Boekema, E.J., and Caffarri, S. (2012). Functional analyses of the plant photosystem I-light-harvesting complex II supercomplex reveal that light-harvesting complex II loosely bound to photosystem II is a very efficient antenna for photosystem I in state II. The Plant cell 24: 2963–78.

Ganeteg, U., Külheim, C., Andersson, J., and Jansson, S. (2004). Is each light-harvesting complex protein important for plant fitness? Plant physiology 134: 502–9.

Gastaldelli, M., Canino, G., Croce, R., and Bassi, R. (2003). Xanthophyll binding sites of the CP29 (Lhcb4) subunit of higher plant photosystem II investigated by domain swapping and mutation analysis. The Journal of biological chemistry 278: 19190–8.

Genty, B., Briantais, J.M., and Baker, N.R. (1989). The relationship between the quantum yield of photosynthetic electron transport and quenching of chlorophyll fluorescence. iochimica et Biophysica Acta 990: 87–92.

Gerotto, C., Alboresi, A., Giacometti, G.M., Bassi, R., and Morosinotto, T. (2012). Coexistence of plant and algal energy dissipation mechanisms in the moss Physcomitrella patens. The New phytologist 196: 763–73.

Gerotto, C. and Morosinotto, T. (2013). Evolution of photoprotection mechanisms upon land colonization: evidence of PSBS-dependent NPQ in late Streptophyte algae. Physiologia plantarum.

Gibbons, C., Montgomery, M.G., Leslie, A.G., and Walker, J.E. (2000). The structure of the central stalk in bovine F(1)-ATPase at 2.4 A resolution. Nature structural biology 7: 1055–61.

Gilmore, A.M. (1997). Mechanistic aspects of xanthophyll cycle-dependent photoprotection in higher plant chloroplasts and leaves. Physiologia Plantarum 99: 197–209.

Gilmore, A.M. and Ball, M.C. (2000). Protection and storage of chlorophyll in overwintering evergreens. Proceedings of the National Academy of Sciences of the United States of America 97: 11098–101.

Gilmore, A.M. and Yamamoto, H.Y. (1992). Dark induction of zeaxanthin-dependent nonphotochemical fluorescence quenching mediated by ATP. Proceedings of the National Academy of Sciences of the United States of America 89: 1899–903.

Glime, J. (2007). Bryophyte Ecology. Volume 1. Physiological Ecology. (Ebook sponsored by Michigan Technological University and the International Association of Bryologists.).

Gobets, B. and van Grondelle, R. (2001). Energy transfer and trapping in photosystem I. Biochimica et biophysica acta 1507: 80–99.

Gradinaru, C.C., van Stokkum, I.H.M., Pascal, A.A., van Grondelle, R., and van Amerongen, H. (2000). Identifying the Pathways of Energy Transfer between Carotenoids and Chlorophylls in LHCII and CP29. A Multicolor, Femtosecond Pump−Probe Study. The Journal of Physical Chemistry B 104: 9330–9342.

Graham, L.E. (1993). Origin of land plants.

Green, B.R. and Durnford, D.G. (1996). THE CHLOROPHYLL-CAROTENOID PROTEINS OF OXYGENIC PHOTOSYNTHESIS. Annual review of plant physiology and plant molecular biology 47: 685–714.

Guskov, A., Kern, J., Gabdulkhakov, A., Broser, M., Zouni, A., and Saenger, W. (2009). Cyanobacterial photosystem II at 2.9-A resolution and the role of quinones, lipids, channels and chloride. Nature structural & molecular biology 16: 334–42.

Hager, A. and Holocher, K. (1994). Localization of the xanthophyll-cycle enzyme violaxanthin de-epoxidase within the thylakoid lumen and abolition of its mobility by a (light-dependant) pH decrease. Planta: 581–589.

Haldrup, A., Naver, H., and Scheller, H.V. (1999). The interaction between plastocyanin and photosystem I is inefficient in transgenic Arabidopsis plants lacking the PSI-N subunit of photosystem I. The Plant journal : for cell and molecular biology 17: 689–98.

Haniewicz P., De Sanctis D., Büchel C., Schröder W.P., Loi M.C., Kieselbach T., Bochtler M., Piano D. Isolation of monomeric photosystem II that retains the subunit PsbS. Photosynth Res (2013) 118:199–207

Harbinson, J. and Foyer, C.H. (1991). Relationships between the Efficiencies of Photosystems I and II and Stromal Redox State in CO(2)-Free Air : Evidence for Cyclic Electron Flow in Vivo. Plant physiology 97: 41–9.

Harrer, R., Bassi, R., Testi, M.G., and Schäfer, C. (1998). Nearest-neighbor analysis of a photosystem II complex from Marchantia polymorpha L. (liverwort), which contains reaction center and antenna proteins. European journal of biochemistry / FEBS 255: 196–205.

Harrison, C.J., Roeder, A.H.K., Meyerowitz, E.M., and Langdale, J.A. (2009). Local cues and asymmetric cell divisions underpin body plan transitions in the moss Physcomitrella patens. Current biology. CB 19: 461–71.

Havaux, M., Eymery, F., Porfirova, S., Rey, P., and Dörmann, P. (2005). Vitamin E protects against photoinhibition and photooxidative stress in *Arabidopsis thaliana*. The Plant cell 17: 3451–69.

Havaux, M. and Niyogi, K.K. (1999). The violaxanthin cycle protects plants from photooxidative damage by more than one mechanism. Proceedings of the National Academy of Sciences of the United States of America 96: 8762–7.

Heber, U., Azarkovich, M., and Shuvalov, V. (2007). Activation of mechanisms of photoprotection by desiccation and by light: poikilohydric photoautotrophs. Journal of experimental botany 58: 2745–59.

Heber, U., Bilger, W., and Shuvalov, V.A. (2006). Thermal energy dissipation in reaction centres and in the antenna of photosystem II protects desiccated poikilohydric mosses against photo-oxidation. Journal of experimental botany 57: 2993–3006.

Hideg, E., Kálai, T., Hideg, K., and Vass, I. (1998). Photoinhibition of photosynthesis in vivo results in singlet oxygen production detection via nitroxide-induced fluorescence quenching in broad bean leaves. Biochemistry 37: 11405–11.

Hieber, A.D., Kawabata, O., and Yamamoto, H.Y. (2004). Significance of the lipid phase in the dynamics and functions of the xanthophyll cycle as revealed by PsbS overexpression in tobacco and in-vitro de-epoxidation in monogalactosyldiacylglycerol micelles. Plant & cell physiology 45: 92–102.

Hobe, S., Trostmann, I., Raunser, S., and Paulsen, H. (2006). Assembly of the major light-harvesting chlorophyll-a/b complex: Thermodynamics and kinetics of neoxanthin binding. The Journal of biological chemistry 281: 25156–66.

Hofmann, A.H., Codón, A.C., Ivascu, C., Russo, V.E., Knight, C., Cove, D., Schaefer, D.G., Chakhparonian, M., and Zrÿd, J.P. (1999). A specific member of the Cab multigene family can be efficiently targeted and disrupted in the moss Physcomitrella patens. Molecular & general genetics : MGG 261: 92–9.

Hohe, A., Egener, T., Lucht, J.M., Holtorf, H., Reinhard, C., Schween, G., and Reski, R. (2004). An improved and highly standardised transformation procedure allows efficient production of single and multiple targeted gene-knockouts in a moss, Physcomitrella patens. Current genetics 44: 339–47.

Holt, N.E., Fleming, G.R., and Niyogi, K.K. (2004). Toward an understanding of the mechanism of nonphotochemical quenching in green plants. Biochemistry 43: 8281–9.

Holt, N.E., Zigmantas, D., Valkunas, L., Li, X.-P., Niyogi, K.K., and Fleming, G.R. (2005). Carotenoid cation formation and the regulation of photosynthetic light harvesting. Science (New York, N.Y.) 307: 433–6.

Horton, P. and Hague, A. (1988). Studies on the induction of chlorophyll fluorescence in isolated barley protoplasts. IV. Resolution of non-photochemical quenching. Biochim Biophys Acta 932.

Horton, P. and Ruban, A.V. (1992). Regulation of Photosystem II. Photosynthesis Research 34: 375–385.

Jackowski, G., Kacprzak, K., and Jansson, S. (2001). Identification of Lhcb1/Lhcb2/Lhcb3 heterotrimers of the main light-harvesting chlorophyll a/b-protein complex of Photosystem II (LHC II). Biochimica et biophysica acta 1504: 340–5.

Jackson, S.A., Fagerlund, R.D., Wilbanks, S.M., and Eaton-Rye, J.J. (2010). Crystal structure of PsbQ from Synechocystis sp. PCC 6803 at 1.8 A: implications for binding and function in cyanobacterial photosystem II. Biochemistry 49: 2765–7.

Jahns, P., Latowski, D., and Strzalka, K. (2009). Mechanism and regulation of the violaxanthin cycle: The role of antenna proteins and membrane lipids. Biochimica et Biophysica Acta (BBA) - Bioenergetics 1787: 3–14.

Jahns, P., Polle, A., and Junge, W. (1988). The photosynthetic water oxidase: its proton pumping activity is short-circuited within the protein by DCCD. The EMBO journal 7: 589–94.

Jansson, S. (1999). A guide to the Lhc genes and their relatives in Arabidopsis/IT>. Trends in plant science 4: 236–240.

Jensen, P.E., Bassi, R., Boekema, E.J., Dekker, J.P., Jansson, S., Leister, D., Robinson, C., and Scheller, H.V. (2007). Structure, function and regulation of plant photosystem I. Biochimica et biophysica acta 1767: 335–52.

Jensen, P.E., Haldrup, A., Rosgaard, L., and Scheller, H.V. (2003). Molecular dissection of photosystem I in higher plants: topologu, structure and function. Physiologia Plantarum : An International Journal for Plant Biology 119: 313–321.

Johnson, M.P., Goral, T.K., Duffy, C.D.P., Brain, A.P.R., Mullineaux, C.W., and Ruban, A.V. (2011). Photoprotective energy dissipation involves the reorganization of photosystem II light-harvesting complexes in the grana membranes of spinach chloroplasts. The Plant cell 23: 1468–79.

Jordan, P., Fromme, P., Witt, H.T., Klukas, O., Saenger, W., and Krauss, N. (2001). Three-dimensional structure of cyanobacterial photosystem I at 2.5 A resolution. Nature 411: 909–17.

Kamisugi, Y., von Stackelberg, M., Lang, D., Care, M., Reski, R., Rensing, S.A., and Cuming, A.C. (2008). A sequence-anchored genetic linkage map for the moss, Physcomitrella patens. The Plant journal : for cell and molecular biology 56: 855–66.

Kammerer, W. and Cove, D.J. (1996). Genetic analysis of the effects of re-transformation of transgenic lines of the moss Physcomitrella patens. Molecular & general genetics : MGG 250: 380–2.

Karp, G. (1996). Cell and Molecular Biology Sons, John.

Kenrick, P. and Crane, P. (1997). The origin and early diversification of land plants. (Washington, London: Smithsonian Institution Press).

Kiss, A. Z., Ruban, A. V. & Horton, P. The PsbS protein controls the organization of the photosystem II antenna in higher plant thylakoid membranes. *J. Biol. Chem.* 283, 3972-3978 (2008).

Klimmek, F., Sjödin, A., Noutsos, C., Leister, D., and Jansson, S. (2006). Abundantly and rarely expressed Lhc protein genes exhibit distinct regulation patterns in plants. Plant physiology 140: 793–804.

Knox, J.P. and Dodge, A.D. (1985). Singlet oxygen and plants. Photochemistry 24: 889–896.

Kouril, R., Zygadlo, A., Arteni, A.A., de Wit, C.D., Dekker, J.P., Jensen, P.E., Scheller, H.V., and Boekema, E.J. (2005). Structural characterization of a complex of photosystem I and light-harvesting complex II of *Arabidopsis thaliana*. Biochemistry 44: 10935–40.

Kouřil, R., Wientjes, E., Bultema, J.B., Croce, R., and Boekema, E.J. (2013). High-light vs. low-light: effect of light acclimation on photosystem II composition and organization in *Arabidopsis thaliana*. Biochimica et biophysica acta 1827: 411–9.

Kovács, L., Damkjaer, J., Kereïche, S., Ilioaia, C., Ruban, A.V., Boekema, E.J., Jansson, S., and Horton, P. (2006). Lack of the light-harvesting complex CP24 affects the structure and function of the grana membranes of higher plant chloroplasts. The Plant cell 18: 3106–20.

Koziol, A.G., Borza, T., Ishida, K.-I., Keeling, P., Lee, R.W., and Durnford, D.G. (2007). Tracing the evolution of the light-harvesting antennae in chlorophyll a/b-containing organisms. Plant physiology 143: 1802–16.

Krause, G.H. (1988). Photoinhibition of photosynthesis. An evaluation of damaging and protective mechanisms. Physiologia Plantarum 74: 566–574.

Krauss, N., Schubert, W.D., Klukas, O., Fromme, P., Witt, H.T., and Saenger, W. (1996). Photosystem I at 4 A resolution represents the first structural model of a joint photosynthetic reaction centre and core antenna system. Nature structural biology 3: 965–73.

Krieger, A., Moya, I., and Weis, E. (1992). Energy-dependent quenching of chlorophyll a fluorescence: effect of pH on stationary fluorescence and picosecond-relaxation kinetics in thylakoid membranes and Photosystem II preparations. Biochimica et Biophysica Acta (BBA) - Bioenergetics 1102: 167–176.

Krieger-Liszkay, A. (2005). Singlet oxygen production in photosynthesis. Journal of experimental botany 56: 337–46.

Kurisu, G., Zhang, H., Smith, J.L., and Cramer, W.A. (2003). Structure of the cytochrome b6f complex of oxygenic photosynthesis: tuning the cavity. Science (New York, N.Y.) 302: 1009–14.

Kühlbrandt, W., Wang, D.N., and Fujiyoshi, Y. (1994). Atomic model of plant light-harvesting complex by electron crystallography. Nature 367: 614–21.

Külheim, C., Agren, J., and Jansson, S. (2002). Rapid regulation of light harvesting and plant fitness in the field. Science (New York, N.Y.) 297: 91–3.

Lam, E., Oritz, W., Mayfield, S., and Malkin, R. (1984). Isolation and Characterization of a Light-Harvesting Chlorophyll a/b Protein Complex Associated with Photosystem I. Plant physiology 74: 650–5.

Lang, D., Weiche, B., Timmerhaus, G., Richardt, S., Riaño-Pachón, D.M., Corrêa, L.G.G., Reski, R., Mueller-Roeber, B., and Rensing, S.A. (2010). Genome-wide phylogenetic comparative analysis of plant transcriptional regulation: a timeline of loss, gain, expansion, and correlation with complexity. Genome biology and evolution 2: 488–503.

Lang, D., Zimmer, A.D., Rensing, S.A., and Reski, R. (2008). Exploring plant biodiversity: the Physcomitrella genome and beyond. Trends in plant science 13: 542–9.

Larkum, A.W.D., Douglas, S., and Raven, J.A. (2003). Photosynthesis in Algae (Springer).

Lemeille, S., Willig, A., Depège-Fargeix, N., Delessert, C., Bassi, R., and Rochaix, J.-D. (2009). Analysis of the chloroplast protein kinase Stt7 during state transitions. PLoS biology 7: e45.

Leonelli L., Erickson E., Lyska D. and Niyogi K.K. Transient expression in Nicotiana benthamiana for rapid functional analysis of genes involved in non-photochemical quenching and carotenoid biosynthesis. Plant J. 2016 Nov; 88(3):375-386.

Leoni, C., Pietrzykowska, M., Kiss, A.Z., Suorsa, M., Ceci, L.R., Aro, E.-M., and Jansson, S. (2013). Very rapid phosphorylation kinetics suggest a unique role for Lhcb2 during state transitions in Arabidopsis. The Plant journal : for cell and molecular biology 76: 236–46.

Li, X.-P., Gilmore, A.M., Caffarri, S., Bassi, R., Golan, T., Kramer, D., and Niyogi, K.K. (2004). Regulation of photosynthetic light harvesting involves intrathylakoid lumen pH sensing by the PsbS protein. The Journal of biological chemistry 279: 22866–74.

Li, X.-P., Gilmore, A.M., and Niyogi, K.K. (2002a). Molecular and global time-resolved analysis of a psbS gene dosage effect on pH- and xanthophyll cycle-dependent nonphotochemical quenching in photosystem II. The Journal of biological chemistry 277: 33590–7.

Li, X.-P., Muller-Moule, P., Gilmore, A.M., and Niyogi, K.K. (2002b). PsbS-dependent enhancement of feedback de-excitation protects photosystem II from photoinhibition.

Proceedings of the National Academy of Sciences of the United States of America 99: 15222–7.

Li, X.P., Björkman, O., Shih, C., Grossman, A.R., Rosenquist, M., Jansson, S., and Niyogi, K.K. (2000). A pigment-binding protein essential for regulation of photosynthetic light harvesting. Nature 403: 391–5.

Li, Z., Wakao, S., Fischer, B.B., and Niyogi, K.K. (2009). Sensing and responding to excess light. Annual review of plant biology 60: 239–60.

Liu, Z., Yan, H., Wang, K., Kuang, T., Zhang, J., Gui, L., An, X., and Chang, W. (2004). Crystal structure of spinach major light-harvesting complex at 2.72 A resolution. Nature 428: 287–92.

Lucinski, R., Schmid, V.H.R., Jansson, S., and Klimmek, F. (2006). Lhca5 interaction with plant photosystem I. FEBS letters 580: 6485–8.

Lunde, C., Jensen, P.E., Haldrup, A., Knoetzel, J., and Scheller, H.V. (2000). The PSI-H subunit of photosystem I is essential for state transitions in plant photosynthesis. Nature 408: 613–5.

Ma, Y.-Z., Holt, N.E., Li, X.-P., Niyogi, K.K., and Fleming, G.R. (2003). Evidence for direct carotenoid involvement in the regulation of photosynthetic light harvesting. Proceedings of the National Academy of Sciences of the United States of America 100: 4377–82.

Malkin, R. and Niyogi, K.K. (2000). No Title. In: Biochemistry and Molecular Biology of Plants, B.B. Buchanan, W. Gruissem, and R.Jones, eds. American Society of Plant Physiologists, Rockville, MD.: 575–577.

Maurino, V.G. and Peterhansel, C. (2010). Photorespiration: current status and approaches for metabolic engineering. Current opinion in plant biology 13: 249–56.

McCarty, R.E., Evron, Y., and Johnson, E.A. (2000). THE CHLOROPLAST ATP SYNTHASE: A Rotary Enzyme? Annual review of plant physiology and plant molecular biology 51: 83–109.

Melis, A. (1999). Photosystem-II damage and repair cycle in chloroplasts: what modulates the rate of photodamage ? Trends in plant science 4: 130–135.
Merchant, S.S. et al. (2007). The Chlamydomonas genome reveals the evolution of key animal and plant functions. Science (New York, N.Y.) 318: 245–50.

Miller, R. et al. (2010). Changes in transcript abundance in Chlamydomonas reinhardtii following nitrogen deprivation predict diversion of metabolism. Plant phys. 154: 1737–52.

Miloslavina, Y., Wehner, A., Lambrev, P.H., Wientjes, E., Reus, M., Garab, G., Croce, R., and Holzwarth, A.R. (2008). Far-red fluorescence: a direct spectroscopic marker for LHCII oligomer formation in non-photochemical quenching. FEBS letters 582: 3625–31.

Mimuro, M. and Katoh, T. (1991). Carotenoids in photosynthesis: absorption, transfer and dissipation of light energy. Pure and Applied Chemistry 63: 123–130.

Minagawa, J. (2011). State transitions--the molecular remodeling of photosynthetic supercomplexes that controls energy flow in the chloroplast. Biochimica et biophysica acta 1807: 897–905.

Minagawa, J. and Takahashi, Y. (2004). Structure, function and assembly of Photosystem II and its light-harvesting proteins. Photosynthesis research 82: 241–63.

Mitchell, P. (1961). Coupling of phosphorylation to electron and hydrogen transfer by a chemi-osmotic type of mechanism. Nature 191: 144–8.

Moore, A.L., Joy, A., Tom, R., Gust, D., Moore, T.A., Bensasson, R.V., and Land, E.J. (1982). Photoprotection by carotenoids during photosynthesis: motional dependence of intramolecular energy transfer. Science (New York, N.Y.) 216: 982–4.

Morosinotto, T., Baronio, R., and Bassi, R. (2002). Dynamics of chromophore binding to Lhc proteins in vivo and in vitro during operation of the xanthophyll cycle. The Journal of biological chemistry 277: 36913–20.

Mozzo, M., Passarini, F., Bassi, R., van Amerongen, H., and Croce, R. (2008). Photoprotection in higher plants: the putative quenching site is conserved in all outer light-harvesting complexes of Photosystem II. Biochimica et biophysica acta 1777: 1263–7.

Mullet, J.E., Burke, J.J., and Arntzen, C.J. (1980a). A developmental study of photosystem I peripheral chlorophyll proteins. Plant physiology 65: 823–7.
Mullet, J.E., Burke, J.J., and Arntzen, C.J. (1980b). Chlorophyll proteins of photosystem I. Plant physiology 65: 814–22.

Murata, N. (1969). Control of excitation transfer in photosynthesis. I. Light-induced change of chlorophyll a fluorescence in Porphyridium cruentum. Biochimica et biophysica acta 172: 242–51.

Müller, P., Li, X.P., and Niyogi, K.K. (2001). Non-photochemical quenching. A response to excess light energy. Plant physiology 125: 1558–66.

Müller-Moulé, P., Havaux, M., and Niyogi, K.K. (2003). Zeaxanthin deficiency enhances the high light sensitivity of an ascorbate-deficient mutant of Arabidopsis. Plant physiology 133: 748–60.

Müller, M. G. *et al*. Singlet energy dissipation in the photosystem II light-harvesting complex does not involve energy transfer to carotenoids. *ChemPhysChem* **11**, 1289-1296 (2010).

Nakazato, K., Toyoshima, C., Enami, I., and Inoue, Y. (1996). Two-dimensional crystallization and cryo-electron microscopy of photosystem II. Journal of molecular biology 257: 225–32.

Nelson, N. and Ben-Shem, A. (2004). The complex architecture of oxygenic photosynthesis. Nature reviews. Molecular cell biology 5: 971–82.

Nelson, N. and Ben-Shem, A. (2005). The structure of photosystem I and evolution of photosynthesis. BioEssays : news and reviews in molecular, cellular and developmental biology 27: 914–22.

Nield, J., Funk, C., and Barber, J. (2000a). Supermolecular structure of photosystem II and location of the PsbS protein. Philosophical transactions of the Royal Society of London. Series B, Biological sciences 355: 1337–44.

Nield, J., Orlova, E.V., Morris, E.P., Gowen, B., van Heel, M., and Barber, J. (2000b). 3D map of the plant photosystem II supercomplex obtained by cryoelectron microscopy and single particle analysis. Nature structural biology 7: 44–7.

Nilkens, M., Kress, E., Lambrev, P., Miloslavina, Y., Müller, M., Holzwarth, A.R., and Jahns, P. (2010). Identification of a slowly inducible zeaxanthin-dependent component of non-photochemical quenching of chlorophyll fluorescence generated under steady-state conditions in Arabidopsis. Biochimica et biophysica acta 1797: 466–75.

Niyogi, K.K. (1999). Photoprotection revisited: Genetic and Molecular Approaches. Annual review of plant physiology and plant molecular biology 50: 333–359.
Niyogi, K.K. (2000). Safety valves for photosynthesis. Current opinion in plant biology 3: 455–60.

Niyogi, K.K., Grossman, A.R., and Björkman, O. (1998). Arabidopsis mutants define a central role for the xanthophyll cycle in the regulation of photosynthetic energy conversion. The Plant cell 10: 1121–34.

Niyogi, K.K., Li, X.-P., Rosenberg, V., and Jung, H.-S. (2005). Is PsbS the site of non-photochemical quenching in photosynthesis? Journal of experimental botany 56: 375–82.

Niyogi, K.K., Shih, C., Soon Chow, W., Pogson, B.J., Dellapenna, D., and Björkman, O. (2001). Photoprotection in a zeaxanthin- and lutein-deficient double mutant of Arabidopsis. Photosynthesis research 67: 139–45.

Niyogi, K.K. and Truong, T.B. (2013). Evolution of flexible non-photochemical quenching mechanisms that regulate light harvesting in oxygenic photosynthesis. Current opinion in plant biology 16: 307–14.

van Oort, B., Alberts, M., de Bianchi, S., Dall'Osto, L., Bassi, R., Trinkunas, G., Croce, R., and van Amerongen, H. (2010). Effect of antenna-depletion in Photosystem II on excitation energy transfer in *Arabidopsis thaliana*. Biophysical journal 98: 922–31.

Ozawa, S.-I., Onishi, T., and Takahashi, Y. (2010). Identification and characterization of an assembly intermediate subcomplex of photosystem I in the green alga Chlamydomonas reinhardtii. The Journal of biological chemistry 285: 20072–9.

Pan, X., Li, M., Wan, T., Wang, L., Jia, C., Hou, Z., Zhao, X., Zhang, J., and Chang, W. (2011). Structural insights into energy regulation of light-harvesting complex CP29 from spinach. Nature structural & molecular biology 18: 309–15.

Paulsen, H., Finkenzeller, B., and Kühlein, N. (1993). Pigments induce folding of light-harvesting chlorophyll a/b-binding protein. European journal of biochemistry / FEBS 215: 809–16.

Peers, G., Truong, T.B., Ostendorf, E., Busch, A., Elrad, D., Grossman, A.R., Hippler, M., and Niyogi, K.K. (2009). An ancient light-harvesting protein is critical for the regulation of algal photosynthesis. Nature 462: 518–21.

Peng, L., Fukao, Y., Fujiwara, M., Takami, T., and Shikanai, T. (2009). Efficient operation of NAD(P)H dehydrogenase requires supercomplex formation with photosystem I via minor LHCI in Arabidopsis. The Plant cell 21: 3623–40.

Peng, L. and Shikanai, T. (2011). Supercomplex formation with photosystem I is required for the stabilization of the chloroplast NADH dehydrogenase-like complex in Arabidopsis. Plant physiology 155: 1629–39.

Peter, G.F. and Thornber, J.P. (1991a). Biochemical composition and organization of higher plant photosystem II light-harvesting pigment-proteins. The Journal of biological chemistry 266: 16745–54.

Peter, G.F. and Thornber, J.P. (1991b). Electrophoretic Procedures for Fractionation of Photosystem-I and Photosystem-II pigment-Proteins of Higher Plants and for Determination of Their Subunit Composition. Methods in.

Peterson, R.B. and Havir, E.A. (2000). A nonphotochemical-quenching-deficient mutant of *Arabidopsis thaliana* possessing normal pigment composition and xanthophyll-cycle activity. Planta 210: 205–14.

Pfannschmidt, T., Nilsson, A., Tullberg, A., Link, G., and Allen, J.F. (1999). Direct transcriptional control of the chloroplast genes psbA and psaAB adjusts photosynthesis to light energy distribution in plants. IUBMB life 48: 271–6.

Pinnola A., Dall'Osto L., Gerotto C., Morosinotto T., Bassi R., Alboresi A. (2013) Zeaxanthin binds to light-harvesting complex stress-related protein to enhance nonphotochemical quenching in Physcomitrella patens. Plant Cell 25, 3519–3534

Pinnola A., Ghin L., Gecchele E., Merlin M., Alboresi A., Avesani L., Pezzotti M., Capaldi S., S Cazzaniga S., and Bassi R. 'Heterologous Expression of Moss Light-harvesting Complex Stress- related 1 (LHCSR1), the Chlorophyll a-Xanthophyll Pigment-protein Complex Catalyzing Non- photochemical Quenching, in Nicotiana sp.', J Biol Chem. 2015 Oct 2; 290(40): 24340–24354.

Pinnola A., Staleva-Musto H., Capaldi S., Ballottari M., Bassi R. and Polívka T. Electron transfer between carotenoid and chlorophyll contributes to quenching in the LHCSR1 protein from Physcomitrella patens. Biochim Biophys Acta. 2016 Dec;1857(12):1870-1878.

Plumley, F.G. and Schmidt, G.W. (1987). Reconstitution of chlorophyll a/b light-harvesting complexes: Xanthophyll-dependent assembly and energy transfer. Proceedings of the National Academy of Sciences of the United States of America 84: 146–50.

Pogson, B., McDonald, K.A., Truong, M., Britton, G., and DellaPenna, D. (1996). Arabidopsis carotenoid mutants demonstrate that lutein is not essential for photosynthesis in higher plants. The Plant cell 8: 1627–39.

Powles, S.B. and Björkman, O. (1982). Photoinhibition of photosynthesis: effect on chlorophyll fluorescence at 77K in intact leaves and in chloroplast membranes of Nerium oleander. Planta 156: 97–107.

Prasil, O., Adir, N., and Ohad, I. (1992). Dynamics of photosystem II: Mechanism of photoinhibition and recovery processes. In The Photosystems: Stucture, Function and Molecular Biology J. Barber, ed (Elsevier).

Pribil, M., Pesaresi, P., Hertle, A., Barbato, R., and Leister, D. (2010). Role of plastid protein phosphatase TAP38 in LHCII dephosphorylation and thylakoid electron flow. PLoS biology 8: e1000288.

Prigge, M.J. and Bezanilla, M. (2010). Evolutionary crossroads in developmental biology: Physcomitrella patens. Development (Cambridge, England) 137: 3535–43.

Quatrano, R.S., McDaniel, S.F., Khandelwal, A., Perroud, P.-F., and Cove, D.J. (2007). Physcomitrella patens: mosses enter the genomic age. Current opinion in plant biology 10: 182–9.

Ramel, F., Birtic, S., Ginies, C., Soubigou-Taconnat, L., Triantaphylidès, C., and Havaux, M. (2012). Carotenoid oxidation products are stress signals that mediate gene responses to singlet oxygen in plants. Proceedings of the National Academy of Sciences of the United States of America 109: 5535–40.

Remelli, R., Varotto, C., Sandonà, D., Croce, R., and Bassi, R. (1999). Chlorophyll binding to monomeric light-harvesting complex. A mutation analysis of chromophore-binding residues. The Journal of biological chemistry 274: 33510–21.

Rensing, S.A. et al. (2008). The Physcomitrella genome reveals evolutionary insights into the conquest of land by plants. Science (New York, N.Y.) 319: 64–9.

Rensing, S.A., Ick, J., Fawcett, J.A., Lang, D., Zimmer, A., Van de Peer, Y., and Reski, R. (2007). An ancient genome duplication contributed to the abundance of metabolic genes in the moss Physcomitrella patens. BMC evolutionary biology 7: 130.

Rensing, S.A., Rombauts, S., Van de Peer, Y., and Reski, R. (2002). Moss transcriptome and beyond. Trends in plant science 7: 535–8.

Richard, C., Ouellet, H., and Guertin, M. (2000). Characterization of the LI818 polypeptide from the green unicellular alga Chlamydomonas reinhardtii. Plant molecular biology 42: 303–16.

Rintamäki, E., Salonen, M., Suoranta, U.M., Carlberg, I., Andersson, B., and Aro, E.M. (1997). Phosphorylation of light-harvesting complex II and photosystem II core proteins shows different irradiance-dependent regulation in vivo. Application of phosphothreonine antibodies to analysis of thylakoid phosphoproteins. The Journal of biological chemistry 272: 30476–82.

Rivadossi, A., Zucchelli, G., Garlaschi, F.M., and Jennings, R.C. Light absorption by the chlorophyll a-b complexes of photosystem II in a leaf with special reference to LHCII. Photochemistry and photobiology 80: 492–8.

Rochaix, J.-D. (2007). Role of thylakoid protein kinases in photosynthetic acclimation. FEBS letters 581: 2768–75.

Rochaix, J.-D., Lemeille, S., Shapiguzov, A., Samol, I., Fucile, G., Willig, A., and Goldschmidt-Clermont, M. (2012). Protein kinases and phosphatases involved in the acclimation of the photosynthetic apparatus to a changing light environment. Philosophical transactions of the Royal Society of London. Series B, Biological sciences 367: 3466–74.

Ruban, A.V. (2012). The Photosynthetic Membrane: Molecular Mechanisms and Biophysics of Light Harvesting (Wiley).

Ruban, A.V., Berera, R., Ilioaia, C., van Stokkum, I.H.M., Kennis, J.T.M., Pascal, A.A., van Amerongen, H., Robert, B., Horton, P., and van Grondelle, R. (2007). Identification of a mechanism of photoprotective energy dissipation in higher plants. Nature 450: 575–8.

Ruban, A.V., Lee, P.J., Wentworth, M., Young, A.J., and Horton, P. (1999). Determination of the stoichiometry and strength of binding of xanthophylls to the photosystem II light harvesting complexes. The Journal of biological chemistry 274: 10458–65.

Ruban, A.V., Pascal, A.A., Robert, B., and Horton, P. (2002). Activation of zeaxanthin is an obligatory event in the regulation of photosynthetic light harvesting. The Journal of biological chemistry 277: 7785–9.

Rubinstein, C.V., Gerrienne, P., de la Puente, G.S., Astini, R.A., and Steemans, P. (2010). Early Middle Ordovician evidence for land plants in Argentina (eastern Gondwana). The New phytologist 188: 365–9.

Ruuska, S.A., Caemmerer, Von, S., Badger, M.R., Andrews, T.J., Price, G.D., and Robinson, S.A. (2000). Xanthophyll cycle, light energy dissipation and electron transport in transgenic tobacco with reduced carbon assimilation capacity. Aust. J. Plant Physiol. 27.

Saga, G., Giorgetti, A., Fufezan, C., Giacometti, G.M., Bassi, R., and Morosinotto, T. (2010). Mutation analysis of violaxanthin de-epoxidase identifies substrate-binding sites and residues involved in catalysis. The Journal of biological chemistry 285: 23763–70.

Sanderson, M.J., Thorne, J.L., Wikström, N., and Bremer, K. (2004). Molecular evidence on plant divergence times. American journal of botany 91: 1656–65.

Schaefer, D.G. (2001). Gene targeting in Physcomitrella patens. Current opinion in plant biology 4: 143–50.

Schaefer, D.G. and Zrÿd, J.P. (1997). Efficient gene targeting in the moss Physcomitrella patens. The Plant journal : for cell and molecular biology 11: 1195–206.

Schaefer, D.G. and Zrÿd, J.P. (2001). The moss Physcomitrella patens, now and then. Plant physiology 127: 1430–8.

Scheller, H.V., Jensen, P.E., Haldrup, A., Lunde, C., and Knoetzel, J. (2001). Role of subunits in eukaryotic Photosystem I. Biochimica et biophysica acta 1507: 41–60.

Schipper, O., Schaefer, D., Reski, R., and Flemin, A. (2002). Expansins in the bryophyte Physcomitrella patens. Plant molecular biology 50: 789–802.

Schreiber, U. and Neubauer, C. (1990). O2-dependent electron flow, membrane energization and the mechanism of non-photochemical quenching of chlorophyll fluorescence. Photosynthesis Research 25: 279–293.

Scott, A.C. and Glasspool, I.J. (2006). The diversification of Paleozoic fire systems and fluctuations in atmospheric oxygen concentration. Proceedings of the National Academy of Sciences of the United States of America 103: 10861–5.

Shapiguzov, A., Ingelsson, B., Samol, I., Andres, C., Kessler, F., Rochaix, J.-D., Vener, A.V., and Goldschmidt-Clermont, M. (2010). The PPH1 phosphatase is specifically involved in LHCII dephosphorylation and state transitions in Arabidopsis. Proceedings of the National Academy of Sciences of the United States of America 107: 4782–7.

Shaw, A.J., Szövényi, P., and Shaw, B. (2011). Bryophyte diversity and evolution: windows into the early evolution of land plants. American journal of botany 98: 352–69.

Shikanai, T., Munekage, Y., and Kimura, K. (2002). Regulation of proton-to-electron stoichiometry in photosynthetic electron transport: physiological function in photoprotection. Journal of plant research 115: 3–10.

Shikanai, T., Munekage, Y., Shimizu, K., Endo, T., and Hashimoto, T. (1999). Identification and characterization of Arabidopsis mutants with reduced quenching of chlorophyll fluorescence. Plant & cell physiology 40: 1134–42.

Standfuss, J. and Kühlbrandt, W. (2004). The three isoforms of the light-harvesting complex II: spectroscopic features, trimer formation, and functional roles. The Journal of biological chemistry 279: 36884–91.

Standfuss, J., Terwisscha van Scheltinga, A.C., Lamborghini, M., and Kühlbrandt, W. (2005). Mechanisms of photoprotection and nonphotochemical quenching in pea light-harvesting complex at 2.5 A resolution. The EMBO journal 24: 919–28.

Stock, D., Leslie, A.G., and Walker, J.E. (1999). Molecular architecture of the rotary motor in ATP synthase. Science (New York, N.Y.) 286: 1700–5.

Storf, S., Stauber, E.J., Hippler, M., and Schmid, V.H.R. (2004). Proteomic analysis of the photosystem I light-harvesting antenna in tomato (Lycopersicon esculentum). Biochemistry 43: 9214–24.

Stroebel, D., Choquet, Y., Popot, J.-L., and Picot, D. (2003). An atypical haem in the cytochrome b(6)f complex. Nature 426: 413–8.

Sugiura, C., Kobayashi, Y., Aoki, S., Sugita, C., and Sugita, M. (2003). Complete chloroplast DNA sequence of the moss Physcomitrella patens: evidence for the loss and relocation of rpoA from the chloroplast to the nucleus. Nucleic acids research 31: 5324–31.

Szabó, I., Bergantino, E., and Giacometti, G.M. (2005). Light and oxygenic photosynthesis: energy dissipation as a protection mechanism against photo-oxidation. EMBO reports 6: 629–34.

Takahashi, H., Iwai, M., Takahashi, Y., and Minagawa, J. (2006). Identification of the mobile light-harvesting complex II polypeptides for state transitions in Chlamydomonas reinhardtii. Proceedings of the National Academy of Sciences of the United States of America 1_0_3_: 477–82.

Tardy, F. and Havaux, M. (1996). Photosynthesis, chlorophyll fluorescence, light-harvesting system and photoinhibition resistance of a zeaxanthin-accumulating mutant of *Arabidopsis thaliana*. Journal of photochemistry and photobiology. B, Biology 3_4_: 87–94.

Teardo, E., de Laureto, P.P., Bergantino, E., Dalla Vecchia, F., Rigoni, F., Szabò, I., and Giacometti, G.M. (2007). Evidences for interaction of PsbS with photosynthetic complexes in maize thylakoids. Biochimica et biophysica acta 1767: 703–11.

Telfer, A. (2005). Too much light? How beta-carotene protects the photosystem II reaction centre. Photochemical & photobiological sciences : Official journal of the European Photochemistry Association and the European Society for Photobiology 4: 950–6.

Telfer, A., Bishop, S., Phillips, D., and Barber, J. (1994). Isolated photosynthetic reaction center of photosystem II as a sensitizer for the formation of singlet oxygen. Detection and quantum yield determination using a chemical trapping technique. J. Biol. Chem. 269: 13244–13253.

Teramoto, H., Ono, T., and Minagawa, J. (2001). Identification of Lhcb gene family encoding the light-harvesting chlorophyll-a/b proteins of photosystem II in Chlamydomonas reinhardtii. Plant & cell physiology 42: 849–56.

Terasawa, K., Odahara, M., Kabeya, Y., Kikugawa, T., Sekine, Y., Fujiwara, M., and Sato, N. (2007). The mitochondrial genome of the moss Physcomitrella patens sheds new light on mitochondrial evolution in land plants. Mol. biology and evolution 24: 699–709.

Testi, M.G., Croce, R., Polverino-De Laureto, P., and Bassi, R. (1996). A CK2 site is reversibly phosphorylated in the photosystem II subunit CP29. FEBS letters 399: 245–50.

Thornber, J.P., Stewart, J.C., Hatton, M.W., and Bailey, J.L. (1967). Studies on the nature of chloroplast lamellae. II. Chemical composition and further physical properties of two chlorophyll-protein complexes. Biochemistry 6: 2006–2014.

Tjus, S.E., Møller, B.L., and Scheller, H.V. (1998). Photosystem I is an early target of photoinhibition in barley illuminated at chilling temperatures. Plant physiology 116: 755–64.

Tjus, S.E., Scheller, H.V., Andersson, B., and Møller, B.L. (2001). Active oxygen produced during selective excitation of photosystem I is damaging not only to photosystem I, but also to photosystem II. Plant physiology 125: 2007–15.

T.K. Ahn, T.J. Avenson, M. Ballottari, Y.C. Cheng, K.K. Niyogi, R. Bassi and G.R. Fleming, 'Architecture of a charge-transfer state regulating light harvesting in a plant antenna protein', Science 320, 794-797 (2008).

Tokutsu, R., Kato, N., Bui, K.H., Ishikawa, T., and Minagawa, J. (2012). Revisiting the supramolecular organization of photosystem II in Chlamydomonas reinhardtii. The Journal of biological chemistry 287: 31574–81.

Tokutsu, R. and Minagawa, J. (2013). Energy-dissipative supercomplex of photosystem II associated with LHCSR3 in Chlamydomonas reinhardtii. Proceedings of the National Academy of Sciences of the United States of America 110: 10016–21.

Vainonen, J.P., Hansson, M., and Vener, A.V. (2005). STN8 protein kinase in Arabidopsis thaliana is specific in phosphorylation of photosystem II core proteins. The Journal of biological chemistry 280: 33679–86.

Vallon, O., Bulte, L., Dainese, P., Olive, J., Bassi, R., and Wollman, F.A. (1991). Lateral redistribution of cytochrome b6/f complexes along thylakoid membranes upon state transitions. Proceedings of the National Academy of Sciences of the United States of America 88: 8262–6.

Verhoeven, A., Adams, I., Demmig-Adams, B., Croce, R., and Bassi, R. (1999). Xanthophyll cycle pigment localization and dynamics during exposure to low temperatures and light stress in vinca major. Plant physiology 1_2_0_: 727–38.

Wallsgrove, R.M., Turner, J.C., Hall, N.P., Kendall, A.C., and Bright, S.W. (1987). Barley mutants lacking chloroplast glutamine synthetase-biochemical and genetic analysis. Plant physiology 83: 155–8.

Walters, R.G. and Horton, P. (1993). Theoretical assessment of alternative mechanisms for non-photochemical quenching of PS II fluorescence in barley leaves. Photosynthesis research 36: 119–39.

Waters, E.R. (2003). Molecular adaptation and the origin of land plants. Molecular phylogenetics and evolution 29: 456–63.

Wientjes, E., van Amerongen, H., and Croce, R. (2013a). LHCII is an antenna of both photosystems after long-term acclimation. Biochimica et biophysica acta 1827: 420–6.

Wientjes, E., van Amerongen, H., and Croce, R. (2013b). Quantum yield of charge separation in photosystem II: functional effect of changes in the antenna size upon light acclimation. The journal of physical chemistry. B 117: 11200–8.

Wientjes, E. and Croce, R. (2011). The light-harvesting complexes of higher-plant Photosystem I: Lhca1/4 and Lhca2/3 form two red-emitting heterodimers. The Biochemical journal 433: 477–85.

Wientjes, E., Drop, B., Kouil, R., Boekema, E.J., and Croce, R. (2013c). During state 1 to state 2 transition in *Arabidopsis thaliana*, the photosystem II supercomplex gets phosphorylated but does not disassemble. The Journal of biological chemistry 288: 32821–6.

Wientjes, E., Oostergetel, G.T., Jansson, S., Boekema, E.J., and Croce, R. (2009). The role of Lhca complexes in the supramolecular organization of higher plant photosystem I. The Journal of biological chemistry 284: 7803–10.

Wollman, F.A. (2001). State transitions reveal the dynamics and flexibility of the photosynthetic apparatus. The EMBO journal 20: 3623–30.

Yakushevska, A.E., Jensen, P.E., Keegstra, W., van Roon, H., Scheller, H.V., Boekema, E.J., and Dekker, J.P. (2001). Supermolecular organization of photosystem II and its associated light-harvesting antenna in *Arabidopsis thaliana*. European journal of biochemistry / FEBS 268: 6020–8.

Yakushevska, A.E., Keegstra, W., Boekema, E.J., Dekker, J.P., Andersson, J., Jansson, S., Ruban, A.V., and Horton, P. (2003). The structure of photosystem II in Arabidopsis: localization of the CP26 and CP29 antenna complexes. Biochemistry 42: 608–13.

Yamakawa, H. and Itoh, S. (2013). Dissipation of excess excitation energy by drought-induced nonphotochemical quenching in two species of drought-tolerant moss: desiccation-induced acceleration of photosystem II fluorescence decay. Biochemistry 52: 4451–9.

Yamamoto, H.Y. and Kamite, L. (1972). The effects of dithiothreitol on violaxanthin de-epoxidation and absorbance changes in the 500-nm region. Biochimica et biophysica acta 267: 538–43.

Yamamoto, H.Y., Wang, Y., and Kamite, L. (1971). A chloroplast absorbance change from violaxanthin de-epoxidation. A possible component of 515 nm changes. Biochemical and biophysical research communications 42: 37–42.

Zhang, S. and Scheller, H.V. (2004). Light-harvesting complex II binds to several small subunits of photosystem I. The Journal of biological chemistry 279: 3180–7.

Zheleva, D., Sharma, J., Panico, M., Morris, H.R., and Barber, J. (1998). Isolation and characterization of monomeric and dimeric CP47-reaction center photosystem II complexes. The Journal of biological chemistry 273: 16122–7.

Zhu, S.-H. and Green, B.R. (2010). Photoprotection in the diatom Thalassiosira pseudonana: role of LI818-like proteins in response to high light stress. Biochimica et biophysica acta 1797: 1449–57.

Zouni, A., Witt, H.T., Kern, J., Fromme, P., Krauss, N., Saenger, W., and Orth, P. (2001). Crystal structure of photosystem II from Synechococcus elongatus at 3.8 A resolution. Nature 409: 739–43.

Chapter 1
Expression of *Pp*LHCSR1 in *Arabidopsis thaliana* *npq4* mutant

Abstract

Non-photochemical quenching (NPQ) of chlorophyll fluorescence is a process essential for the regulation of photosynthesis and protection from light in excess. As previously mentioned, in vascular plants this process is triggered by a luminal pH sensor, the PSBS protein, which transduces chloroplast lumen acidification, induced by excess light, into a quenching reaction occurring within specific interacting chromophore-bound light-harvesting proteins (LHC). In algae, such as *Chlamydomonas reinhardtii,* stress-related light-harvesting proteins (LHCSR) fulfill both pH sensing and quenching reactions, due to their capacity of binding chlorophylls and xanthophylls. In the case of the moss *Physcomitrella patens*, an evolutionary intermediate between algae and plants, both PSBS and LHCSR proteins are active in quenching. Plants and mosses have a very similar organization of thylakoid membranes thus suggesting LHCSR might be active in plants. In this chapter we verified this hypothesis by overexpressing the *Pplhcsr1* gene into the *psbs-less* mutant of *Arabidopsis thaliana*, called *npq4, which* is inactive in NPQ. The transformants exhibited a light-dependent quenching activity, although reduced respect to *P. patens*, which allowed analysis of factors controlling quenching activity. In addition, LHCSR1 ability to bind pigments, its zeaxanthin-dependence for quenching and its localization within thylakoid compartment are discussed.

Introduction

The need for a balance between light harvesting and photoprotection is one of the key driving forces that shaped adaptation of photosynthetic eukaryotic organisms on Earth. Non Photochemical Quenching (NPQ) of chlorophyll fluorescence is a key mechanism for the dissipation of excess absorbed energy (Genty et al., 1990; Muller, 2001; Baker, 2008). NPQ is a multi-pathway process that consists of several components occur with different induction and relaxation kinetics: qE, a flexible, rapidly reversible type of NPQ which is induced by the buildup of a high thylakoid ΔpH in the presence of excess light, qT which is the phosphorylation-related migration of major LHCII between PSI and PSII known as state transition, and qI the photoinhibitory quenching caused by the slow and reversible inactivation of PSII reaction centers. NPQ is deeply dependent on Light Harvesting Complexes (LHC), a large superfamiliy of nuclear encoded proteins that bind chlorophylls and carotenoids. qE, the fastest component of NPQ, is fully dependent on thylakoid lumen acidification, a light-driven phenomenon that is also necessary for ATPase activity (Kramer et al., 1999; Kanazawa and Kramer, 2002; Horton et al., 1996). The plant-type S subunit of Photosystem II (PSBS) is active in *Arabidopsis thaliana* (Li et al., 2000) and is generally considered the trigger of qE in vascular plants (Niyogi and Truong, 2013). An ancient light-harvesting complex stress-related protein called LHCSR is the key activator of qE in *Chlamydomonas reinhardtii* (Peers et al., 2009) and an homologous called LHCX has the same role in *Phaeodactylum tricornutum* (Bailleul et al., 2010). PSBS and LHCSR are two phylogenetically and structurally distict proteins (Niyogi and Truong, 2013; Engelken et al., 2010). Both proteins are responding to thylakoid lumen acidification obtained under excess light conditions. Both proteins interact directly with LHC proteins associated to Photosystem II (PSII) and this interaction is priming the quenching of their chlorophyll fluorescence (Wilk et al., 2013; Tokutsu and Minagawa, 2013; Teardo et al., 2007). In this scenario, it was shown that PSBS protein aquired its activity before LHCSR was lost. In fact in the moss *Physcomitrella patens* both PSBS and LHCSR are accumulated and they act independently to turn on qE (Alboresi et al., 2010; Gerotto et al., 2012). LHCSR proteins share several common features (Dittami et al., 2010), but differences have been described. In fact, in *C. reinhardtii* LHCSR is accumulated at low level under standard growth conditions and is strongly induced only under stress conditions (e.g. iron starvation or excess light) (Naumann et al., 2007; Peers et al., 2009; Savard et al., 1996).

In *P. patens* the LHCSR protein is accumulated and active also under standard growth conditions even though stress conditions enhance protein accumulation (Gerotto et al., 2011).

Hypothesis and strategy

Thylakoid membrane organisation is a major structural difference that could influence the activity of LHCSR proteins in algae and mosses. Little or no grana stack is formed in unicellular algae while mosses have highly structured thylakoid membranes organisation similar to those of flowering plants (Mullineaux, 2005; Wiedemann et al., 2010). Beside the knowledge aquired during the past fifteen years, there are still lots of opened question about the mechanism of quenching activation and about the reasons that lead to the specialization of PSBS activity in flowering plants. Now it would be interesting to verify the effect of inserting LHCSR in higher plants and study the possible interactions of the expressed protein *in planta*. It has been recently shown that LHCSR1 protein, responsible for non-photochemical quenching in the moss *P. patens* can be expressed in *N. tabacum* (Pinnola et al., 2015) by exploiting the properties of the *agrobacterium*-mediated transformation. In this study, we proceed to the expression of LHCSR1 in *Arabidopsis thaliana* in order to exploit the large variety of mutants available in this plant. In particular, the availability of a mutant lacking PSBS (i.e. *npq4*) allows for a functional analysis of LHCSR1 on the fluorescence properties of the plant in vivo, thus of the fate of chlorophyll excited states which are the substrate of regulation by NPQ and specifically by qE.

We expressed LHCSR1 from *Physcomitrella patens* in PSBS-less, *npq4 Arabidopsis thaliana* mutant plants. The choice of this specific mutant, unable to perform NPQ, was made in order to ensure that any quenching activity that we would see would be due to the presence of LHCSR1.

Material and Methods

A brief description of all the methods, procedures and materials followed in this study for the generation of thylakoids, plasmid constructs and transgenic plants, is presented in the following chapters. All these techniques are described later in detail, in the 'Appendix' section.

Cloning of LHCSR1 cDNA, Arabidopsis transformation and screening

The fragment corresponding to *LHCSR1* (Locus name Phpat.009G013900) was amplified from *P. patens* total cDNA obtained from 6 days old plants grown on minimum medium, RNA was isolated using TRI Reagent® Protocol (T9424, Sigma-Aldrich) and cDNA was synthetized using M-MLV Reverse Transcriptase (M1302, Sigma-Aldrich) and Oligo$(dT)_{23}$ (O4387, Sigma-Aldrich). Primers including *attB* sequences for the gateway technology (Invitrogen™) were designed to anneal 27 base pairs upstream of the ATG codon (PpLHCSR1attB1 5'-GGGGACAAGTTTGTACAAAAAAGCAG GCTCCAATCTCGAGCTTTTGCT-3') and 107 base pairs downstream of the stop codon (*Pp* LHCSR1attB5'- GGGGACCACTTTGTACAAGAAAGCTGGGTCGACT GCGAATCAATCAGA A-3'). The 966 base pairs PCR product was first cloned in pDONR™221 Vector (12536-017, Invitrogen™) and then recombined into the pH7WG2 binary vector (Karimi et al., 2002) to make the *35S::LHCSR1* construct. The accuracy of the cloning was verified by DNA digestion and sequencing and the plasmid was transferred in *Agrobacterium tumefaciens* strain GV3101 (Zhang et al., 2006). *Arabidopsis* plants were transformed by the floral dip method and transgenic plants were selected on Moorashige-Skoog medium supplemented by hygromycin (25 mg L^{-1}) and carbenicillin (100 mg L^{-1}) (Zhang et al., 2006). Ten days after sowing on selective medium, plants were transferred in pots and three weeks after the expression of LHCSR1 transgene was assayed by western blotting.

Plant material and growth conditions

Physcomitrella patens wild-type protonemal tissue was grown in Petri dishes containing minimum $PPNO_3$ medium (Ashton et al., 1979) enriched with 0.5% glucose and solidified with 0.8% plant agar. In-plate material was grown under controlled light and temperature conditions: 24°C, 16-h light/8-h dark photoperiod with a light intensity of 40 µmol photons m^{-2} s^{-1}. *Arabidopsis thaliana* wild-type plants (ecotype *Columbia*) were grown in controlled conditions of 8-h light/16-h dark with a light intensity of 100 µmol photons m^{-2} s^{-1} under stable temperature (23°C in light / 20°C in dark) for 4 weeks. Transgenic lines were grown on selective Moorashige and Skoog (MS) medium containing hygromycin-B (25mg L^{-1}) for the first 10 days under 16-h light and 8-h dark photoperiod (40 µmol photons m^{-2} s^{-1}, 24°C) and then followed the growth conditions of *A. thaliana* wild- type plants for 3 weeks.

Gel Electrophoresis

Total leaf extracts from transgenic *A. thaliana* plants were homogenized using plastic pestels in Laemmli buffer with 62.5 mM Tris pH 6.8, 10% glycerol, 5% SDS, 5%2-mercaptoethanol and loaded on a 15% (w/v) separating acrylamide gel (75:1 acrylamide/bis-acrylamide) with 6M Urea. After SDS-PAGE gel electrophoresis, proteins were transferred by western-blot on a polyvinylidene fluoride (PVDF) transfer membrane (Millipore) with the use of a Bio-rad blot system and developed using specific LHCSR and CP43 antibodies produced in the laboratory.

Thylakoid isolation

Stacked thylakoids were purified from about 25-days old *A. thaliana* wild-type and transgenic plants (Berthold et al., 1981). Detached leaves from dark-adapted plants were harvested and homogenized in cold extraction buffer containing 0.02M Tricine-KOH pH 7.8, 0.4M NaCl, 0.002M $MgCl_2$, 0.5% milk powder, and protease inhibitors 0.005M e-aminocaproic acid, 0.001M phenyl-methylsulfonyl fluoride and 0.001M benzamidine added right before the isolation. Homogenized leaves were then filtered, centrifuged at 1500g for 15 min at 4°C and then resuspended in a hypotonic buffer of 0.02M Tricine-KOH pH 7.8, 0.005M $MgCl_2$, 0.15M NaCl and the pre-mentioned concentrations of protease inhibitors. Resuspended thylakoids were centrifuged for 10min at 10,000g (4°C) followed by a second resuspension in a sorbitol buffer (0.01M HEPES-KOH pH 7.5, 0.4M Sorbitol, 0.015M NaCl and 0.005M $MgCl_2$). Thylakoid membranes were quantified and either used directly or stored in -80^{o}C. Stroma and grana separation was performed as previously described (Morosinotto et al., 2010).

Pigment-protein complexes separation with Deriphat-PAGE

Non-denaturating Deriphat-PAGE was performed as previously described (Peter et al., 1991) with some modifications: stacking gel of 3.5% (w/v) acrylamide (38:2 acrylamide/bis-acrylamide) and separating acrylamide gel was prepared at different fixed or gradient concentration depending on the purposes. Acrylamide concentrations are specified along the text. Thylakoids from WT and transgenic plants corresponding to a final chlorophyll concentration of 0.5mg were washed with 5mM EDTA and then resuspended in 10mM HEPES pH 7.5. Samples were then solubilized with 0.8% n-*Dodecyl* α-D-*maltoside* and 10 mM HEPES pH 7.5 by vortexing thoroughly for 1min.

Solubilized samples were kept 10 min in ice and then centrifuged at 15,000g for 10min to pellet any insolubilized material and then loaded.

Thylakoid membranes fractionation

Solubilization protocol was performed as in (Morosinotto et al., 2010). Stacked thylakoids were resuspended in 0.02 M HEPES-KOH, pH 7.5, 0.015 M NaCl, 0.005 M $MgCl_2$ buffer at 1 mg Chl/ml and solubilized at 4 °C for 20 min in slow agitation with different amounts of β-DM ranging from 0.16 to 0.49% (w/v), always in the presence of 0.015 M NaCl, 0.005 M MgCl2 and 0.02 M HEPES-KOH, pH 7.5. Unsolubilized thylakoids were pelleted by centrifugation at 3.500 X g for 5 min. Partially solubilized grana membranes were instead pelleted with a further 30 min centrifugation at 40.000 X g. Solubilized complexes and small membrane patches remained instead in the supernatant. Membrane pellet was washed with 0.015 M NaCl, 0.005 M MgCl2 and 0.02 M HEPES-KOH, pH 7.5, centrifuged for 30 min at 30.000 X g and finally resuspended in 0.4 M Sorbitol, 0.01 M HEPES-KOH, pH 7.5, 0.015 M NaCl, 0.005 M MgCl2 frozen in liquid nitrogen and stored at –80°C until use.

Fluorescence measurements

In vivo chlorophyll fluorescence was measured in room temperature, directly on detached leaves from 45min dark-adapted *A. thaliana* plants by FC 800MF closed FluorCam Video-imaging system (Photon Systems Instruments) and Dual Pulse-Amplitude Modulated (PAM-100) fluorometer. For every measurement a saturating pulse of 4000 μmol photons m^{-2} s^{-1} and actinic light with an intensity of 1200 or 800 μmol photons m^{-2} s^{-1} were applied. Fv/Fm and NPQ parameters were calculated as (Fm−Fo)/Fm and (Fm−Fm′)/Fm′ respectively.

Pigment composition analysis (HPLC)

A. thaliana leaves, inside 1.5mL eppendorfs, were frozen in liquid nitrogen and homogenized using plastic pestles. Pigments were extracted in 80% cold acetone and analyzed by High-Pressure Liquid Chromatography (HPLC) after two steps of centrifugation at maximum speed for 15 min at 4°C.

Results

1.1 LHCSR1 expression in *A. thaliana npq4* mutant

The coding sequence of LHCSR1 was amplified from cDNA synthetized from *P. patens* protonema grown on minimum medium and cloned in pH7WG2 under the control of the constitutive promoter 35S. LHCSR1 is physiologically expressed at high levels in *P. patens* and the use of a strong promoter should guarantee high levels of LHCSR1 mRNA without undesired silencing effects. *Agrobacterium*-mediated transformation with *35S::LHCSR1* construct was first of all adopted on *npq4* mutant plants which lack PSBS and qE and therefore allow the visualization of any LHCSR-dependent NPQ activation. After *agrobacterium*-mediated transformation of *npq4* plants following the flower-dip method (see appendix) transgenic seeds were collected, purified following a standard purification protocol and let for 10 days to grow on selection petri dishes containing Murashige and Skoog medium supplemented with hygromicine-B. Two different series of resistant plants were transferred on soil, together with *A. thaliana* wild-type and *npq4* control plants and after 3 weeks leaves were collected and total extracts were analyzed by western blotting using specific home-made antibodies, raised against the *in vitro* refolded LHCSR1 protein. In order to make sure that the immunoreaction of anti-LHCSR antibody was specific to the transgenic protein and not to the cross-reaction with other LHC expressed by *A. thaliana*, total protein extracts from wild-type and *npq4* plants were also analyzed by western blot with no reaction being detected. On the contrary, the core subunit of PSII super complex CP43 was detected in all samples. As a further control, thylakoid proteins from *P. patens* were used and in this case both LHCSR1 and LHCSR2 were detected. The apparent molecular weight of LHCSR1 expressed by *A. thaliana* matches with the one of the native LHCSR1 protein accumulated in *P. patens* thylakoid membranes, suggesting that LHCSR1 was expressed in its mature form in the selected transgenic lines. All of the 14 independent T1 lines resistant to hygromicine-B expressed LHCSR1 with only small differences in the amount of protein accumulated. We decided to carry on our study on those lines that had the highest accumulation (e.g. O1.2, Figure 1.1 B, lines N1.3 and P1.3, Figure 1.1 C) and the T2 generation of 5 lines was collected for further characterization.

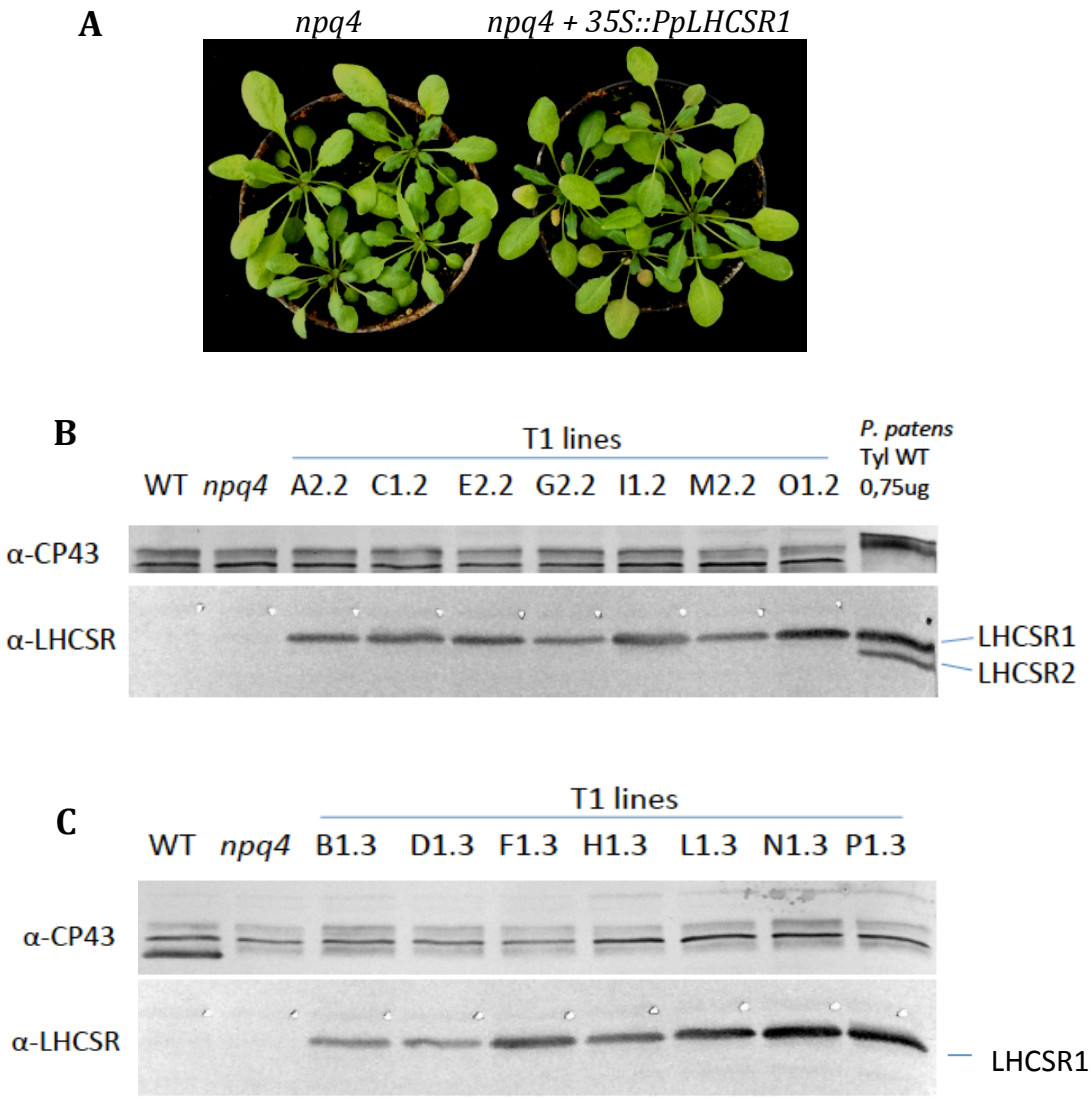

Figure 1.1. **Biochemical characterization of 35S::LHCSR1 transformed lines.** *(A) A. thaliana transgenic lines were selected on agar plates and then transferred in pots in a short-day photoperiod growth chamber (right). Control npq4 plants of the same age were also grown in the same conditions (left). (B,C) Western blot analysis was performed on total proteins extracted by grinding one leaf disk directly in 100 µL of loading buffer, one tenth of the volume was loaded on SDS-PAGE. Proteins of wild-type and npq4 plants were loaded as a control as well as the equivalent of 1 µg of Chls of thylakoid proteins purified from wild-type P. patens plants. The primary antibody used for the analysis is indicated on the left side of the membrane while the band corresponding either to P. patens LHCSR1 or LHCSR2 is indicated on the left side.*

1.2 LHCSR1 localization in *A. thaliana* thylakoid membranes

To verify that LHCSR1 was actually imported to the chloroplast and inserted in thylakoid membranes, we have purified thylakoid proteins from *A. thaliana* 35S::LHCSR1 complemented but also control *npq4* mutant plants and we have analyzed them by SDS-PAGE through Coomassie staining (Figure 1.2 A) and western blotting (Figure 1.2 B). A band with the apparent molecular weight of LHCSR1 is present in a region comprised between Lhcb3 and Lhcb6 exclusively in 35S::LHCSR1 complemented plants but not in *npq4*. No other major change could be highlighted between the two genotypes (Figure 1.2 A). Western blot analysis confirmed that anti-LHCSR antibody reacted against the *P. patens* protein accumulated in thylakoid membranes of 35S::LHCSR1 (Figure 1.2 B). Also in this case, *P. patens* wild-type and *lhcsr1lhcsr2* ko thylakoid membranes were used as additional controls for western blot analysis. LHCSR1 and LHCSR2 were detected in the wild-type thylakoids plants but not in *lhcsr* ko (Figure 1.2 B). CP43 was used as a loading control and was present in similar amounts in all samples (Figure 1.2 B). LHCSR1 of *P. patens* is clearly accumulated in thylakoid membranes of *A. thaliana*.

Earliest reports described LHCSR as a member of the LHC superfamily that is easily extracted from thylakoid membranes in *C. reinhardtii* (Richard et al., 2000). On this basis, we proceeded to the gentle solubilization of stacked thylakoid membranes using n-Dodecyl a-D-maltoside (a-DM) to verify if LHCSR conserved this property of easy extraction also when expressed in *A. thaliana*. The use of a-DM followed by two centrifugation steps at 40000 g resulted in the purification of two fractions, on one side a pellet enriched in grana membranes and on the other side a supernatant containing stroma lamellae and all the membrane portions exposed to the stroma compartment (referred to as supernatant (Sup) or simply stromal membranes). The same samples were also analyzed by SDS-PAGE followed by Coomasie staining (Figure 1.2 C). Fractionation results showed that complexes typically localized in stroma-exposed membranes (e.g. ATP synthase proteins) are highly accumulated in the supernatant fraction while LHCII, Lhcb3 and Lhcb6 are enriched in grana partitions (Figure 1.2 C). A band at the apparent molecular weight of LHCSR1 appears to be more abundant in the supernatant fraction. This result is also supported by western blot analyses (Figure 1.2 D) indicating that LHCSR1 is a protein easily extracted out of thylakoid membranes and partitioning with thylakoid stroma components PSI and ATPase rather than with PSII components of grana stacks.

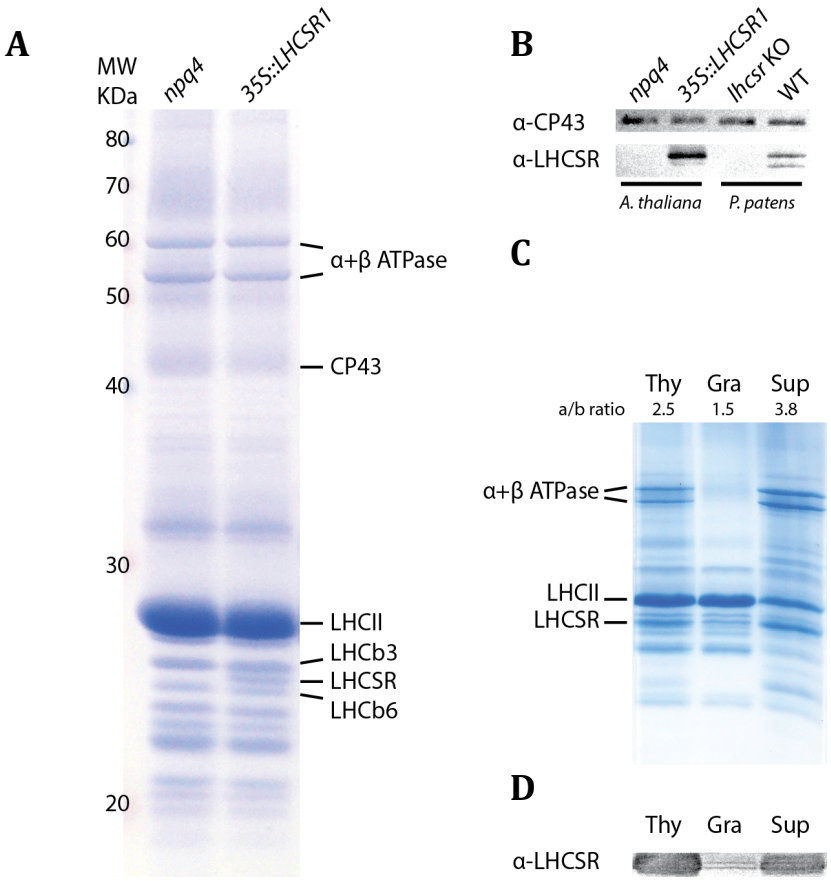

Figure 1.2. *A. thaliana* thylakoid membrane fractionation and analysis of LHCSR distribution in the individual fractions. *A) Coomassie-stained SDS-PAGE separation of thylakoid proteins isolated from npq4 plants and npq4 plants expressing LHCSR1 (35S::LHCSR1). The identity of LHCSR1 and other bands is indicated on the right side of the gel. B) Western blot analysis of thylakoid proteins isolated from A. thaliana npq4 plants and npq4 plants expressing LHCSR1 (35S::LHCSR1). As an external control, WT and lhcsr KO thylakoid proteins were also loaded on the gel. C) Coomassie-stained SDS-PAGE separation of proteins of thylakoid membranes (Thy), grana fraction (Gra) and the supernatant obtained after thylakoid solubilization and grana precipitation (Sup). Gels were loaded on a chlorophyll basis (4 µg for Thy and 2.7 µg for Gra and Sup), the chlorophyll a/b ratio is indicated over the gel. D) Western blot analysis of LHCSR1 distribution in the fractions described in panel C, in this case four times less material was loaded on the SDS-PAGE.*

In order to have additional evidence of the presence and easy extraction of LHCSR1 in *A. thaliana* thylakoids we repeated the thylakoid grana and stromal membranes separation process, this time by using different concentrations of a-DM detergent. Grana (Gra) and stromal membranes (Sup) fractions were separated after pelleting down and solubilizing thylakoid samples from *A. thaliana* wild-type and 35S::LHCSR1 plants, with 0.16, 0.24, 0.32, 0.39 and 0.47% of a-DM (see materials and methods in this section). Also in this case, western blot analysis and Coomasie staining followed fractionation. The pellet and supernatant samples (corresponding respectively to grana partition membranes and stromal-membrane derived solubilized matherial, Morosinotto

et al. 2010) were loaded in alternate slots on SDS-PAGE gels, in an increasing a-DM concentration used for solubilization (0.16-0.47% w/v) and in a Chl basis of 0.5 ug per sample. Results showed increasing levels of LHCSR1 accumulated in the stromal membrane fractions as the concentration of detergent increased. In contrast the protein is detected in much lower levels in the grana fractions, as a-DM concentration gets higher. As for the controls, LHCSR1 can be clearly seen in the thylakoid membranes of *P. patens* wild-type and *A. thaliana* 35S::LHCSR1 complement plants in contrast to *A. thaliana npq4* where the protein is completely absent. As an additional control, the upper part of the membrane was developed against a-CP43.

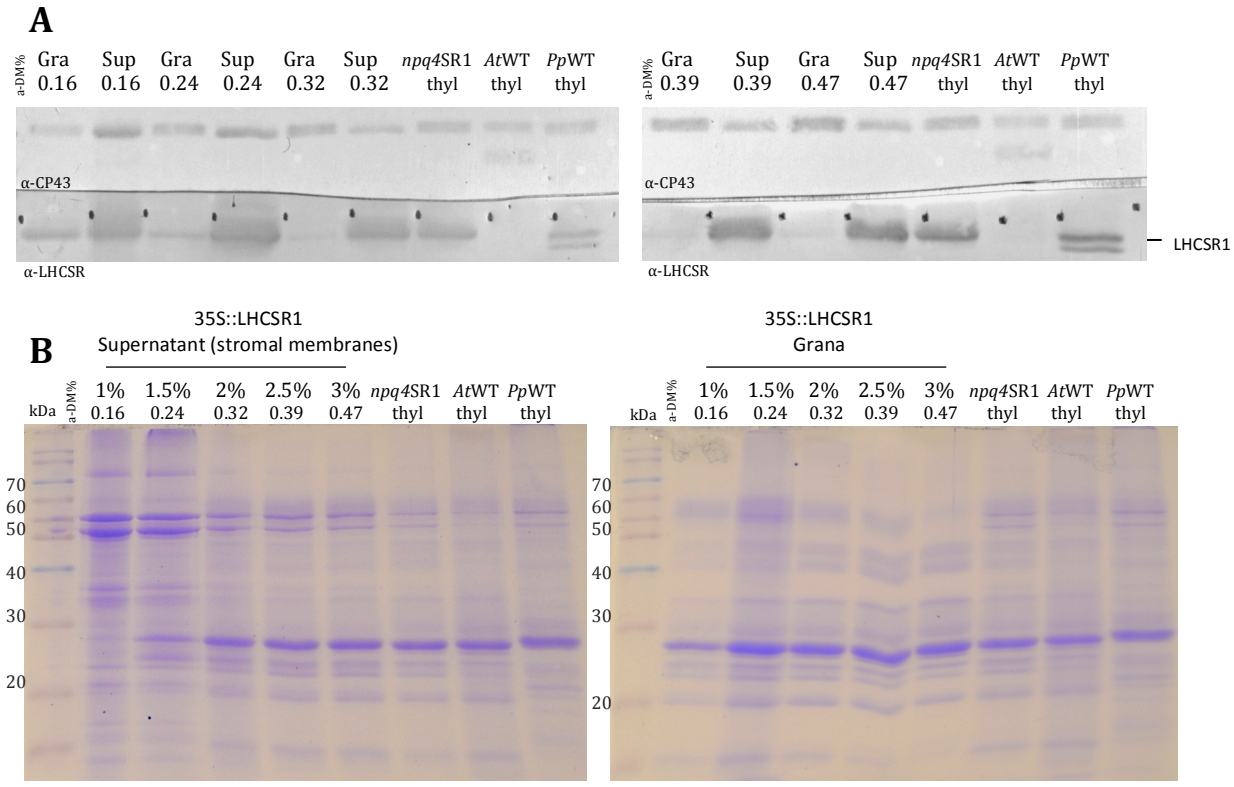

Figure 1.3. Grana and stromal membranes separation from 35S::LHCSR1 thylakoids and fractionation with different a-DM concentrations. *(A) Western blot analysis of LHCSR1 distribution in the separated grana and stromal membrane (supernatant) fractions from each solubilization. Grana (Gra) and stromal membrane (Sup) fractions solubilized with a-DM ranging from 0.16-0.47%, were loaded alternately on SDS-PAGE gels (detergent concentration increases from left to right). Equal amount of thylakoids from A. thaliana 35S::LHCSR1, wild-type and P.patens wild-type were loaded as controls. All samples were loaded on a Chl basis of 0.5ug (B) Coomassie staining of fractionated stromal membrane (left) and grana partitions (right) from 35S::LHCSR1 thylakoid membranes. Samples are presented with an increasing a-DM concentration. All samples were loaded on a Chl basis of 2ug.*

1.3 Separation of pigment-binding complexes

LHCSR protein has been described as a pigment binding complex both in *C. reinhardtii* and *P. patens* (Bonente et al., 2011; Pinnola et al., 2013). In order to make sure that LHCSR1 is a pigment-binding protein complex also when heterologously expressed in *A. thaliana*, we solubilized *npq4* and 35S::LHCSR1 thylakoids and resolved different pigment binding complexes by a native Deriphat-PAGE (Figure 1.4A). There is no major difference in chlorophyll distribution between the two genotypes analyzed indicating that the accumulation of LHCSR1 in thylakoid membranes does not alter the overall structure of PS super-complexes. A difference was, however, detected in the region comprised between LHCII trimers and free pigments. In fact two bands are substantially more abundant in 35S::LHCSR1 than in *npq4* thylakoid membranes. The first band migrates halfway between LHCII trimers and LHC monomers and can be attributed to LHC dimers, while the second band appears below LHC monomers and therefore can be attributed to an LHC-pigment complex of small molecular weight (Figure 1.4 A).

Next step was to analyze by western blotting the region of the gel between LHCII trimers and free pigments both for *npq4* and 35S::LHCSR1 complemented plants (Figure 1.4 B). This portion of the native page was cut in 8 slices of about 0.5 cm height each which were separately smashed and eluted in a buffer containing 20 mM Hepes pH 7.8, 0.03 % α-DM and 50 % w/v glicerol for 2 hours. After centrifugation at 13000 x g at 4°C, one third of each fraction was used for SDS-PAGE analysis and western blotting using anti-LHCSR antibody (Figure 1.4 B). As expected, no signal corresponding to LHCSR1 was detected in *npq4* plants, confirming the high specificity of our anti-LHCSR antibody. The sample corresponding to 35S::LHCSR1 had no signal corresponding to the free pigments region while the strongest signal corresponded to the two bands mentioned above, the one corresponding to LHC dimers and the one migrating below LHC monomers (Figure 1.4 B). Lower level of reactivity was detected in the area between the two strongly reactive bands but not at lower MW, suggesting the low-molecular weight band might derive from the dissociation of the high-molecular weight band during separation.

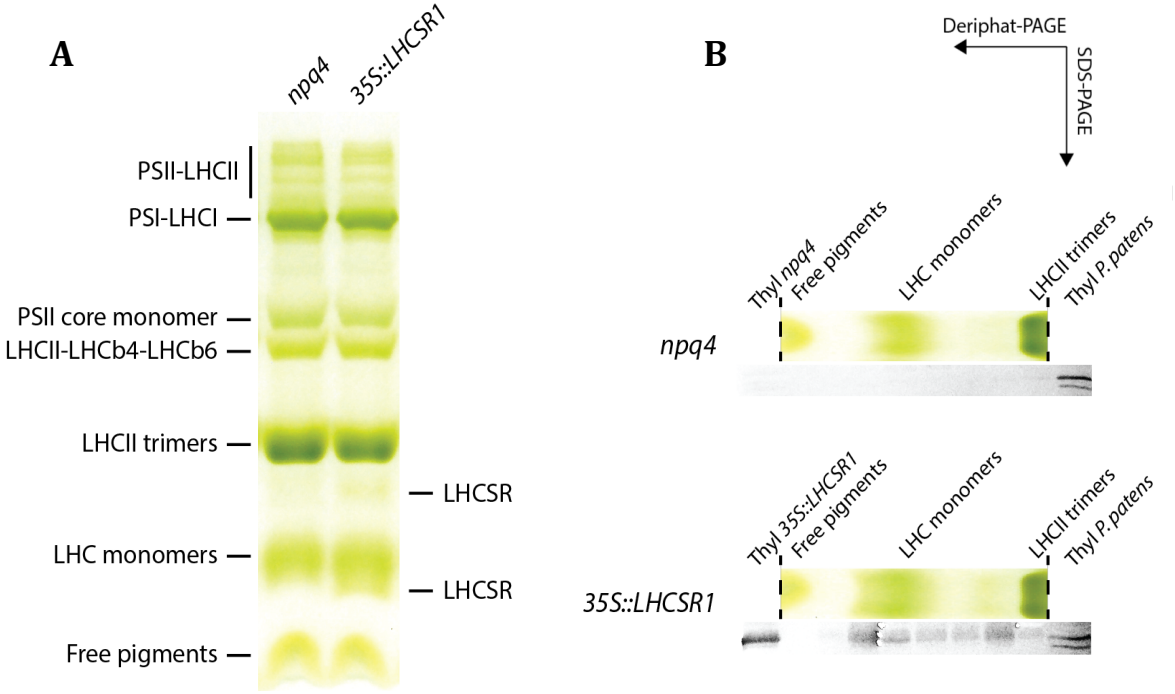

Figure 1.4. **Deriphat-PAGE analysis of A. thaliana thylakoid membrane protein complexes.** ***(****A) Thylakoid membranes (30 µg of Chls) of npq4 and 35S::LHCSR1 plants solubilized with 0,8 % (w/v) α-DM was subjected to deriphat-PAGE. PSII and PSI complexes, together with various combinations of LHCs are resolved and indicated on the left side of the gel. Complexes more abundant in 35S::LHCSR1 than in npq4 plants are labeled as LHCSR on the right side of the gel. (B) Western blot analysis of the region between free pigments and LHCII trimers of the deriphat-PAGE shown in panel A. Both npq4 and 35::LHCSR1 samples were taken in account. Proteins were extracted from the gel reloaded on SDS-PAGE. Each gel has two controls, an aliquot of the same thylakoids used for deriphat-PAGE (Thyl npq4 and Thyl 35S::LHCSR1) and an aliquot of thylakoids of P. patens wild-type plants (thyl. P. patens).*

1.4 Spectroscopic analysis of pigment-binding complexes

In order to investigate the spectroscopic properties of the regions where LHCSR1 migrated, we repeated the pigment-binding super-complexes separation by resolving them with Deriphat-PAGE. For this, 150ug Chl of thylakoids from the transgenic 35S::LHCSR1 and control wild-type plants were solubilized with a-DM and loaded on a Deriphat-PAGE gel of fixed acrylamide concentration. Also in this case, upon separation of α-DM solubilized thylakoids a difference in the region between LHCII trimers and free pigments can be highlighted, with a green band being present only in the 35S::LHCSR1 lane. A faint green band appearing between the LHCII trimers and LHCII monomers in both lanes can be possibly attributed to LHCII dimers as a result of solubilization. Immuno-blotting of the middle part of the gel into a poly-vinylidene fluoride (PVDF) membrane was then performed in order to detect the migration of the LHCSR protein with anti-LHCSR antibodies. Also in this case two differential immuno-reactions were observed consistent with the location of LHCSR1 in the previous Deriphat-PAGE analysis, one corresponding to LHCII dimers and a broader one migrating below LHCII

monomers (Figure 1.5A). The band appearing below LHCII trimers was not further analysed as its properties are affected by the co-migration with the LHCII dimers.

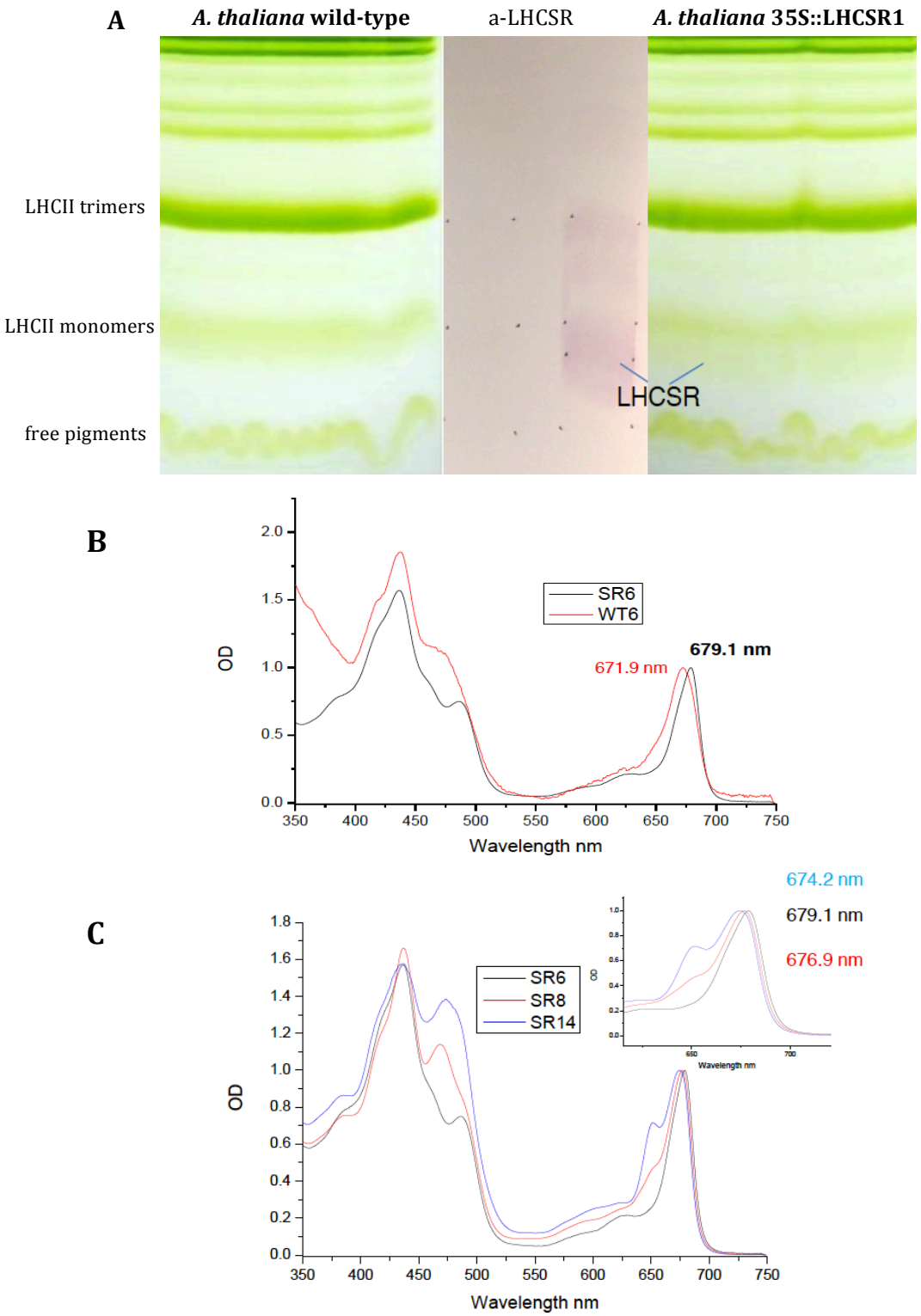

Figure 1.5. Resolution and spectroscopic analysis of 35S::LHCSR1 pigment-binding complexes. *(A) Deriphat-PAGE (7%) of At WT and At npq4+35S::LHCSR1 unstacked thylakoids, solubilized in 0.8% α-DM. Bands were cut directly from the gel and eluted in 10mM HEPES/0.03% α-DM. Eluted fractions were immunoblotted against α-LHCSR antibody. Absorption spectra was taken for all eluted fractions. (B) Spectroscopic comparison of eluted band 6 from At WT and At npq4+35S::PpLHCSR1. (C) Absorption spectra of band 6 (LHCSR1), fraction 8 (LHCII monomers) and band 14 (LHCII trimers) of At npq4+35S::LHCSR1.*

Next step was fractionation and spectroscopic analysis for the remaining part of the gel. For this, a broad molecular mass range (20-100-kD), including LHC monomers, was cut into thin slices (0.5 cm height) that were grinded and eluted in a buffer solution containing 20 mM Hepes pH 7.8, 0.03 % α-DM and 50 % w/v glicerol for 2 hours. After centrifugation, one third from each slice (around 200ul) was submitted to absorption spectroscopy. Absorption spectra of the fractions eluted from this gel region showed the presence of a complex characterized by a Qy absorption peak red-shifted to 679.1 nm versus 671.9nm of the corresponding area of the gel in the *A. thaliana* wild-type lane (Figure 1.5B).

1.5 NPQ activity of *Pp*LHCSR1 in *A. thaliana*

1.5.1 NPQ measurements using fluorescence video-imaging

After assessing the successful expression of LHCSR1 and its accumulation in thylakoid membranes of *A. thaliana npq4* plants, which are completely impared in qE because of the lack of PSBS expression, we proceeded to test the quenching activity of the protein *in planta.* As previously mentioned, the activity of PSBS and LHCSR is additive and independent in *P. patens* plants (Alboresi et al., 2010; Gerotto et al., 2012). To this direction, we measured the chlorophyll fluorescence quenching of wild-type, *npq4* plants and 14 independent 35S::LHCSR1 complemented plants by video-imaging following a standard procedure for *A. thaliana*. The protocol consisted of a 45min dark adaptation of leaves that will be measured, followed by a 5min NPQ light induction using white actinic light (*1200 μmol m^{-2} s^{-1})* and a 5min phase of dark recovery. When the protocol was applied for the first time, all genotypes analyzed had the same fluorescence profile and the expression of LHCSR1 did not lead to any special increase of quenching activity (Figure 1.6, first row panels). However, when the illumination period was applied for the second time (Figure 1.6, second row panels) a more pronounced quenching was detected in 35S::LHCSR1 lines if compared to *npq4*. Two additional NPQ measurements were applied showing an even further pronounced chlorophyll fluorescence quenching in 35S::LHCSR1 lines between the second and the third measurements while was very similar between the third and the fourth measurement (Figure 1.6, third and fourth row panels). All measurements are the result of three repetitions per genotype in the case of *A. thaliana* wild-type and *npq4* and an average of 3 replicas per line in the case of the 35S::LHCSR1 complemented plants. Due to the large numbers of lines, a simplified figure with given below, including the two control genotypes (wild-type, *npq4*) and an

average of nine independent 35S::LHCSR1 lines with similar level of protein accumulation (Figure 1.7).

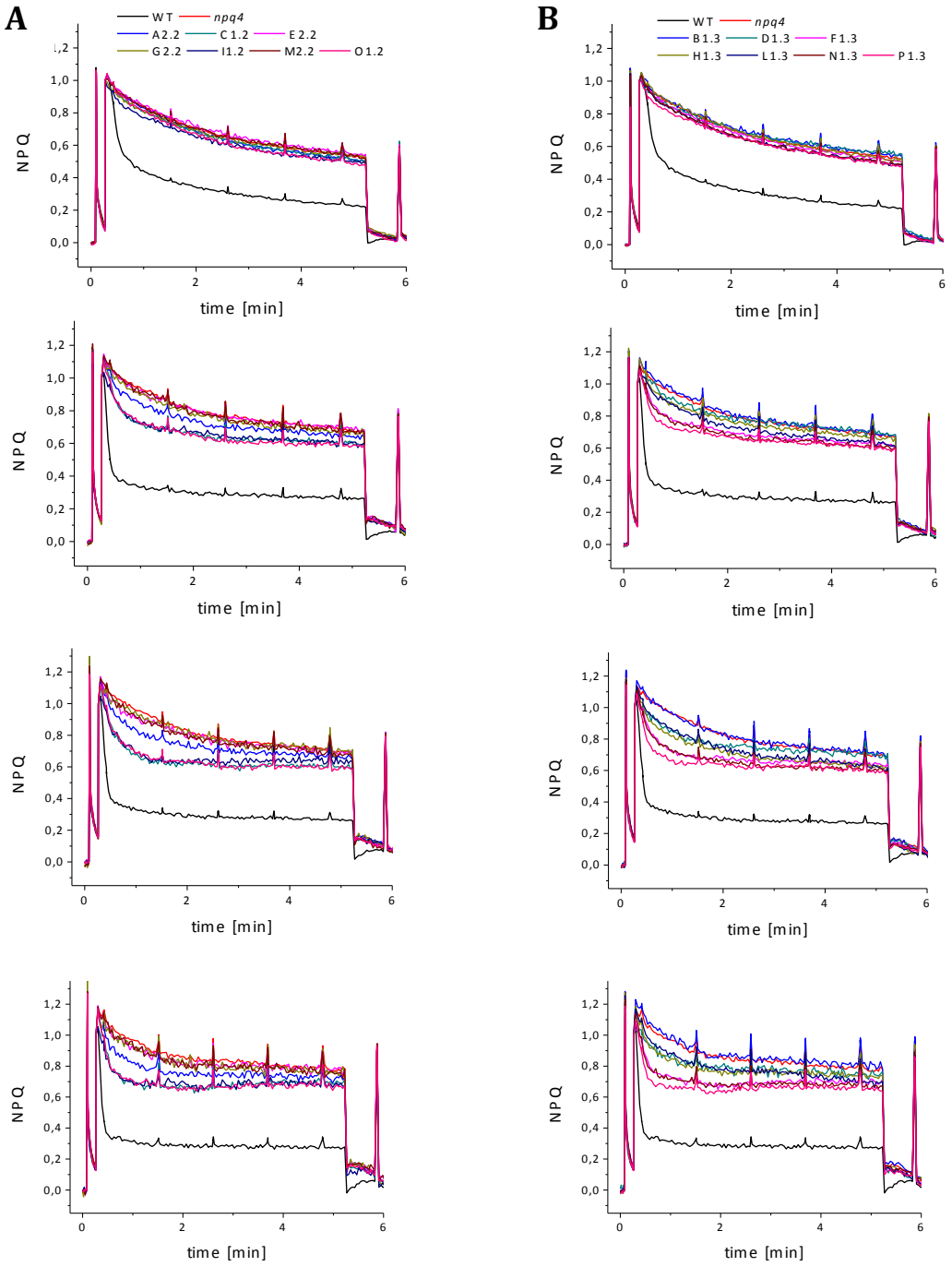

Figure 1.6. Chlorophyll fluorescence quenching in independent 35S::LHCSR1 lines. *A. thaliana plants from two different series (series 1 on the left, series 2 right) were dark adapted for 45 minutes before measurement. After an Fm measurement, NPQ was induced by 5 minutes of white actinic light (1200 µmol m^{-2} s^{-1}; white bar) followed by 5 minutes of dark relaxation. After that, the same protocol was repeated three successive times. (A) Fluorescence induction curve measured for 7 independent lines (series 1). Control wild-type and npq4 line are indicated with black and red respectively. (B) Fluorescence induction measured for another 7 independent lines (series 2).*

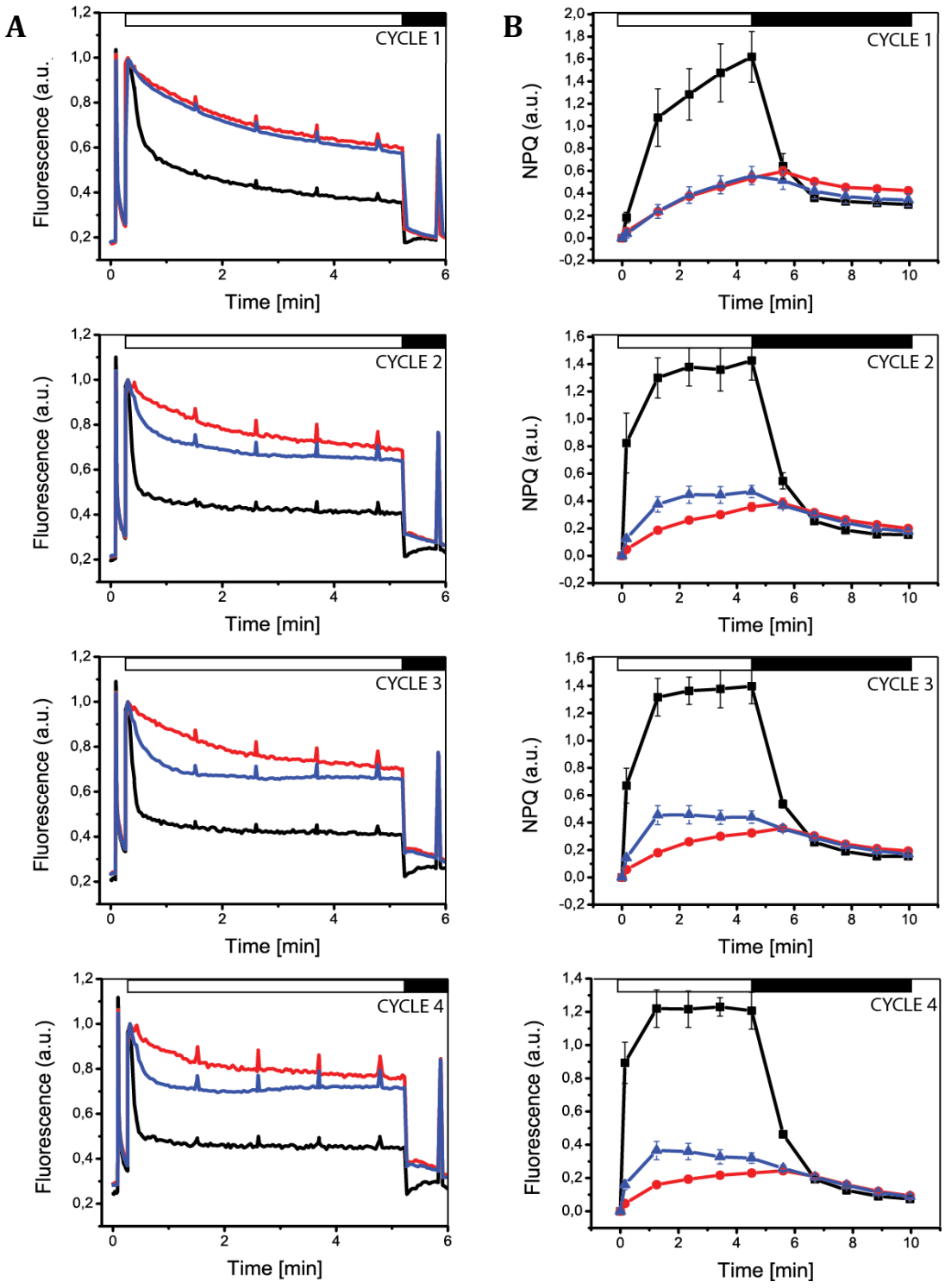

Figure 1.7. Chlorophyll fluorescence quenching in independent 35S::LHCSR1 lines. *(A) Fluorescence induction curve and (B) NPQ, calculated as quenching of maximal fluorescence (Fm - Fm')/Fm' for every saturating flash. Black line, WT (n=3). Red line, npq4 (n=3). Blue line, 35S::LHCSR1 (n=9 independent T1 lines). As before, A. thaliana plants were dark adapted for 45 minutes before measurement. After an Fm measurement, NPQ was induced by 5 minutes of white actinic light (1200 µmol m^{-2} s^{-1}; white bar) followed by 5 minutes of dark relaxation (CYCLE 1). After that, the same protocol was repeated three successive times (CYCLES 2 to 4). Each panel indicates the measuring cycle.*

The same genotypes were tested using two additional different measuring protocol, this time by using just one cycle of NPQ but with an extended period of illumination and dark recovery, thus avoiding intermediate dark recovery cycles and allowing zeaxanthin to accumulate continuously. For this, leaves from 35S::LHCSR1 and control *npq4* plants were dark adapted for 45 minutes, followed by two NPQ measurement protocols: **Protocol 1**, using 10 minutes of actinic light treatment followed by 15 minutes of dark recovery and **protocol 2** which included 30 minutes of actinic light and a 15-minute dark relaxation period.

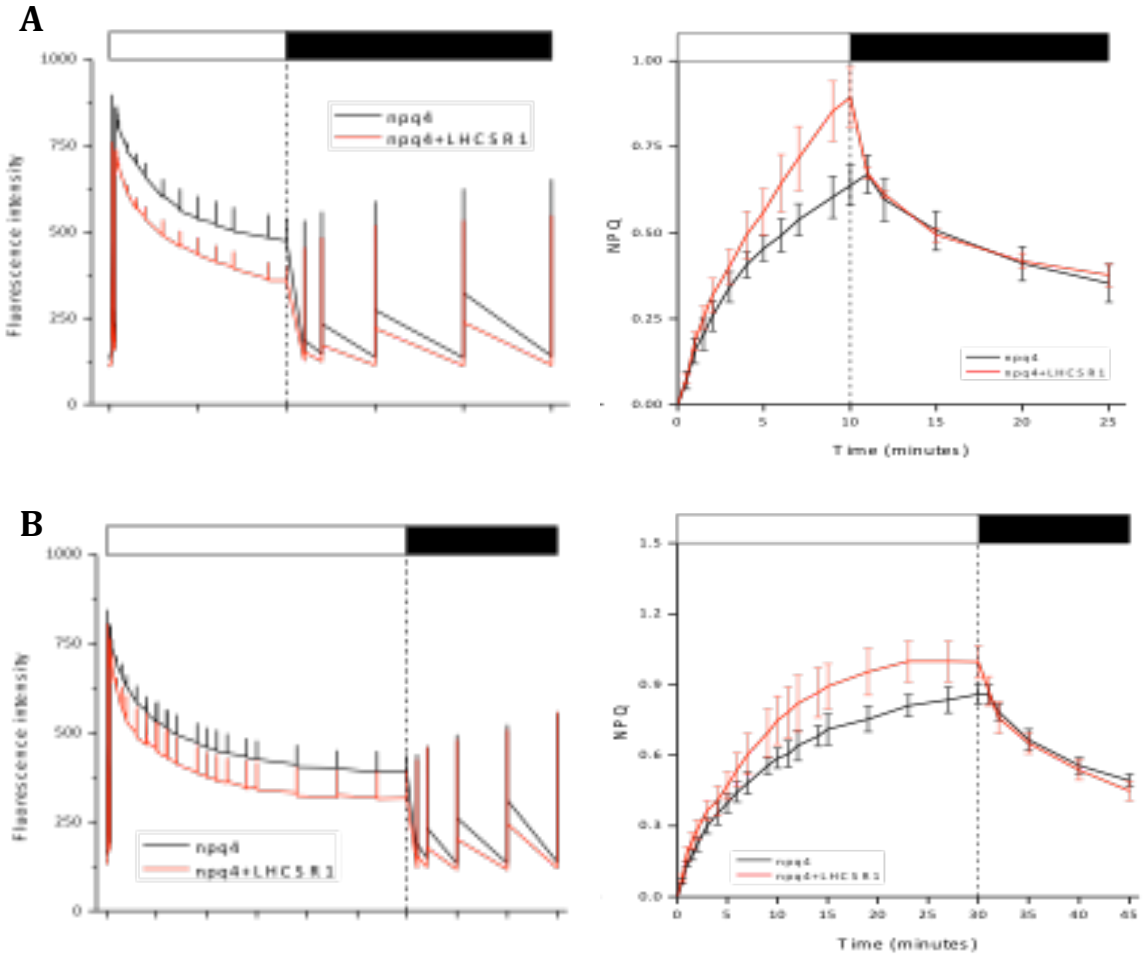

Figure 1.8. NPQ induction in 35S::LHCSR1 lines using different measuring protocols. *NPQ of Chl fluorescence was measured on leaves detached of 4-5-weak old plants at room temperature. The results of two different measuring protocols are presented: Protocol 1 includes 10 minute of actinic light treatment (800) followed by 15 min of dark recovery (upper panels) while protocol 2 has an extended actinic light treatment of 30 minutes and 15 minutes of dark recovery (lower panels). A) Fluorescence induction curve for each of the measuring protocols applied. B) NPQ, calculated as quenching of maximal fluorescence (Fm - Fm')/Fm' for every saturating flash. Black line, npq4 (n=5). Red line, 35S::PpLHCSR1 (n=5). A. thaliana leaves were dark adapted for 45 minutes. After an Fm measurement, NPQ was induced by either 10 or 30 minutes of white actinic light (800 µmol m^{-2} s^{-1}; white bar) followed by 15 minutes of dark relaxation in a single measurement cycle.*

	10' light and 15'dark		30' light and 15'dark	
Genotype	NPQ_{max}	qE	NPQ_{max}	qE
npq4	0.64±0.06	0.23±0.05	0.86±0.04	0.30±0.03
*npq4+35S::*LHCSR1	0.89±0.09	0.48±0.09	1.00±0.09	0.45±0.06

Table I. NPQ and qE calculation of measured control and 35S::LHCSR1 plants. *Results for each genotype after measurement with two different protocols. The maximum NPQ as well as qE (fast relaxation) are presented. qE is calculated as the last point in the light phase minus the second point in the dark.*

As seen in Figure 1.8, LHCSR-complemented plants have an increased NPQ amplitude compared to the non-transformed lines, while as calculated in table they exhibited a higher dark recovery when the actinic light was switched off in both of the measuring protocols used ($qE_{LHCSR1} = 0.89$ *vs* $qE_{control} = 0.64$).

1.5.2 NPQ measurement using pulse-amplitude modulated fluorescence (PAM)

In order to verify the observed quenching activity of LHCSR1, we refined the NPQ analysis by pulse-amplitude modulated (PAM) measurements. We chose two plant lines with high LHCSR1 accumulation (lines O1 and P1) and followed a protocol similar to the one we used for the video-imaging fluorescence measurements. Leaves from control *npq4* plants and the two transgenic 35S::LHCSR1 lines were dark adapted for 45minutes and then measured in a series of double NPQ with extended light period and dark recovery: 10min of white actinic light, 10min of dark relaxation and then another 10min of actinic light followed by an additional 10min dark recovery. The quenching observed during the actinic phase treatment was visible both at 800 μmol photons m^{-2} s^{-1} and 1200 μmol photons m^{-2} s^{-1} and corresponded to higher qE activity during the dark recovery. The quenching observed during the actinic phase treatment was visible at 1200 μmol photons m^{-2} s^{-1} and corresponded to higher qE activity during the dark recovery. As seen in Figures 1.9A,B during the first actinic light treatment there were little differences between *npq4* plants and the 35S::LHCSR1 complemented line as in the case of NPQ measurement with video-imaging fluorescence, while a clear difference emerged during the first dark relaxation.

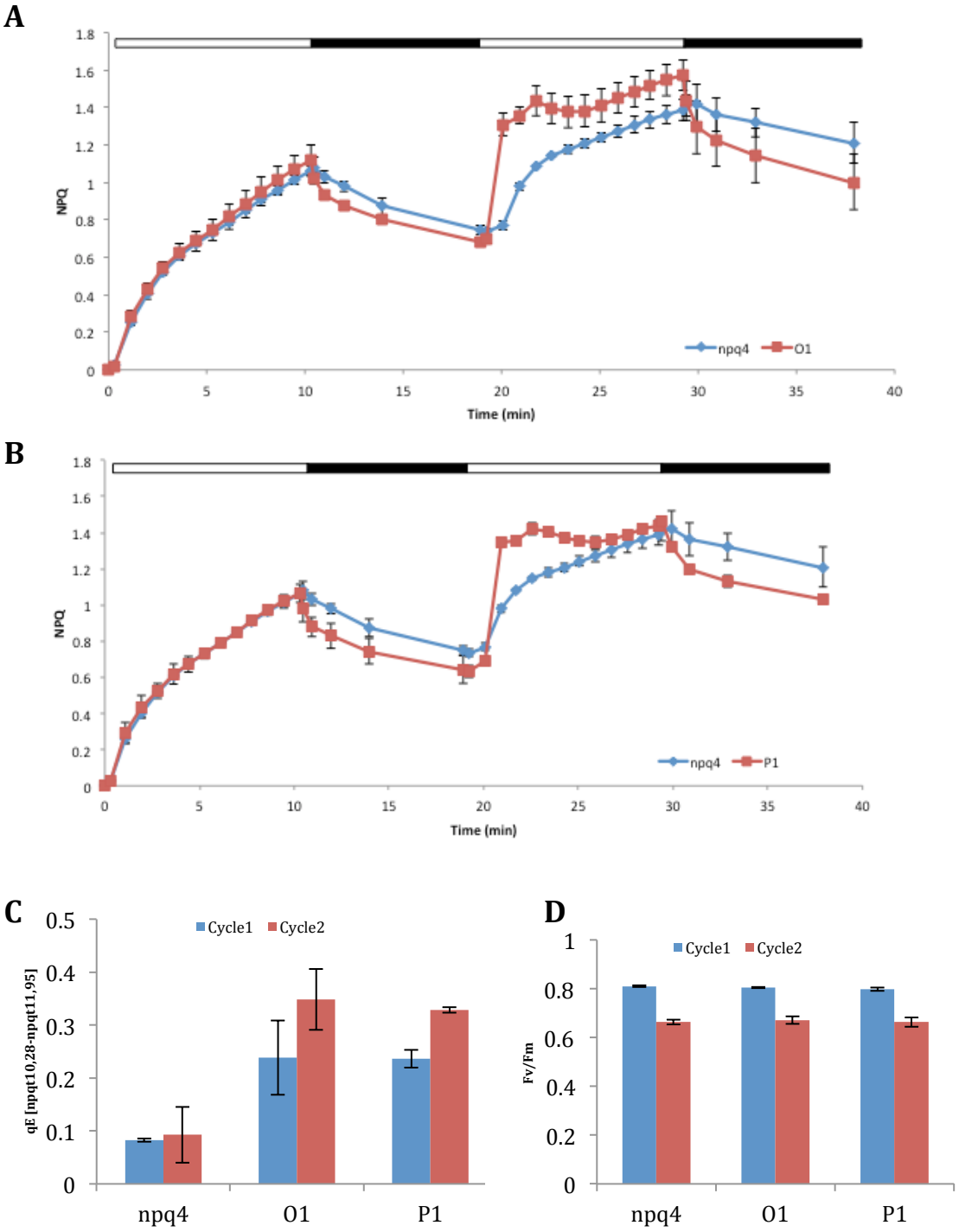

Figure 1.9. NPQ measured using pulse-amplitude modulated fluorescence. *NPQ of dark adapted leaves from A. thaliana npq4 and two 35S::LHCSR1 plant lines (O1, P1) was in a standard light treatment/dark recovery protocol. (A) Two successive NPQ cycles using 1200 µmol photons m^{-2} s^{-1} of actinic light (10min light treatment/10min dark recovery). Light and dark periods are indicated with white and black bars respectively. Genotypes measured: A. thaliana npq4 (blue line), 35S::LHCSR1 line O1 (red line). Measurements are the average of three replicas. (B) Two successive NPQ cycles using 1200 µmol photons m^{-2} s^{-1}. Genotypes measured: A. thaliana npq4 (blue line), 35S::LHCSR1 line O1 (red line), (C) Calculation of NPQ relaxation (qE) calculated as the last point during light phase minus the second point in the dark. (D) Calculation of Fv/Fm parameter.*

In fact, a sudden NPQ relaxation was detected two minutes after the actinic light was switched off (Figure 1.9A). When the second measurement was started, NPQ rose quickly in the 35S::LHCSR1 complemented lines, showing , in addition, a much faster dark recovery than in *npq4* if compared to the kinetic during the first cycle of NPQ. The lines lacking PSBS (control *npq4*) had a qE value of 0.068 at the fourth point of dark relaxation of the second measurement at 1200 μmol photons m^{-2} s^{-1} while transgenic lines expressing LHCSR1 had a qE of 0.427 and 0.306 (Figure 1.9C).

1.6 LHCSR1 and zeaxanthin accumulation

As previously observed from the video-imaging fluorescence and PAM measurements, the activity of LHCSR1 in *A. thaliana* was detected only after repeated cycles of NPQ measurements. In the last PAM measurement described above (Figure 1.9) an immediate increase of NPQ in the 35S::LHCSR1 complemented lines was detected right after the second cycle of illumination was initiated. Since a first 10-minute period of illumination was performed in advance, we hypothesized that zeaxanthin accumulated during that first actinic treatment was the reason behind the pronounced LHCSR-dependent quenching at the start of the second. To determine the pigment content of both *npq4* and LHCSR1-complemeted *npq4* plants during the PAM double-NPQ measurements, chlorophyll and carotenoid content was measured by HPLC.

The pigment content of leaf samples before the NPQ measurement (dark-adapted state), during NPQ (state of illumination) and right after the light phase of NPQ (dark-adaptation) was measured. Results from HPLC analysis showed that zeaxanthin content in all phases for both genotypes is the same (Table I) with the LHCSR1-complemented plants showing an increasing chlorophyll quenching activity during the light phase but also activation of qE in the first minute of dark recovery during the second NPQ cycle (Figure 1.9).

	Chl *a/b*	Car/Chl	V+A+Z	DEP	Neo	Vio	Ant	Lut	Zea	β-car
T_0_Dark										
npq4	2.59 ± 0.08	26.4 ± 1.1	2.6 ± 0.2		4.0 ± 0.2	2.6 ± 0.2		12.5 ± 0.5		6.4 ± 0.7
Line O1	2.65 ± 0.09	27.1 ± 1.4	3.3 ± 0.8		3.9 ± 0.1	3.3 ± 0.8		12.8 ± 0.5		6.2 ± 0.1
Line P1	2.60 ± 0.05	28.5 ± 1.7	3.6 ± 0.8		4.2 ± 0.4	3.6 ± 0.8		13.7 ± 0.9		5.9 ± 0.6
T_{10}_Light										
npq4	2.50 ± 0.07	26.6 ± 0.7	3.4 ± 0.1	0.53 ± 0.07	4.1 ± 0.2	1.4 ± 0.2	0.3 ± 0.1	12.8 ± 0.5	1.7 ± 0.3	6.3 ± 0.2
Line O1	2.59 ± 0.13	26.7 ± 1.2	4.3 ± 0.1	0.44 ± 0.04	3.9 ± 0.3	2.2 ± 0.1	0.4 ± 0.0	12.9 ± 1.0	1.7 ± 0.2	5.7 ± 0.7
Line P1	2.59 ± 0.03	28.1 ± 0.9	4.7 ± 0.2	0.48 ± 0.02	4.1 ± 0.1	2.2 ± 0.2	0.4 ± 0.0	13.4 ± 0.1	2.0 ± 0.1	5.8 ± 0.5
T_{20}_Dark										
npq4	2.60 ± 0.09	26.7 ± 2.7	3.4 ± 0.2	0.53 ± 0.01	4.0 ± 0.7	1.3 ± 0.1	0.6 ± 0.0	12.6 ± 1.6	1.5 ± 0.1	6.7 ± 0.6
Line O1	2.65 ± 0.08	26.4 ± 1.1	4.2 ± 0.4	0.42 ± 0.03	3.6 ± 0.1	2.1 ± 0.3	0.6 ± 0.1	12.6 ± 0.3	1.5 ± 0.1	6.0 ± 0.5
Line P1	2.58 ± 0.06	28.1 ± 2.4	4.7 ± 1.2	0.48 ± 0.02	4.1 ± 0.4	2.2 ± 0.7	0.6 ± 0.1	13.6 ± 1.2	2.0 ± 0.4	5.7 ± 0.3
T_{30}_Light										
npq4	2.48 ± 0.03	27.6 ± 1.4	3.6 ± 0.2	0.63 ± 0.01	4.3 ± 0.3	1.2 ± 0.1	0.3 ± 0.1	13.4 ± 0.6	2.1 ± 0.1	6.3 ± 0.6
Line O1	2.63 ± 0.01	27.1 ± 2.0	4.4 ± 0.6	0.54 ± 0.03	3.8 ± 0.3	1.9 ± 0.4	0.4 ± 0.1	13.0 ± 1.0	2.2 ± 0.2	5.9 ± 0.1
Line P1	2.60 ± 0.07	28.1 ± 1.2	4.4 ± 0.5	0.61 ± 0.01	4.1 ± 0.3	1.5 ± 0.2	0.4 ± 0.0	13.5 ± 0.9	2.5 ± 0.3	6.2 ± 0.2
T_{40}_Dark										
npq4	2.53 ± 0.03	27.6 ± 0.9	3.6 ± 0.2	0.59 ± 0.02	4.2 ± 0.2	1.2 ± 0.1	0.6 ± 0.1	13.2 ± 0.4	1.8 ± 0.2	6.6 ± 0.2
Line O1	2.55 ± 0.06	26.5 ± 1.1	4.0 ± 0.6	0.51 ± 0.02	3.8 ± 0.1	1.6 ± 0.3	0.7 ± 0.1	13.1 ± 0.8	1.7 ± 0.2	5.7 ± 0.6
Line P1	2.54 ± 0.09	27.6 ± 0.8	4.1 ± 0.5	0.56 ± 0.03	4.1 ± 0.1	1.5 ± 0.3	0.7 ± 0.0	13.4 ± 0.8	2.0 ± 0.3	6.1 ± 0.4

Table II: Photosynthetic pigment content of *Arabidopsis thaliana npq4* mutant and *35S::LHCSR1* transgenic lines. Pigment content was determined mimicking the two consecutive periods of illumination with white light used for NPQ measurements (1200 mmol photons m^{-2} s^{-1}, 25 min, 24°C). Data are normalized to 100 Chl a + b molecules and are expressed as mean SD (n = 3). T_0_Dark are plants dark adapted for 45 min, T_{10}_Light are plants illuminated for 10 minutes during the first NPQ measurement, T_{20}_Dark are plants that recovered for ten minutes during the first NPQ cycle, T_{30}_Light are plants illuminated for ten minutes during the second NPQ cycle and T_{40}_Dark are plants that recovered for ten minutes during the second NPQ cycle.

As mentioned in chapter 1, the activity of LHCSR1 protein in *P. patens* depends on the conversion of violaxanthin into zeaxanthin through the xanthophyll cycle and the strong accumulation of the latter. Previous studies have shown that NPQ activation in *P. patens* strongly depends on zeaxanthin accumulation, especially for its LHCSR-dependent component. This was observed by the decrease in chlorophyll fluorescence quenching induced by the *vde* KO mutation on *psbs lhcsr* KO plants both *in vitro* and *in vivo* upon excess light treatment (Pinnola et al., 2013). Since LHCSR-dependent mechanisms activating NPQ in *P. patens* depend on zeaxanthin and VDE mutants are impaired in their capacity to resist excess light treatments, we decided to perform a similar experiment in order to verify that the quenching activity of LHCSR1 expressed in *A. thaliana* depends also on zeaxanthin accumulation. To this direction we performed another set of NPQ

measurements, this time by infiltrating dark-adapted leaves from *A. thaliana* wild-type and 35S:: LHCSR1 plants with dithiothreitol (DTT). DTT acts as an inhibitor of violaxanthin de-epoxidase enzyme (VDE) thus blocking the removal of epoxy groups from violaxanthin to produce zeaxanthin. Dark-adapted leaves from *A. thaliana npq4* and transgenic LHCSR1 plants were infiltrated with or without DTT and NPQ measurement was performed as before (successive cycles of 1200 µmol photons m^{-2} s^{-1}). Infiltration of plants with the DTT-less buffer had, as expected, no effect in NPQ amplitude and dark-recovery apart from the already seen quenching activity in LHCSR1-complemented plants. However, this quenching activity but also de-activation of qE in dark was completely lost upon infiltration of transgenic plants with the buffer containing DTT (Figure 1.10A,B).

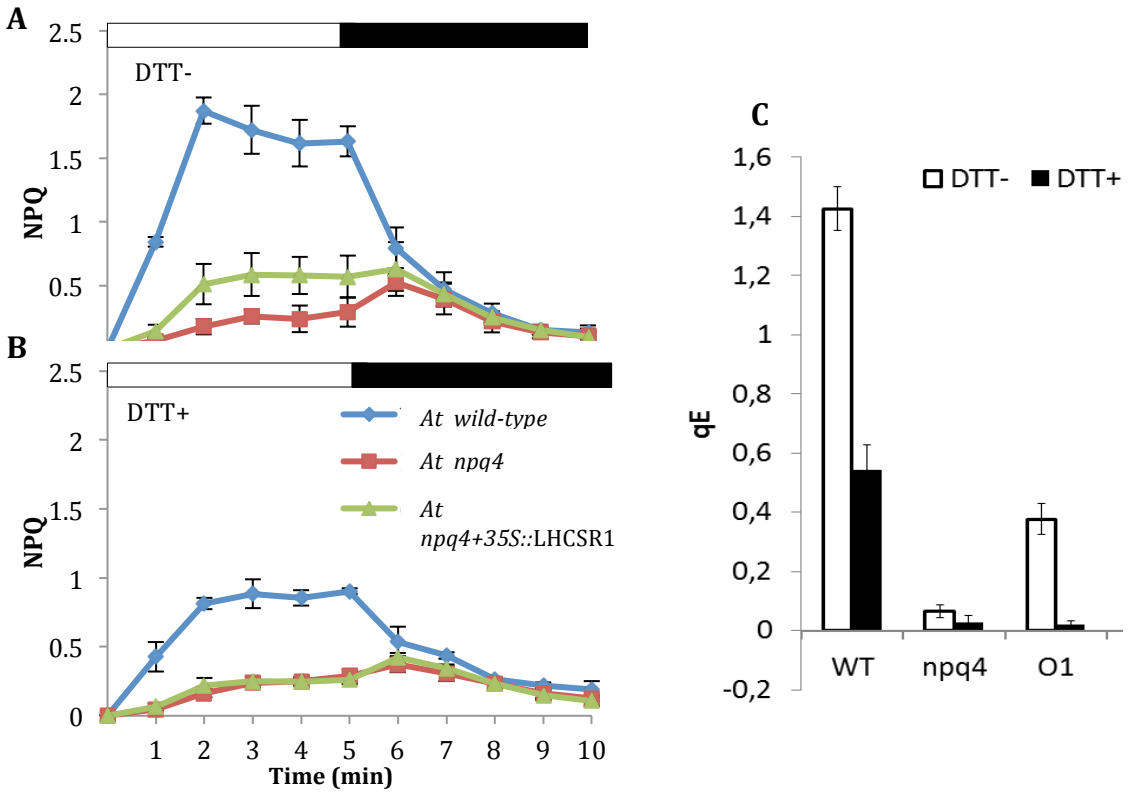

Figure 1.10. NPQ measurement after infiltration of A. thaliana leaves with DTT. *Dark-adapted leaves from A. thaliana wild-type and 35S::LHCSR1 were infiltrated with DTT, inhibiting VDE enzyme thus blocking zexanthin production. Successive cycles of NPQ were applied according to a standard protocol (5' actinic light / 5' dark recovery). Results showed from the final NPQ cycle (A) NPQ chart of wild-type, 35S::LHCSR1 and npq4 genotypes infiltrated with a DTT-less buffer (control), presented with blue, green and red lines respectively (B) NPQ chart of wild-type, 35S::LHCSR1 and npq4 genotypes infiltrated with DTT (the line colors represent the same genotypes as in the previous chart), (C) NPQ recovery (qE) of each genotype (infiltrated with and without DTT) calculated as the last point in the light phase minus the second point in the dark. All NPQ charts are results of three replicas.*

1.7 Correlation between LHCSR1 accumulation and NPQ activity

LHCSR1 from *P. patens* is expressed in *A. thaliana*, PSBS-less, *npq4* plants, having a quenching activity during repeating cycles of illumination and a dark recovery once the light is switched off. As a first attempt to understand if these events correlated positively to the amount of expressed LHCSR1 leaves from 35S::LHCSR1-complemented lines with low and high qE relaxation level were selected. Leaves from 3 low qE lines (qE < 0.05) and 3 high qE lines (qE > 0.15) were homogenized creating two individual samples. Four different Chl concentrations (0.5, 1, 2 and 4 ug) were loaded for each sample and raised against homemade a-LHCSR and a-CP43 antibodies. As additional controls, total extracts from *A. thaliana npq4* and *P. patens* wild-type plants were also loaded. Results showed that the lines with lower qE accumulated LHCSR in lower levels, compared to the higher qE lines (Figure 1.11).

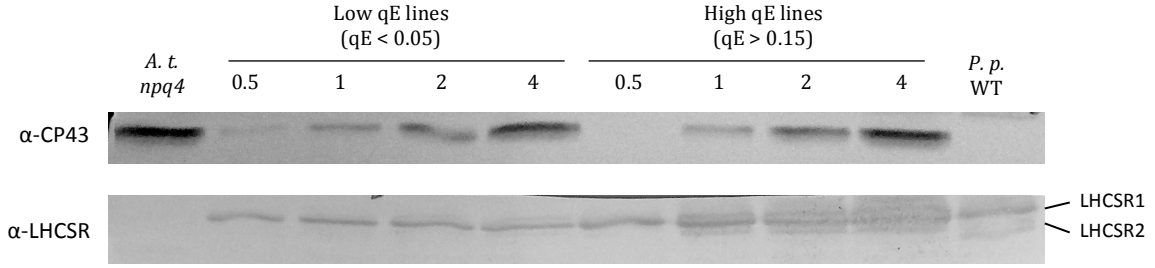

Figure 1.11. Immuno-blotting of 35S::LHCSR1 lines with different qE relaxation. *Total leaf extracts from plant lines showing low qE (homogenized leaves from 3 independent lines with qE<0.05, left part) and high qE relaxation (homogenized leaves from 3 lines with qE>0.15, right part) were loaded on a SDS-PAGE gel and immuno-blotted against a-LHCSR and a-CP43 antibodies. Four different amounts of Chl (0.5 - 4 ug) were loaded for the two homogenized samples. As additional controls A. thaliana npq4 and P. patens wild-type extracts were also loaded (4 ug Chl for each one). At: Arabidopsis thaliana; Pp WT: Physcomitrella patens wild type.*

In order to verify the correlation between quenching activity and LHCSR1 accumulation, leaves from 35S::LHCSR1-complemented plant lines (T2, n=9) were dark adapted and measured for their NPQ activity following a standard protocol (4 successive cycles of 5min actinic light treatment and 5 min of dark relaxation, Figure 1.12A). Total leaf extracts from the same lines were analyzed by western blot and developed against homemade LHCSR antibodies (Figure 1.12B), expressing the protein in different levels. After extracting LHCSR1 intensity for each plant line sample, the maximum NPQ (NPQ max) but also the fast dark recovery of the mechanism (qE) values were plotted together with the LHCSR1 accumulation level. In both cases there is a positive correlation between LHCSR1 accumulation and either NPQ induction (R^2=0.933) or qE relaxation (R^2=0.929, Figure 1.12C).

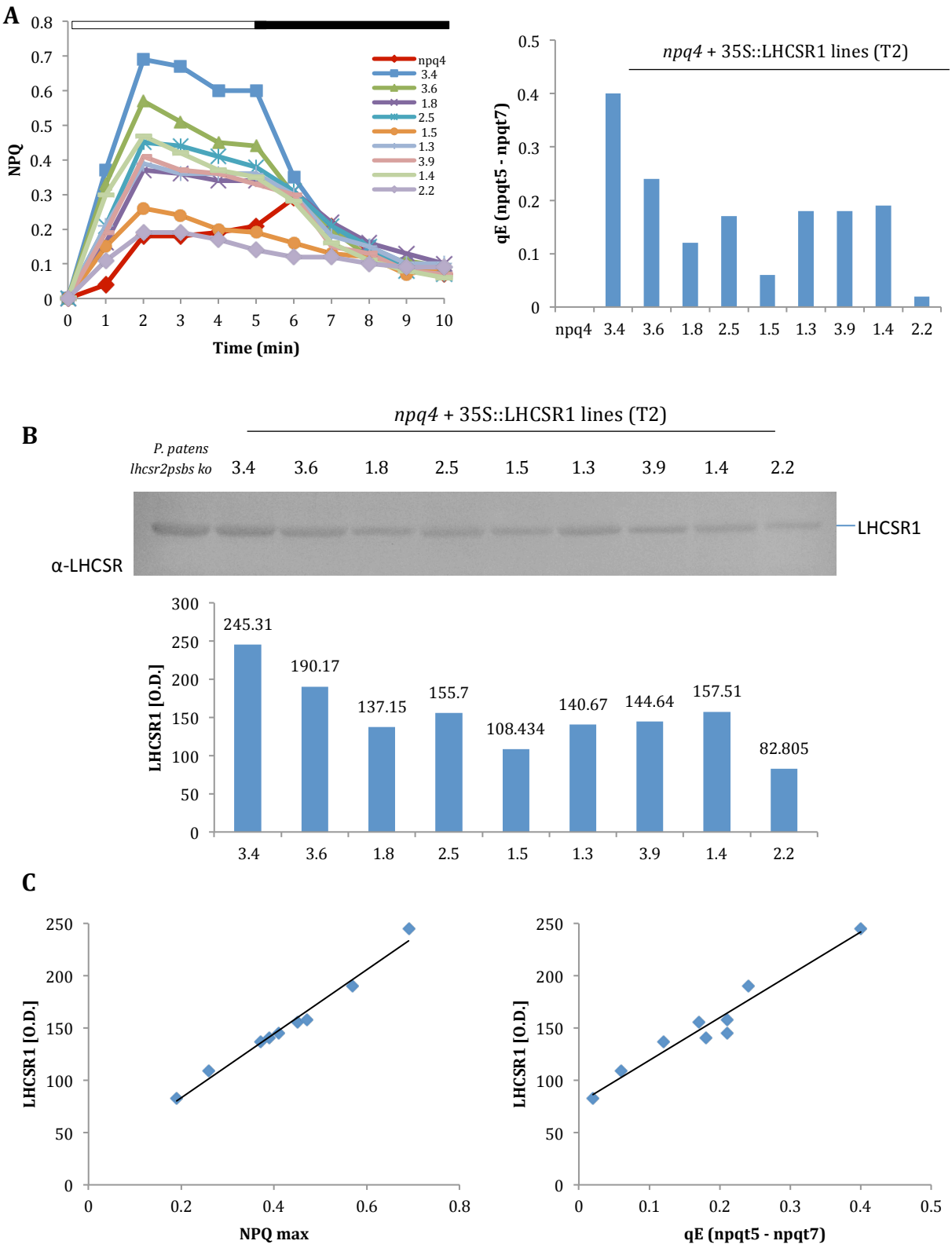

Figure 1.12. Correlation between NPQ activity and LHCSR1 accumulation. *(A) NPQ of T2 independent 35S::PpLHCSR1 lines (n=9) measured using a specific protocol (4 cycles of 5min actinic light, 5min of dark recovery). White and black bars represent the light and dark phase. NPQ chart of the final cycle is presented on the left, qE recovery calculated as the last point in the light phase minus the second point in the dark phase (npq t5 – npq t7) is shown on the right, (B) After NPQ measurement total leaf extracts from each line were loaded on a SDS-PAGE on a basis of 0.75ug Chl and immuno-blotted against a-LHCSR homemade antibodies. P. patens lhcsr2psbs ko thylakoids were loaded as control, (C) The protein intensity of each sample is calculated and plotted together with the maximum NPQ yielding a positive correlation of R^2=0.9804 (left chart) and the qE recovery with a positive correlation of R^2=0.944 (right chart).*

1.8 LHCSR1 in *A. thaliana*: Dependence on light intensity

In order to better understand the quenching activity of LHCSR1 *in planta*, three *At* 35S::LHCSR1 lines with high and intermediate NPQ activity were selected and measured using different light intensities. More specifically, NPQ was measured on leaves from transgenic plants of the same age, starting from a very low light intensity (100uE) up to a light intensity of 1000uE. Before each measurement leaves were dark-adapted for 45min, pre-treated with actinic light (800uE) for 15min in order to have an equal amount of zeaxanthin in all lines and left to relax for 10min in the dark. Leaves from *A. thaliana* wild-type and *npq4* plants of the same age were used as controls. When low light was applied, an initial activation of NPQ occurs in all *A. thaliana* genotypes, which rapidly drops due to activation of the downstream ATPase dissipating the established ΔpH for ATP synthesis. However, as the intensity of actinic light increases, plants activate NPQ with *Pp*LHCSR1 complemented lines showing activity right from 200uE (Figure 1.13).

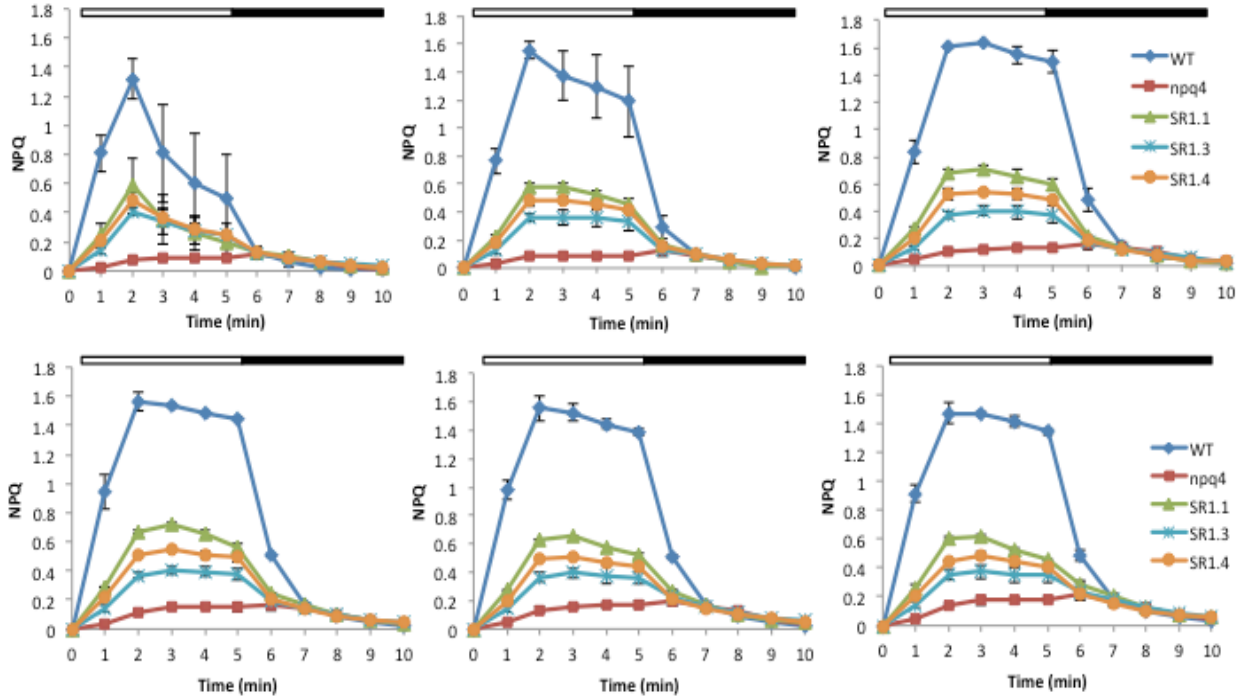

Figure 1.13. Testing 35S::LHCSR1 lines in various light intensities. *Three different At npq4+35S::PpLHCSR1 lines with high and intermediate NPQ activation were tested in a variety of actinic light intensities. Leaves were dark adapted for 45min, pre-treated with 800uE of actinic light for 15min and left to relax in the dark for 10min before the NPQ measurement. Each measurement corresponds to one single NPQ cycle of 5min actinic light and 5min dark recovery. From top left to right: 100uE, 200uE, 400uE, 600uE, 800uE and 1000uE of actinic light. Leaves from At npq4 (red line) and At wild-type (blue line) were used as controls.*

Discussion

The moss *Physcomitrella patens* is an evolutionary intermediate between higher plants and green algae as both PSBS and LHCSR act in an additive way catalyzing a strong NPQ activity, with LHCSR1 being the major NPQ trigger (Alboresi et al., 2010; Gerotto et al., 2012). In addition, in *P. patens* the xanthophyll zeaxanthin serves an essential role on the control of LHCSR-dependent NPQ (Pinnola et al., 2013). Recent studies on the biochemical properties of LHCSR1 using heterologous expression systems such as *N.tabacum* and *N. benthamiana* together with information coming from recombinant proteins refolded *in vitro* have shown that LHCSR1 can be correctly folded binding mainly chlorophyll a (Pinnola et al., 2015). In this chapter we showed the heterologous expression of LHCSR1, in the thylakoid membranes of the *Arabidopsis thaliana npq4* mutant and studied the NPQ activity of the generated LHCSR1-complemented transgenic plants.

The strategy adopted was the heterologous expression of *P. patens* LHCSR1 in A. *thaliana npq4*, as this mutant lacks PSBS protein and so the observed quenching activity would be attributed only to the presence of LHCSR1. Moreover, *A. thaliana* contains all the chromophores needed for LHCSR protein folding and can be easily treated *in vivo* with high light in order to accumulate sufficient amounts of zeaxanthin, essential for LHCSR1 activity. Finally, *agrobacterium*-mediated transformation of *A. thaliana* used throughout this work, is a well-known and broadly used method which allows screening of different constructs in different plant genotypes before moving to higher throughput expression systems.

The heterologous-expressed LHCSR1 protein was correctly addressed to thylakoid membranes with an apparent molecular weight identical to that of *P. patens* thylakoids observed in SDS-PAGE, strongly suggesting a correct targeting and processing of the pre-protein encoded by the construct. This was verified also during the screening of the T2 and T3 generations where the protein was expressed in higher levels due to the presence of homozygous transgenic plants.

Separation of grana and stromal-membrane compartments by solubilization with a-DM from extracted thylakoids of LHCSR1-complemented plants, showed that the protein was mainly accumulated in the stromal partitions of thylakoids with only a small amount being present in the grana region, consistent with the localization data from LHCSR1-complemented N. *benthamiana* plants (Pinnola et al., 2015). The clear differences in the

Chl a/b ratio (2.5 for thylakoids, 1.5 for grana fraction and 3.8 for stroma-exposed membranes) demonstrate that the fractions originate from distinct compartments of the thylakoid membrane. This result was further verified by grana and stromal membranes fractionation with different a-DM concentrations, showing increasing accumulation of LHCSR1, as the a-DM concentration used for the solubilization of stromal membranes gets higher. This result is also supported by western blot analysis, indicating that LHCSR1 is a protein easily extracted out of thylakoid membranes and suggesting its localization in the stromal exposed thylakoid domains. Even though the factors leading to the localization of the protein in the stromal membranes are not yet known, it may be attributed to the affinity of LHCSR1 with one or more proteins that co-localize in the same compartement.

Further characterization focused on the formation of a pigment binding complex and spectroscopic properties. Non-denaturing Deriphat-PAGE was previously applied as a fast method for purification of LHCSR proteins from *P. patens* owing to the higher mobility in this type of gels with respect to other non-recombinant monomeric LHCs. The accumulation of LHC minor antenna proteins has a stabilizing effect on super-complexes stability (Caffarri et al., 2009; de Bianchi et al., 2011) but LHCSR1 has not such a structural role when expressed in *npq4 A. thaliana* plants, as seen from the overall distribution of LHC-complexes. LHSCR1 was isolated by protein elution from the fragment of the fast-running monomeric bands. Spectroscopic analysis of the eluted fragments revealed a pigment-binding protein with properties similar to recombinant *C. reinhardtii* LHCSR3 refolded *in vitro* (Bonente et al, 2011) and a red-shifted Q_y absorption peak at approximately 679.1 nm, which interestingly matches that of the purified LHCSR1 from *P. patens*. The activity of LHCSR1 protein has been evaluated measuring NPQ kinetics of LHCSR1-complemented plants with respect to non-transformed *npq4*.

NPQ kinetics was obtained by applying different measuring protocols either with video-imaging or pulse-modulated amplitude fluorescence. In both cases results indicated a partial NPQ activity, which was revealed only after successive short cycles or single cycles of prolonged strong light treatment were applied, clearly indicating a zeaxanthin build-up. This is consistent to the fact that in the homologous system (*P. patens*) LHCSR1 is strictly zeaxanthin dependent (Pinnola et al., 2013). LHCSR1 zeaxanthin dependence was confirmed after infiltration of LHCSR1-complement plants with dithiothreitol (DTT), an inhibitor of VDE enzyme in the xanthophyll cycle, which blocks

the conversion of violaxanthin into zeaxanthin. Loss of NPQ activity in the DTT-infiltrated LHCSR1-complemented plants clearly suggested the need of zeaxanthin in the LHCSR1-dependent NPQ.

NPQ activity of the heterogously expressed LHCSR1 was tested using a variety of light intensities, ranging from 100 to 1000 μmol photons m^{-2} s^{-1}. A transient NPQ activity was observed in low light (200 μmol photons m^{-2} s-1) in the LHCSR1-complemented lines in contrast to control *npq4*, showing that this activity is not present in the absence of PSBS but is recovered in the presence of LHCSR1. Induction of transient NPQ during illumination of dark-adapted plants, with low light intensities used has been previously described as the effect of quenching from PSII core complex (Finazzi et al. 2004). In addition, interaction between PSBS subunit and the PSII core has been reported in *N. tabacum* (Haniewicz et al., 2013) implying that LHCSR might replace PSBS in this low-light quenching effect, possibly by interacting directly with PSII core.

Finally there is a positive correlation between the maximum exhibited NPQ or the qE dark relaxation and the accumulation of LHCSR1. Transgenic lines expressing LHCSR1 in lower level exhibit not only lower NPQ but also lower qE in contrast with lines accumulating higher levels of the protein.

Conclusion

Heterologous expression of LHCSR1 in *A. thaliana npq4* mutant yields a pigment-binding protein with properties similar to those of LHCSR1 from *P. patens*. The protein is partially active in NPQ induction after several cycles of illumination due to a high zeaxanthin build-up after each light treatment. However, LHCSR1-complemented plants never reach the *A. thaliana* or *P. patens* wild-type NPQ levels probably due to the localization of the protein in the stromal membranes of thylakoids which is rich in LHCII in mosses but not in plants (Pinnola et al. 2015) and probably quenching only a small fraction of LHCII in *A. thaliana*. Zeaxanthin is undoubtedly essential for this partial activity with VDE-inhibited LHCSR1-complemented plants behaving like control *npq4*.

Bibliography

Alboresi, A., Gerotto, C., Giacometti, G.M., Bassi, R., and Morosinotto, T. (2010). Physcomitrella patens mutants affected on heat dissipation clarify the evolution of photoprotection mechanisms upon land colonization. Proc. Natl. Acad. Sci. U. S. A. 107: 11128–33.

Ashton, N.W., Grimsley, N.H., and Cove, D.J. (1979). Analysis of gametophytic development in the moss, Physcomitrella patens, using auxin and cytokinin resistant mutants. Planta 144: 427–435.

Bailleul, B., Rogato, A., de Martino, A., Coesel, S., Cardol, P., Bowler, C., Falciatore, A., and Finazzi, G. (2010). An atypical member of the light-harvesting complex stress-related protein family modulates diatom responses to light. Proc. Natl. Acad. Sci. U. S. A. 107: 18214–9.

Baker, N.R. (2008). Chlorophyll fluorescence: a probe of photosynthesis in vivo. Annu. Rev. Plant Biol. 59: 89–113.

Berthold, D.A., Babcock, G.T., and Yocum, C.F. (1981). A highly resolved, oxygen-evolving photosystem II preparation from spinach thylakoid membranes. FEBS Lett. 134: 231–234.

Betterle, N., Ballottari, M., Zorzan, S., De Bianchi, S., Cazzaniga, S., Dall'Osto, L., Morosinotto, T., and Bassi, R. (2009). Light-induced Dissociation of an Antenna Hetero-oligomer Is Needed for Non-photochemical Quenching InductionS. J. Biol. Chem. 284: 15255–15266.

De Bianchi, S., Betterle, N., Kouril, R., Cazzaniga, S., Boekema, E., Bassi, R., and Dall'Osto, L. (2011). Arabidopsis mutants deleted in the light-harvesting protein Lhcb4 have a disrupted photosystem II macrostructure and are defective in photoprotection. Plant Cell 23: 2659–79.

Bonente, G., Ballottari, M., Truong, T.B., Morosinotto, T., Ahn, T.K., Fleming, G.R., Niyogi, K.K., and Bassi, R. (2011). Analysis of LhcSR3, a protein essential for feedback de-excitation in the green alga Chlamydomonas reinhardtii. PLoS Biol. 9: e1000577.

Bonente, G., Howes, B.D., Caffarri, S., Smulevich, G., and Bassi, R. (2008). Interactions between the photosystem II subunit PsbS and xanthophylls studied in vivo and in vitro. J. Biol. Chem. 283: 8434–45.

Caffarri, S., Kouřil, R., Kereïche, S., Boekema, E.J., and Croce, R. (2009). Functional architecture of higher plant photosystem II supercomplexes. Eur. Mol. Biol. Organ. J. 28: 3052–3063.

Dittami, S.M., Michel, G., Collén, J., Boyen, C., and Tonon, T. (2010). Chlorophyll-binding proteins revisited--a multigenic family of light-harvesting and stress proteins from a brown algal perspective. BMC Evol. Biol. 10: 365.

Engelken, J., Brinkmann, H., and Adamska, I. (2010). Taxonomic distribution and origins of the extended LHC (light-harvesting complex) antenna protein superfamily. BMC Evol. Biol. 10: 233.

Finazzi G., Johnson G.N., Dall'osto L., Joliot P., Wollman F.A., and Bassi R. (2004) A zeaxanthin independent nonphotochemical quenching mechanism localized in the photosystem II core complex. PNAS vol. 101 no. 33, 12375–12380,

Genty, B., Harbinson, J., Briantais, J.M., and Baker, N.R. (1990). The relationship between non-photochemical quenching of chlorophyll fluorescence and the rate of photosystem 2 photochemistry in leaves. Photosynth. Res. 25: 249–57.

Gerotto, C., Alboresi, A., Giacometti, G.M., Bassi, R., and Morosinotto, T. (2012). Coexistence of plant and algal energy dissipation mechanisms in the moss Physcomitrella patens. New Phytol. 196: 763–73.

Gerotto, C., Alboresi, A., Giacometti, G.M., Bassi, R., and Morosinotto, T. (2011). Role of PSBS and LHCSR in Physcomitrella patens acclimation to high light and low temperature. Plant. Cell Environ. 34: 922–32.

Haniewicz P., De Sanctis D., Büchel C., Schröder W.P., Loi M.C., Kieselbach T., Bochtler M., Piano D. Isolation of monomeric photosystem II that retains the subunit PsbS. Photosynth Res (2013) 118:199–207

Horton, P., Ruban, A. V., and Walters, R.G. (1996). REGULATION OF LIGHT HARVESTING IN GREEN PLANTS. Annu. Rev. Plant Physiol. Plant Mol. Biol. 47: 655–684.

Kanazawa, A. and Kramer, D.M. (2002). In vivo modulation of nonphotochemical exciton quenching (NPQ) by regulation of the chloroplast ATP synthase. Proc. Natl. Acad. Sci. U. S. A. 99: 12789–94.

Karimi, M., Inzé, D., and Depicker, A. (2002). GATEWAY vectors for Agrobacterium-mediated plant transformation. Trends Plant Sci. 7: 193–5.

Kramer, D.M., Sacksteder, C.A., and Cruz, J.A. (1999). How acidic is the lumen? Photosynth. Res. 60: 151–163.

Kukuczka, B., Magneschi, L., Petroutsos, D., Steinbeck, J., Bald, T., Powikrowska, M., Fufezan, C., Finazzi, G., and Hippler, M. (2014). Proton Gradient Regulation5-Like1-Mediated Cyclic Electron Flow Is Crucial for Acclimation to Anoxia and Complementary to Nonphotochemical Quenching in Stress Adaptation. Plant Physiol. 165: 1604–1617.

Li, X.-P., Björkman, O., Shih, C., Grossman, A.R., Rosenquist, M., Jansson, S., and Niyogi, K.K. (2000). A pigment-binding protein essential for regulation of photosynthetic light harvesting. Nature 403: 391–5.

Li, X.-P., Gilmore, A.M., Caffarri, S., Bassi, R., Golan, T., Kramer, D., and Niyogi, K.K. (2004). Regulation of photosynthetic light harvesting involves intrathylakoid lumen pH sensing by the PsbS protein. J. Biol. Chem. 279: 22866–74.

Liguori, N., Roy, L.M., Opacic, M., Durand, G., and Croce, R. (2013). Regulation of light harvesting in the green alga Chlamydomonas reinhardtii: the C-terminus of LHCSR is the knob of a dimmer switch. J. Am. Chem. Soc. 135: 18339–42.

Muller, P. (2001). Non-Photochemical Quenching. A Response to Excess Light Energy. PLANT Physiol. 125: 1558–1566.

Mullineaux, C.W. (2005). Function and evolution of grana. Trends Plant Sci. 10: 521–5.

Naumann, B., Busch, A., Allmer, J., Ostendorf, E., Zeller, M., Kirchhoff, H., and Hippler, M. (2007). Comparative quantitative proteomics to investigate the remodeling of bioenergetic pathways under iron deficiency in Chlamydomonas reinhardtii. Proteomics 7: 3964–79.

Niyogi, K.K. and Truong, T.B. (2013). Evolution of flexible non-photochemical quenching mechanisms that regulate light harvesting in oxygenic photosynthesis. Curr. Opin. Plant Biol. 16: 307–14.

Peers, G., Truong, T.B., Ostendorf, E., Busch, A., Elrad, D., Grossman, A.R., Hippler, M., and Niyogi, K.K. (2009). An ancient light-harvesting protein is critical for the regulation of algal photosynthesis. Nature 462: 518–521.

Peter, G.F., Takeuchi, T., and Philip Thornber, J. (1991). Solubilization and two-dimensional electrophoretic procedures for studying the organization and composition of photosynthetic membrane polypeptides. Methods 3: 115–124.

Pinnola, A., Dall'osto, L., Gerotto, C., Morosinotto, T., Bassi, R., and Alboresi, A. (2013). Zeaxanthin Binds to Light-Harvesting Complex Stress-Related Protein to Enhance Nonphotochemical Quenching in Physcomitrella patens. Plant Cell 25: 3519–34.

Pinnola, A., Ghin, L., Gecchele, E., Merlin, M., Alboresi, A., Avesani, L., Pezzotti, M., Capaldi, S., Cazzaniga, S., and Bassi, R. (2015). Heterologous expression of moss LHCSR1: the Chlorophyll a-xanthophyll pigment-protein complex catalyzing Non-Photochemical Quenching, in Nicotiana sp. J. Biol. Chem.

Richard, C., Ouellet, H., and Guertin, M. (2000). Characterization of the LI818 polypeptide from the green unicellular alga Chlamydomonas reinhardtii. Plant Mol. Biol. 42: 303–16.

Savard, F., Richard, C., and Guertin, M. (1996). The Chlamydomonas reinhardtii LI818 gene represents a distant relative of the cabI/II genes that is regulated during the cell cycle and in response to illumination. Plant Mol. Biol. 32: 461–73.

Teardo, E., de Laureto, P.P., Bergantino, E., Dalla Vecchia, F., Rigoni, F., Szabò, I., and Giacometti, G.M. (2007). Evidences for interaction of PsbS with photosynthetic complexes in maize thylakoids. Biochim. Biophys. Acta 1767: 703–11.

Tokutsu, R. and Minagawa, J. (2013). Energy-dissipative supercomplex of photosystem II associated with LHCSR3 in Chlamydomonas reinhardtii. Proc. Natl. Acad. Sci. U. S. A. 110: 10016–21.

Wiedemann, G., Hermsen, C., Melzer, M., Büttner-Mainik, A., Rennenberg, H., Reski, R., and Kopriva, S. (2010). Targeted knock-out of a gene encoding sulfite reductase in the moss Physcomitrella patens affects gametophytic and sporophytic development. FEBS Lett. 584: 2271–8.

Wilk, L., Grunwald, M., Liao, P.-N., Walla, P.J., and Kühlbrandt, W. (2013). Direct interaction of the major light-harvesting complex II and PsbS in nonphotochemical quenching. Proc. Natl. Acad. Sci. U. S. A. 110: 5452–6.

Zhang, X., Henriques, R., Lin, S.-S., Niu, Q.-W., and Chua, N.-H. (2006). Agrobacterium-mediated transformation of *Arabidopsis thaliana* using the floral dip method. Nat. Protoc. 1: 641–6.

Chapter 2

An *in vivo* analysis of factors controlling LHCSR1 activity through heterologous expression in *Arabidopsis thaliana*

Abstract

Carotenoids fulfill several important functions in photosynthesis. They have a major role in photoprotection; they contribute to the assembly and stability of photosynthetic complexes and act as photoreceptors. Photoprotection is catalyzed through the quenching of chlorophyll triplets, the scavenging of singlet oxygen and other ROS, and the heat dissipation of excess singlet excited states (NPQ). Xanthophylls play a major role aslo in the cases of mosses such as *P. patens.* LHCSR1 the major NPQ activator in *P. patens,* is proved to be extremely dependent on the presence and accumulation of the xanthophyll zeaxanthin. Having successfully expressed LHCSR1 in the thylakoid membranes of *A. thaliana npq4*, the NPQ activity of the protein was uncovered after applying repeated cycles of illumination, implying that its prolonged activity is due to the accumulation of zeaxanthin during each cycle. This hypothesis was biochemically verified by measuring NPQ of transgenic plant leaves infiltrated with DTT, an inhibitor of VDE enzyme, causing the loss of LHCSR1-induced quenching. In order to genetically verify the essential need of zeaxanthin, the full coding sequence of LHCSR1 was inserted in the *A. thaliana npq1npq4*, a mutant unable to synthetize zeaxanthin and resistant plants were screened for protein expression and fluorescence quenching. In addition, the impact of another xanthophyll, lutein, in the LHCSR1 expression and activity was studied in the lutein-less *A. thaliana lut2npq4* mutant. In both cases LHCSR1 protein could be expressed but with contrasting effects in the activation of NPQ mechanism. Wanting to investigate the factors limiting LHCSR1 activity *in planta*, LHCSR1 full coding sequence was also inserted in *A. thaliana* mutants altered in LHCII composition. For this, *ch1lhcb5*, a mutant completely deficient of antenna system due to the lack of Chl b and the *NoMnpq4* mutant lacking minor antennae CP24, CP26 and CP29 but also PSBS were complemented *in vivo* with LHCSR1 in order to investigate any possible interaction of the protein with the antenna system of PSII.

I. Impact of carotenoid composition on LHCSR1 expression and activity.

I.1 Introduction

Through daytime plants get exposed to different levels of sunlight, ranging from limiting conditions to very high levels of illumination. Photoprotection mechanisms are essential, helping the removal of harmful reactive intermediates such as Chl triplets and singlet oxygen. Through photoprotection, damage of the photosynthetic apparatus is prevented and the efficiency of photosynthesis maintained. Carotenes and xanthophylls play an essential role in photoprotection: under excess light, plants synthesize a specific carotenoid, zeaxanthin, with enhanced photoprotective properties (see Introduction).

Zeaxanthin is of particular interest because it is absent in dark or low light conditions and accumulates in excess light only, as produced from the diepoxide xanthophyll violaxanthin (Demmig-Adams, 1989) by the violaxanthin de-epoxidase (VDE) enzyme (Bugos and Yamamoto, 1996). Zeaxanthin is known to be involved in multiple photoprotective reactions with different timescales, including two mechanisms quenching ^{1}Chl*, namely feedback de-excitation quenching qE (Niyogi et al., 1997; Holt NE et al., 2005), in the timescale of seconds to minutes and qZ, a component of photo-inhibitory quenching (qI), which provide sustained quenching upon exposure to excess light (Dall'Osto et al., 2005) by replacing Viola into binding sites of LHC proteins (Morosinotto et al., 2002). Increasing thermal dissipation of ^{1}Chl* can effectively protect reaction centers from over-excitation, thus reducing the probability of intersystem crossing and singlet oxygen formation in the LHCs. In addition, zeaxanthin has been proposed to scaveng $^1O_2$ *, and preventing lipid peroxidation (Havaux et al., 1991) upon release from the pH dependent V1 binding site of the major LHCII complex (Caffarri et al., 2001) into the lipid phase. Previous results (Havaux and Niyogi, 1999) demonstrated that *npq1* mutant of *Arabidopsis thaliana*, which is defective in the light-dependent conversion of violaxanthin into zeaxanthin, showed increased photo-inhibition and lipid peroxidation with respect to *A. thaliana* wild-type when plants are exposed to high light. Other studies have proved that the high light-induced binding of zeaxanthin to key proteins located in between the major antenna proteins and PSII reaction centers plays a major role in enhancing photoprotection by modulating the yield of potentially dangerous chlorophyll-excited states and preventing the production of singlet oxygen *in vivo* (Dall'Osto et al., 2012). Finally, recent studies have proved the crucial role of zeaxanthin

in the LHCSR-dependent activation of non-photochemical quenching (NPQ) in the moss *Physcomitrella patens*. Generation of mutants lacking the de-epoxidation VDE enzyme, thus being unable in zeaxanthin synthesis, showed a near-complete loss of NPQ activity in high light conditions (Pinnola et al., 2013).

Xanthophylls, besides their role in photoprotection and LHC assembly, are also needed for photosystem I core translation and stability. The *A. thaliana nox* mutant lacking carotenoid hydroxylases, has shown a linear relation between the abundance of Lhcb proteins connected to PSII, controlling its antenna size, and the total amount of PSI-LHCI complex as is functional to the maintenance of physiological redox poise of plastoquinone pool during acclimative response to light intensity (Dall'Osto et al., 2013). Carotenoids and xanthophylls are also essential for the structure of light-harvesting complexes. Lutein binds to site L1 of all LHC proteins, whose occupancy is indispensable for protein folding and quenching chlorophyll triplets (Dall'Osto et al. 2006). Recent structural studies on LHCII and minor antenna CP29 isolated from spinach showed that four or three carotenoid-binding domains are present per LHCII monomer or CP29 respectively (Pan et al., 2012). These regions are occupied by lutein (L1, L2) neoxanthin (N1) and violaxanthin (V1) in LHCII while in the case of CP29 by lutein (L1), violaxanthin (L2) and neoxanthin (N1). Beside this, xanthophylls are also effective in energy transfer and/or take active part in NPQ as shown in the case of LHCSR1 in the moss *P. patens.* As a member of the light-harvesting complex (LHC) superfamily LHCSR1 has as well four carotenoid-binding sites within its structure one of which is occupied by lutein. To this direction, *in vivo* LHCSR1 complementation of mutant plants with altered carotenoid/xanthophyll composition could yield important information on the structure and activity of the protein since absence of these components could have a direct effect on its stability and expression of LHCSR1.

Material and Methods

Plant culture

Arabidopsis thaliana wild-type (ecotype *Columbia*), *npq4*, *npq1npq4*, *lut2npq4*, *NoMnpq4* and *ch1lhcb5* plants were grown in controlled conditions of 8-h light/16-h dark with a light intensity of 100 μmol photons m^{-2} s^{-1} under stable temperature (23^{o}C in light / 20^{o}C in dark) for 4 weeks. Transgenic lines were grown on selective Moorashige and Skoog (MS) medium containing hygromycin-B (25mg L^{-1}) for the first 10 days under 16-

h light and 8-h dark photoperiod (40 µmol photons m^{-2} s^{-1}, 24°C) and then followed the growth conditions of *A. thaliana* wild- type plants for 3 weeks.

Cloning of LHCSR1 cDNA, Arabidopsis transformation and screening

The fragment corresponding to *LHCSR1* (Locus name Phpat.009G013900) was amplified from *P. patens* total cDNA obtained from 6 days old plants grown on minimum medium, RNA was isolated using TRI Reagent® Protocol (T9424, Sigma-Aldrich) and cDNA was synthetized using M-MLV Reverse Transcriptase (M1302, Sigma-Aldrich) and Oligo$(dT)_{23}$ (O4387, Sigma-Aldrich). Primers including attB sequences for the gateway technology (Invitrogen™) were designed to anneal 27 base pairs upstream of the ATG codon (*Pp*LHCSR1attB1 5'-GGGGACAAGTTTGTACAAAAAAGCAGG CTCCAATCTCGAGCTTTTGCT-3') and 107 base pairs downstream of the stop codon (*Pp*LHCSR1attB2 5'-GGGGACCACTTTGTACAAGAAAGCTGGGTCGACTGCGAA TCAATCAGAA-3'). The 966 base pairs PCR product was first cloned in pDONR™221 Vector (12536-017, Invitrogen™) and then recombined into the pH7WG2 binary vector (Karimi et al., 2002) to make the *35S::LHCSR1* construct. The accuracy of the cloning was verified by sequencing and the plasmid was transferred in *Agrobacterium tumefaciens* strain GV3101 (Zhang et al., 2006). *Arabidopsis* plants were transformed by the floral dip method and transgenic plants were selected on MS medium supplemented by hygromycin (25 mg L^{-1}) and carbenicillin (100 mg L^{-1}). Ten days after sowing on selective medium, plants were transferred in pots and three weeks after the expression of LHCSR1 transgene was assayed by western blotting.

Gel Electrophoresis

Total leaf extracts from transgenic *A. thaliana* plants were homogenized using plastic pestels in Laemmli buffer with 62.5 mM Tris pH 6.8, 10% glycerol, 5% SDS, 5%2-mercaptoethanol and loaded on a 15% (w/v) separating acrylamide gel (75:1 acrylamide/bis-acrylamide) with 6M Urea. After SDS-PAGE gel electrophoresis, proteins were transferred by western-blot on a polyvinylidene fluoride (PVDF) transfer membrane (Millipore) with the use of a Biorad blot system and developed using specific LHCSR and CP43 antibodies produced in the laboratory.

Thylakoid isolation

Stacked thylakoids were purified from about 25-days old *A. thaliana* wild-type and transgenic plants (Berthold et al., 1981). Detached leaves from dark-adapted plants were harvested and homogenized in cold extraction buffer containing 0.02M Tricine-KOH pH 7.8, 0.4M NaCl, 0.002M $MgCl_2$, 0.5% milk powder, and protease inhibitors 0.005M e-aminocaproic acid, 0.001M phenyl-methylsulfonyl fluoride and 0.001M benzamidine added right before the isolation. Homogenized leaves were then filtered, centrifuged at 1500g for 15 min at 4°C and then resuspended in a hypotonic buffer of 0.02M Tricine-KOH pH 7.8, 0.005M $MgCl_2$, 0.15M NaCl and the pre-mentioned concentrations of protease inhibitors. Resuspended thylakoids were centrifuged for 10min at 10,000g (4°C) followed by a second resuspension in a sorbitol buffer (0.01M HEPES-KOH pH 7.5, 0.4M Sorbitol, 0.015M NaCl and 0.005M $MgCl_2$). Stromal membranes and grana separation was performed as previously described (Morosinotto 2010).

Pigment-protein complexes separation with Deriphat-PAGE

Non-denaturating Deriphat-PAGE was performed as previously described (Peter et al., 1991) with some modifications: stacking gel of 3.5% (w/v) acrylamide (38:2 acrylamide/bis-acrylamide) and separating acrylamide gel was prepared at different fixed or gradient concentration depending on the purposes. Acrylamide concentrations are specified along the text. Thylakoids from wild-type and transgenic plants corresponding to a final chlorophyll concentration of 0.5mg were washed with 5mM EDTA and then resuspended in 10mM HEPES pH 7.5. Samples were then solubilized with 0.8% n-*Dodecyl* α-D-*maltoside* and 10 mM HEPES pH 7.5 by vortexing thouroughly for 1min. Solubilized samples were kept 10 min in ice and then centrifuged at 15,000g for 10min to pellet any insolubilized material and then loaded.

NPQ measurements

In vivo chlorophyll fluorescence was measured in room temperature, directly on detached leaves from 45min dark-adapted *A. thaliana* plants by FC 800MF closed FluorCam Video-imaging system (Photon Systems Instruments) and Dual Pulse-Amplitude Modulated (PAM-100) fluorometer. For every measurement a saturating pulse of 4000 μmol photons m^{-2} s^{-1} and actinic light with an intensity of 1200 or 800 μmol

photons m^{-2} s^{-1} were applied. Fv/Fm and NPQ parameters were calculated as (Fm−Fo)/Fm and (Fm−Fm′)/Fm′ respectively.

Results

In order to investigate the role of carotenoids in the stable expression and quenching activity of LHCSR1, the 35S::LHCSR1 construct was introduced in two double *A. thaliana* mutants: 1) *npq1npq4*, a mutant unable to accumulate zeaxanthin due to the lack of VDE enzyme which inhibits the conversion of violaxanthin into zeaxanthin and 2) *lut2npq4*, the lutein-less *A. thaliana* mutant which is defective in the lycopene e-cyclase and therefore lacks production of lutein from a-lycopene. The choice of the *npq1npq4* double mutant was made in order to verify whether LHCSR1 could be expressed in the absence of zeaxanthin. Also this experiment allows us to verify that LHCSR1-dependent NPQ activity *in planta* depends on zeaxanthin as in the case of *P. patens*. Complementary to that, *in vivo* complementation of the *lut2npq4* genotype will verify whether LHCSR1-requires lutein for activity or, like in plants, lack of lutein can be compensated by zeaxanthin (Dall'Osto et al. 2006).

I.2.1 Expression in *A.thaliana npq1npq4* mutant

The pH7WG2/LHCSR1 construct was used in order to complement *npq1npq4* plants with LHCSR1 from *P. patens*. Transformation of zeaxanthin-deficient plants was performed using the *A. tumefaciens* dip-floral method and was followed by selection of T1 resistant transgenic lines on plates with MS medium supported with hygromycin-B (25mg L^{-1}). Resistant lines were moved on soil and left to grow for 3-4 weeks. As seen in Figure 2.1A, no major difference in the size or shape of the transformed plants was observed. Leaves from control and 35S::LHCSR1 complemented plants were collected, followed by western blot analysis of total protein extracts against specific LHCSR antibodies. Screening with western blot resulted into 18 stable lines accumulating LHCSR1. The plant lines with the highest protein accumulation were isolated (i.e. lines #1, #3 and #4, Figure 2.1B) and left to grow in order to produce seeds for the analysis of T2 generation. Following the same selection procedure on MS medium plates enriched in hygromycin-B, resistant T2 plants were screened by western blot analysis, verifying that LHCSR1 can be expressed and processed to its mature form in the absence of zeaxanthin (Figure 2.1C).

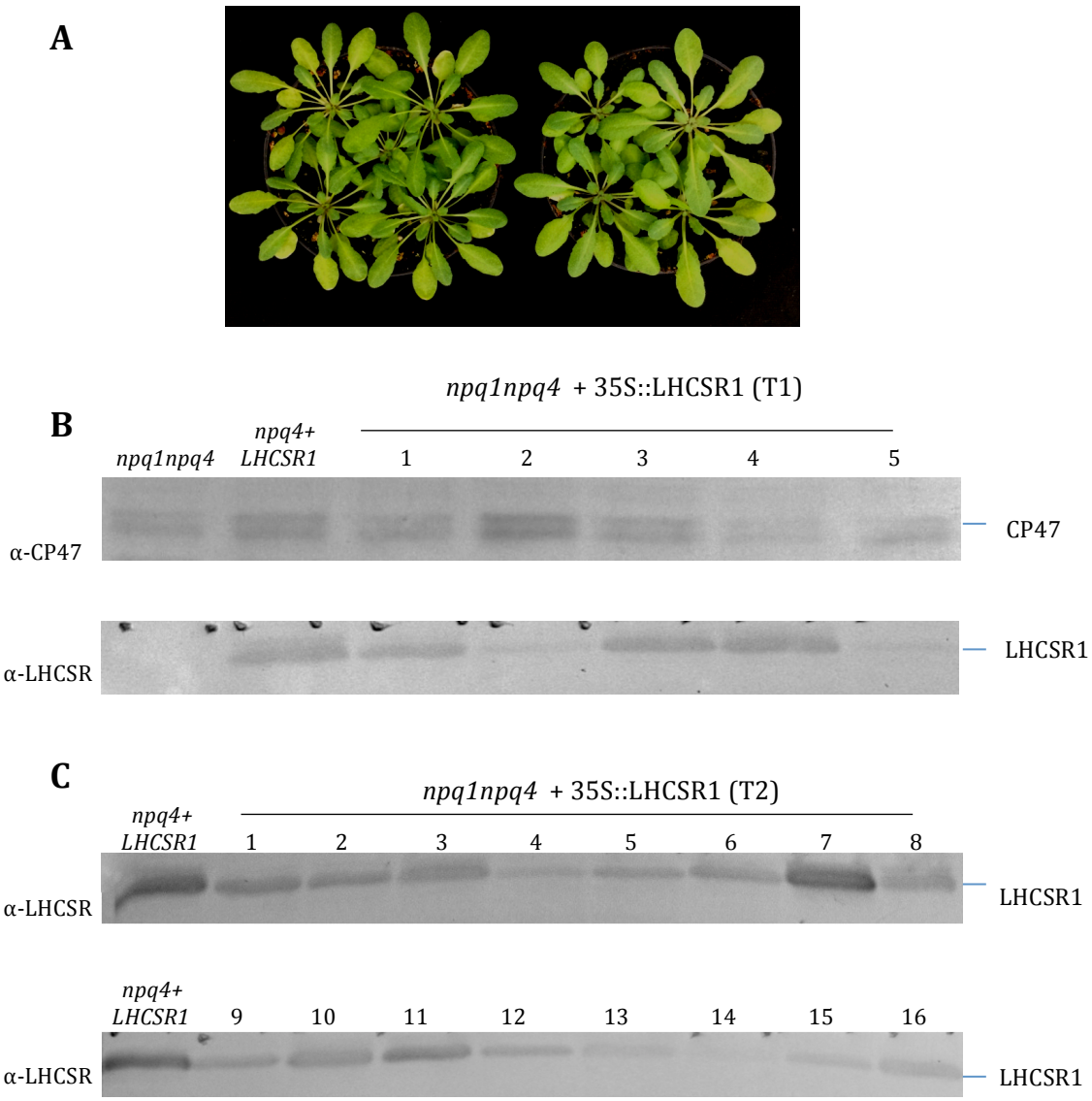

Figure 2.1. **Immunological screening of *npq1npq4* + 35S::LHCSR1 transformed lines.** *(A) A. thaliana transgenic lines were selected on agar plates and then transferred in pots in a short-day photoperiod growth chamber (right). Control npq1npq4 plants of the same age were also grown in the same conditions (left). (B) Western blot analysis of the T1 generation was performed on total proteins extracted by grinding one leaf disk directly in 100 µL of loading buffer, one tenth of the volume was loaded on SDS-PAGE. Proteins of non-transformed npq1npq4 and npq4+35S::LHCSR1 plants were loaded as controls. The primary antibody used for the analysis is indicated on the left side of the membrane while the band corresponding either to P. patens LHCSR1 or CP47 is indicated on the right side (C) Western blot analysis of 16 independent plant lines from the T2 generation. Samples loaded on a Chl basis of 0.75ug.*

I.2.2 LHCSR1 quenching activity in *A. thaliana npq1npq4*, Zea-less plants

As indicated by previous studies in *P. patens*, zeaxanthin plays a crucial role for the activity of LHCSR1 since *vde* KO mutants are shown to be unable in activating the NPQ mechanism (Pinnola et al., 2013). As seen in Chapter 1, we performed a biochemical verification of the direct zeaxanthin dependence of LHCSR1 in NPQ by infiltrating 35S::LHCSR-complemented *npq4* plants with DTT and by measuring the NPQ activity upon successive cycles of illumination. The infiltrated plants lost completely their ability to perform fluorescence quenching as well as the capacity to convert violaxanthin into zeaxanthin via VDE enzyme, which is known to be inhibited by DTT. The *in vivo* complementation of the *npq1npq4* double mutant further details the target of DTT inhibition is specifically VDE. The NPQ activity of complemented plants was analyzed by video-imaging and PAM fluorometry. Previous work (see Chapter 1) showed that qE activity could be restored in *A. thaliana npq4* plants, impaired in qE, by expression of LHCSR1. Here, we used the double mutant *npq1npq4* to verify the dependence of LHCSR1-dependent qE activity on zeaxanthin.

To this aim, we measured the chlorophyll fluorescence quenching of npq1*npq4* plants and of 7 independent 35S::LHCSR1 complemented plants by video-imaging following a standard procedure for *A. thaliana*. The protocol consisted of a 45-min dark adaptation of leaves that were measured by applying4 successive cycles of 5-min NPQ light induction using white actinic light (1200 μmol m^{-2} s^{-1}) and a 5-min phase of dark recovery. Upon the first illumination, all genotypes analyzed showed the same fluorescence profile irrespective from the expression level of LHCSR1.Moreover, the quenching activity was the same also during the following cycles of illumination without any major difference between *npq1npq4* (control) and the complemented *npq1npq4*-LHCSR1 plants. In order to verify the result of the short successive cycles measurement, transgenic *npq1npq4* + 35S::LHCSR1 and control *npq1npq4* lines were measured using two additional protocols: Protocol I, performing one single cycle of 10min actinic light (800 μmol photons m^{-2} s^{-1}) and followed by 15min of dark recovery and protocol II, with one single cycle of 30min actinic light (800 μmol photons m^{-2} s^{-1}) and 15min of dark recovery.

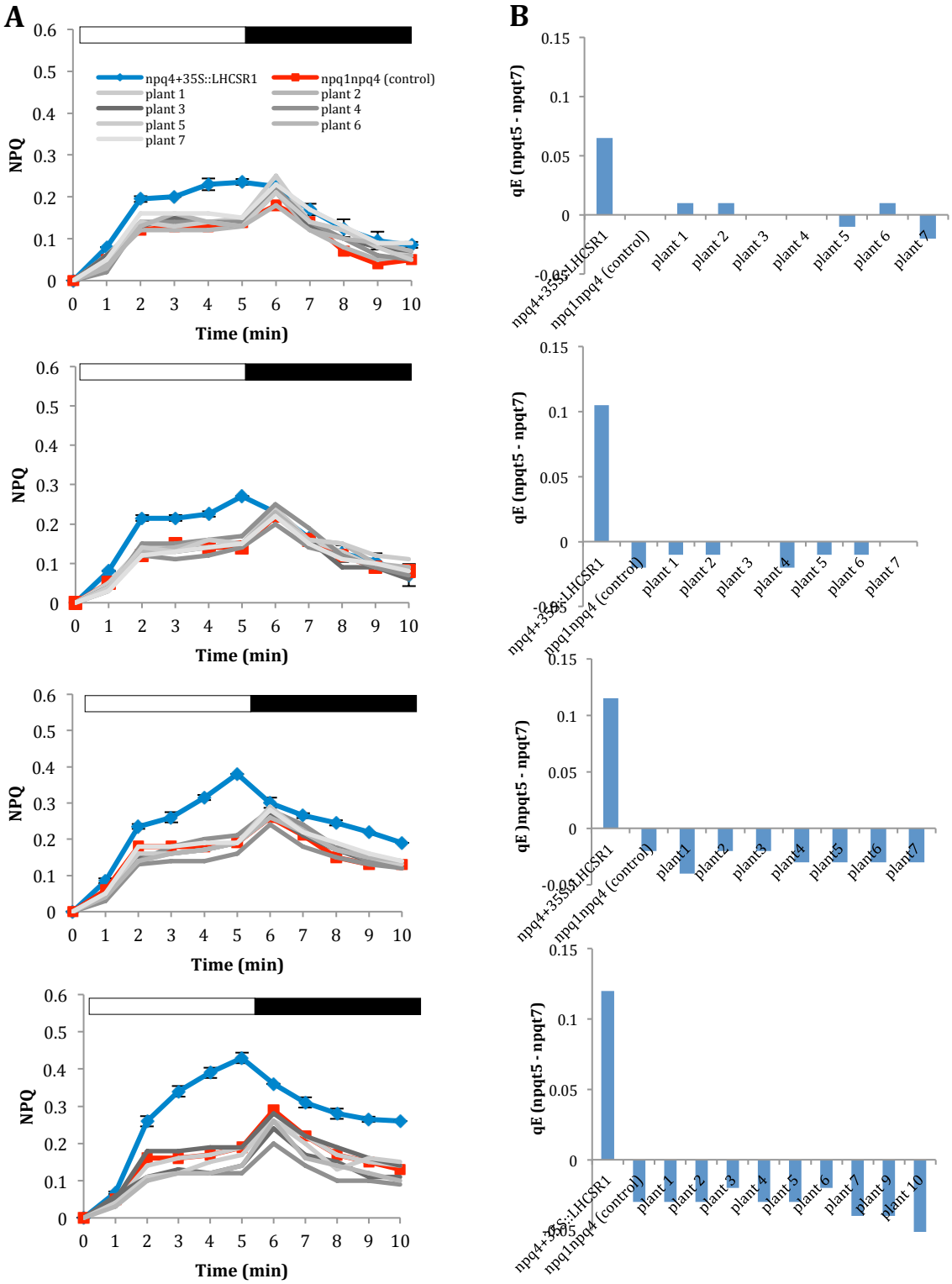

Figure 2.2. NPQ induction in *npq1npq4* + 35S::LHCSR1 lines using fluorescence video-imaging. *NPQ of Chl fluorescence was measured on leaves detached of 4-5-week old plants at room temperature. The results of 4 successive NPQ cycles are presented. Protocol: 5 minute of actinic light treatment (800) followed by 5 min of dark recovery. A) NPQ, calculated as quenching of maximal fluorescence (Fm - Fm')/Fm' for every saturating flash. Blue line, npq4 + 35S::LHCSR1 (n=3). Red line, non-transformed npq1npq4 (control). A. thaliana leaves were dark adapted for 45 minutes. After an Fm measurement, NPQ was induced by 5min of white actinic light (800 µmol m^{-2} s^{-1}; white bar) followed by 5min of dark relaxation, repeated for 4 measuring cycles. From top to bottom, cycles 1-4. B) qE fast recovery calculated as the last point in the light minus the second point in the dark phase (qE = $npqt_5$ - $npqt_7$).*

LHCSR1 was successfully expressed, giving stable transgenic lines. However when measured for their quenching activity these lines did not present any major difference, under any of the measuring protocols. More specifically the 35S::LHCSR1-complemented *npq1npq4* plants showed almost identical NPQ values during each performed illumination cycle in both protocols with respect to the non-complemented *npq1npq4* plants (Protocol I: $NPQ_{control} = 0.55$ *vs.* $NPQ_{LHCSR1}=0.6$; protocol II: $NPQ_{control} = 0.74$ *vs.* $NPQ_{LHCSR1}=0.79$, Table 2B). As for the qE relaxation during the dark phase, the measured values were very low with no difference between the two genotypes (Protocol I: $qE_{control} = 0.18$ *vs.* $qE_{LHCSR1} = 0.16$; Protocol II: $qE_{control} = 0.29$ *vs.* $qE_{LHCSR1} = 0.25$, Table 2A).

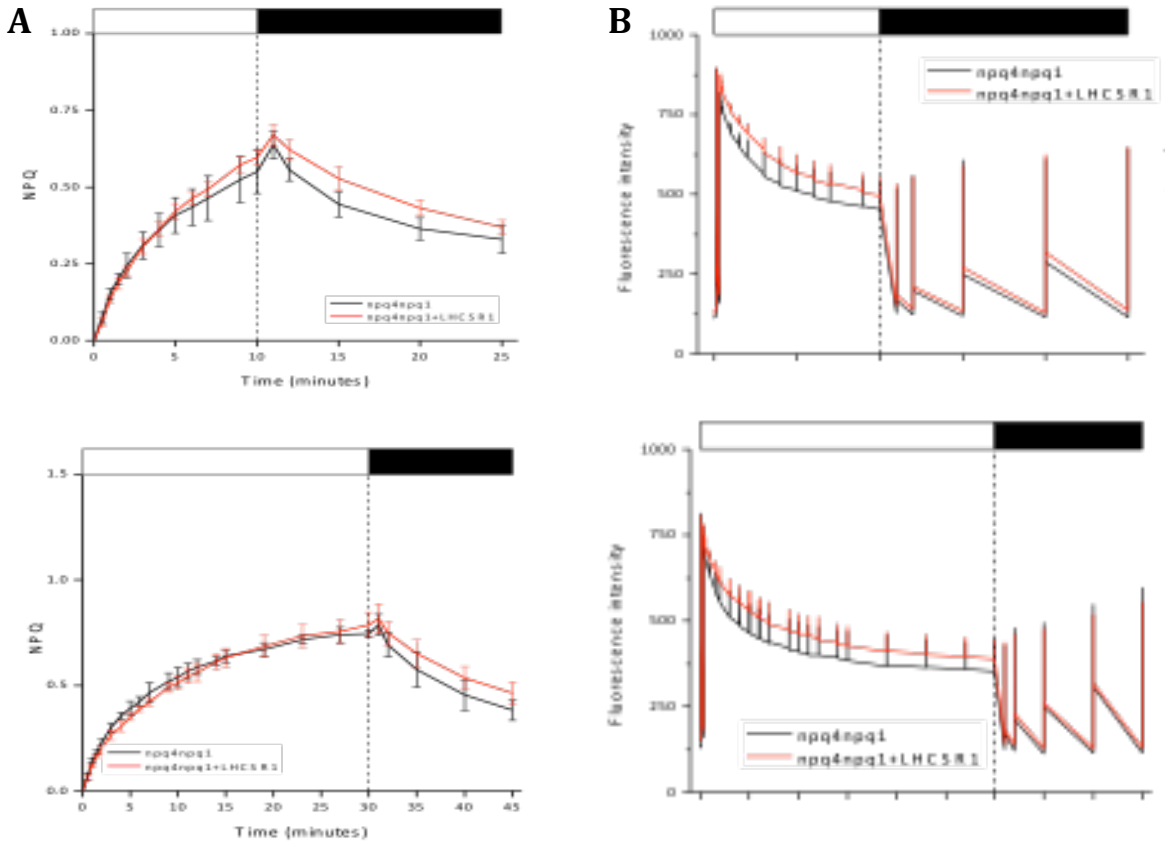

Figure 2.3. NPQ induction in *npq1npq4* + 35S::LHCSR1 lines using different measuring protocols. *NPQ of Chl fluorescence was measured on leaves detached of 4-5-week old plants at room temperature. The results of two different measuring protocols are presented: Protocol I, 10 minute of actinic light treatment (800) followed by 15 min of dark recovery (upper panels) while protocol II has an extended actinic light treatment of 30 minutes and 15 minutes of dark recovery (lower panels). A) NPQ, calculated as quenching of maximal fluorescence (Fm - Fm')/Fm' for every saturating flash. Black line, npq1npq4 (n=5). Red line, npq1npq4+35S::LHCSR1 (n=5). A. thaliana leaves were dark adapted for 45 minutes. After an Fm measurement, NPQ was induced by either 10 or 30 minutes of white actinic light (800 µmol m^{-2} s^{-1}; white bar) followed by 15 minutes of dark relaxation in a single measurement cycle. Protocol I, upper left chart; Protocol II, lower left chart. B) Fluorescence induction curve for each measuring protocol. Protocol I, upper right chart; Protocol II, lower right chart.*

	10’ light and 15’dark		30’ light and 15’dark	
Genotype	NPQ_{max}	qE	NPQ_{max}	qE
npq1npq4	0.55±0.07	0.18±0.04	0.74±0.02	0.29±0.06
npq1npq4+LHCSR1	0.60±0.03	0.16±0.03	0.79±0.06	0.25±0.02

Table 2A. NPQ and qE calculation of measured *npq1npq4* control and 35S::LHCSR1 plants. *Results for each genotype after measurement with two different protocols. The maximum NPQ as well as qE (fast relaxation) are presented. qE is calculated as the last point in the light phase minus the second point in the dark.*

I.2.3 NPQ measurements using pulse-amplitude modulated fluorescence (PAM)

NPQ activity of LHCSR1-complemented *npq1npq4* plants was also refined by PAM measurements. Using two different actinic light intensities (800, 600 photons m^{-2} s^{-1}), 45min dark-adapted leaves from *npq1npq4* control plants and 35S::LHCSR1-compemented lines were illuminated for 10 minutes, followed by a 10-minute dark relaxation. PAM results indicated that there is no observed difference in NPQ amplitude between control and LHCSR1-complemented plants with the last ones being unable to recover when actinic light is off (qE = -0.053, Figure 2.4 A,B). These data are in agreement with what was observed using the previously tested protocols by fluorescence video-imaging.

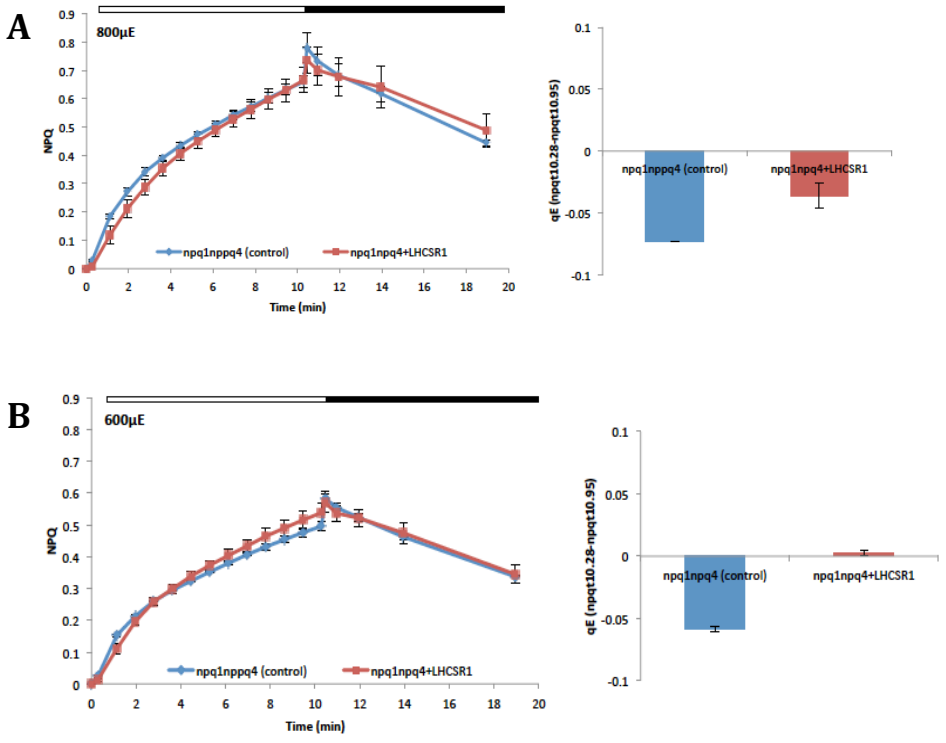

Figure 2.4. NPQ measured using pulse-amplitude modulated fluorescence. *NPQ of dark adapted leaves from A. thaliana npq1npq4 and 35S::LHCSR1 plant lines was measured using two different actinic light intensities in a standard light treatment/dark recovery protocol A) NPQ induction using 800 µmol photons m^{-2} s^{-1} of actinic light (10min light treatment/10min dark recovery). Genotypes measured: A. thaliana npq1npq4 (blue line), 35S::LHCSR1 line (red line). Measurements are the average of three replicas. B) Two successive NPQ cycles using 600 µmol photons m^{-2} s^{-1}. Genotypes measured: A. thaliana npq1npq4 (blue line), 35S::LHCSR1 line O1 (red line).*

I.2.4 Expression in *A. thaliana lut2npq4* mutant

Following the *agrobacterium*-mediated transformation method, the full coding sequence of LHCSR1 was integrated into *A. thlaliana lut2npq4* plants, followed by growth under stable light and temperature conditions for 3-4 weeks. Seeds from the first generation plants were collected, sterilized and placed on MS medium plates enriched with antibiotics for the selection of resistant plants. After selection on hygromycin-B, resistant plants were transferred to soil and left to grow for 3 weeks, with no major phenotypic differences between control and 35S::LHCSR1–complemented *lut2npq4* plants. Leaves from each plant line were collected and total protein extracts were obtained and screened by western blot against LHCSR antibody. Total protein extracts from *A. thaliana* wild-type and *npq4* plants were also used as negative controls of the specificity of the LHCSR antibody against the transgenic protein. In total 17 hygromycin-B-resistant *lut2npq4* plants of the first generation expressed LHCSR1, accumulating the protein on different levels.

As previously done with *npq4* + 35S::LHCSR1 we decided to continue the analysis of the second generation *lut2npq4* + 35S::LHCSR1 plants by further selecting lines with the highest level of LHCSR1 accumulation (e.g. lines #1, #2, #5, #15, Figure 2.5B). To this direction, the selected resistant plants were left to grow enough in order to produce mature siliques and seeds were again collected, sterilized and grown on selective hygromycin petri plates. Resistant plants of the second generation were screened again by western blot in order to check the accumulation of LHCSR1 protein. Indeed, LHCSR1 was successfully expressed with a more homogenous distribution among the population of plants analyzed (Figure 2.5C)

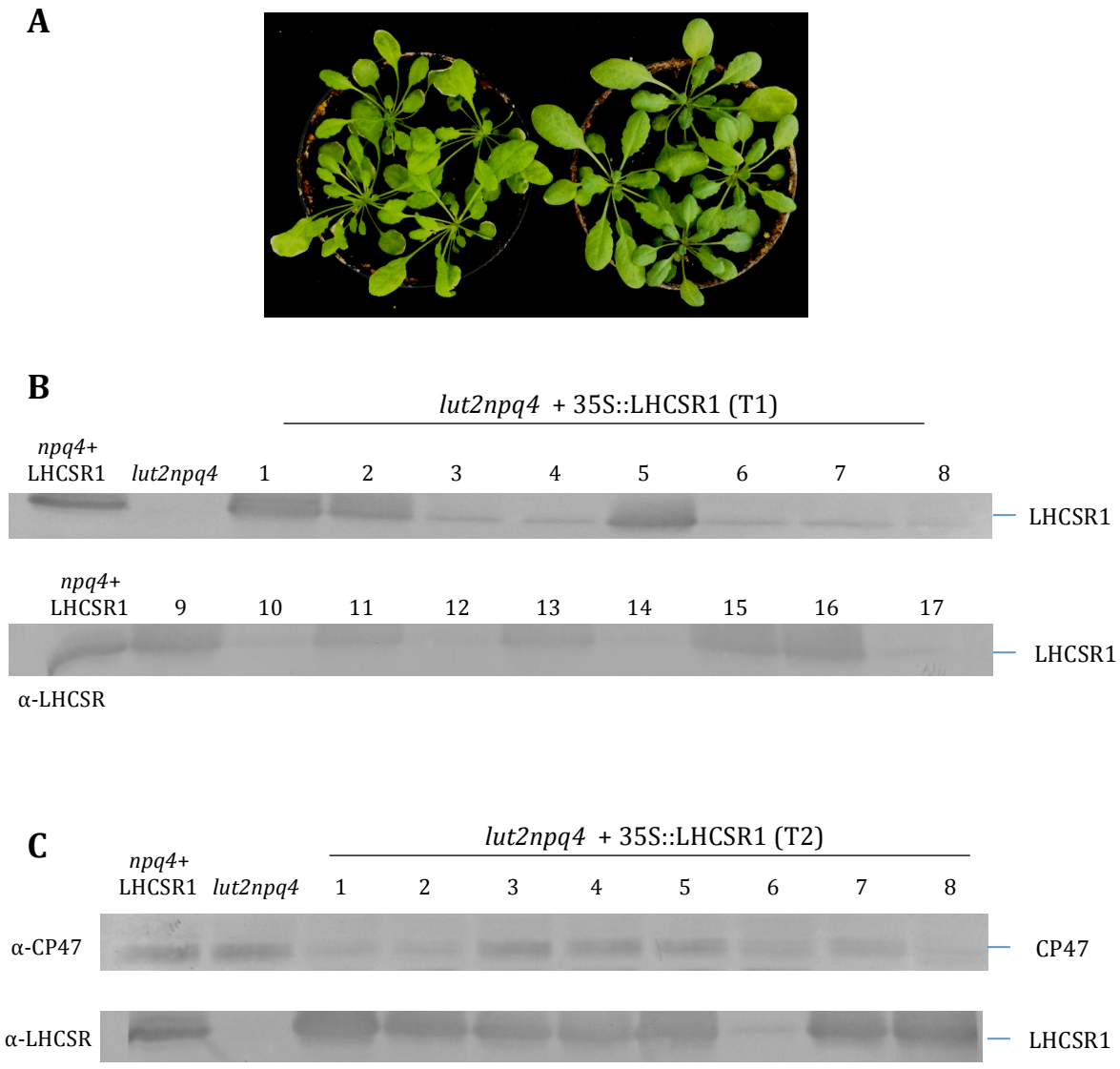

Figure 2.5. **Immunological screening of *lut2npq4* + 35S::LHCSR1 transformed lines.** *A) A. thaliana transgenic lines were selected on agar plates supplemented with hygromicine-B and then transferred in soil pots in a short-day photoperiod growth chamber under controlled temperature conditions for 3-4 weeks (right). Control lut2npq4 plants of the same age were also grown in the same conditions (left). B) Western blot analysis of the T1 generation was performed on total proteins extracted by grinding one leaf disk directly in 100 µL of loading buffer, one tenth of the volume was loaded on SDS-PAGE. Proteins of non-transformed lut2npq4 and transgenic npq4+35S::LHCSR1 plants were loaded as controls. The primary antibody used for the analysis is indicated on the left side of the membrane while the band corresponding either to P. patens LHCSR1 or CP47 is indicated on the right side C) Western blot analysis of 8 independent plant lines from the T2 generation.*

I.2.5 LHCSR1 quenching activity in *A. thaliana lut2npq4*

Upon verifying the presence of the protein, 35S::LHCSR1-complemeted *lut2npq4* plant lines were tested for their quenching activity. NPQ induction of all T1 transformed lines was measured by fluorescence video-imaging following a standard procedure for *A. thaliana*. The protocol included 45-min dark adaptation of leaves, followed by four successive cycles of 10-min NPQ light induction using white actinic light (*1200 μmol m^{-2} s^{-1})* and a 10-min phase of dark recovery. When the protocol was applied for the first time there was no major difference in the NPQ induction of both 35S::LHCSR1 and control genotypes analyzed (Figure 2.6, first row panels). However, when the illumination period was applied for the second time (Figure 2.6, second row panels) a more pronounced quenching was detected in 35S::LHCSR1 lines if compared to *lut2npq4* control line. Two additional NPQ measurements were applied showing an even further pronounced NPQ activity in 35S::LHCSR1 lines between the second and the third measurements while quenching was similar between the third and the fourth measurement (Figure 2.6, A). The same results were observed also for the fast qE relaxation. During the first cycle of illumination there was no significant difference in qE between 35S::LHCSR1-complemented and control lines, in contrast with the third and fourth illumination cycles where the lines expressing LHCSR1 showed higher qE. The same genotypes were tested using two additional different measuring protocols, this time by using just one cycle of NPQ but with an extended period of illumination and dark recovery. For this reason, leaves from 35S::LHCSR1 and control *lut2npq4* plant lines of the same age were dark adapted for 45 minutes and measured using two NPQ protocols. In protocol A, plants were subjected to 10 minutes of white actinic light treatment followed by 15 minutes of dark recovery while protocol B included an extended 30-min illumination period followed by a 15-min dark relaxation. Results from protocol A showed just a small difference emerging between 35S::LHCSR1 and control *lut2npq4* lines during the actinic light phase while no immediate recovery was observed for both genotypes upon switching off the actinic light (Figure 2.7A). Using protocol B the difference in NPQ amplitude during the light period became more evident with the 35S::LHCSR1 line showing higher NPQ induction (Figure 2.7B) The difference between the two genotypes measured, applied also for the fast qE component with the 35S::LHCSR1 line showing a recovery rate within the first minute of dark relaxation with respect to the *lut2npq4* control which is not recovering directly when the light is switched off.

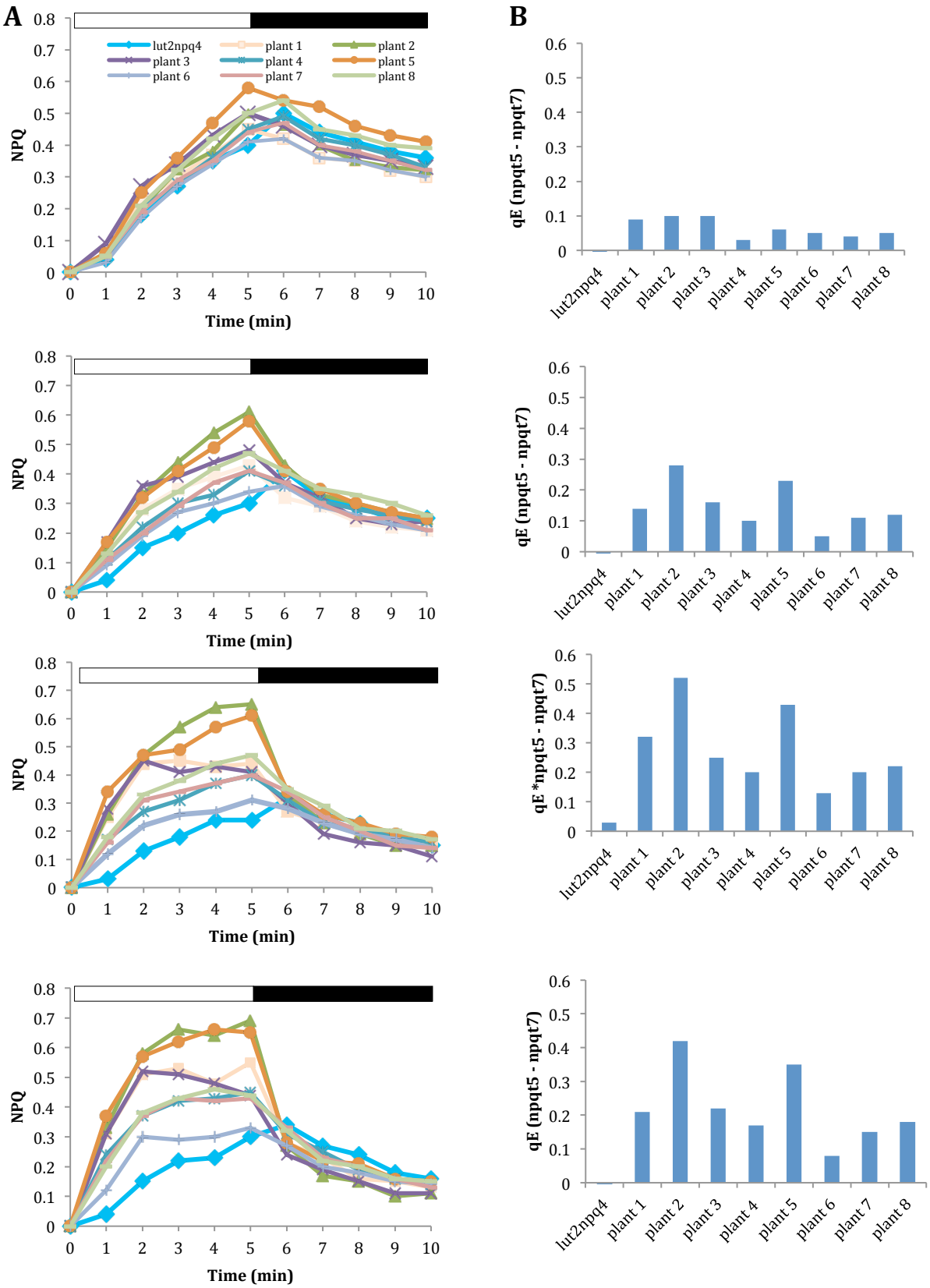

Figure 2.6. NPQ induction in *lut2npq4* + 35S::LHCSR1 lines using fluorescence video-imaging. *NPQ of Chl fluorescence was measured on leaves detached of 4-5-week old plants at room temperature. The results of 4 successive NPQ cycles are presented. Protocol: 5 minute of actinic light treatment (800) followed by 5 min of dark recovery. A) NPQ, calculated as quenching of maximal fluorescence (Fm - Fm')/Fm' for every saturating flash. Bright blue line, non-transformed lut2npq4 (control). A. thaliana leaves were dark adapted for 45 minutes. After an Fm measurement, NPQ was induced by 5min of white actinic light (800 µmol m^{-2} s^{-1}; white bar) followed by 5min of dark relaxation, repeated for 4 measuring cycles. From top to bottom, cycles 1-4. B) qE fast recovery calculated as the last point in the light minus the second point in the dark phase (qE = $npqt_5$ - $npqt_7$). From upper to lower panels, cycles 1-4*

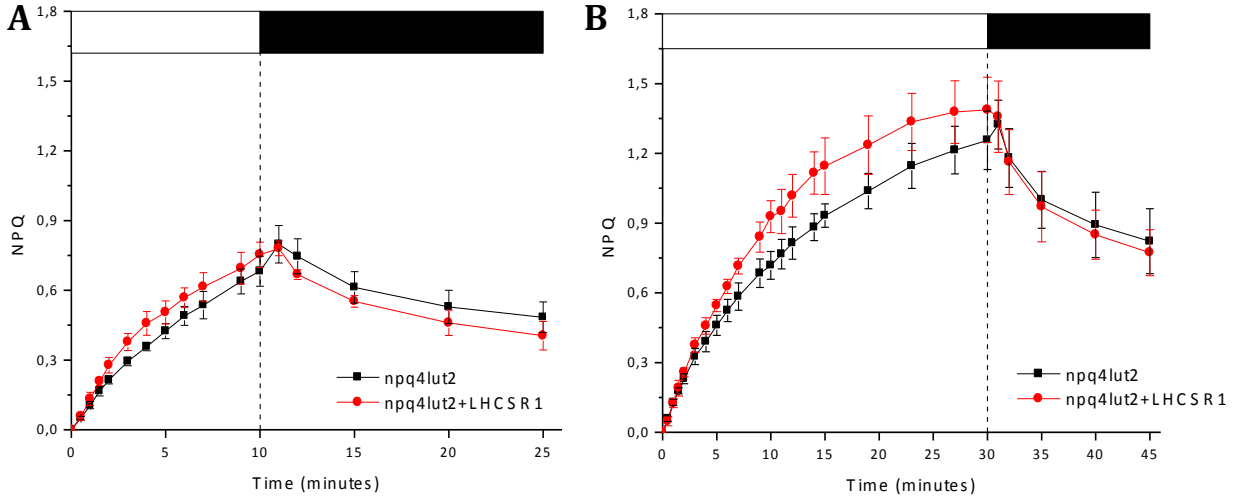

	10' light and 15'dark		30' light and 15'dark	
Genotype	NPQ_{max}	qE	NPQ_{max}	qE
lut2npq4	0.68	0.06	1.25	0.09
lut2npq4+LHCSR1	0.75	0.08	1.39	0.23

Figure 2.7 . NPQ induction in *lut2npq4* + 35S::LHCSR1 lines using different measuring protocols. *NPQ of Chl fluorescence was measured on leaves detached of 4-5-week old plants at room temperature. The results of two different measuring protocols are presented: (A) Protocol I, 10 minute of actinic light treatment (800) followed by 15 min of dark recovery while (B) protocol II has an extended actinic light treatment of 30 minutes and 15 minutes of dark recovery. NPQ, calculated as quenching of maximal fluorescence (Fm - Fm')/Fm' for every saturating flash. Black line, lut2npq4 (n=3). Red line, lut2npq4 + 35S::LHCSR1 (n=3). A. thaliana leaves were dark adapted for 45 minutes. After an Fm measurement, NPQ was induced by either 10 or 30 minutes of white actinic light (800 µmol m^{-2} s^{-1}; white bar) followed by 15 minutes of dark relaxation in a single measurement cycle. Protocol I, upper left chart; Protocol II, lower left chart.* ***Table 2B.*** *NPQ and qE values from two different protocols. qE calculated as the last point in the light period minus the second point in the dark.*

I.2.6 Correlation between LHCSR1 accumulation and NPQ activity

In order to verify the correlation between quenching activity and LHCSR1 accumulation, leaves from 35S::LHCSR1-complemented plant lines (T2, n=8) were dark adapted and measured for their NPQ activity following a standard protocol (4 successive cycles of 10min actinic light treatment and 10min of dark relaxation, Figure 2.8A). Total leaf extracts from the same lines were analyzed by western blot and developed against homemade LHCSR antibodies (Figure 2.8B), accumulating the protein at different levels. The maximum NPQ (NPQ max) but also the fast dark recovery of the mechanism (qE) values for each plant line sample were plotted together with the LHCSR1 accumulation level. In both cases there is a positive correlation between LHCSR1 accumulation (Figure 2.8C).

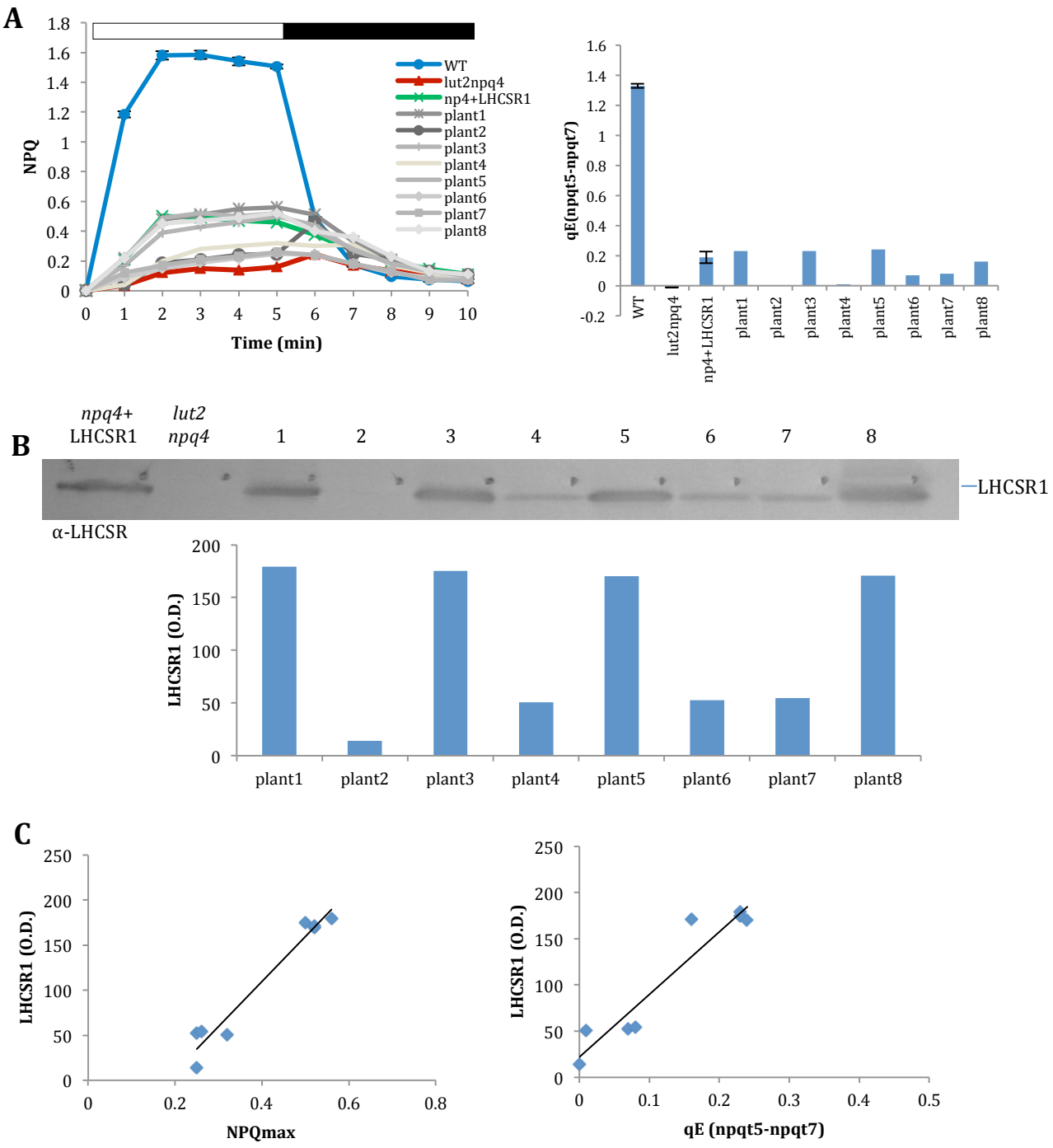

Figure 2.8. Correlation between NPQ activity and LHCSR1 accumulation in *lut2npq4* plants. *A) NPQ of T2 independent 35S::PpLHCSR1 lines (n=8) measured using a specific protocol (4 cycles of 5min actinic light, 5min of dark recovery). White and black bars represent the light and dark phase. NPQ chart of the final cycle is presented on the left, qE recovery calculated as the last point in the light phase minus the second point in the dark phase (npq t5 – npq t7) is shown on the right, B) After NPQ measurement total leaf extracts from each line were loaded on a SDS-PAGE on a basis of 0.75ug Chl and immuno-blotted against a-LHCSR homemade antibodies. P. patens lhcsr2psbs ko thylakoids were loaded as control, C) The protein intensity of each sample is calculated and plotted together with the maximum NPQ giving a positive correlation of R^2=0.952 (left chart) and the qE recovery with a positive correlation of R^2=0.911 (right chart).*

II. LHCSR1 interactions with antenna system subunits

II.1 Introduction

Oxygenic photosynthesis is performed in the chloroplast by a series of reactions, which transform sunlight energy into readily used chemical energy. Absorption of light, excitation energy transfer (EET) and electron transfer are the primary events of the photosynthetic light phase and take place in the core complexes of the two photosystems: PSI and PSII (Schatz et al., 1988; Melkozernov et al., 2000; Gobets, 2001; Croce, 2004; Busch, 2011; Croce and van Amerongen, 2013). Photosystem II (PSII), a large supra-molecular pigment–protein complex is located in the thylakoid membranes of plants, algae and cyanobacteria. Its reaction center consists of several subunits carrying the cofactors for electron transport and forms, together with the proteins CP43 and CP47, the PSII core complex (Ferreira et al., 2004; Umena et al., 2011). Around the PSII core complex a peripheral antenna system is organized. The PSII antenna system is composed by two types of antennae: (i) the trimeric LHCII, by far the most abundant and (ii) the monomeric LHCs, namely CP24, CP26 and CP29. Among the antenna complexes of PSII, the minor antennae are of particular interest since they bridge the inner antennae CP43/CP47 with the outer LHCII trimers within the PSII supercomplex (Harrer et al., 1998). Although CP24, CP26 and CP29 complexes are homologous and are expected to share a common three-dimensional organization on the basis of the structural data available (Liu et al., 2004; Pan et al., 2011), they cannot be exchanged between each other in the super-complexes. In addition, the location of these complexes in between LHCII and the PSII reaction center makes them crucial for controlling EET from LHCII, to the core subunits.

Depletion of specific monomeric LHCs *in vivo* was shown to impair the organization of photosynthetic complexes within grana partitions and to negatively affect electron transport rates and photoprotection capacity (de Bianchi et al., 2010). Evidence that these gene products have been conserved over at least 350 million years of evolution (Durnford et al., 2003) strongly indicates that each complex has a specific role in the PSII function over the highly variable conditions of the natural environment. Recent studies on double *A. thaliana* mutants *ko*CP26/CP24 and *ko*CP29/CP24, and from a mutant lacking all minor antennae (NoM) have shown that in the absence of all minor LHCs, the functional connection of LHCII to the PSII cores appears to be seriously impaired whereas the disconnected LHCII is substantially quenched (Dall'Osto et al., 2014).

One of the major structural components of the light-harvesting complexes is chlorophyll b (Chlb). It is synthetized from Chla in a reaction catalyzed by the chlorophyllide oxygenase (CAO) , a single-gene encoded enzyme located in the inner envelope/thylakoid membrane of chloroplasts. The main functions of Chlb are the absorption and transfer of light energy, assembly of light harvesting complexes and regulation of antenna size. As no redundant genes or biochemical pathway is available for CAO, mutations in the *cao* gene result in the loss of Chlb (Tanaka et al., 1998), cause structural changes and affect the plant function. Lack of Chlb affects the abundance LHC proteins and pigment-protein complexes (Bassi et al 1985; Falbel et al., 1996). Mutants without Chlb fail to accumulate significant amount of light harvesting Chl a/b binding proteins, leading to the reduction in photosynthetic unit size and the development of an abnormal thylakoid membrane system. The ultrastructure of chloroplast of this mutant has been the object of contrasting reports: Chen et al., 2007 have shown decreased grana lamellae and slightly swelling thylakoid while early reports (Bassi et al. 1985) showed well developed grana stacks.

Loss of Chlb affects the plant function in various ways. It affects the phenotype of plants and leaf becomes pale green in color. There is retardation of growth, delay of flowering and reduction in leaf area (Lin et al., 2003). Besides this, lack of Chlb affects energy dissipation processes, like energy dependent quenching and state transition. Non-photochemical quenching is decreased (Gilmore et al., 1996) without affecting, however, photochemical efficiency Fv/Fm, (Lin et al., 2003).

Ch1 (chlorina) is a pale-green *A. thaliana* mutant lacking completely Chlb (Espineda et al., 1999) and is completely devoid of photosystem II (PSII) chlorophyll-protein antenna complexes (Havaux et al., 2007). Loss of the normal structural architecture around the PSII reaction centers in Chl b–less plant mutants has significant effects on the functionality of the PSII core reaction center complexes, including loss of non-photochemical quenching (NPQ), impaired oxidizing side of PSII and reduced grana stacking, which leads to enhanced sensitivity to PSII photo-inactivation (Leverenz et al., 1992; Havaux and Tardy, 1997; Kim et al., 2009).

Recent studies have shown that transient expression of LHCSR1 in heterologous systems like *N. tabacum* results into the accumulation of the protein in its mature form. LHCSR1 localizes in the chloroplast thylakoid membranes, and is correctly folded with chlorophyll *a* and xanthophylls but without chlorophyll *b*, an essential chromophore for plants and algal LHC proteins (Pinnola et al., 2015). *In vivo* insertion of LHCSR1 in a

Chlb-less *Arabidopsis* mutant could give answers on the stability of the protein in the absence of Chlb but also on the requirement of interacting pigment-binding complexes for the quenching activity of the protein.

Results

Minor antennae of LHCII play a major role within PSII since they contribute in the transfer of energy connecting the antenna system with the PSII core. In order to investigate the role of minor antennae in the stable expression and quenching activity of LHCSR1 protein and wanting to see if the Lhcb monomers could be the limiting factors of LHCSR1 activity, the 35S::LHCSR1 construct was introduced into *NoMnpq4*, a mutant lacking *lchb* genes which encode CP24, CP26 and CP29 minor antennae. In this context, the Chlb-less *A. thaliana* mutant *ch1lhcb5* which is completely deficient of antenna system was *in vivo* transformed with LHCSR1 in order to verify whether the protein can be accumulated in the absence of Chlb but also if it can complement NPQ activity in the complete absence of LHCII.

II.2.1 LHCSR1 expression in *A.thaliana NoMnpq4* and *ch1lhcb5* mutants

The pH7WG2/LHCSR1 construct was used in order to complement *NoMnpq4* and *ch1lhcb5* plants with LHCSR1 from *P. patens*. Transformation of minor and major antenna mutant plants was performed using the *A. tumefaciens* dip-floral method and was followed by selection of T1 resistant transgenic lines on plates with MS medium supported with hygromycin-B (25mg L^{-1}). Resistant lines were moved on soil and left to grow for 3-4 weeks. Leaves from control and 35S::LHCSR1 complemented plants were collected, followed by western blot analysis of total protein extracts against specific LHCSR antibodies.

II.2.1.1 LHCSR1 expression in *A. thaliana NoMnpq4*

Total leaf extracts from 35S::LHCSR1-complemented *NoMnpq4* plants were loaded on an SDS-PAGE gel and developed against homemade a-LHCSR antibody by western blot analysis. As additional controls, extracts from *P. patens*, *A. thaliana npq4* + 35S::LHCSR1 and non-transformed *NoMnpq4* plants were also loaded. Results of the first generation resistant plants (T1) revealed 6 lines expressing LHCSR1. The lines (i.e.

#1, #4, #8, #9, #12 and #14, Figure 2.9) were isolated for further characterization of the T2 plant generation.

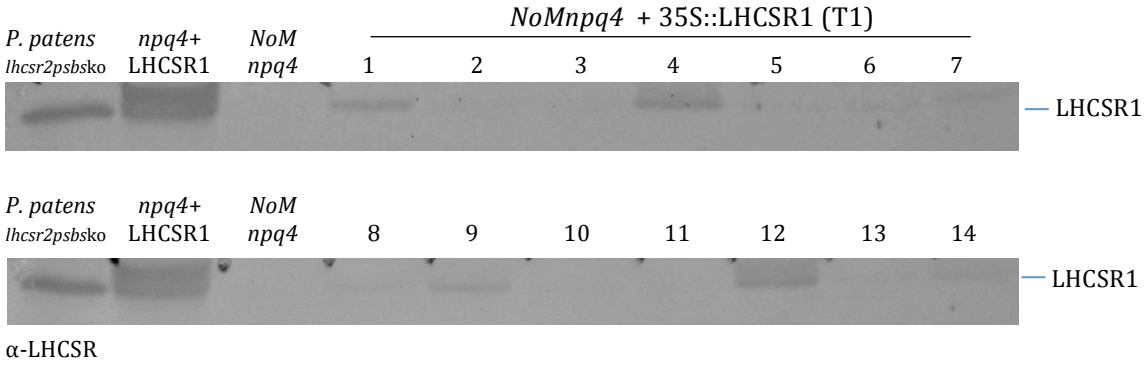

Figure 2.9. Screening of *NoMnpq4* + 35S::LHCSR1 transformed lines by western blot. *Western blot analysis of the T1 generation was performed on total proteins extracted by grinding one leaf disk directly in 100 µL of loading buffer, one tenth of the volume was loaded on SDS-PAGE. Protein extracts from P. patens lhcsr2psbs ko, non-transformed NoMnpq4 and transgenic NoMnpq4+35S::LHCSR1 plants were loaded as controls (first three lanes respectively in each blot filter). The primary antibody used for the analysis is indicated on the left side of the membrane while the band corresponding either to P. patens LHCSR1 or is indicated on the right side.*

II.2.1.2 LHCSR1 expression in *A. thaliana ch1lhcb5*

First, there are no major differences observed in the phenotype between transformed and control plants. Screening of the first plant generation (T1) with western blot resulted into 5 stable lines, which accumulate LHCSR1. All plant lines accumulating LHCSR1 were isolated (lines #1 - #5, Figure 2.10B) and left to grow until seeds were ready to collect for the analysis of T2 plant generation. Following the same selection procedure on MS medium plates enriched in hygromycin-B, 24 resistant plants of T2 generation were screened by western blot analysis, verifying that LHCSR1 can be expressed and processed to its mature form in the absence of Chlb. Lines with the highest protein accumulation were collected and stored for future characterization of T3 generation (i.e. lines #2, #3, #4, #8 and #18, Figure 2.10C).

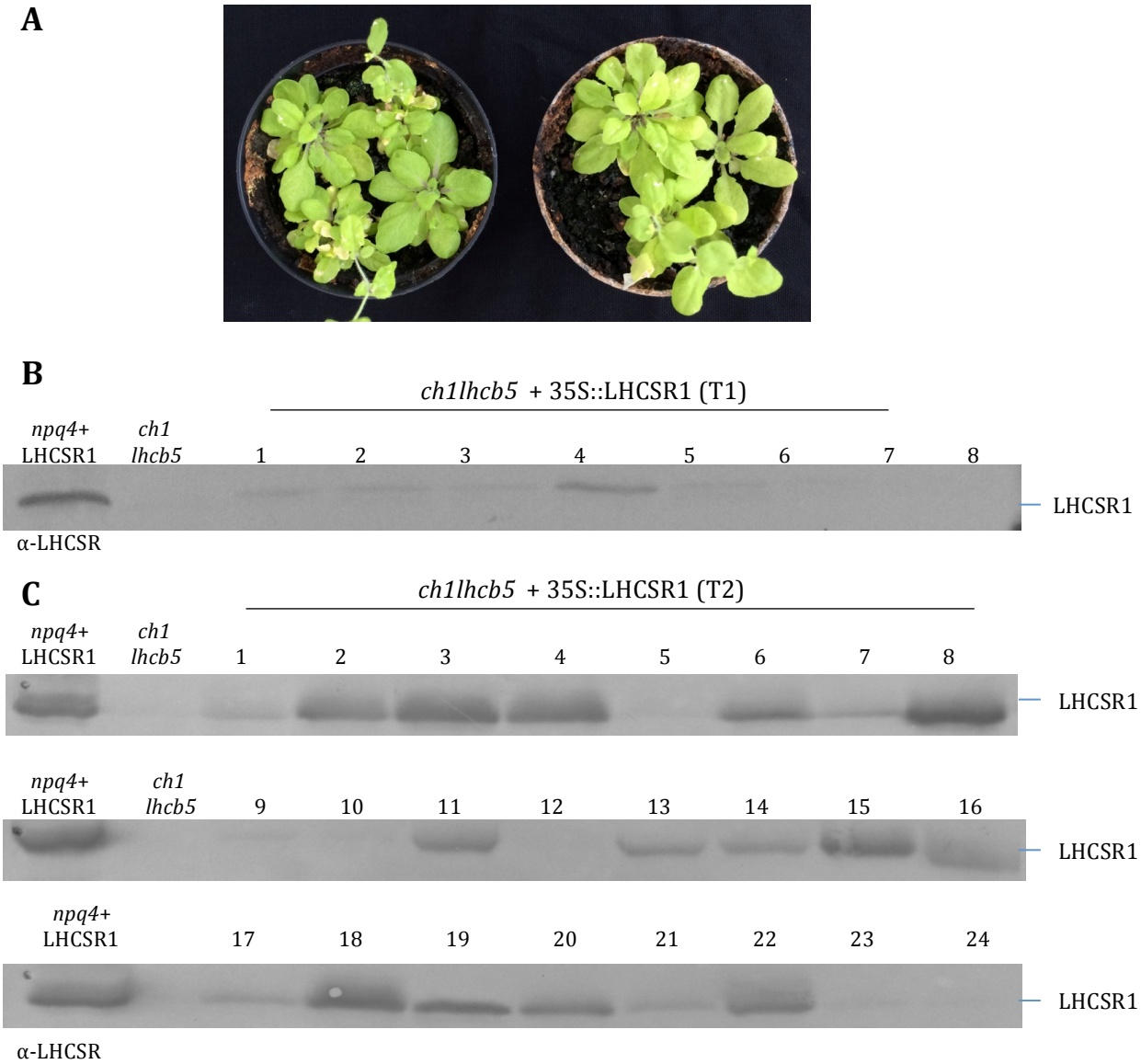

Figure 2.10. Biochemical characterization of *ch1lhcb5* + 35S::LHCSR1 transformed lines. *A) A. thaliana transgenic lines were selected on agar plates supplemented with hygromicine-B and then transferred in soil pots in a short-day photoperiod growth chamber under controlled temperature conditions for 3-4 weeks (right). Control ch1lhcb5 plants of the same age were also grown in the same conditions (left). B) Western blot analysis of the T1 generation was performed on total proteins extracted by grinding one leaf disk directly in 100 µL of loading buffer, one tenth of the volume was loaded on SDS-PAGE. Proteins of non-transformed ch1lhcb5 and transgenic npq4+35S::LHCSR1 plants were loaded as controls. The primary antibody used for the analysis is indicated on the left side of the membrane while the band corresponding either to P. patens LHCSR1 is indicated on the right side C) Western blot analysis of 24 independent plant lines from the T2 generation.*

II.2.2 LHCSR1 quenching activity in *NoMnpq4* and *ch1lhcb5* plants

After successful expression of LHCSR1 in the thylakoid membranes of *A. thaliana NoMnpq4* and *ch1lhcb5* antenna mutants, stable transgenic lines were tested for their NPQ activity in a series of fluorescence video-imaging measurements. All of these measurements were performed on dark-adapted leaves detached from 35S::LHCSR1 and control plants of the same age. The protocols used were the same as for all LHCSR1-

complemented plants, consisted of 4 successive 5-min actinic light cycles with an intermediate 5-min dark recovery phase.

II.2.2.1 LHCSR1 activity in *A. thaliana NoMnpq4*

When the first cycle of NPQ was applied there was no significant difference between control and independent 35S::LHCSR1-complemented plant lines (n=14). The same phenotype was observed when the protocol was applied for a second type, having both control and transgenic plants showing no activity. Even after two more NPQ cycles, there was no trace of quenching activity during the light period and no recovery during the dark period. Both the transgenic and control *NoMnpq4* plant lines remain completely 'flat' during all measuring cycles (Figure 2.11). The same phenotype is observed for the fast recovery (qE) when the actinic light was switch off, with no difference between control and 35S::LHCSR1-complemented plant lines (Figure 2.12)

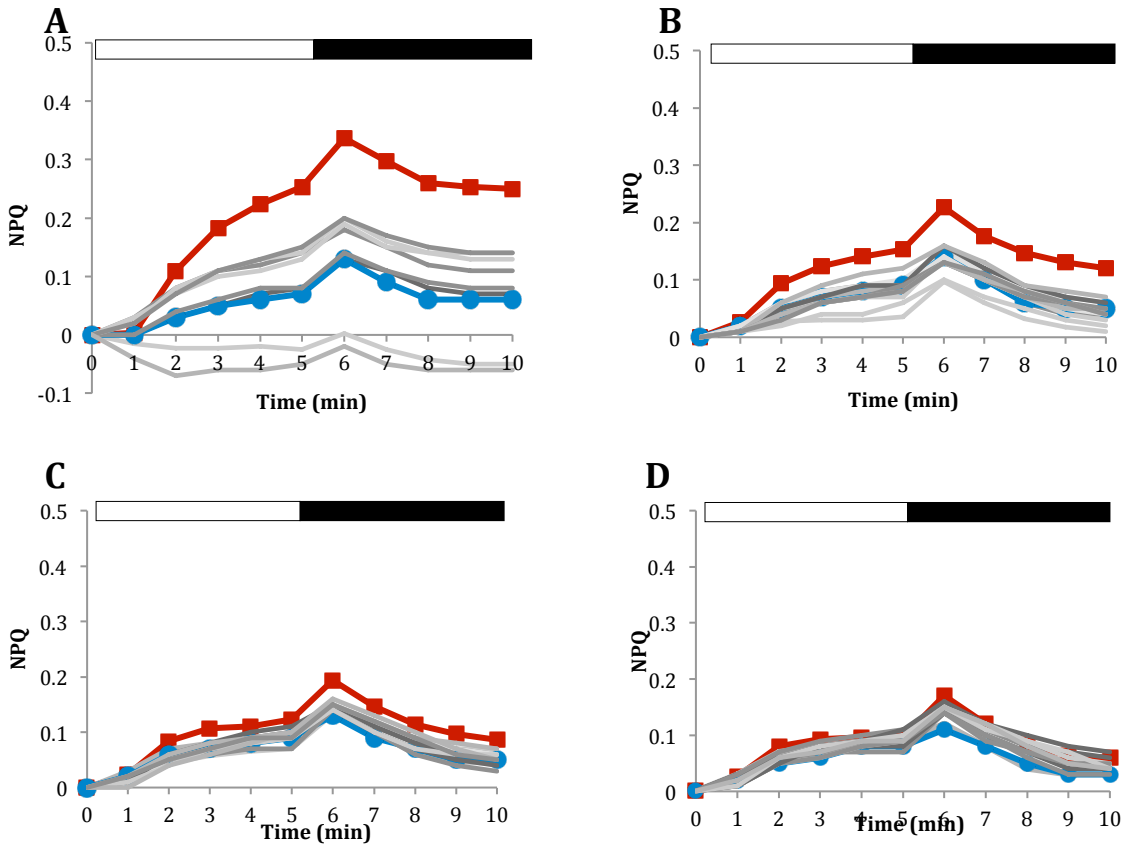

Figure 2.11. NPQ induction in *NoMnpq4* + 35S::LHCSR1 lines using fluorescence video-imaging. *NPQ of Chl fluorescence was measured on leaves from 14 independent NoMnpq4 + 35S::LHCSR1 lines detached of 4-5-week old plants at room temperature. The results of 4 successive NPQ cycles are presented. Protocol: 5 minute of actinic light treatment followed by 5 min of dark recovery. NPQ, calculated as quenching of maximal fluorescence (Fm - Fm')/Fm' for every saturating flash. Blue line, non-transformed NoMnpq4; red line, npq4. A. thaliana leaves were dark adapted for 45 minutes. After an Fm measurement, NPQ was induced by 5min of white actinic light (1200 µmol m^{-2} s^{-1}; white bar) followed by 5min of dark relaxation, repeated for 4 measuring cycles (A-D, cycles 1-4).*

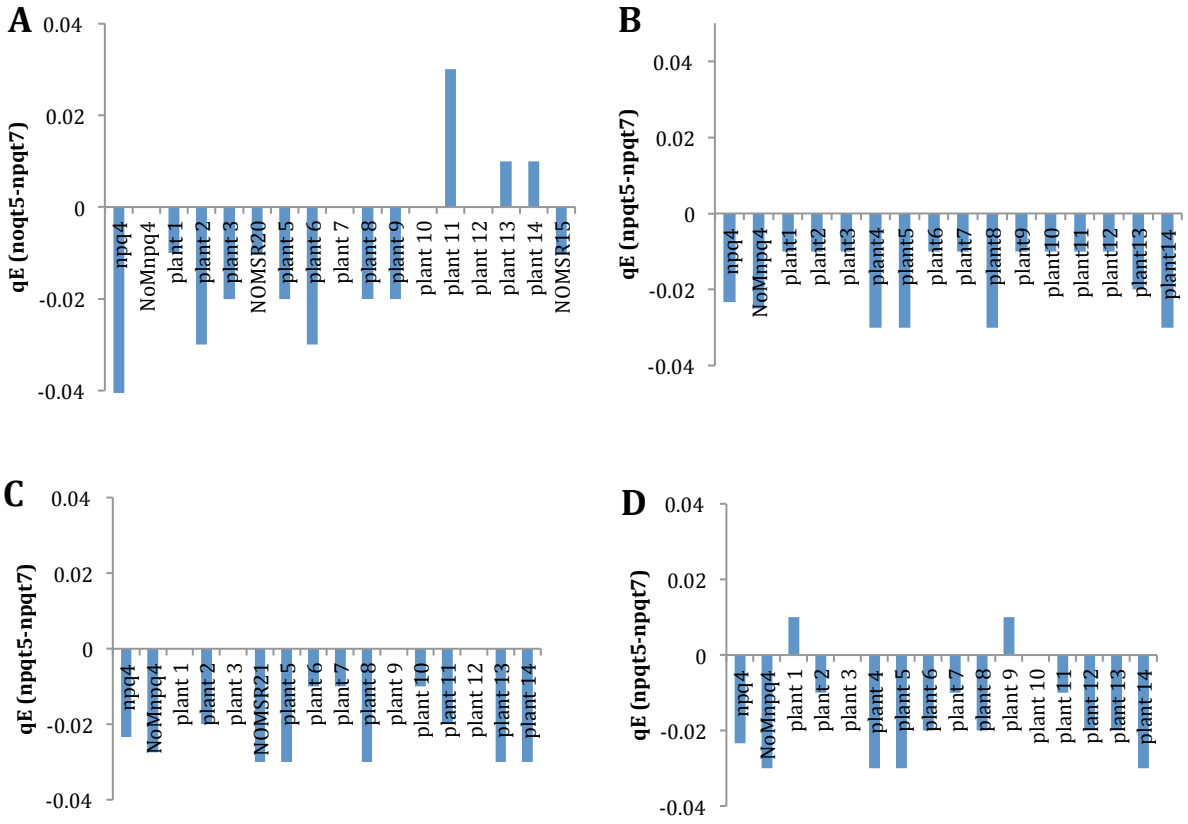

Figure 2.12. Fast recovery (qE) *NoMnpq4* + 35S::LHCSR1 lines using fluorescence video-imaging. *qE of 14 independent NoMnpq4 + 35S::LHCSR1 lines was measured on dark-adapted leaves detached of 4-5-week old plants at room temperature. The results of 4 successive NPQ cycles are presented. Protocol: 5 minute of actinic light treatment followed by 5 min of dark recovery. qE calculated as the last point in the light phase minus the second point in the dark (qE = npqt5 – npqt7, see figure 2.11). Leaves from npq4 and non-transformed NoMnpq4 plants were used as controls. (A-D: cycles 1-4).*

II.2.2.2 LHCSR1 activity in *A. thaliana ch1lhcb5*

Chlorophyll fluorescence quenching of control *ch1lhcb5* and 7 independent 35S::LHCSR1 complemented plants accumulating high levels of LHCSR1 protein (i.e. #2, #3, #4, #8, #11, Figure 2.10 C) was measured by video-imaging following a standard procedure for *A. thaliana*. The protocol consisted of a 45-min dark adaptation of leaves, followed by 4 successive cycles of 5-min NPQ light induction using white actinic light (1200 µmol m^{-2} s^{-1}) and a 5-min phase of dark recovery. When the protocol was applied for the first time, all genotypes analyzed had the same fluorescence profile (NPQ_{ch1} = 0.44 vs. $NPQ_{ch1+LHCSR1}$ = 0.46) with some 35S::LHCSR1-complemented lines having a lower NPQ activation with respect to the control *ch1lhcb5*. In fact the quenching activity appears to be the same also during the following three cycles of illumination without any major difference between control and complemented *ch1lhcb5* plants (Figure 2.13 A).

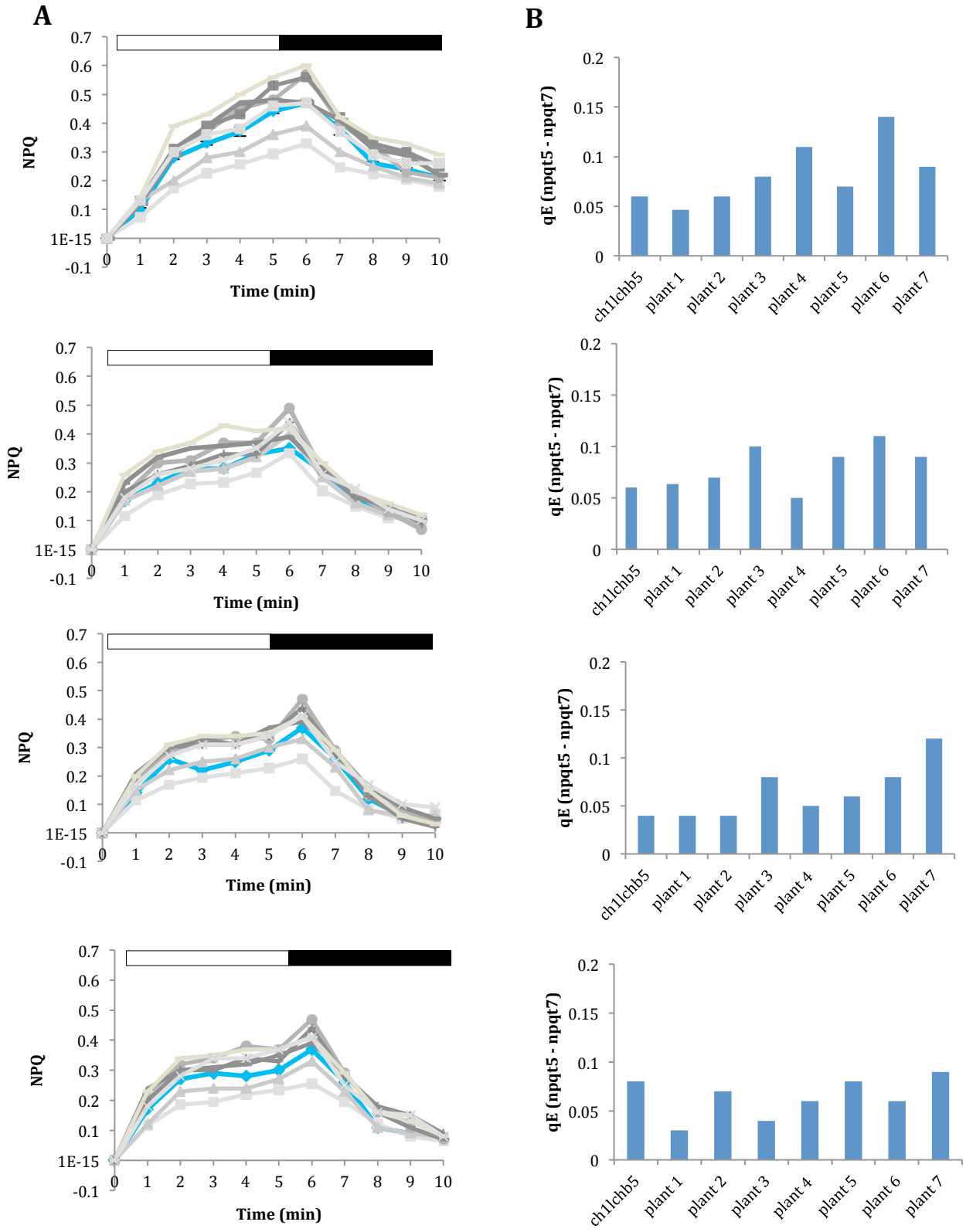

Figure 2.13. NPQ induction in *ch1lhcb5* + 35S::LHCSR1 lines using fluorescence video-imaging. *NPQ of Chl fluorescence was measured on leaves detached of 4-5-week old plants at room temperature. The results of 4 successive NPQ cycles are presented. Protocol: 5 minute of actinic light treatment (1200 µmol m^{-2} s^{-1}; white bar) followed by 5 min of dark recovery (black bar). A) NPQ, calculated as quenching of maximal fluorescence (Fm - Fm')/Fm' for every saturating flash. Bright blue line, non-transformed ch1lhcb5 (control). A. thaliana leaves were dark adapted for 45 minutes. After an Fm measurement, NPQ was induced by 5min of white actinic light followed by 5min of dark relaxation, repeated for 4 measuring cycles. From top to bottom, cycles 1-4. B) qE fast recovery calculated as the last point in the light minus the second point in the dark phase (qE = $npqt_5$ - $npqt_7$). From upper to lower panels, cycles 1-4*

II.2.3 LHCSR1 accumulation in the thylakoid membranes of *A. thaliana*

To verify that LHCSR1 was actually imported to the chloroplast and inserted in thylakoid membranes, we have purified thylakoid proteins from *A. thaliana* 35S::LHCSR1 complemented backgrounds but also control *npq4* plants and we have analyzed them by SDS-PAGE through coomassie staining (Figure 2.14, A) and western blotting (Figure 2.14, B). A band with the apparent molecular weight of LHCSR1 is present in a region exclusively in 35S::LHCSR1-complemented plants but not in *npq4*. No other major change could be highlighted between control and complemented genotypes (Figure 2.14, B), apart from the absence of LHCII and monomeric Lhcb subunits in the *ch1lhcb5* sample due to the lack of Chlb. Western blot analysis confirmed that anti-LHCSR antibody reacts against the *P. patens* protein accumulated in thylakoid membranes of 35S::LHCSR1-complemented backgrounds (Figure 2.14, B). Also in this case, *P. patens* and *A. thaliana wild-type* thylakoid membranes were used as additional controls for western blot analysis. LHCSR1 and LHCSR2 were detected in *P. patens* wild-type thylakoids but not in *A.thaliana* wild-type (Figure 2.14, B).

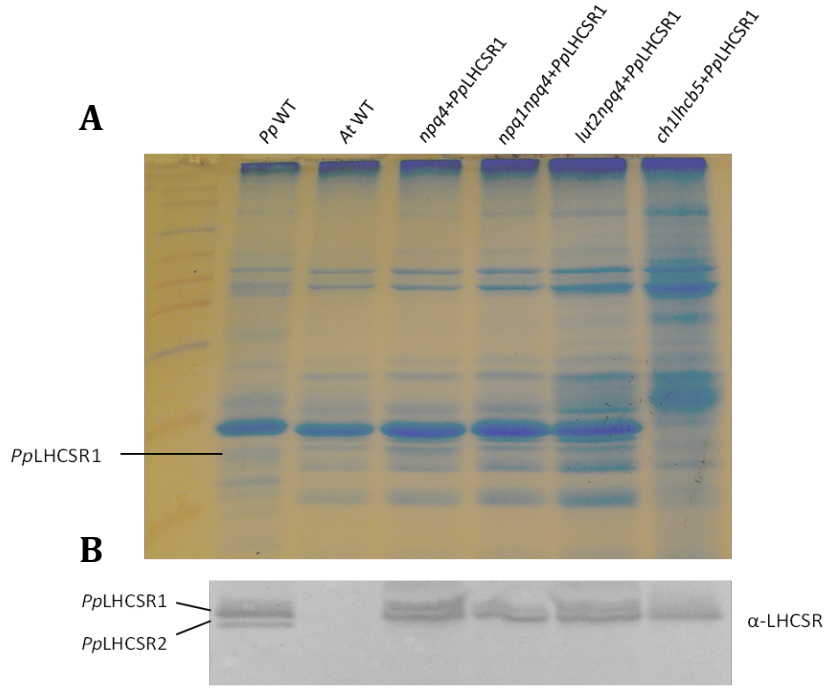

Figure 2.14. Coomasie-staining and western blot analysis of 35S::LHCSR1-complemented *A. thaliana* mutants. *A) Coomassie-stained SDS-PAGE separation of thylakoid proteins isolated from 35S::LHCSR1-complemented A. thaliana plants. The identity of LHCSR1 is indicated on the right side of the gel. Thylakoids from P. patens and A. thaliana wild-type thylakoids were loaded as controls. B) Western blot analysis of thylakoid proteins isolated from 35S::LHCSR1-complemented A. thaliana plants and developed against a-LHCSR antibody. As an external control, thylakoid proteins from P. patens and A. thaliana wild-type were also loaded on the gel. Genotypes loaded (from left to right): P. patens wild-type, A. thaliana wild-type, npq4 + 35S::LHCSR1, npq1npq4 + 35S::LHCSR1, lut2npq4 + 35S::LHCSR1 and ch1lhcb5 + 35S::LHCSR1. Samples were loaded on a Chl basis of 2ug for the coomassie staining and 1ug for the western blot analysis.*

II.2.4 Abundance of LHCSR1 in the thylakoid membranes of *A. thaliana*

The abundance of LHCSR1 in the thylakoid fraction of the different *A. thaliana* expression systems was determined by immuno-titration, using as a reference the purified His-tag LHCSR1 from *N. tabacum* (Figure 2.15, A). Different thylakoid amounts from 35S::LHCSR1-complemented *A. thaliana* mutants (0.25, 0.5, 1, 1.25 ug Chl) were loaded on a SDS-polyacrylamide gel, together with serial dilutions of His-tag LHCSR1 (0.006, 0.012, 0.025, 0.05 ug Chl). Reactivity of α-LHCSR antibody and intensity of LHCSR1 from each sample were evaluated by densitometric analysis of immunoreactions. The amount of protein was calculated for 1ug Chl per genotype: 0.06 ug of protein are present in LHCSR1-complemented *npq4* thylakoids as well as in *npq1npq4* background. Slightly less LHCSR1 is present in the thylakoids of *lut2npq4* (0.044ug/1ug Chl) while the lower amount of LHCSR1 was calculated for the complemented *ch1lhcb5* (0.015 ug protein).

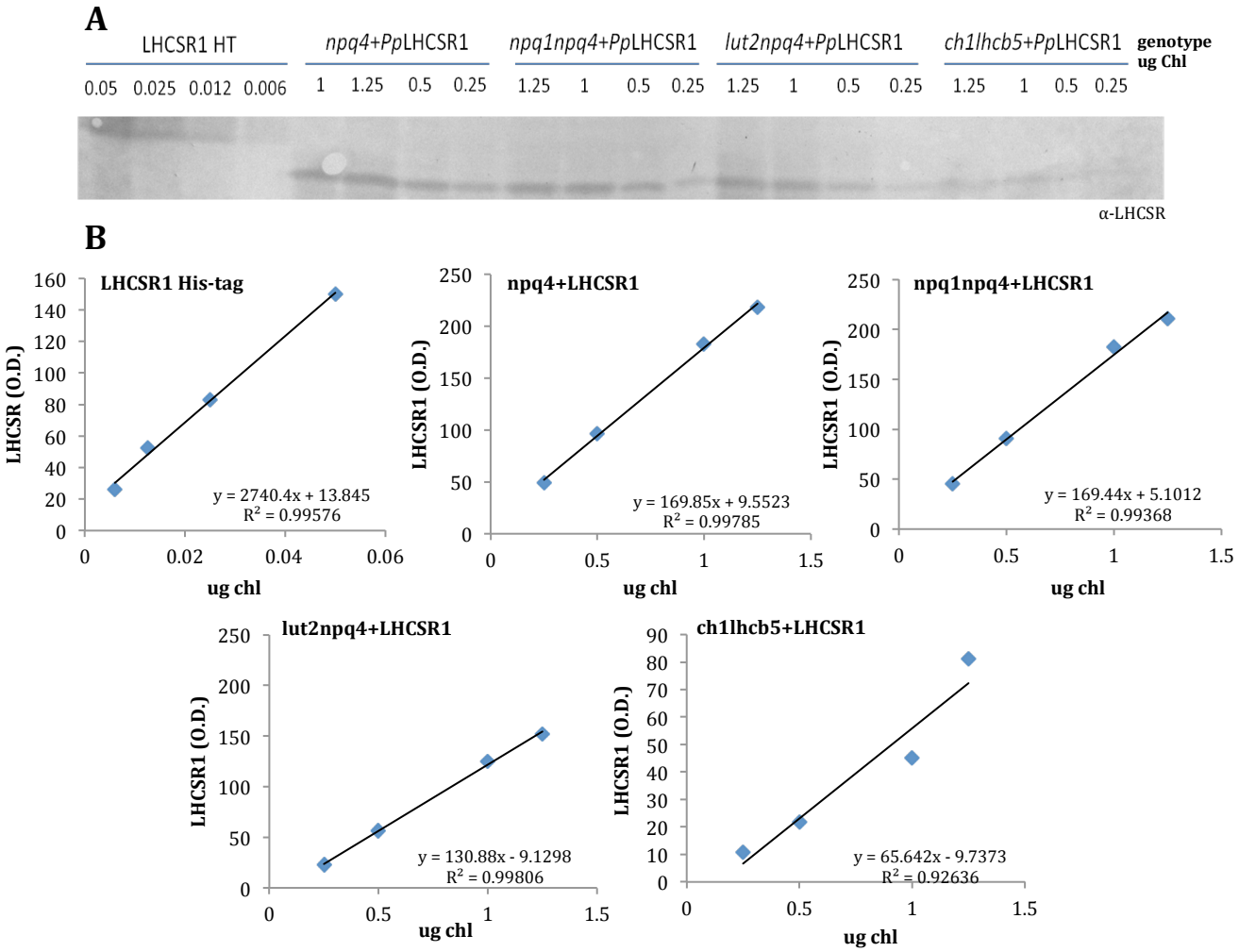

Figure 2.15. Abundance of LHCSR1 protein in different *A. thaliana* expression backgrounds. *A) LHCSR1 immunotitration of thylakoids from different 35S::LHCSR1-complemented A. thaliana mutants. Different thylakoid amounts (0.25, 0.5, 1, 1.25 ug Chl) were loaded on a SDS-polyacrylamide gel together with serial dilutions of His-tag LHCSR1 (0.006, 0.012, 0.025, 0.05 ug Chl) as a reference. B) Correlation between intensity of LHCSR1 signal and ug of Chl loaded. Amount of LHCSR1 was estimated on the basis of ug of Chl of LHCSR1/ug Chl of thylakoids:* ***npq4*** *= 0.06,* ***npq1npq4*** *= 0.059,* ***lut2npq4*** *= 0.044,* ***ch1lhcb5*** *= 0.015*

Discussion

The pigment-binding protein LHCSR1, member of the LHC family, is responsible for the activation of NPQ in the moss *Physcomitrella patens* (Alboresi et al., 2010; Gerotto et al., 2012). The activity of LHCSR1 is strictly zeaxanthin-dependent since lack of this specific xanthophyll leads to loss of NPQ induction (Pinnola et al., 2013). Following the heterologous expression strategy previously applied for the PSBS-less *npq4* (Chapter 1), we proceeded with the 35S::LHCSR1 *in vivo* complementation of *Arabidopsis thaliana* mutants altered either in the carotenoid content or antenna system composition and studied the NPQ activity of the generated LHCSR1-complemented transgenic plants.

In vivo complementation of *A. thaliana npq1npq4*, the *vde* KO mutant unable to accumulate zeaxanthin resulted in several transgenic plant lines accumulating LHCSR1 in thylakoid membranes. The heterologous-expressed LHCSR1 protein was correctly addressed to the thylakoid membranes of 35S::LHCSR1-complemeted *npq1npq4* plants with a molecular weight identical to that of *P. patens* thylakoids observed in SDS-PAGE. This was verified also during the screening of the T2 generation where the protein was expressed in higher levels due to the presence of homozygous transgenic plants, making sure that the protein is expressed in its mature form. However, when several cycles of white actinic light where applied these plants were unable to induce NPQ verifying the extreme dependence of LHCSR1-induced NPQ on zeaxanthin. This result is in agreement with the inhibition of zeaxanthin synthesis in 35S::LHCSR1-complemeted *npq4* plants by DTT (inhibitor of VDE enzyme) performed in the previous chapter, in which DTT-infiltrated lines subjected to the same NPQ measuring protocol as *npq1npq4*, lost their NPQ activity and qE recovery.

Lutein binds to site L1 of all LHC proteins, whose occupancy is indispensable for protein folding and quenching chlorophyll triplets (Dall'Osto et al. 2006). LHC Recent structural studies on Light-Harvesting Complex II (LHCII) and minor antenna CP29 isolated from spinach show that four or three carotenoid-binding regions are present per LHCII monomer or CP29 respectively (Pan et al., 2012). These regions are occupied by lutein (L1, L2) neoxanthin (N1) and violaxanthin (V1) in LHCII while in the case of CP29 by lutein (L1), violaxanthin (L2) and neoxanthin (N1). As a member of the light-harvesting complex (LHC) superfamily, LHCSR1 has as well four carotenoid-binding sites within its structure one of which is occupied by lutein. Absence of this carotenoid could have a direct or effect on the stability or expression of LHCSR1 leading to a wrong

protein folding and degradation. Surprisingly, *in vivo* complementation of *A. thaliana lut2npq4* plants completely deficient of lutein, generated transgenic plant lines expressing LHCSR1 protein in a similar level, something that was also verified in the T2 generation of transgenic plants. Thus, absence of lutein does not de-stabilize LHCSR1, which remains stable in thylakoid membranes. This is consistent with the conservation of LHC proteins in *lut2* mutant (Pogson et al. 1996; Dall'Osto et al. 2006) although with a different aggregation state, i.e. the LHCII complex trimers were disrupted into monomers.

Recent results on the isolated LHCSR protein showed the formation of a lutein radical cation in quenching conditions (Pinnola et al. 2016) despite the very strong requirement of zeaxanthin for qE activity (Pinnola et al. 2015). When NPQ was measured, the majority of these lines activated NPQ on a level similar to that of *npq4* plants complemented with LHCSR1. This relatively stable expression of LHCSR1 protein in the absence of lutein but also the quenching activity are indicative of lutein being dispensable for *Pp*LHCSR1-dependent NPQ activity, suggesting lutein and zeaxanthin can lead to the same function in the fundamental physico-chemical process responsible for quenching. A similar conclusion was reached in *A. thaliana* (Li X. et al., 2002; Li Z. et al., 2009) where, however, PSBS rather than LHCSR1 triggers NPQ. We conclude that the properties of zeaxanthin and lutein makes them particularly suited for quenching reactions within pigment-binding complexes irrespective from whether they bind to LHCSR or to other LHC antenna proteins which are in charge of quenching reactions in PSBS-dependent systems.

Once light energy is captured by the LHCII antenna system it is channeled towards PSII reaction center, where charge separation occurs. Monomeric Lhcb subunits of LHCII or else minor antennae CP24, CP26 and CP29 play a crucial role in this energy transfer since they are the connecting link between the major LHCII antennas and PSII reaction center. *In vivo* complementation of *A. thaliana NoMnpq4, a* mutant lacking these monomeric subunits and also PSBS protein, led to transgenic plant lines accumulating LHCSR1 in thylakoid membranes, thus proving expression of LHCSR1 is independent from monomeric LHC proteins. However, the protein is not active in the generated *NoMnpq4*-LHCSR1 plants even after several cycles of strong illumination were applied, having no significant difference from the control *NoMnpq4*. In this context, *in vivo* complementation of the *Arabidopsis* Chlb-less mutant *ch1*, completely devoid of antenna system, generated T2 homozygous plants over-expressing LHCSR1. Like in the case of

NoMnpq4, there is no significant difference in the quenching activity between 35S::LHCSR1-complemented *ch1lhcb5* and control plants, showing that LHCSR1 cannot rescue NPQ phenotype in the absence of antenna system. These findings suggest that subunits of LHCII (i.e. one or more of the monomeric Lhcb subunits) could be quenching partners of LHCSR1, thus allowing for a partial quenching activity in the *Arabidopsis* backgrounds where both the major LHCII and minor antennae are present (i.e *npq4*).

LHCSR1 can be successfully imported to the chloroplast and inserted in thylakoid membranes as shown from the Coomassie staining and western blot analysis of purified thylakoid proteins from *A. thaliana* 35S::LHCSR1-complemented backgrounds. A band with the apparent molecular weight of LHCSR1 is present exclusively in 35S::LHCSR1 complemented plants but not to in *npq4*, strongly suggesting a correct targeting and processing of the pre-protein encoded by the constructs. Immunotitration of LHCSR1 coming from thylakoids of transformed *A. thaliana* backgrounds showed that expression of LHCSR1 in *A. thaliana npq4* gives a yield of 0.06 ug Chl LHCSR1/ ug Chl thylakoids, similar to the one from 35S::LHCSR1-complemented *npq1npq4,* while expression in the lutein-less *lut2npq4* has a slightly lower yield of 0.044. These results are in agreement with recent studies on the stable expression of LHCSR using heterologous systems such as *N.tabacum* and *N. benthamiana* with an LHCSR1 yield of up to 0.036 ug Chl of LHCSR1/ug Chl of thylakoids.

PpLHCSR1 in A. thaliana				
Genotype	**Main background characteristics**	**LHCSR1 accumulation**	**NPQ activity**	**qE component**
npq4	no PSBS	yes	yes	partial recovery
npq1npq4	no Zeaxanthin, no PSBS	yes	no effect	no recovery
lut2npq4	no Lutein, no PSBS	yes	yes	partial recovery
NoMnpq4	absence of minor antennae, no PSBS	yes	no effect	no recovery
ch1lhcb5	Absence of Chl *b*	yes	no effect	no effect

Table 2C. *Pp*LHCSR1 in different *A. thaliana* backgrounds. *This table presents all the results obtained from the in vivo complementation of several A. thaliana mutants with LHCSR1 from P. patens. Information on the genetic profile of each used background, the accumulation of LHCSR1 in the thylakoid membranes, NPQ activity and the qE fast recovery component are presented.*

Conclusion

Heterologous expression of LHCSR1 in *A. thaliana* carotenoid mutants *npq1npq4* and *lut2npq4* mutant yields an LHCSR1 protein addressed in the thylakoid membranes. In the case of *vde* KO mutant, *npq1npq4*, the protein is inactive in NPQ induction after several cycles of illumination due to lack of violaxanthin de-epoxidation into zeaxanthin, thus verifying the extreme zeaxanthin dependence of LHCSR1 (Chapter 1). In contrast, LHCSR1-complemented *lut2npq4* plants in which LHCSR1 protein is also successfully expressed, maintain their partial quenching activity showing that LHCSR1 activity and expression are independent of lutein. Finally, insertion of LHCSR1 in *A. thaliana* antenna mutants *NoMnpq4* and *ch1lhcb5* showed that the protein could be successfully expressed. However, induction of NPQ with white actinic light of high intensity in these mutants does not lead to any significant quenching activity, implying that subunits of the LHCII antenna system are essential for the LHCSR1 activity *in planta*.

Bibliography

Bugos RC, Yamamoto HY (1996) Molecular cloning of violaxanthin de-epoxidase from romaine lettuce and expression in Escherichia coli. Proc. Natl. Acad. Sci. U. S. A 93: 6320-6325.

Busch A., Hippler M., The structure and function of eukaryotic photosystem I, Biochim. Biophys. Acta Bioenerg. 1807 (2011) 864–877.

Caffarri S, Croce R, Breton J, Bassi R (2001) The major antenna complex of photosystem II has a xanthophyll binding site not involved in light harvesting. J. Biol. Chem. 276: 35924-35933.

Chen Xi, Zhang W, Xie Y, Lu W, Zhang R (2007) Comparative proteomics of thylakoid membrane from a chlorophyll b-less rice mutant and its wild type. Plant Sci 173: 397-407

Croce R., H. van Amerongen, Natural strategies for photosynthetic light harvesting, Nat. Chem. Biol. 10 (2014) 492–501.

Croce R., H. van Amerongen, Light-harvesting in photosystem I, Photosynth. Res. 116 (2013) 153–166.

Dall'Osto L, Caffarri S, Bassi R (2005) A mechanism of nonphotochemical energy dissipation, independent from Psbs, revealed by a conformational change in the antenna protein CP26. Plant Cell 17: 1217-1232.

Dall'Osto L, Lico C, Alric J, Giuliano G, Havaux M, Bassi R. (2006). Lutein is needed for efficient chlorophyll triplet quenching in the major LHCII antenna complex of higher plants and effective photoprotection in vivo under strong light. BMC Plant Biol. 2006 Dec 27;6:32

Dall'Osto, L., Holt, N.E., Kaligotla, S., Fuciman, M., Cazzaniga, S., Carbonera, D., Frank, H.A., Alric, J., and Bassi, R. (2012). Zeaxanthin protects plant photosynthesis by modulating chlorophyll triplet yield in specific light-harvesting antenna subunits. The Journal of biological chemistry.

Dall'Osto L., Unlü C., Cazzaniga S., H. van Amerongen (2014). Disturbed excitation energy transfer in *Arabidopsis thaliana* mutants lacking minor antenna complexes of photosystem II. Biochimica et Biophysica Acta 1837 (2014) 1981–1988.

D.G. Durnford, J.A. Price, S.M.McKim, M.L. Sarchfield, Light-harvesting complex gene expression is controlled by both transcriptional and post-transcriptional mechanisms during photoacclimation in Chlamydomonas reinhardtii, Physiol. Plant. 118 (2003) 193–205.

De Bianchi S., Ballottari M., Dall'Osto L., Bassi R., Regulation of plant light harvesting by thermal dissipation of excess energy, Biochem. Soc. Trans. 38 (2010) 651–660.

Demmig-Adams B, Winter K, Kruger A, Czygan FC (1989) in Photosynthesis. Plant Biology Vol.8, ed. Briggs, W. R. (Alan R. Liss, New York), pp. 375-391.

Espineda, C.E., Linford, A.S., Devine, D., and Brusslan, J.A. (1999). The AtCAO gene, encoding chlorophyll a oxygenase, is required for chlorophyll b synthesis in *Arabidopsis thaliana*. Proc. Natl. Acad. Sci. USA 96: 10507–10511.

Falbel TG, Staehelin LA (1996) Partial block in the early steps of the chlorophyll synthesis pathway: A common feature of chlorophyll b-deficient mutants. Physiol Plant 97: 311-320

Gilmore A, Hazlett T, Debrunner P, Govindjee (1996) PS II Chl a fluorescence lifetimes and intensity are independentof the antenna size difference between barley wild type and chlorina mutants: photochemical quenching andxanthophylls cycle dependent non-photochemical quenching of fluorescence. Photosynth Res 48: 171-187

Gobets B., R. van Grondelle, Energy transfer and trapping in photosystem I, Biochim. Biophys. Acta Bioenerg. 1507 (2001) 80–99.

Harrer R. Bassi R., Testi M.G., Schäfer C (1998) Nearest-neighbor analysis of a Photosystem II complex from *Marchantia polymorpha* L. (liverwort), which contains reaction center and antenna proteins. Febs Journal Volume 255, Issue 1, 196–205

Havaux M, Gruszecki I, Dupont I, Leblanc RM (1991) Increased heat emission and its relationship to the xanthophyll cycle in pea leaves exposed to strong light stress. J. Photochem. Photobiol. B 8: 361-370.

Havaux, M., and Tardy, F. (1997). Thermostability and photostability of photosystemII in leaves of the Chlorina-f2 barleymutant deficient in lightharvesting chlorophyll a/b protein complexes. Plant Physiol. 113: 913–923.

Havaux M, Niyogi KK (1999) The violaxanthin cycle protects plants from photooxidative damage by more than one mechanism. Proc. Natl. Acad. Sci. U. S. A 96: 8762-8767.

Havaux, M., Dall'Osto, L., and Bassi, R. (2007). Zeaxanthin has enhancedantioxidant capacity with respect to all other xanthophylls in Arabidopsis leaves and functions independent of binding to PSII antennae. Plant Physiol. 145: 1506–1520.

Holt NE et al. (2005) Carotenoid cation formation and the regulation of photosynthetic light harvesting. Science 307: 433-436

H. van Amerongen, J.P. Dekker, Light harvesting in photosystem II, Light-harvesting antennas in photosynthesis, Kluwer Academic Publishers, 2003, pp. 219–251.

H. van Amerongen, Croce R. , Light harvesting in photosystem II, Photosynth. Res. 116 (2013) 251–263.

Kim, E.-H., Li, X.-P., Razeghifard, R., Anderson, J.M., Niyogi, K.K., Pogson, B.J., and Chow, W.S. (2009). The multiple roles of lightharvesting chlorophyll a/b-protein complexes define structure and optimize function of Arabidopsis chloroplasts: A study using two chlorophyll b-less mutants. Biochim. Biophys. Acta 1787: 973–984.

Leverenz, J.W., Öquist, G., and Wingsle, G. (1992). Photosynthesis and photoinhibition in leaves of chlorophyll b-less barley in relation to absorbed light. Physiol. Plant. 85: 495–502.

Li Z, Ahn TK, Avenson TJ, Ballottari M, Cruz JA, Kramer DM, Bassi R, Fleming GR, Keasling JD, Niyogi KK. Lutein accumulation in the absence of zeaxanthin restores nonphotochemical quenching in the *Arabidopsis thaliana* npq1 mutant. Plant Cell. 2009 Jun;21(6):1798-812

Lin Z-F, Peng C-L, Lin G-Z, Ou Z-Y, Yang C-W, Zhang J-L (2003) Photosynthetic characteristics of two new chlorophyll b-less rice mutants. Photosynthetica 41: 61-67

Liu Z.F., H.C. Yan, K.B. Wang, T.Y. Kuang, J.P. Zhang, L.L. Gui, X.M. An, W.R. Chang, Crystal structure of spinach major light-harvesting complex at 2.72 Angstrom resolution, Nature 428 (2004) 287–292.

Melkozernov A.N., S. Lin, R.E. Blankenship, Excitation dynamics and heterogeneity of energy equilibration in the core antenna of photosystem I from the cyanobacterium Synechocystis sp. PCC 6803, Biochemistry 39 (2000) 1489–1498.

Morosinotto T, Baronio R, Bassi R (2002) Dynamics of chromophore binding to Lhc proteins in vivo and in vitro during operation of the xanthophyll cCycle. J. Biol. Chem. 277: 36913-36920.

Nelson N., A. Ben-Shem, The complex architecture of oxygenic photosynthesis, Nat. Rev. Mol. Cell Biol. 5 (2004) 971–982.

Nelson N., C.F. Yocum, Structure and function of photosystems I and II, Annu. Rev. Plant Biol. 57 (2006) 521–565.

Niyogi KK, Björkman O, Grossman AR (1997) Chlamydomonas xanthophyll cycle mutants identified by video imaging of chlorophyll fluorescence quenching. Plant Cell 9: 1369-1380.

Pan, X., Li, M., Wan, T., Wang, L., Jia, C., Hou, Z., Zhao, X., Zhang, J., and Chang, W. (2011). Structural insights into energy regulation of light-harvesting complex CP29 from spinach. Nature structural & molecular biology 18: 309–15.

Pinnola A., Dall'Osto L., Gerotto C., Morosinotto T., Bassi R., Alboresi A. (2013) Zeaxanthin binds to light-harvesting complex stress-related protein to enhance nonphotochemical quenching in Physcomitrella patens. Plant Cell 25, 3519–3534

Pinnola A., Staleva-Musto H., Capaldi S., Ballottari M., Bassi R. and Polívka T. Electron transfer between carotenoid and chlorophyll contributes to quenching in the LHCSR1 protein from Physcomitrella patens. Biochim Biophys Acta. 2016 Dec;1857(12):1870-1878.

Schatz G.H., Brock H., Holzwarth A.R., Kinetic and energetic model for the primary processes in photosystem-II, Biophys. J. 54 (1988) 397–405.

Tanaka A, Ito H, Tanaka R, Tanaka NK., Yoshida K, Okada K (1998) Chlorophyll a oxygenase (CAO) is involved in chlorophyll b formation from chlorophyll a. Proc Natl Acad Sci USA 95: 12719-12723

Veerman J., F.K. Bentley, J.J. Eaton-Rye, C.W. Mullineaux, S. Vasil'ev, D. Bruce, The PsbU subunit of photosystem II stabilizes energy transfer and primary photochemistry in the phycobilisome — photosystem II assembly of Synechocystis sp. PCC 6803, Biochemistry 44 (2005) 16939–16948

Chapter 3
Towards LHCSR1 *in vivo* mutational analysis

Abstract

In normal light conditions, pigments of antenna systems can efficiently capture light energy and channel it towards the reaction center. However, in high light conditions the absorption of energy often exceeds the rate of photochemical reactions, leading to the production of highly reactive oxygen species that can damage the photosynthetic apparatus and inhibit photosynthesis. Non-photochemical quenching (NPQ) is one of the major photoprotection mechanisms adapted by algae, mosses and higher plants in order to overcome excess light stress. LHCSR proteins, members of the LHC family are proven to be effectively tuned from light harvesting to excess energy quenching. In the case of green algae such as *C. reinhardtii*, LHCSR3 can activate NPQ in high light conditions whereas in the moss *P. patens* the major NPQ activator is another LHCSR member called LHCSR1. Quenching reactions are activated by conformational changes that control pigment-pigment interaction within the multi-chromophore pigment-proteins. Since most amino-acid residues responsible for Chl-binding coordination are conserved within members of LHC family, a mutational analysis approach could give interesting information on the identity of crucial chromophores and the nature of the reaction involved. To this direction, a library of LHCSR1 mutants altered in Chl-binding sites was generated by using two different expression systems, an heterologous (*A. thaliana npq4*) and an homologous system (*P. patens psbslhcsr2* KO). Mutants were generated by *in vivo* transformation and screened for their LHCSR1 accumulation and NPQ activity.

Introduction

In photosynthetic eukaryotes, members of a multigenic family called Light Harvesting Complexes (LHC) compose the antenna system. In higher plants, up to 10 different isoforms have been identified to be associated to Photosystems, respectively Lhca1-4 to PSI and Lhcb1-6 to PSII (Jansson, S. 1999). Four additional isoforms (Lhca5, Lhca6, Lhcb7 and Lhcb8) have been identified from gene sequences but their functional significance is still unclear (Jansson, S. 1999; Klimmek, F. et al. 2006). All these polypeptides share the same evolutionary origin and a common structural organization (Green, B. R. and Durnford, D. G. 1996). They all have three transmembrane and two amphipathic helices, indicated respectively as A-C and D-E (Liu, Z. et al. 2004).

Chlorophyll (Chl) binding sites (Kühlbrandt, W. et al. 1994; Liu, Z. et al. 2004) can be conserved among LHC proteins or changed in their selectivity for Chla vs. Chlb depending on the conservation of the nucleophylic aminoacid residues, which provide coordination of the central Mg^{2+} Chl ligands and the chemical nature of interacting side-chains. Eight residues are conserved in all LHC proteins (Jansson, S. 1999) as identified in several LHC proteins: Lhcb1, Lhcb4, Lhca1, Lhca3 and Lhca4 (Bassi, R. et al. 1999; Morosinotto, T. et al. 2002b; Morosinotto, T. et al. 2005b; Mozzo, M. et al. 2006; Remelli, R. et al. 1999) by site-specific mutagenesis thus obtaining specific loss of chromophores or affinity changing for Chl a vs Chl b (Bassi, R. et al. 1999; Remelli, R. et al. 1999). Although sequence conservation is high among LHC proteins suggesting strong structural similarity, a specific role for each member is suggested by conservation of at least 10 LHC isoforms through the green lineage (Alboresi et al., 2006) and by fitness reduction in mutants lacking specifically LHC members in a natural environment (Ganeteg, U. et al. 2004) although the molecular mechanism differentially involved in their function are still mostly unclear.

In vitro reconstitution studies on Lhcb subunits have indicated specific Chl-sites such as Chl A2 (Ruban et al., 2007) or Chl A5 (Passarini et al., 2009) as potential candidates for energy quenching (Ahn et al., 2008). More recent studies on LHCSR3 from *C. reinhardtii* indicate Chl A3 (Liguori et al., 2016) as lowest energy state, which is located close to the lumen and to the pH-sensing region of the protein while studies on LHCSR1 from *P. patens* indicate that a possible quenching site in LHCSR1 can be observed between a Chl-carotenoid pair (Pinnola et al., 2016).

Strategy

As reported in Chapter 1, we could express LHCSR1 from *P. patens* in the thylakoid membranes of *A. thaliana npq4* plants. Recent studies have focused their efforts on the mutational analysis of several LHC components, mainly by *in vitro* reconstitution of mutant proteins with very interesting results. With the aim of investigating the role of specific chlorophylls in the quenching activity and properties of LHCSR1 *in vivo*, we proceeded to a mutational analysis study by site-directed mutagenesis using *A. thaliana* as an heterologous protein expression tool. Site-directed mutagenesis allows operating specific and intentional changes to the DNA sequence of a gene and therefore to any aminoacid in the gene product. To this direction, we initiated a series of *A. thaliana in vivo* transformations, using destination vectors which carry mutated versions of LHCSR1 on specific Chl-binding residues. These mutated LHCSR1 versions were generated using specific pairs of primers which introduce single point mutations on *lhcsr1* locus by substituting individual Chl-binding residues with others residues unable to co-ordinate porphyrins. Resistant plants were screened by western blotting for protein expression and by fluorescence video-imaging for NPQ activity. A limitation of the Arabidopsis heterologous expression system is the low amplitude of the quenching activity detected with wild-type sequence already, thus making the accuracy of phenotypes difficult. To overcome this problem we attempted parallel analysis using homologous recombination, a specific advantage of the in *P. patens,* system. Here we report on the construction of mutant genotypes and preliminary analysis of NPQ phenotypes *in vivo*.

Identification of Chl-binding sites

The alignment of LHCSR1 and LHCSR2 sequences from *P. patens* versus LHCSR3 from *Chlamydomonas reinhardtii*, Lhcb1 and Lhcb4 from *A. thaliana* shows that eight amino acid residues responsible for Chl binding among members of the LHC family (Kühlbrandt et al., 1994; Bassi et al., 1999; Liu et al., 2004) are conserved, i.e., residues coordinating four Chl *a*–specific sites (A1, A2, A4, and A5) and two Chl*a*/Chl *b* sites (A3 and B5). The two other residues (B3 and B6 sites) are not conserved with respect to LHCII. The transmembrane helices and the putative chlorophyll-binding ligands are highly conserved through the LHC family members (Pichersky and Jansson, 1996). Sequence homology between LHCII and LHCSR1 in the transmembrane helices A, B

and C and the amphipathic helix D, where Chl-binding residues have been located is very high thus suggesting a common structure.

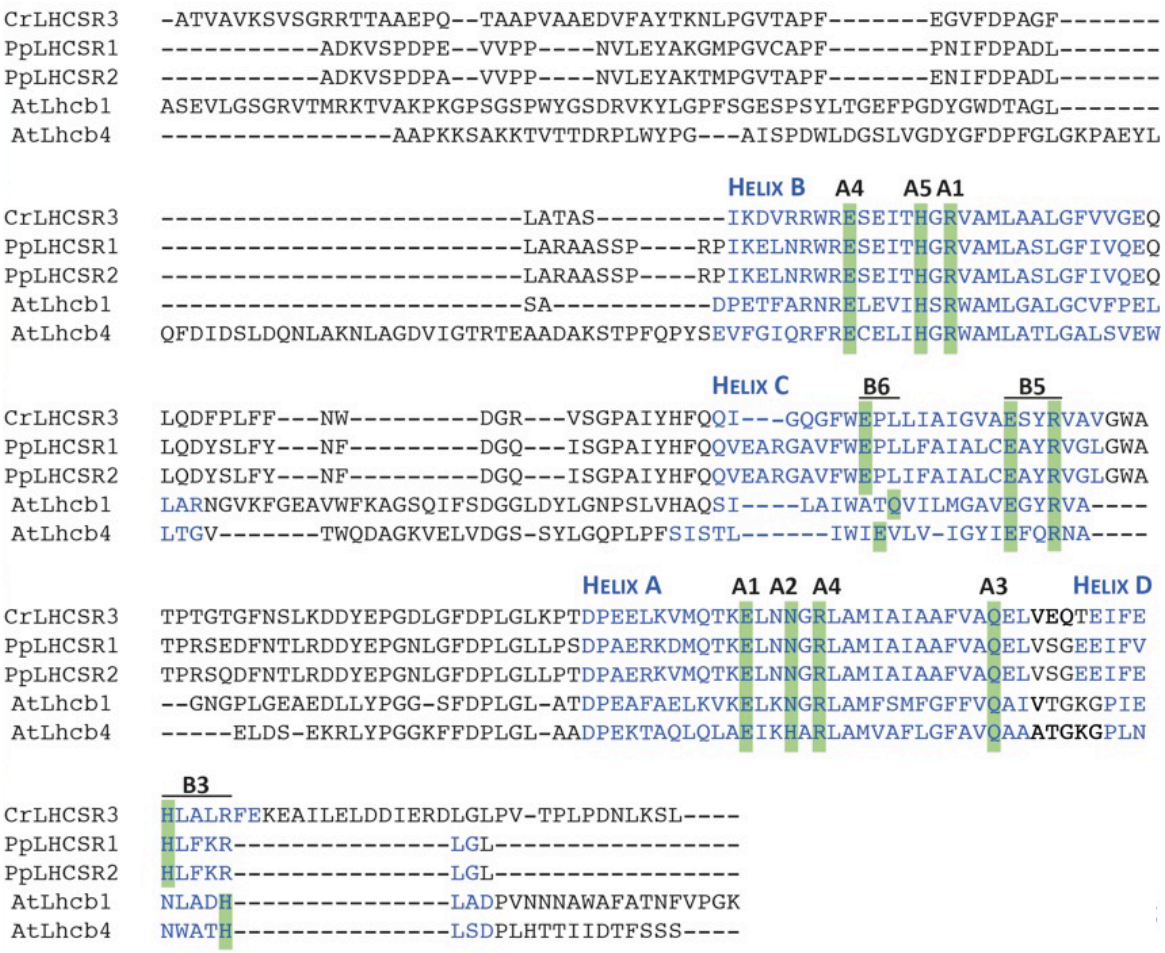

Figure 3.1. Sequence alignment of LHC binding proteins. *Sequence alignment for five LHC protein coming from three different organisms are presented. Respective protein sequences are: LHCSR3 from C. reinhardtii, LHCSR1 and LHCSR2 from P. patens, Lhcb1 and Lhcb4 from A. thaliana. Blue color indicates transmembrane domains; green color indicates Chl-coordinating residues.*

Point mutations in the LHCSR1 gene sequence

After identification of the Chl-binding sites, the codons for Chl-coordinating residues were mutated to apolar residues with similar steric hindrance using specific primers. A total number of six primer pairs were designed in order to alter the codons responsible for identity of Chl-binding residues in the following sites: Chl A2 (Chl 612), Chl A3 (Chl 613) and Chl B3 (Chl 614), Chl A5 (Chl 603), Chl B5 (Chl 609) and Chl B6 (Chl 606). Each set of primers introduced a single point mutation to *lhcsr1* gene, to an individual residue responsible for chlorophyll binding. In the case of Chl B5 in which ligands form ion pairs with two amino acids, the analysis has been done on the single mutant, since previous *in vitro* analysis of double mutants in CP29 showed reduced stability of the refolded complex (Bassi et al., 1999).

Site	LHCSR1 helix	LHCSR1 position	Mutated to
A2 (Chl612)	A	Asn 212	Phe
A3 (Chl613)	A	Gln 226	Leu
A5 (Chl603)	B	His 99	Phe
B3 (Chl614)	D	His 237	Leu
B5 (Chl609)	C	Glu 159	Val
B6 (Chl606)	C	Glu 149	Gln

Table 3A. Point mutations on LHCSR1 Chl-binding sites. *Six point mutations were introduced for six different residues coordinating Chl-binding sites, mutating them to apolar residues with similar steric hindrance. The Chl-binding site, LHCSR1 helix and mutation are presented.*

Site-directed mutagenesis and generation of mutant plasmid vectors

In the case of *A. thaliana*, the QuickChange™ site-directed mutagenesis technology was used in order to create mutant versions of LHCSR1. Having the pH7WG2/LHCSR1 construct as a DNA template (pH7WG2 vector integrated with the *lhcsr1* gene, see appendix), each set of primers was used in a series of PCR reactions in order to obtain pH7WG2 constructs carrying LHCSR1 with modified Chl-binding sites (pH7WG2/LHCSR1*).

Site	Forward primer (5'-3')	Reverse primer (5'-3')	Mutation (from-to)
A2 (Chl612)	AAA GAG CTC AAC TTC GGG CGT CTT GCC ATG	CAT GGC AAG ACG CCC GAA GTT GAG CTC TTT	N-F
A3 (Chl613)	GCT GCC TTC GTT GCG CTG GAG TTG GTC TCG	GCA GAC CAA CTC CAG CGC AAC GAA GGC AGC	Q-L
A5 (Chl603)	GAG TCT GAG ATT ACC TTC GGC CGT GTG GCC	GGC CAC ACG GCC GAA GGT AAT CTC AGA CTC	H-F
B3 (Chl614)	GAG ATC TTC GTG CTT TTG TTC AAG AGA TTG GGC	GCC CAA TCT CTT GAA CAA AAG CAC GAA GAT	H-L
B5 (Chl609)	GCC ATC GCT CTT TGC GTG GCC TAC AGA GTT	AAC TCT GTA GGC CAC GCA AAG AGC GAT GGC	E-V
B6 (Chl606)	GGC GAA CAG CAA GGG CTG CCA GAA CAC GGC	GCC GTG TTC TGG CAG CCC TTG CTG TTC GCC	E-Q

Table 3B. DNA primer sets for the generation of single-point mutations in *LHCSR1* gene. *Six DNA primer sets were specifically designed in order to alter Chl coordinating codons into apolar residues unable to bind pigments. The Chl-binding site as well as the forward and reverse primer (5'-3' direction) for the introduction of each individual mutation are presented. Amino-acids: N=asparagine; F=phenyalanine; Q=glutanime; L=leucine; H=histidine; E=glutamic acid; V=valine*

Each construct was checked by DNA digestion and sequencing in order to ensure that the whole *lhcsr1* locus was present (ATG to STOP codon) together with the correct mutation and without any additional alterations. The mutated pH7WG2/LHCSR1* constructs were later inserted in *A. tumefaciens* GV3103 competent cells in order to be

used for the transformation of *A. thaliana npq4* plants *via* the floral dip method (see Appendix).

In the case of *P. patens* the same primers were used in the QuickChange™ site-directed mutagenesis method, having the BHRf/LHCSR1 construct as a DNA template (BHRf destination vector for *P. patens* integrated with the *lhcsr1* gene). The double *P. patens psbslhcsr2* KO mutant in which NPQ activity is strongly decreased was used as a transformation background since it lacks PSBS and LHCSR2 and the only qE triggering protein left is LHCSR1. By this, the original *lhcsr1* gene could be 'exchanged' through homologous recombination with its mutated *lhcsr1* sequence variant. Also in this case, all mutated BHRf/LHCSR1* constructs were checked by DNA digestion and sequencing and they were used for the *in vivo* transformation of *P. patens* protoplasts upon verification that the *lhcsr1* locus with each mutation was present (see Appendix).

Materials and Methods

Plant culture

Protonemal tissue of *P. patens*, Gransden WT strain, was grown on minimum PpNO3 medium (Ashton et al., 1979) solidified with 0.8% Plant Agar (Duchefa Biochemie). Plants were propagated under sterile conditions on 9cm petri dishes overlaid with a cellophane disk (A.A. Packaging Limited), as previously described (Trouiller et al., 2006). Plates were placed in a growth chamber under controlled conditions: 22°C day/21°C night temperature, 16 h light/8 h dark photoperiod and a light intensity of 20 $\mu mol.m^{-2}.s^{-1}$. *Arabidopsis thaliana* wild-type plants (ecotype *Columbia*) were grown in controlled conditions of 8-h light/16-h dark with a light intensity of 100 µmol photons m^{-2} s^{-1} under stable temperature (23°C in light / 20°C in dark) for 4 weeks. Transgenic lines were grown on selective Moorashige and Skoog (MS) medium containing hygromycin-B (25mg L^{-1}) for the first 10 days under 16-h light and 8-h dark photoperiod (40 µmol photons m^{-2} s^{-1}, 24°C) and then followed the growth conditions of *A. thaliana* wild- type plants for 3 weeks.

Site-directed mutagenesis

Mutations were generated as described (Yukenberg et al., 1991) using the QuikChange™ site-directed mutagenesis kit (Stratagene). In the case of *P. patens* a PstI restriction site was first created. PstI is a silent mutation in the BHRf plasmid with the

genetic sequence LHCSR1 already integrated (BHRf/LHCSR1). This approach was used during the screening phase to discriminate transformed mosses, which have at the same time the mutant and the wild-type genes. By sequencing, we confirmed the DNA mutation and used again the site directed mutagenesis on the plasmid produced (BHRf/LHCSR1) to integrate the mutations that will silence the chlorophyll-binding sites. In the case of *A. thaliana* site directed mutagenesis was used in the pH7WG2/LHCSR1 construct, generating vectors, which carried the mutated version of LHCSR1. DNA sequencing in all stages of cloning verified the presence of the mutations.

Protoplast transformation in P. patens

Genomic *P. patens* protonemal DNA was extracted (Allen et al., 2006) and used as starting template for all molecular cloning. All regions upstream and downstream of target coding sequences were amplified by PCR and sub-cloned into pGEM-T Vector (catalog no. A3600; Promega). Region from *lhcsr1* (locus XM_001776900) gene was successively cloned into BHRf plasmid (kindly provided by F. Nogue, Institute National de la Recherche Agronomique, Versailles, France). Transformation of *P. patens* was performed as in the study made by Schaefer and Zrÿd (Schaefer and Zrÿd, 1997) with minor modifications.

Agrobacterium*-mediated transformation of *A. thaliana

Agrobacterium GV3101 cells were transformed with the plasmid pH7WG2/LHCSR1* constructs carrying mutated versions of the protein in specific Chl-binding sites, using a standard transformation protocol. *A. thaliana npq4* plants were then transformed by the floral dip method and transgenic plants were selected on MS medium supplemented by hygromycin (25 mg L^{-1}) and carbenicillin (100 mg L^{-1}) (Zhang et al., 2006). Ten days after sowing on selective medium, plants were transferred in pots and three weeks after the expression of LHCSR1 transgene was assayed by western blotting.

NPQ measurements

In vivo chlorophyll fluorescence in *P. patens* and *A. thaliana* mutants was measured at room temperature by FC 800MF closed FluorCam Video-imaging system (Photon Systems Instruments) and Dual Pulse-Amplitude Modulated (PAM-100) fluorometer. For every measurement a saturating pulse of 4000 μmol photons m^{-2} s^{-1} and actinic light with

an intensity of 1200 or 800 µmol photons m^{-2} s^{-1} were applied. Fv/Fm and NPQ parameters were calculated as (Fm−Fo)/Fm and (Fm−Fm′)/Fm′ respectively.

Thylakoid extraction, SDS/PAGE and Western blotting analysis.

Thylakoids from protonemal tissue (10 - 12 day old plants) were prepared using an *Arabidopsis* protocol with minor modifications (Alboresi et al., 2008). After SDS/PAGE, proteins were transferred onto a nitrocellulose membrane (Sartorious AG) using a blot system from Biorad and were detected with specific polyclonal antibodies produced in the laboratory.

Results

I. Mutant LHCSR1 expression in an heterologous system

I.1 Mutated LHCSR1 expression in the thylakoid membranes of *A. thaliana*

After the successful cloning of LHCSR1, the construction of pH7WG2/LHCSR1* vectors integrated with mutated version of the *lhcsr1* encoding sequence and the transformation of *A. tumefaciens* GV3101 cells, we proceeded to the transformation of *A. thaliana npq4* plants. We exploited the *agrobacterium*-mediated transformation method adopted on *npq4* mutant plants, which lack PSBS and qE and therefore allow the detection of any LHCSR1-dependent NPQ activation. After transformation, plants were left to grow for 1-2 weeks until mature siliques were formed. Transgenic seeds were collected, purified following a standard purification protocol and selected on petri dishes containing Murashige and Skoog medium supplemented with hygromycin-B. After selection, 10-day old resistant plants were transferred from the selection dishes directly on soil and left to grow in a growth chamber under standard light and temperature conditions for about 3-4 weeks. Leaves from all transgenic plant lines carrying different LHCSR1 mutations were collected for screening. Total protein extracts were analyzed by western blotting using specific homemade α-LHCSR antibodies raised against the *in vitro* refolded LHCSR1 protein. In order to make sure that the immunoreaction of a-LHCSR antibody was specific to the transgenic protein and not due to cross-reactions with other LHC expressed by *A. thaliana*, total protein extracts from non-transformed *npq4* plants were also analyzed as control without any reaction detected. In the case of mutations A2 (Chl 612), A3 (Chl 613) and B6 (Chl 606) the apparent molecular weight of LHCSR1 expressed matched with the one of the non-mutated LHCSR1 in *A. thaliana* and also with

the native LHCSR1 protein accumulated in *P. patens* thylakoid membranes. In contrast, all the analyzed plant lines coming from the transformations with A5 (Chl 603) and B5 (Chl 609) constructs were unable to accumulate LHCSR1. All independent resistant 35S::LHCSR1* T1 lines (ChlA2 = 4 lines, ChlA3 = 5 lines, ChlB6 = 6 lines) expressed LHCSR1 with only small differences in the amount of protein accumulated. In the case of Chl A2 we could analyze also the T2 generation. T1 lines with the highest LHCSR1 accumulation were isolated and left to grow to seed production. Transgenic T1 seeds were collected, purified, selected on MS/hygromycin-B plates and resistant T2 plants were moved on soil. After 3-4 weeks growth under stable light and temperature conditions, total protein extracts from 35S::LHCSR1*A2 complemented plants of the second generation were analyzed by western blotting. Results revealed a more homogenous plant population with LHCSR1*A2 being accumulated in higher levels with respect to T1 generation.

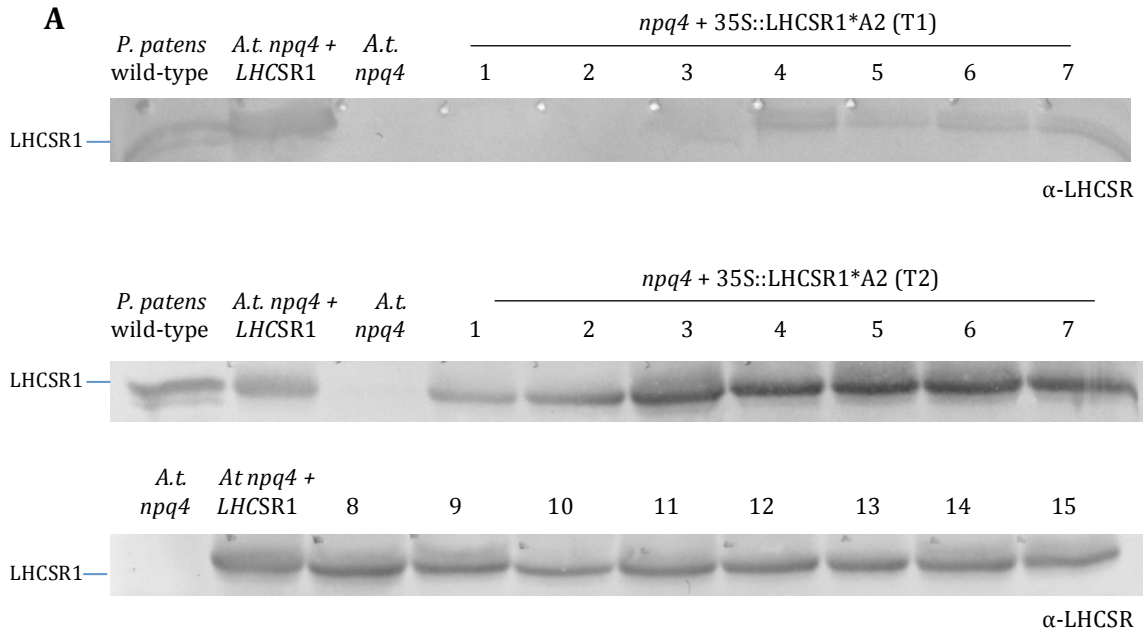

Figure 3.2. Immunoblotting of mutated 35S::LHCSR1 transformed lines. *A) Screening of T1 and T2 generation of LHCSR1*A2 mutants. Western blot analysis was performed on total proteins extracted by grinding one leaf disk directly in 100 µL of loading buffer; one tenth of the volume was loaded on SDS-PAGE. Proteins of P. patens wild-type, A. thaliana 35S::LHCSR1 and npq4 plants were loaded as controls. The primary antibody used for the analysis is indicated on the right side of the membrane while the band corresponding either to P. patens LHCSR1 or LHCSR2 is indicated on the left side.*

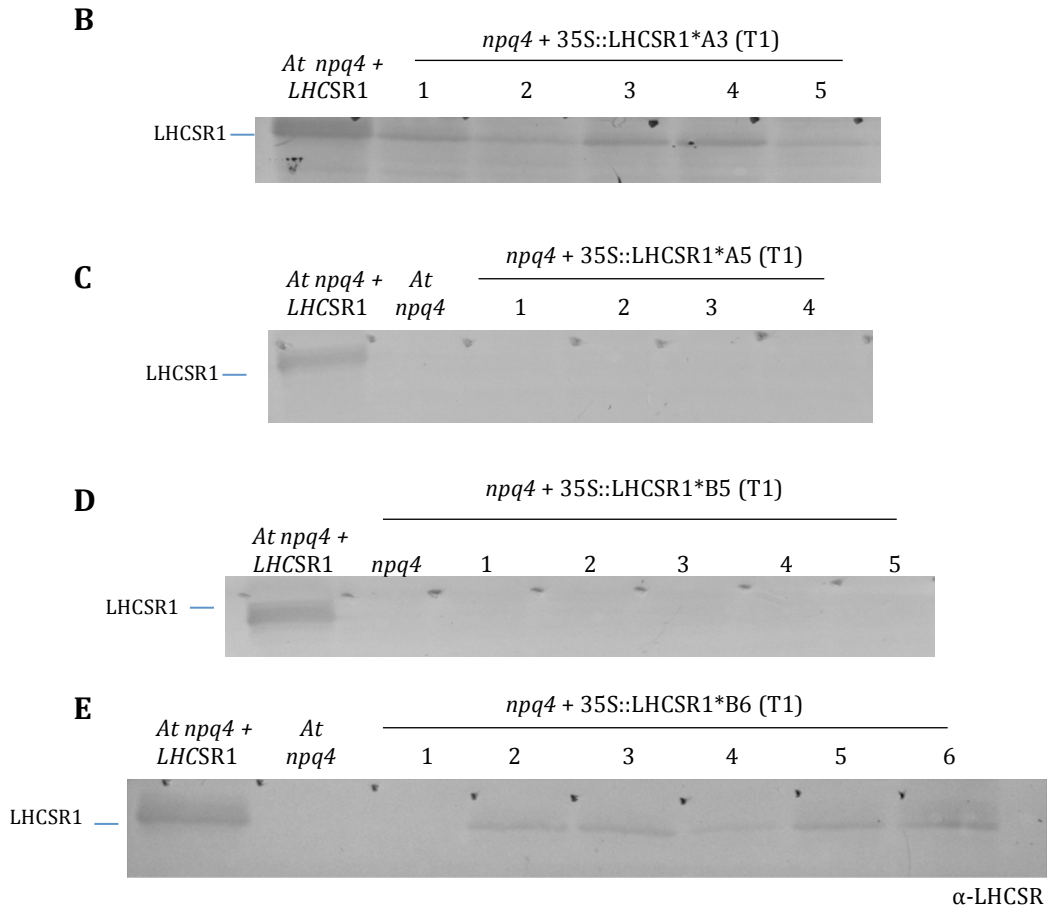

Figure 3.2 (cont.). Immuno-blotting of mutated 35S::LHCSR1 transformed lines. *A) Screening of T1 and T2 generation of LHCSR1*A2 mutants. Western blot analysis was performed on total proteins extracted by grinding one leaf disk directly in 100 µL of loading buffer; one tenth of the volume was loaded on SDS-PAGE. Proteins of P. patens wild-type, A. thaliana 35S::LHCSR1 and npq4 plants were loaded as controls. The primary antibody used for the analysis is indicated on the right side of the membrane while the band corresponding either to P. patens LHCSR1 or LHCSR2 is indicated on the left side B) Western blot analysis of 6 independent LHCSR1*A3 plant lines. C) Western blot analysis of total extracts from LHCSR1*A5 plant lines. D) Western blot analysis of LHCSR1*B5 plant lines E) Western blot analysis of LHCSR1*B6 plant lines. Total extracts from non-mutated 35S::LHCSR1 and npq4 were used as positive and negative controls respectively.*

I.2 Verification of *lhcsr* locus by PCR and DNA sequencing

In order to verify whether the *lhcsr1* locus was present, genomic DNA was extracted from selected T1 mutated 35S::LHCSR1-complemented plant lines using a standard DNA extraction protocol for *A. thaliana* and amplified with PCR, using specific DNA primers. Results indicated that *lhcsr1* locus could be successfully amplified for all mutated LHCSR1 plant lines verifying the successful integration of *lhcsr1* locus. PCR products were purified following a standard purification protocol and sent for DNA sequencing in order to verify the presence of each mutation. Sequencing results indeed verified the expected alteration for each Chl-binding site (see Appendix).

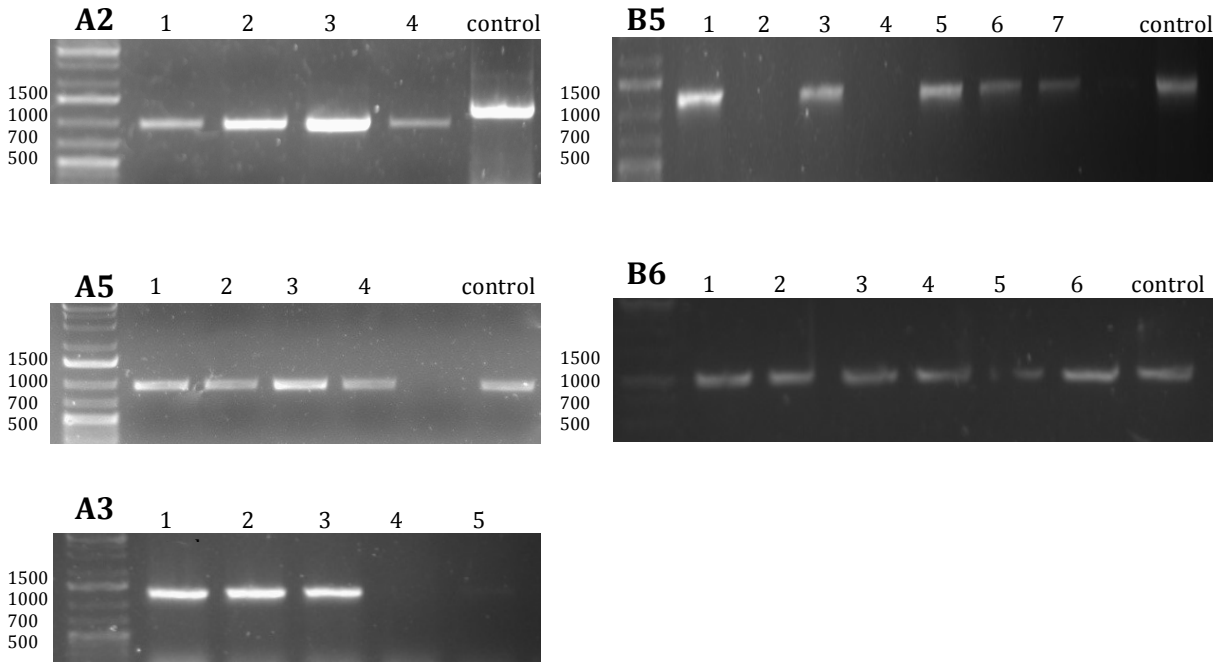

Figure 3.3. LHCSR1 PCR amplification from extracted mutant 35S::LHCSR1 plant DNA . *DNA from transgenic mutant 35S::LHCSR1 plant lines was extracted following a standard extraction protocol for A. thaliana and amplified by PCR using lhcr1 specific primers. The amplified lhcr1 locus (966bp) is shown in all lanes. Each Chl mutation is indicated on the top of each figure.*

I.3 Effect of single-point Chl mutations on the LHCSR1 quenching activity

In order to assess the impact of each individual chlorophyll mutation on the NPQ activity, all different mutant 35S::LHCSR1 lines were analyzed using fluorescence video-imaging. Measurements were initiated with Chl A2 and Chl A5, as these were the mutations from which transgenic lines were obtained first. For the measuring protocol, mutant 35S::LHCSR1-complemented leaves were detached from each plant line, dark adapted for 45 minutes and measured using one single cycle of 30min actinic light illumination (800 $\mu mol\ m^{-2}\ s^{-1}$) and 15min of dark recovery. In all measurements, qE recovery is calculated as the last point in the light phase minus the second point during dark relaxation.

Chl A2 (Chl 612)

A. thaliana A2 mutant plants did not show any significant difference in quenching activity with respect to the *npq4* control plants when actinic light was applied. By applying 30 minutes of light treatment and 15min of dark recovery, there is no significant difference in the amplitude between the A2 and the *npq4* plants (NPQ_{A2} = 0.51 vs.

NPQ_{npq4} = 0.50) and there is no drop in qE when actinic light is turned off. In contrast, the non-transformed 35S::LHCSR1 control line shows NPQ activity when actinic light is applied and a qE recovery when the light is off (qE_{SR1} = 0.24 vs. qE_{A2} = 0.065).

Chl A5 (Chl 603)

As in the case of Chl A2, *A. thaliana,* Chl A5 mutant lines have no significant difference in NPQ induction with respect to *npq4*. In fact the difference is observed when the actinic light is switched off with the NPQ of A5 plants rising higher instead of immediately relaxing in the dark. This result is consistent with the protein not being detected by western blot analysis, even though *lhcsr1* DNA sequence could be successfully amplified. In contrast, the un-transformed 35S::LHCSR1 control line shows NPQ activity when actinic light is on and a higher qE when the light is switched off (qE_{SR1} = 0.24 vs. qE_{A5} = 0.05).

Chl A3 (Chl 613)

Most of LHCSR1-expressing A3 mutant plants that were tested showed low activation of NPQ when actinic light was applied, but with a qE higher of the value calculated for *npq4* and Chls A2 and A5 when the actinic light was switched off (qE_{SR1} = 0.24, qE_{npq4} = 0.04 , qE_{A3} = 0.15).

Chl B5 (Chl 609)

As in the case of A2 and A5, when a 30-min actinic light treatment was applied there was no quenching activity for the B5 mutant plant lines (all lines are similar to *npq4*). This was expected since LHCSR1 protein could not be found in the thylakoid membranes of the 35S::LHCSR1*A5 plants during immuno-blotting analysis (qE_{SR1} = 0.24, qE_{npq4} = 0.04 , qE_{B5} = 0.055)

Chl B6 (Chl 606)

In the case of mutation B6, all independent plant lines showed a quenching activity. Applying a 30-min actinic light treatment, all plant lines show NPQ amplitude similar to the one of the non-transformed 35S::LHCSR1 control line, clearly higher than *npq4* negative control plants thus implying that mutation of the Chl B6 had no negative effect in the LHCSR1 activity (qE_{SR1} = 0.24, qE_{npq4} = 0.04 , qE_{B6} = 0.195).

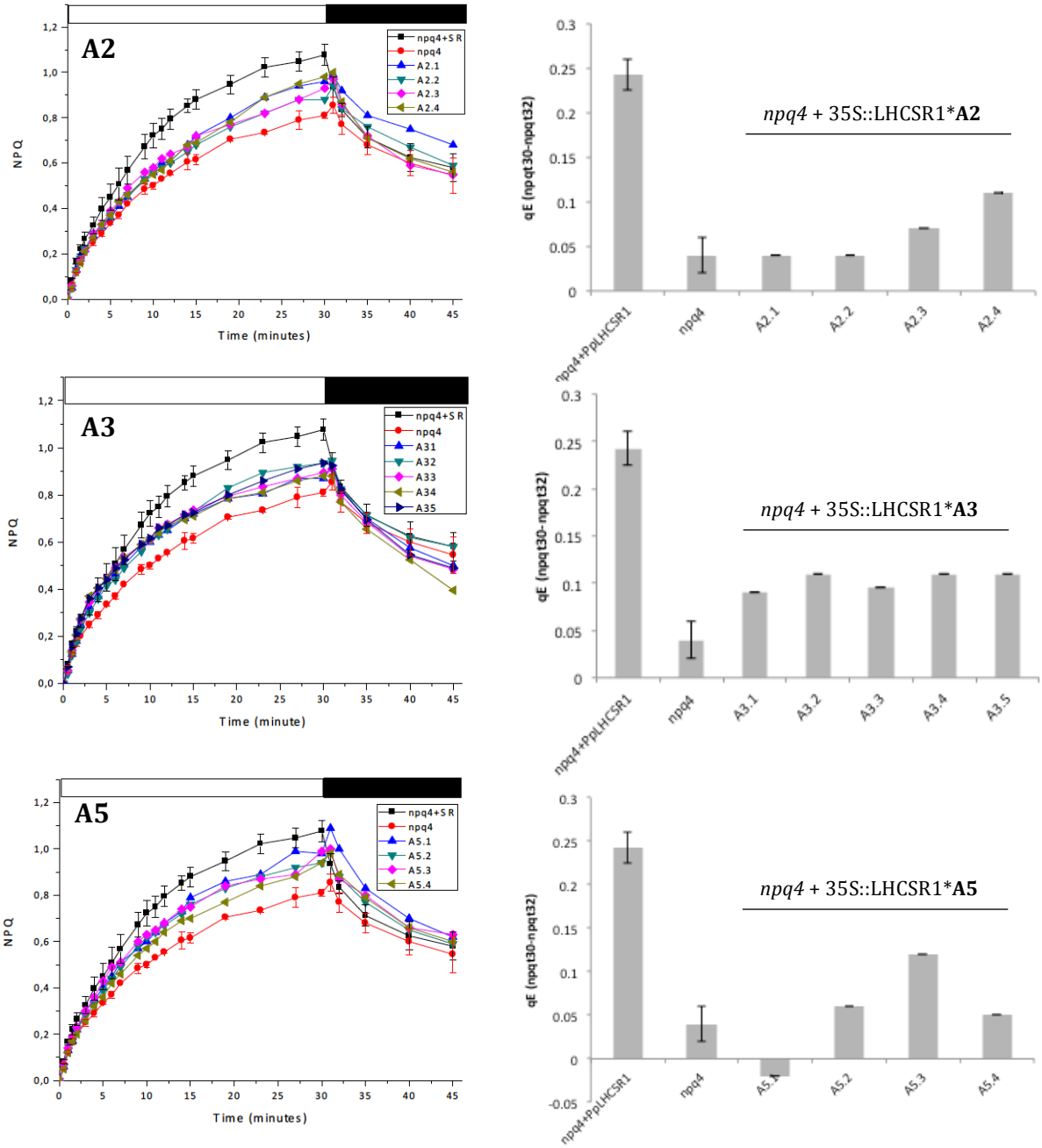

Figure 3.4. NPQ induction in *A. thaliana* 35S::LHCSR1* Chl mutant plants. *A. thaliana npq4 complemented with 35S::LHCSR1 mutated in ChlA2, ChlA3, ChlA5, ChlB5 and ChlB6 respectively. Plants were dark adapted for 45min and NPQ was measured using a standard protocol of 30min actinic light (800uE) and 15min of dark recovery. Non-transformed A. thaliana npq4 (red line) and non-mutated npq4+LHCSR1 (black line) plants of the same age were used as controls. Right panels: qE (fast recovery) of mutated lines calculated as the last point in the light phase minus the second point in the dark phase. Each mutation is indicated in the top of each graph.*

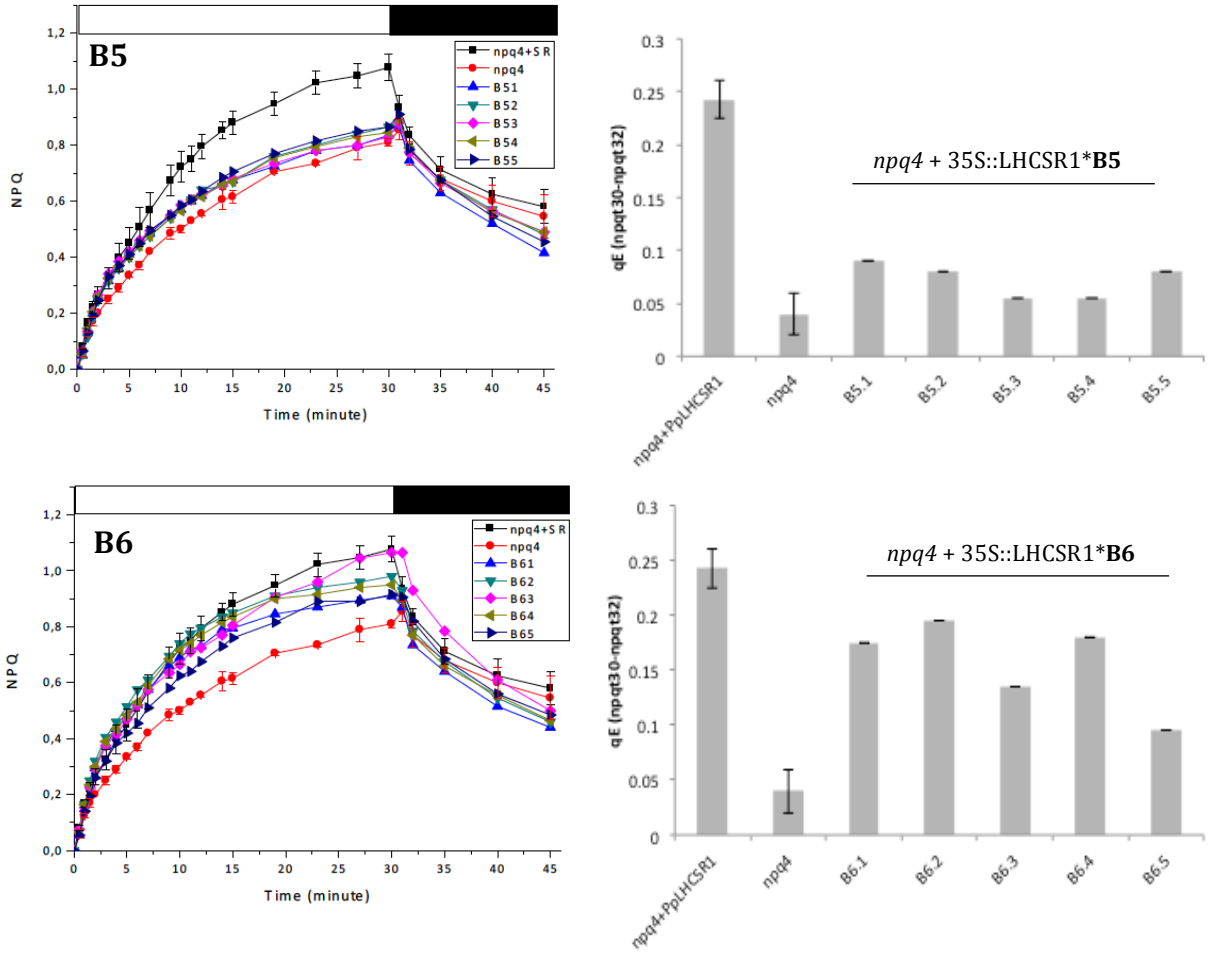

Figure 3.4 (cont.). NPQ induction in *A. thaliana* 35S::LHCSR1* Chl mutant plants. *A. thaliana npq4 complemented with 35S::LHCSR1 mutated in ChlA2, ChlA3, ChlA5, ChlB5 and ChlB6 respectively. Plants were dark adapted for 45min and NPQ was measured using a standard protocol of 30min actinic light (800uE) and 15min of dark recovery. Non-transformed A. thaliana npq4 (red line) and non-mutated npq4+LHCSR1(black line) plants of the same age were used as controls. Right panels: qE (fast recovery) of mutated lines calculated as the last point in the light phase minus the second point in the dark phase. Each mutation is indicated in the top of each graph.*

II. Mutant LHCSR1 expression in an homologous system

II.1 Proof of concept (Mutation STOP)

Before starting *P. patens* protoplast transformation with the Chl mutations, we decided to verify the possibility of integrating point mutations *in vivo* as well as the efficiency of homologous recombination. This preliminary work included the integration of a 'STOP' codon in *lhcsr1* that would lead to a truncated, non-functional LHCSR1 protein (change Tyr128 residue (TAC) into a TAG stop codon), observing the corresponding genotype (mutant mosses with reduced or no NPQ response) after protoplast transformation. Using BHRf – the destination vector for *P. patens* – the mutated *lhcsr1* sequence would go exactly at the same position as the non-mutated *lhcsr1* allele under the control of the

endogenous promoter via homologous recombination. The STOP mutation was introduced using the QuickChange^{TM} mutagenesis kit exactly as in the case of the other mutations. A pair of specific DNA primers (*Pp*LHCSR1$_{STOP}$F: 5'-ACCTTGAGGGAC GACTAGGAGCCCGGCAAC-3', *Pp*LHCSR1$_{STOP}$R: 5'-GTTGCCGGGCTCCTAGTC GTCCCTCAAGGT-3' was used together with the BHRf/LHCSR1 plasmid construct (parental DNA template) generating a new BHRf/LHCSR1*STOP vector by PCR. The correct sequence of the generated vector was verified with DNA digestion and sequencing and then inserted into *P. patens lhcsr2psbs* KO protoplasts. Transgenic colonies were tested for their resistance against antibiotic-supplemented $PPNH_4$ petri dishes (2 selection rounds on zeocin and hygromycin, see Appendix) Out of the 27 generated colonies, only 7 managed to pass the double antibiotic selection rounds showing a transformation efficiency of 25%, consistent to the efficiency reported for *P. patens* transformation protocols in literature. Resistant moss plants were additionally grown on $PPHN_4$ medium enriched with glucose. Protonemal tissue from 7-day old moss colonies was collected, homogenized and the total protein extracts were challenged with homemade a-LHCSR antibodies. Non-transformed extracts from *P. patens* wild-type, *lhcsr2psbs* KO mosses but also from a moss colony that did not pass the resistance test were loaded as additional controls. Western blot analysis showed no LHCSR1 expression for any of the resistant *lhcsr2psbs* KO + LHCSR1*STOP samples in contrast with the control lines where LHCSR1 could be accumulated (LHCSR1 and LHCSR2 in the case of *P. patens* wild-type).

The same moss colonies were later tested for their NPQ activity via fluorescence video-imaging, by applying a standard NPQ protocol (10min of strong actinic light followed by 10min of dark relaxation) on dark-adapted samples. More specifically, 7-day old STOP-mutant moss plants were dark adapted for 45min and then exposed to 1200 μmol photons m^{-2} s^{-1} for 10 minutes in order to induce NPQ. The light period was followed by a 10-minute dark period in order to follow the recovering ability of the mutant mosses. As controls, *P. patens* wild-type and un-transformed *lhcsr2psbs* KO plants were used. Results showed that for the 7 lines in which the STOP mutation is integrated leading to a truncated LHCSR1, there was no NPQ activity in contrast to the control lines, thus verifying the efficiency of the *in vivo* transformation and homologous recombination in *P. patens*.

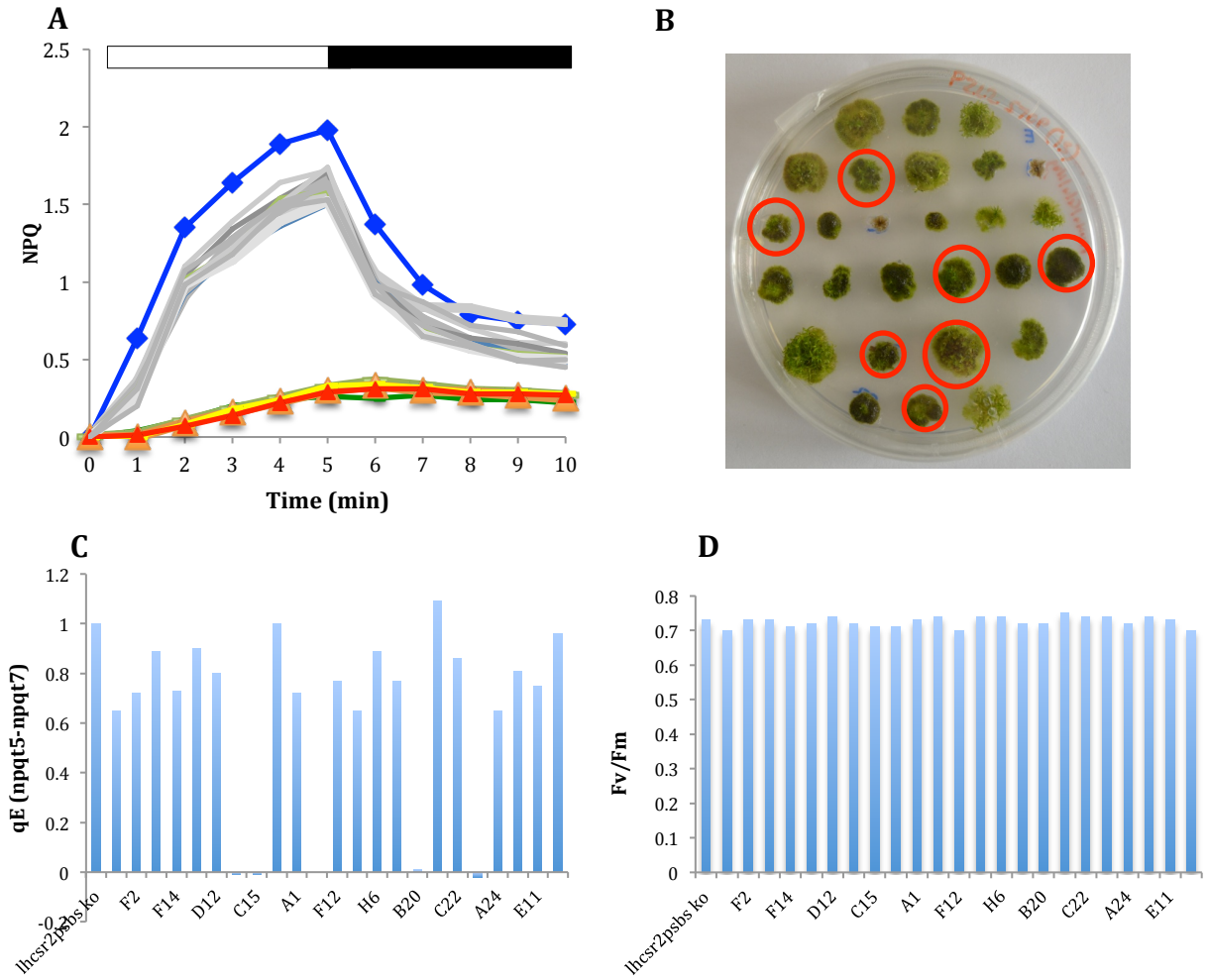

Figure 3.5. NPQ induction in *P. patens* STOP mutant plants. *A) NPQ induction of selected resistant lhcsr2psbs KO + LHCSR1*STOP lines. All plants were dark-adapted for 45-min and measured for their NPQ activation following a standard protocol. NPQ was induced using 1200 actinic light followed by 10min of dark relaxation. Non-transformed lhcsr2psbs KO plants were used as control (bright blue line). Real STOP mutants are indicated with colored lines (red, yellow, green), having almost a no-NPQ phenotype. B) An example of P. patens moss colonies growing on rich PPNH₄ medium. Actual STOP mutants are indicated with a red circle (7 positive colonies out of 27, transformation efficiency of 25%). C) qE (fast recovery) of lines calculated as the last point in the light phase minus the second point in the dark phase. D) Fv/Fm calculation for all measured lines (control and transgenic).*

II.2 LHCSR1 expression in the thylakoid membranes of *P. patens lhcsr2psbs* KO

After verifying the efficiency of the *in vivo* transformation with the STOP mutation, the same procedure was followed for the *in vivo* insertion of Chl-mutated BHRf/LHCSR1*A2 and A5 constructs. After *P. patens lhcsr2psbs* KO protoplast isolation, transformation and selection of resistant colonies on antibiotic-supplemented petri dishes (see Appendix), each resistant moss plant was screened for LHCSR1 expression. A small fragment from each plant was isolated and total protein extracts were loaded on SDS-PAGE gel followed by western blot analysis against LHCSR homemade antibodies. Extracts from *P. patens* wild-type and *lhcsr1lhcsr2psbs* KO mosses were also loaded as additional controls. Results showed that LHCSR1 could be expressed in the

cases of both Chl A2 and Chl A5 with all screened lines accumulating the protein on the same level of non-mutated LHCSR1 line. As expected, extracts coming from the triple *lhcsr1lhcsr2psbs* KO mutant have no signal revealed by α-LHCSR antibody.

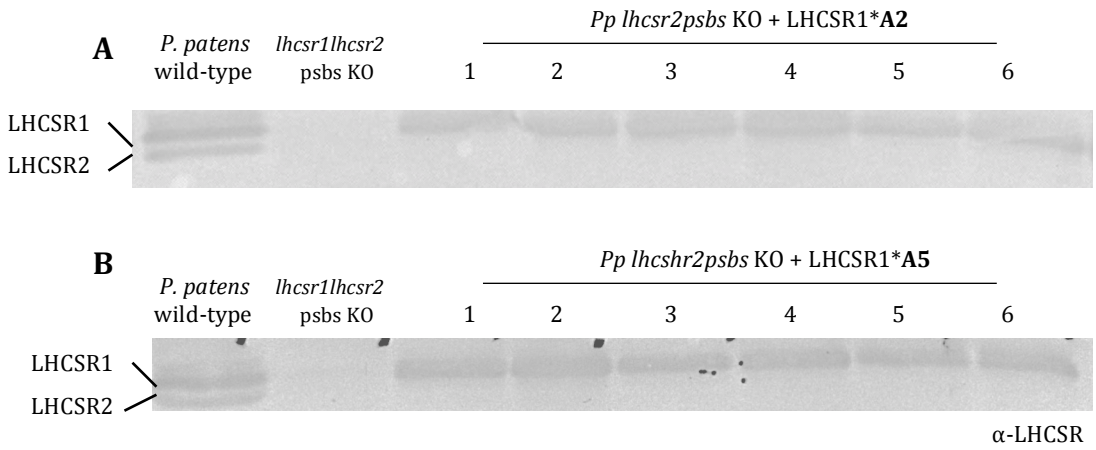

Figure 3.6. Immunological screening of BHRf/LHCSR1*A2 and A5 transformed lines. *Western blot analysis was performed on total proteins from independent lines extracted by grinding a piece of P. patens tissue in 80 µL of loading buffer. Proteins of P. patens wild-type but also the triple lhcsr1lhcsr2psbs KO were loaded as positive and negative controls respectively. The primary antibody used for the analysis is indicated on the right side of the membrane while the band corresponding either to P. patens LHCSR1 or LHCSR2 is indicated on the left side.*

II.3 NPQ activity single-point Chl mutations on the LHCSR1

Resistant LHCSR1-expressing mutant moss plants were analyzed using fluorescence video-imaging. All transgenic mosses were dark-adapted for 45 minutes followed by NPQ measurements using a standard protocol. NPQ was induced using a 10-min period of white actinic light (1200 µmol photons m^{-2} s^{-1}) and then left to relax in the dark for 10 minutes. First, for mutation A2 (10 independent lines) results showed a reduction in NPQ activity during the illumination phase ($maxNPQ_{control}$ = 2.47 vs. $maxNPQ_{A2}$ = 1.5, Figure 3.7, A), while when the light was switch off, transgenic lines managed to recover with only minor differences with respect to the non-transformed *lhcsr2psbs* KO line (Figure 3.7, B).

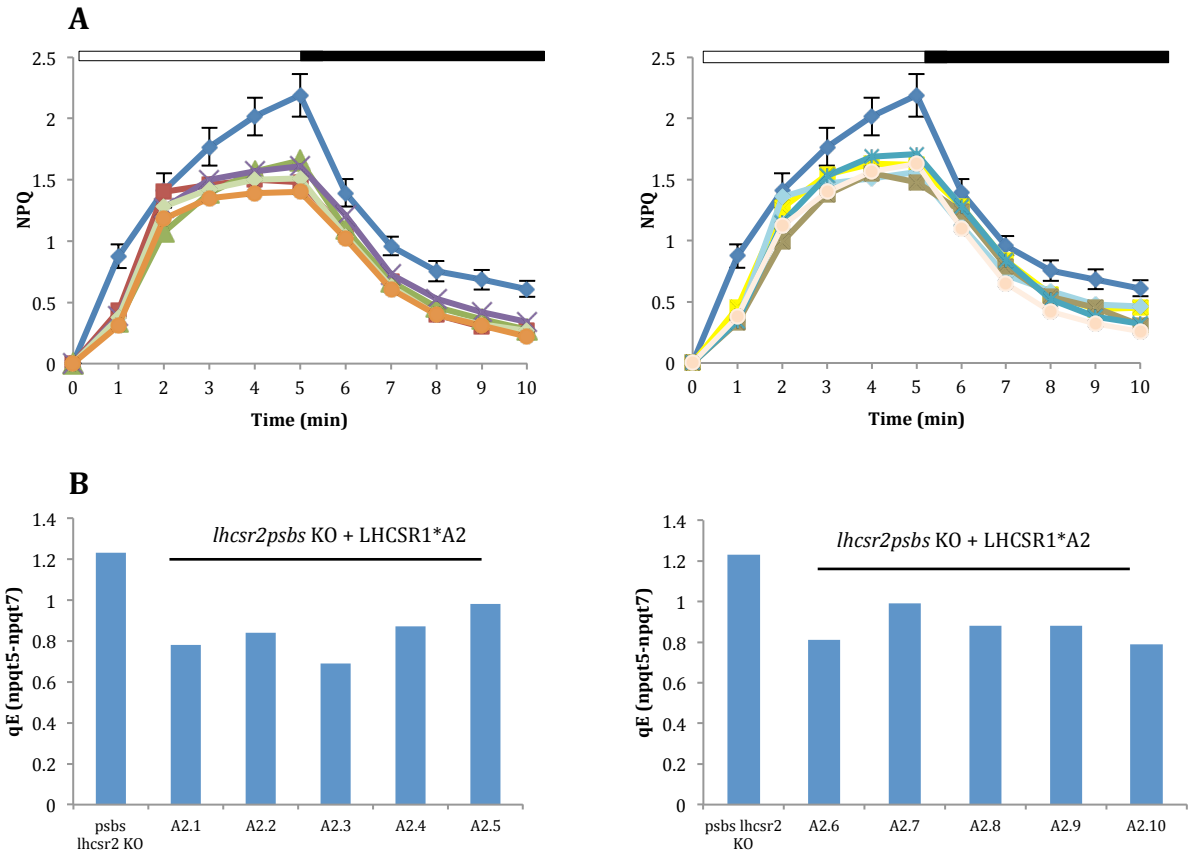

Figure 3.7. NPQ induction in *P. patens* LHCSR1*A2 mutant plants. *A) NPQ induction of selected resistant lhcsr2psbs KO + LHCSR1*A2 lines. All plants were dark-adapted for 45-min and measured for their NPQ activation following a standard protocol. NPQ was induced using 1200 actinic light followed by 10min of dark relaxation. Non-transformed lhcsr2psbs KO plants were used as control (blue line). Possible A2 mutants are indicated with colored lines, all of them below the control line. B) qE (fast recovery) of lines calculated as the last point in the light phase minus the second point in the dark phase.*

For mutation A5 results showed no significant differences in the NPQ induction between LHCSR1*A5-complemented and control *lhcsr2psbs* KO lines during the illumination phase ($maxNPQ_{control}$ = 2.19 vs. $maxNPQ_{A2}$ = 2.07, Figure 3.8, A), while when the light was switch off, transgenic lines managed to recover as much as the un-transformed *lhcsr2psbs* KO line, even if LHCSR1 could be accumulated in levels similar to the *P. patens* wild type (Figure 3.8, B).

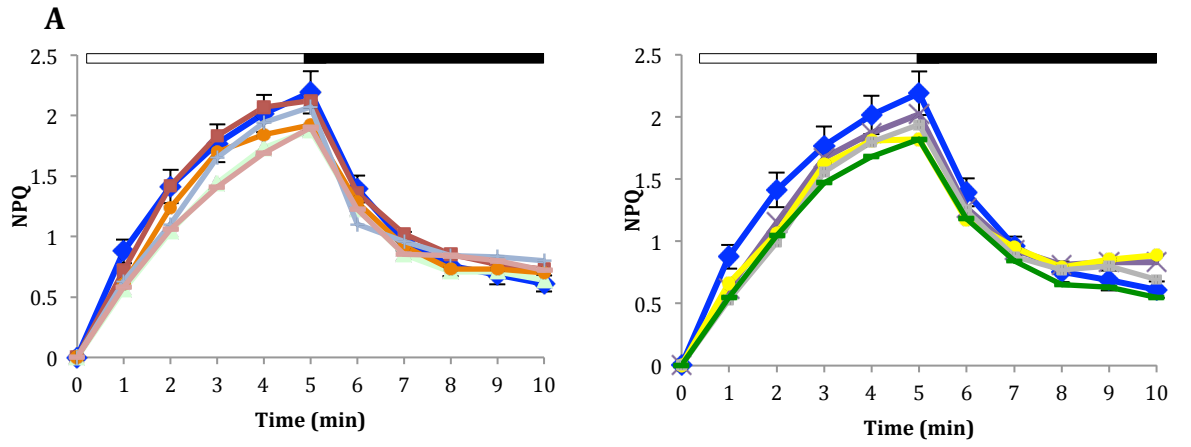

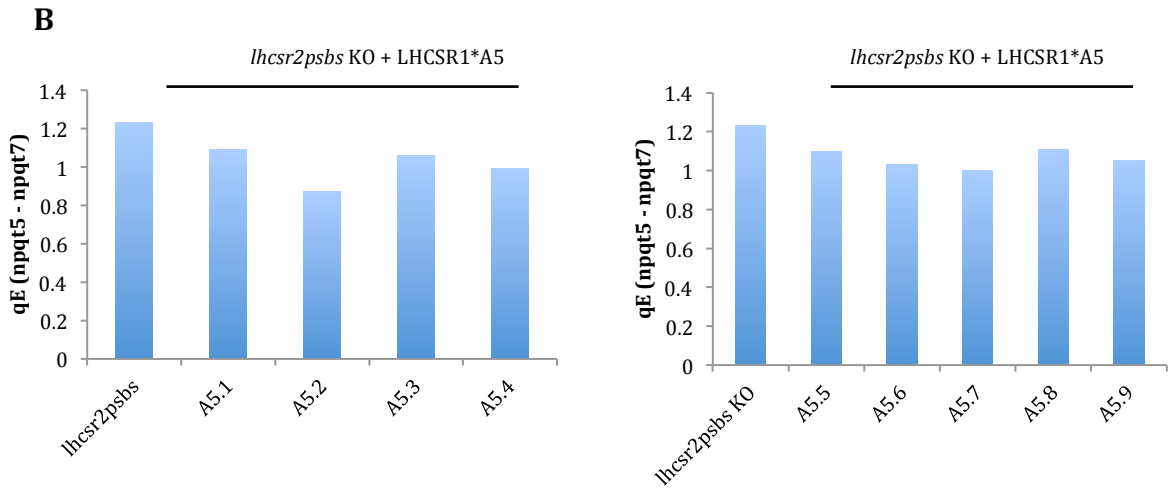

Figure 3.8. NPQ induction in *P. patens* LHCSR1*A5 mutant plants. *A) NPQ induction of selected resistant lhcsr2psbs KO + LHCSR1*A5 lines. All plants were dark-adapted for 45-min and measured for their NPQ activation following a standard protocol. NPQ was induced using 1200 actinic light followed by 10min of dark relaxation. Non-transformed lhcsr2psbs KO plants were used as control (blue line). Possible A5 mutants are indicated with colored lines, all of them below the control line. B) qE (fast recovery) of lines calculated as the last point in the light phase minus the second point in the dark phase.*

Arabidopsis thaliana (*npq4*)				
Mutation	**LHCSR1 accumulation**	**NPQ**	**qE** (fast NPQ component)	**DNA sequenced** (presence of mutation *in vivo*)
A2	Yes	< control	< control	Yes
A3	Yes	< control	< control	Yes
A5	No	< control	< control	Yes
B5	No	< control	< control	Yes
B6	Yes	= control	= control	Yes
Physcomitrella patens (*lhcsr2psbs* ko)				
A2	Yes	< control	= control	Verified in construct – not yet *in vivo*
A5	Yes	= control	= control	Verified in construct – not yet *in vivo*

Table 3C. LHCSR1 Chl mutations in *A. thaliana* and *P. patens*. *This table presents all the preliminary results obtained from the in vivo LHCSR1 mutational analysis in the heterologous system of A. thaliana npq4 and the homologous system of P. patens lhcsr2psbs ko. Information on the mutation introduced, the accumulation of LHCSR1 in the thylakoid membranes, NPQ activity, qE and presence of the mutation in vivo, are shown taking the NPQ activity of the un-mutated LHCSR1 as a reference (referred to as control).*

Discussion

The moss *P. patens* an evolutionary intermediate between algae and land plants is the first organism in which LHCSR and PSBS, have been found together, making this moss a unique model to study the process of NPQ and its evolution from algae to land colonization. Generation of *P. patens lhcsr* and *psbs* KO mutants have showed that both proteins are active in promoting NPQ and contribute to photoprotection under high light stress conditions with LHCSR1 being the major activator of this photoprotection mechanism (Alboresi et al., 2010).

Eight residues are conserved in all LHC proteins (Jansson, S. 1999) as identified in several LHC proteins: Lhcb1, Lhcb4, Lhca1, Lhca3 and Lhca4 (Bassi, R. et al. 1999; Morosinotto, T. et al. 2002b; Morosinotto, T. et al. 2005b; Mozzo, M. et al. 2006; Remelli, R. et al. 1999) by site-specific mutagenesis. The sequence alignment of LHCSR1 and LHCSR2 from *P. patens* versus LHCSR3 from *Chlamydomonas reinhardtii*, Lhcb1 and Lhcb4 from *A. thaliana* shows that these eight amino acid residues responsible for Chl binding among members of the LHC family (Kühlbrandt et al., 1994; Bassi et al., 1999; Liu et al., 2004) are conserved also in LHCSR1.

An attempt to introduce mutations in the conserved LHCSR1 Chl-binding sites in *vivo* was performed. To this aim, a library of pH7WG2 plasmid constructs carrying mutated versions of LHCSR on Chl-binding sites was created by single-point direct mutagenesis, mutating the codons for the Chl-coordinating residues to apolar residues with similar steric hindrance using specific primers. These constructs were used for *in vivo* transformation using the *A. thaliana* heterologous system as an expression tool. The *Arabidopsis* background used was the PSBS-less *npq4*, in order to ensure that the quenching activity observed would be only due to the presence of LHCSR1. Preliminary screening results revealed mutant plant lines for Chl 612 (Chl A2), Chl 613 (Chl A3), Chl 603 (Chl A5), Chl 609 (Chl B5) and Chl 606 (Chl B6), with LHCSR1 expressed in all mutants expect for Chl A5 and Chl B5. This result may suggest that absence of Chl A5 and Chl B5 located in close proximity of L2 site of LHCSR1 is important for the stability of the protein *in vivo,* in contrast to Chl A2 and Chl A3, located close to L1 site, which do not seem to have an effect on the protein stability. Absence of Chl B6, located in helix C did not have an effect on the expression of LHCSR1.

Quenching activity of heterologously expressed mutant LHCSR1 was measured by applying a standard NPQ protocol for *A. thaliana*. Preliminary results showed that most

of the mutations tested had a lowering effect on the partial activity of LHCSR1, since the genotypes generated behaved closely alike the un-transformed *npq4*. Only lines mutated in Chl B6 have the same NPQ activity as the control non-mutated LHCSR1, suggesting that absence of Chl B6 does not inhibit energy quenching. However, these first observations in between different mutations are hard to distinguish due to the low activity of the heterologously expressed LHCSR1. A different approach would include the generation of constructs that allow the protein to be localized in the grana partitions, where it could be more active in quenching.

Mutational analysis was initiated also in the *P. patens* homologous system (*lhcsr2psbs* KO), thus exploiting the unique ability of the moss to perform homologous recombination in order to express mutated forms of LHCSR1 *in vivo*. The same mutations were integrated *in vivo* using BHRf, a specific vector for *P. patens*. The efficiency of the procedure was verified by introducing a STOP mutation in LHCSR1. This mutation consists of the alteration of the Y182 (Tyr) codon into a termination codon, thus leading to a truncated, non-functional LHCSR1 protein. Measurement of fluorescence quenching in resistant STOP transformants resulted to a no-NPQ phenotype upon induction with high actinic light. Preliminary screening results showed LHCSR1-accumulating mosses for both Chl A2 and Chl A5 mutant. Regarding NPQ activity, Chl A2 transformants showed reduced NPQ while Chl A5 lines showed no difference with respect to control *lhcs2psbs* KO lines. This latter result regarding Chl A5 is in contrast with what obtained in the *Arabidopsis* system as for both the accumulation and activity of the protein. In the case of *P. patens* it is possible that the mutation in A5 is not essential for NPQ activity which would be a very interesting result for the interpretation of the recent report that isolated LHCSR1 produces a lutein radical cation upon binding of zeaxanthin and acidification (Pinnola et al. 2016). This would imply that the quenching site in *Physcomitrella* LHCSR1 involves L1 site, the only one that does not undergo exchange with zeaxanthin upon de-epoxidation (Pinnola et al. 2013, Pinnola et al. Unpublished results). It should be underlined, however, that these results must be considered as preliminary since no sequencing of the DNA for confirming the presence of the mutations in *P. patens* mutants has yet been performed. In conclusion we can confirm the complementarity of the *A. thaliana* and *P. patens* systems for the mutation analysis of LHCSR1. It is likely that when the series of analysis initiated here will be accomplished, a map of the choromophore involved in quenching reactions will be obtained.

Bibliography

Ahn Tk., Avenson TJ., Ballottari M., Cheng Y-C., Niyogi KK., Bassi R.,Fleming GR (2008) Architecture of a charge-transfer state regulating light harvesting in a plant antenna protein. Science (New York,NY) 320: 794–7

Bailey,S., Walters,R.G., Jansson,S., and Horton,P. (2001) Acclimation of *Arabidopsis thaliana* to the light environment: the existence of separate low light and high light responses. Planta 213:794-801.

Ballottari,M., Dall'Osto,L., Morosinotto,T., and Bassi,R. (2007) Contrasting behavior of higher plant photosystem I and II antenna systems during acclimation. Journal of Biological Chemistry 282:8947-8958.

Ballottari M, Mozzo M, Girardon J, Hienerwadel R, Bassi R. Chlorophyll triplet quenching and photoprotection in the higher plant monomeric antenna protein Lhcb5. J Phys Chem B. 2013 Sep 26;117(38):11337-48. doi: 10.1021/jp402977y. Epub 2013 Jul 8.

Bassi,R., Croce,R., Cugini,D., and Sandona,D. (1999) Mutational analysis of a higher plant antenna protein provides identification of chromophores bound into multiple sites. Proc.Natl.Acad.Sci.USA 96:10056- 10061.

Dall'Osto,L., Caffarri,S., and Bassi,R. (2005) A mechanism of nonphotochemical energy dissipation, independent from Psbs, revealed by a conformational change in the antenna protein CP26. Plant Cell 17:1217-1232.

Ganeteg,U., Kulheim,C., Andersson,J., and Jansson,S. (2004) Is each light-harvesting complex protein important for plant fitness? Plant Physiol 134:502-509.

Green,B.R. and Durnford,D.G. (1996) The Chlorophyll-carotenoid proteins of oxygenic photosynthesis. Annu.Rev.Plant Physiol.Plant Mol.Biol. 47:685-714.

Havaux,M. and Niyogi,K.K. (1999) The violaxanthin cycle protects plants from photooxidative damage by more than one mechanism. Proc.Natl.Acad.Sci.U.S.A 96:8762-8767.

Holt,N.E., Zigmantas,D., Valkunas,L., Li,X.P., Niyogi,K.K., and Fleming,G.R. (2005) Carotenoid cation formation and the regulation of photosynthetic light harvesting. Science 307:433-436.

Jansson,S. (1999) A guide to the Lhc genes and their relatives in Arabidopsis. Trends Plant Sci. 4:236-240.

Klimmek,F., Sjodin,A., Noutsos,C., Leister,D., and Jansson,S. (2006) Abundantly and rarely expressed Lhc protein genes exhibit distinct regulation patterns in plants. Plant Physiology 140:793-804.

Kovacs,L., Damkjaer,J., Kereiche,S., Ilioaia,C., Ruban,A.V., Boekema,E.J., Jansson,S., and Horton,P. (2006) Lack of the light-harvesting complex CP24 affects the structure and function of the grana membranes of higher plant chloroplasts. Plant Cell 18:3106-3120.

Kühlbrandt,W., Wang,D.N., and Fujiyoshi,Y. (1994) Atomic model of plant light-harvesting complex by electron crystallography. Nature 367:614-621.

Liguori N, Novoderezhkin V, Roy LM, van Grondelle R, Croce R. Excitation dynamics and structural implication of the stress-related complex LHCSR3 from the green alga Chlamydomonas reinhardtii. Biochim Biophys Acta. 2016 Sep;1857(9):1514-23.

Liu,Z., Yan,H., Wang,K., Kuang,T., Zhang,J., Gui,L., An,X., and Chang,W. (2004) Crystal structure of spinach major light-harvesting complex at 2.72 A resolution. Nature 428:287-292.

Mozzo,M., Morosinotto,T., Bassi,R., and Croce,R. (2006) Probing the structure of Lhca3 by mutation analysis. Biochimica et Biophysica Acta-Bioenergetics 1757:1607-1613.

Morosinotto,T., Baronio,R., and Bassi,R. (2002a) Dynamics of Chromophore Binding to Lhc Proteins in Vivo and in Vitro during Operation of the Xanthophyll Cycle. J.Biol.Chem. 277:36913-36920.

Morosinotto,T., Breton,J., Bassi,R., and Croce,R. (2003a) The nature of a chlorophyll ligand in Lhca proteins determines the far red fluorescence emission typical of photosystem I. J.Biol.Chem. 278:49223- 49229.

Morosinotto,T., Castelletti,S., Breton,J., Bassi,R., and Croce,R. (2002b) Mutation analysis of Lhca1 antenna complex. Low energy absorption forms originate from pigment-pigment interactions. J.Biol.Chem. 277:36253-36261.

Morosinotto,T., Mozzo,M., Bassi,R., and Croce,R. (2005b) Pigment-pigment interactions in Lhca4 antenna complex of higher plants photosystem I. Journal of Biological Chemistry 280:20612-20619.

Passarini F, Wientjes E, Hienerwadel R, Croce R (2009). Molecular basis of light harvesting and photoprotection in CP24: unique features of the most recent antenna complex. J Biol Chem 284: 29536-29546

Remelli,R., Varotto,C., Sandona,D., Croce,R., and Bassi,R. (1999) Chlorophyll binding to monomeric light-harvesting complex. A mutation analysis of chromophore-binding residues. J.Biol.Chem. 274:33510-33521.

Rogl,H. and Kuhlbrandt,W. (1999) Mutant trimers of light-harvesting complex II exhibit altered pigment content and spectroscopic features. Biochemistry 38:16214-16222.

Ruban AV, Berera R, Ilioaia C, van Stokkum IHM, Kennis JTM, Pascal A, van Amerongen H, Robert B, Horton P, van Grondelle R (2007). Identification of a mechanism of photoprotective energy dissipation in higher plants. Nature 450: 575-8.

Conclusions

Life on Earth depends directly on the energy obtained by photosynthesis, a process of vital importance, which enables photosynthetic organisms - such as plants and algae - to harvest solar energy and convert it into readily usable energy.

Under normal light conditions, the photosynthetic apparatus can efficiently absorb light energy and use it for CO_2 fixation and the production of organic compounds. However, in high light conditions the energy captured in excess, with respect to the capacity of electron transport activity, leads to over-reduction of the photosynthetic electron transport chain and thus to the saturation of photosynthesis. Higher excitation, longer the time antenna chlorophylls stay in the S1 excited state, which allows for intersystem crossing to triplet state. ^{3}Chl* react with molecular oxygen to yield ROS (Reactive Oxygen Species) which can act as signaling compounds in the acclimatory response but they can also be very harmful for cellular components. In terms of photoprotection, plants have evolved several defense mechanisms in order to face excess light stress and prevent ROS damaging action. One of these, called non-photochemical quenching (NPQ) of chlorophyll fluorescence, is a process essential for the regulation of photosynthesis and plant protection.

In the case of vascular plants NPQ activation relies on PSBS protein, a pH sensor, which transduces chloroplast lumen acidification into a quenching reaction, while in algae an ancient LHC-like protein called LHCSR3, is responsible for the pH sensing and excess energy quenching in high light conditions. The moss *Physcomitrella patens* holds a strategic position in the phylogenetic tree between green algae and land plants, as it constitutively accumulates both PSBS and LHCSR proteins active in NPQ, with LHCSR1 being the major effector.

Land colonization led to loss of LHCSR1 in vascular plants. However, its heterologous expression emerges as an interesting experiment as LHCSR1 could be active in a system from which it was rejected during evolution. Verification of this hypothesis is relevant in order to verify the need of specific interacting partners for LHCSR1 quenching activity: if LHCSR1 is active by itself we can expect quenching upon expression *in planta* while if LHCSR1 needs a specific partner for activity, low or no-NPQ activity is expected, unless this partner is conserved between mosses and higher plants.

This PhD thesis is focused on the functional analysis of *Pp*LHCSR1 protein and its relation to the NPQ photoprotection mechanism through heterologous expression in several *A. thaliana* mutants affected either in chromophore biosynthesis or in antenna system components.

I. Expression of *Pp*LHCSR1 in *Arabidopsis thaliana npq4* mutant

LHCSR1 of *P. patens* is accumulated in its mature form in *A. thaliana*. LHCSR1 was correctly addressed to thylakoid membranes of *A. thaliana* with an apparent molecular weight identical to that of LHCSR1 from *P.patens* thylakoids. Its heterologous expression yields a protein with properties similar to those reported for LHCSR1 in the moss *P. patens,* such as the ability of the protein to fold correctly with chromophores and its direct dependence on zeaxanthin.

LHCSR1, located in the thylakoid stroma-exposed membranes, activates chlorophyll quenching after several cycles of excess light exposure. LHCSR1 showed a partial NPQ activity which was revealed only after successive short cycles of excess light, indicating a zeaxanthin build-up. This decreased NPQ can be attributed to the localization of LHCSR1 in the thylakoid stroma-exposed membranes, which are rich in LHCII in the case of mosses but not in plants. Finally, a transient NPQ in dark-adapted LHCSR1-complemented *npq4* plant lines was observed when low light was applied, implying that there could be a direct interaction between LHCSR1 and the PSII core.

II. An *in vivo* analysis of factors controlling LHCSR1 activity through heterologous expression in *Arabidopsis thaliana*

When expressed in *A. thaliana npq4* constitutively lacking NPQ, LHCSR1 manages to complement only part of the NPQ phenotype. As shown in Chapter 1, a tentative reason for this low activity could be the low LHCII content in the stromal membranes were the LHCSR1 protein is located. Wanting to investigate additional factors limiting LHCSR1 activity *in planta*, the protein was inserted in a series of *A. thaliana* mutants affected in chromophore biosynthesis or lacking specific antenna subunits.

LHCSR1 synthesis is independent from zeaxanthin or lutein accumulation however its activity depends on xanthophyll cycle. LHCSR1-complemented *npq1npq4 plants* (the *vde* KO mutant unable to accumulate zeaxanthin) could normally express LHCSR1. However, these plants were incapable of NPQ induction, confirming the direct dependence of the protein on zeaxanthin. The effect of lutein was also investigated by LHCSR1 insertion in *lut2npq4*, the lutein-less *A. thaliana* mutant defective in the lycopene e-cyclase. *Lut2npq4*-LHCSR1 plants prove that the protein can be normally expressed in the absence of lutein, having a quenching activity similar to *npq4*-LHCSR1 plants. This relatively stable expression as well as the quenching activity, suggest that the role of lutein in LHCSR1-dependent NPQ is dispensable.

LHCSR1 can be expressed in the absence of Chl b, however the protein might need an interaction partner in quenching. LHCSR1 could be expressed in the absence of Chl b as observed in the case of the CAO mutant *ch1*. However, the transgenic *ch1*-LHCSR1 plants did not show NPQ activity. The reason for this phenotype could be the lack of one or more interaction partners for LHCSR1 among LHC subunits. This hypothesis was further empowered for the minor antennae CP24, CP26 and CP29 since *NoMnpq4* plants complemented with LHCSR1 showed a No-NPQ phenotype, suggesting that there could be a need for LHCSR1 interaction with one or more of the monomeric antennae.

III. Towards LHCSR1 *in vivo* mutational analysis

Mutations on LHCSR1 Chl-binding sites were introduced *in vivo* using *A. thaliana npq4* as an expression tool. Western blot screening of resistant plants showed that LHCSR1 could be expressed in the cases of Chl A2 and Chl A3, the chlorophylls located near the lutein-occupied site L1 but also in the case of Chl B6. On the contrary, the protein could not be accumulated in the cases of Chl A5 and Chl B5, the chlorophylls located close to the xanthophyll-binding L2 site. This result suggests that absence of Chl A5 and Chl B5 is important for the stability of the protein *in vivo* in contrast to Chl A2 and Chl A3, which do not seem to have an effect on the protein stability.

Preliminary results showed that most of the mutations tested have a negative effect on the LHCSR1 activity, since the majority of the generated mutants showed an NPQ induction similar to the untransformed *npq4.* The limit of the heterologous expression system is the low amplitude of the signal, decreasing sensitivity in the analysis of the

phenotype. Better signal level was obtaining by repeating the mutation analysis in the homologous system *P. patens* by exploiting the ability of this moss to perform homologous recombination. Here we could prove that in the case of Chl A5 mutant the protein was accumulated. However, this encouraging result needs to be fully confirmed.

We conclude that LHCSR1, an ancient LHC-like protein, responsible for Non-Photochemical Quenching in the moss *P. patens* can be successfully expressed as a pigment-binding protein in *A. thaliana npq4*, maintaining its biochemical properties. Its expression is not affected by the absence of chlorophyll b, lutein or zeaxanthin, however, lack of the latter xanthophyll leads to LHCSR1 inability to induce NPQ. The partial NPQ induction by LHCSR1 can be primarily attributed to its localization in the stroma region of *A. thaliana* thylakoid membranes where LHCII concentration is low, in contrast with the homologous expression system *Physcomitrella patens*. Finally, direct interaction of LHCSR1 with protein subunits of *A. thaliana* LHC antenna system is a likely possibility, since the lack of LHC monomeric subunits impairs NPQ activity and suggests that LHCII subunits of *A. thaliana* cannot sustain the LHCII-LHCSR1 interaction observed in *P. patens.*

Future perspectives

What comes as an important result out of this thesis is the fundamental importance of LHCSR1 in photoprotective response. Apart from academic curiosity on plant evolution and the adaptation to terrestrial environment, further study of LHCSR proteins can provide information in order to optimize the growth of photoautotrophic organisms used for the production of biofuels. Recent studies show that down-regulating NPQ can result into increased biomass productivity in *C. reinhardtii* (Berteotti et al., 2016) while acceleration of NPQ recovery in *N. tabacum* leads to an increase of at least 15% in crop productivity (Kromdijk et al., 2016), making the tuning of NPQ a suitable strategy for the improvement of light use efficiency for biomass and biofuel production in microalgae and higher plants.

For sure there are several open questions and points that could be further improved in order to have a better understanding of LHCSR1 activity in the complex mechanism of NPQ:

- The production of a His-tag version of the protein expressed in *A. thaliana* in order to

facilitate its isolation from different background genotypes and characterization of the pigment-protein complexes.

- Experiments in order to track other LHC members that possibly interact with the protein required in order to elucidate docking site(s) responsible for activation of LHCSR1-mediated NPQ.
- Full accomplishment of *in vivo* mutational analysis also in the homologous expression system of LHCSR1, in order to produce and characterize mutants lacking specific Chl-binding sites.
- Isolation of sufficient amounts of LHCSR1 in either their violaxanthin or zeaxanthin binding forms, in order to attempt crystallization and structure resolution towards elucidation of pigment-pigment interactions activated during quenching.

Appendix

In this chapter all the methods and techniques used in the laboratory during this work are described in detail. In the case of LHCSR1 mutational analysis in the heterologous expression system of *A. thaliana* all cloning procedures are explained by presenting the steps followed for the mutation of Chl A2 as an example. Also, for the case of LHCSR1 mutation of the homologous system of *P. patens,* a first attempt to verify the possibility of integrating point mutations *in planta* as well as the efficiency of homologous recombination are presented by introducing a STOP mutation. The significance of STOP mutation is the alteration of a codon in *lhcsr1* locus, which leads to the generation of a truncated, non-functional protein.

1. Plasmids employed for *P. patens* and *A. thaliana* transformation

During this study different over-expressing lines were produced. Depending on the destination organism, different vectors were employed carrying different antibiotic resistances. In general, the possibility to use different antibiotic resistances is important because it allows combining different mutations in multiple lines. In the case of *P. patens*, regions from PSBS (locus XM_001778511) and LHCSR1 (locus XM_001776900) genes were cloned respectively into BZRf (PSBS) and BHRf (LHCSR1) plasmids. These vectors present a very similar backbone with different resistance cassettes. In all cases 5' and 3' sequences of the target gene were cloned in the Multi Cloning Sites (MCS) at the two end of the resistance cassette, to obtain the substitution of the coding sequence with the antibiotic resistance.

For the study of the protein in an heterologous system (*A. thaliana npq4*), the full-coding sequence from LHCSR1 was cloned in pDONR221 and sub-cloned in the destination vector pH7WG2.

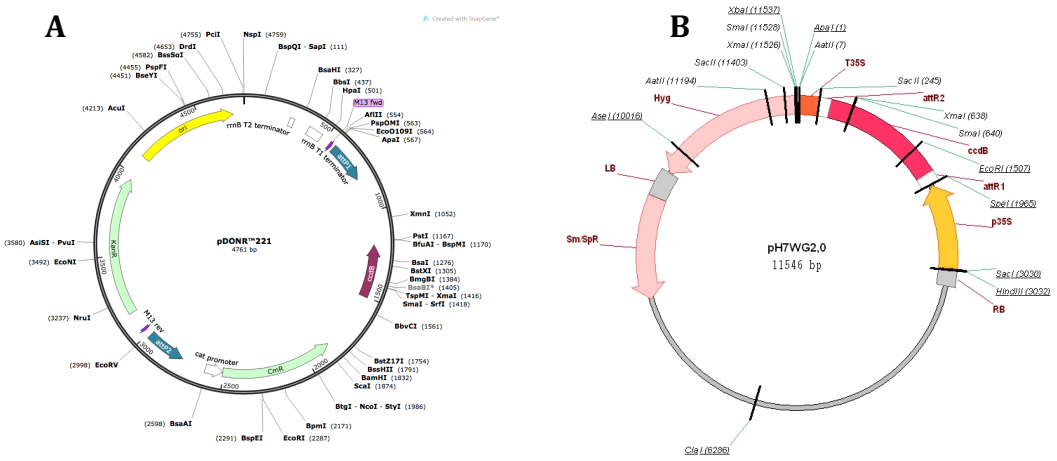

Figure A1. Plasmid vectors used for LHCSR1 cloning in A. thaliana. *A) Entry vector pDONR221 and B) pH7WG2 destination vector.*

pDONR221, which was used as the entry vector is designed to generate attL-flanked entry clones. It includes a series of useful elements such as M13 Forward (-20) and M13 Reverse priming sites (for the sequencing of the insert), two recombination attP sites (attP1, attP2) for recombination cloning of the gene of interest (attB PCR product), Kanamycin resistance gene for selection and pUC origin for replication in *E. coli*. Plasmid vector pH7WG2 was used as a destination vector and it is suitable for easy insertion and expression of genes in plants. Its major characteristics include the strong

Cauliflower Mosaic Virus Promoter CaMV 35S, attR1 and *att*R2 recombination sites, hygromycin resistance cassette and a t35s termination sequence.

2. Cloning of LHCSR1 cDNA and generation of pH7WG2/LHCSR1 construct

The fragment corresponding to *LHCSR1* (Locus name Phpat.009G013900) was amplified from *P. patens* total cDNA obtained from 6 days old plants grown on minimum medium, RNA was isolated using TRI Reagent® Protocol (T9424, Sigma-Aldrich) and cDNA was synthetized using M-MLV Reverse Transcriptase (M1302, Sigma-Aldrich) and Oligo(dT)$_{23}$ (O4387, Sigma-Aldrich). For the cloning procedure we used the Gateway® Technology which is a universal cloning method based on the site-specific recombination properties of bacteriophage lambda in *E. coli* (Bushman et al., 1985; Landy, 1989; Ptashne, 1992).

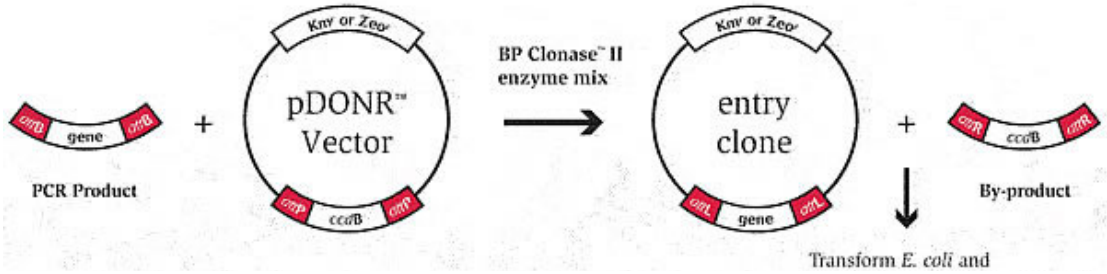

Figure A2. Cloning using the Gateway technology. *The gene of interest (GOI) is amplified with PCR and inserted into an entry vector. Then through the BP reaction the gene of interest is sub-cloned in an entry clone, later transformed in competent DH5a E. coli cells*

This technology provides a rapid and highly efficient way to move DNA sequences into multiple vector systems for functional analysis and protein expression (Hartley et al., 2000). First of all an entry clone is prepared with the sequence of interest inserted in between two sites called attP. pDONR221 which was used as the entry clone, is a vector designed to generate attL-flanked entry clones containing one gene of interest (in our case, *P. patens* LHCSR1) following recombination with an attB expression clone or an attB PCR product. After creating an entry clone, the gene of interest may then be easily shuttled into a large selection of destination vectors (or expression vectors) containing attR sites, using the LR recombination reaction.

The DNA recombination sequences (*att*L, *att*R, *att*B, and *att*P) and the Clonase enzyme mixtures, LR or BP Clonase mediate the lambda recombination reactions. These four types of sites are involved in two reactions as follows: the BP reaction, *att*B × *att*P → _*att*L + *att*R and the LR reaction, *att*L × *att*R → _*att*B + *att*P. All *att* sites contain a central 7-bp overlap region, defined by the cleavage site that largely dictates the specificity of the recombination reaction and up to 4 variations of the BP or LR *att* sites are known (Landy 1989, Cheo et al. 2004). Reactions in which unique *att* sites flanking a gene of interest (GOI) such as *att*B1-GOI-*att*B2, are reacted with pDONR221 vector that includes compatible sites (*att*P1-*att*P2 sites) will result in sequential recombination reactions that transfer the GOI into the pH7WG2 vector backbone, now flanked by *att*L sites (*att*L1-GOI-*att*L2). Because the recombination events that occur within the 7-bp overlap regions are precise, the reading frame and orientation of the transferred DNA are maintained, providing for amino- and/or carboxy-terminal fusion proteins to be rapidly constructed, and conserving the integrity of the transferred DNA sequence. The utility of the system has been enhanced further by introduction of entry and destination vectors, which will allow simultaneous insertion of two, three or four fragments in 1-2 reactions (Karimi et al. 2005).

In our case, the full coding sequence of LHCSR1 from *P. patens* was first cloned in pDON221 exploiting its the *attP*-compatible sites and then sub-cloned into pH7WG2 (the destination vector for *A. thaliana*) using a set of *attB* primers via the BP Clonase reaction The pH7WG2/LHCSR1 cloning strategy is briefly presented in the following page, indicating the DNA primers used for the amplification and the cloning of attB1-*Pplhcsr1*-attB2 insert in pDONR221 entry vector. The entry pDONR221/LHCSR1 clone was then sub-cloned in the pH7WG2 destination vector, which includes attR-sites using the LR Clonase reaction indicated above:

***Pp*LHCSR1 in pDONR221** Attp1 Attp2

CTTTCCTGCGTTATCCCCTGATTCTGTGGATAACCGTATTACCGCCTTTGAGTGAGCTGATACCGCTCGCCGCAG
CCGAACGACCGAGCGCAGCGAGTCAGTGAGCGAGGAAGCGGAAGAGCGCCCAATACGCAAACCGCCTCTCCCCGC
GCGTTGGCCGATTCATTAATGCAGCTGGCACGACAGGTTTCCCGACTGGAAAGCGGGCAGTGAGCGCAACGCAAT
TAATACGCGTACCGCTAGCCAGGAAGAGTTTGTAGAAACGCAAAAAGGCCATCCGTCAGGATGGCCTTCTGCTTA
GTTTGATGCCTGGCAGTTTATGGCGGGCGTCCTGCCCGCCACCCTCCGGGCCGTTGCTTCACAACGTTCAAATCC
GCTCCCGGCGGATTTGTCCTACTCAGGAGAGCGTTCACCGACAAACAACAGATAAAACGAAAGGCCCAGTCTTCC
GACTGAGCCTTTCGTTTTATTTGATGCCTGGCAGTTCCCTACTCTCGCGTTAACGCTAGCATGGATGTTTTCCCA
GTCACGACGTTGTAAAACGACGGCCAGTCTTAAGCTCGGGCCCCAAATAATGATTTTATTTTGACTGATAGTGAC
CTGTTCGTTGCAACAAATTGATGAGCAATGCTTTTTTATAATGCCAACTTTGTACAAAAAAGCTGAACGAGAAAC
GTAAAATGATATAAATATCAATATATTAAATTAGATTTTGCATAAAAAACAGACTACATAATACTGTAAAACACA
ACATATCCAGTCACTATGAATCAACTACTTAGATGGTATTAGTGACCTGTAGTCGACCGACAGCCTTCCAAATGT
TCTTCGGGTGATGCTGCCAACTTAGTCGACCGACAGCCTTCCAAATGTTCTTCTCAAACGGAATCGTCGTATCCA

GCCTACTCGCTATTGTCCTCAATGCCGTATTAAATCATAAAAAGAAATAAGAAAAAGAGGTGCGAGCCTCTTTTT
TGTGTGACAAAATAAAAACATCTACCTATTCATATACGCTAGTGTCATAGTCCTGAAAATCATCTGCATCAAGAA
CAATTTCACAACTCTTATACTTTTCTCTTACAAGTCGTTCGGCTTCATCTGGATTTTCAGCCTCTATACTTACTA
AACGTGATAAAGTTTCTGTAATTTCTACTGTATCGACCTGCAGACTGGCTGTGTATAAGGGAGCCTGACATTTAT
ATTCCCCAGAACATCAGGTTAATGGCGTTTTTGATGTCATTTTCGCGGTGGCTGAGATCAGCCACTTCTTCCCCG
ATAACGGAGACCGGCACACTGGCCATATCGGTGGTCATCATGCGCCAGCTTTCATCCCCGATATGCACCACCGGG
TAAAGTTCACGGGAGACTTTATCTGACAGCAGACGTGCACTGGCCAGGGGGATCACCATCCGTCGCCCGGGCGTG
TCAATAATATCACTCTGTACATCCACAAACAGACGATAACGGCTCTCTCTTTTATAGGTGTAAACCTTAAACTGC
ATTTCACCAGCCCCTGTTCTCGTCAGCAAAAGAGCCGTTCATTTCAATAAACCGGGCGACCTCAGCCATCCCTTC
CTGATTTTCCGCTTTCCAGCGTTCGGCACGCAGACGACGGGCTTCATTCTGCATGGTTGTGCTTACCAGACCGGA
GATATTGACATCATATATGCCTTGAGCAACTGATAGCTGTCGCTGTCAACTGTCACTGTAATACGCTGCTTCATA
GCATACCTCTTTTTGACATACTTCGGGTATACATATCAGTATATATTCTTATACCGCAAAAATCAGCGCGCAAAT
ACGCATACTGTTATCTGGCTTTTAGTAAGCCGGATCCACGCGGCGTTTACGCCCCCCCTGCCACTCATCGCAGTA
CTGTTGTAATTCATTAAGCATTCTGCCGACATGGAAGCCATCACAAACGGCATGATGAACCTGAATCGCCAGCGG
CATCAGCACCTTGTCGCCTTGCGTATAATATTTGCCCATGGTGAAAACGGGGGCGAAGAAGTTGTCCATATTGGC
CACGTTTAAATCAAAACTGGTGAAACTCACCCAGGGATTGGCTGAGACGAAAAACATATTCTCAATAAACCCTTT
AGGGAAATAGGCCAGGTTTTCACCGTAACACGCCACATCTTGCGAATATATGTGTAGAAACTGCCGGAAATCGTC
GTGGTATTCACTCCAGAGCGATGAAAACGTTTCAGTTTGCTCATGGAAAACGGTGTAACAAGGGTGAACACTATC
CCATATCACCAGCTCACCGTCTTTCATTGCCATACGGAATTCCGGATGAGCATTCATCAGGCGGGCAAGAATGTG
AATAAAGGCCGGATAAAACTTGTGCTTATTTTTCTTTACGGTCTTTAAAAAGGCCGTAATATCCAGCTGAACGGT
CTGGTTATAGGTACATTGAGCAACTGACTGAAATGCCTCAAAATGTTCTTTACGATGCCATTGGGATATATCAAC
GGTGGTATATCCAGTGATTTTTTTCTCCATTTTAGCTTCCTTAGCTCCTGAAAATCTCGATAACTCAAAAAATAC
GCCCGGTAGTGATCTTATTTCATTATGGTGAAAGTTGGAACCTCTTACGTGCCGATCAACGTCTCATTTTCGCCA
AAAGTTGGCCCAGGGCTTCCCGGTATCAACAGGGACACCAGGATTTATTTATTCTGCGAAGTGATCTTCCGTCAC
AGGTATTTATTCGGCGCAAAGTGCGTCGGGTGATGCTGCCAACTTAGTCGACTACAGGTCACTAATACCATCTAA
GTAGTTGATTCATAGTGACTGGATATGTTGTGTTTTACAGTATTATGTAGTCTGTTTTTTATGCAAAATCTAATT
TAATATATTGATATTTATATCATTTTACGTTTCTCGTTCAGCTTTCTTGTACAAAGTTGGCATTATAAGAAAGCA
TTGCTTATCAATTTGTTGCAACGAACAGGTCACTATCAGTCAAAATAAAATCATTATTTGCCATCCAGCTGATAT
CCCCTATAGTGAGTCGTATTACATGGTCATAGCTGTTTCCTGGCAGCTCTGGCCCGTGTCTCAAAATCTCTGATG
TTACATTGCACAAGATAAAAATATATCATCATGAACAATAAAACTGTCTGCTTACATAAACAGTAATACAAGGGG
TGTTATGAGCCATATTCAACGGGAAACGTCGAGGCCGCGATTAAATTCCAACATGGATGCTGATTTATATGGGTA
TAAATGGGCTCGCGATAATGTCGGGCAATCAGGTGCGACAATCTATCGCTTGTATGGGAAGCCCGATGCGCCAGA
GTTGTTTCTGAAACATGGCAAAGGTAGCGTTGCCAATGATGTTACAGATGAGATGGTCAGACTAAACTGGCTGAC
GGAATTTATGCCTCTTCCGACCATCAAGCATTTTATCCGTACTCCTGATGATGCATGGTTACTCACCACTGCGAT
CCCCGGAAAAACAGCATTCCAGGTATTAGAAGAATATCCTGATTCAGGTGAAAATATTGTTGATGCGCTGGCAGT
GTTCCTGCGCCGGTTGCATTCGATTCCTGTTTGTAATTGTCCTTTTAACAGCGATCGCGTATTTCGTCTCGCTCA
GGCGCAATCACGAATGAATAACGGTTTGGTTGATGCGAGTGATTTTGATGACGAGCGTAATGGCTGGCCTGTTGA
ACAAGTCTGGAAAGAAATGCATAAACTTTTGCCATTCTCACCGGATTCAGTCGTCACTCATGGTGATTTCTCACT
TGATAACCTTATTTTTGACGAGGGGAAATTAATAGGTTGTATTGATGTTGGACGAGTCGGAATCGCAGACCGATA
CCAGGATCTTGCCATCCTATGGAACTGCCTCGGTGAGTTTTCTCCTTCATTACAGAAACGGCTTTTTCAAAAATA
TGGTATTGATAATCCTGATATGAATAAATTGCAGTTTCATTTGATGCTCGATGAGTTTTTCTAATCAGAATTGGT
TAATTGGTTGTAACACTGGCAGAGCATTACGCTGACTTGACGGGACGGCGCAAGCTCATGACCAAAATCCCTTAA
CGTGAGTTACGCGTCGTTCCACTGAGCGTCAGACCCCGTAGAAAAGATCAAAGGATCTTCTTGAGATCCTTTTTT
TCTGCGCGTAATCTGCTGCTTGCAAACAAAAAAACCACCGCTACCAGCGGTGGTTTGTTTGCCGGATCAAGAGCT
ACCAACTCTTTTTCCGAAGGTAACTGGCTTCAGCAGAGCGCAGATACCAAATACTGTTCTTCTAGTGTAGCCGTA
GTTAGGCCACCACTTCAAGAACTCTGTAGCACCGCCTACATACCTCGCTCTGCTAATCCTGTTACCAGTGGCTGC
TGCCAGTGGCGATAAGTCGTGTCTTACCGGGTTGGACTCAAGACGATAGTTACCGGATAAGGCGCAGCGGTCGGG
CTGAACGGGGGGTTCGTGCACACAGCCCAGCTTGGAGCGAACGACCTACACCGAACTGAGATACCTACAGCGTGA
GCTATGAGAAAGCGCCACGCTTCCCGAAGGGAGAAAGGCGGACAGGTATCCGGTAAGCGGCAGGGTCGGAACAGG
AGAGCGCACGAGGGAGCTTCCAGGGGGAAACGCCTGGTATCTTTATAGTCCTGTCGGGTTTCGCCACCTCTGACT
TGAGCGTCGATTTTTGTGATGCTCGTCAGGGGGGCGGAGCCTATGGAAAAACGCCAGCAACGCGGCCTTTTTACG
GTTCCTGGCCTTTTGCTGGCCTTTTGCTCACATGTT

***Pp*LHCSR1attB1**
GGGGACAAGTTTGTACAAAAAAGCAGGCTCCAATCTCGAGCTTTTGCT

***Pp*LHCSR1attB2**
GGGGACCACTTTGTACAAGAAAGCTGGGTCGACTGCGAATCAATCAGAA

>*Pp*LHCSR1 cds (967bp)

CTCGCTCTGCAACTTTCCTTTCCACTTGGCTCCCGTATTTCCAATCTCGAGCTTTTGCTAGCGTTCTCTGAA
CTGCTTTAGAACCATGGCGATCGCTATGTCCTCCGTGAGCTGCATCTCAGGTGCTAAGCTCTTCTCAACCCC
AGCAGCCTACCAGGTGACTCGCCGCGCCGGCGTTCAGCGGATCAGTGCTGTGGCCGACAAGGTCTCCCCCGA
CCCCGAAGTTGTTCCCCCCAATGTGCTCGAATACGCCAAGGGAATGCCCGGAGTGTGCGCTCCATTCCCAAA
CATCTTCGACCCTGCCGATTTGTTGGCTCGTGCTGCCTCTAGCCCTCGCCCCATCAAGGAATTAAACAGGTG
GAGGGAGTCTGAGATTACCCACGGCCGTGTGGCCATGCTTGCTTCCCTTGGATTCATCGTGCAGGAGCAGCT
CCAGGACTATTCTCTGTTCTACAACTTCGACGGGCAGATCTCTGGCCCTGCCATCTACCACTTCCAGCAGGT
TGAGGCCCGCGGTGCCGTGTTCTGGGAGCCCTTGCTGTTCGCCATCGCTCTTTGCGAGGCCTACAGAGTTGG
ACTTGGGTGGGCTACTCCCCGCTCCGAGGACTTCAACACCTTGAGGGACGACTACGAGCCCGGCAACTTGGG
CTTCGACCCCTTGGGTCTCCTCCCCTCTGACCCCGCCGAAAGGAAGGACATGCAGACCAAAGAGCTCAACAA
CGGGCGTCTTGCCATGATTGCCATTGCTGCCTTCGTTGCGCAGGAGTTGGTCTCGGGTGAAGAGATCTTCGT
GCATTTGTTCAAGAGATTGGGCCTGTAAAGTGACCGTTCATTGTAAATACCTCTCTCAACGACGAACGGCAT
GGGTTGTGTATTTAGAGCAGGGTGGTTAATGAAGCATCTGCACTGAGTTTATTGCAGCTAGAATTCTGATTG
ATTCGCAGTCGTAGCGTTGATGATATCTGCGTGTGCAGAGTGAGCTCTGCCTAATTTTTGAGGCTACAGATG
CTAGTTAGGAGGTGATGCAGTGACGTTTCTCACGGTTGAGAATTGTAACATTTGCGTTCCATGTGAAAATGA
TTTGCAATGAAGGCAACGTTCCAT

3. Site-directed mutagenesis

Apart from the study of the 'wild-type' LHCSR1, this work made a first approach on the mutational analysis of the protein, using *A. thaliana* as a tool for the protein expression and its quenching activity. For this reason a series of plasmid constructs were generated, using different sets of primers introducing a single-point mutation on a residue involved in a chlorophyll-binding site. The technology exploited for this, called *in vitro site-directed mutagenesis*, is used to make point mutations, replace amino acids, and delete or insert single or multiple adjacent amino acids. It is a rapid three-step procedure which generates mutants with greater than 80% efficiency in a single reaction and it is performed using *Pfu Ultra* high-fidelity (HF) DNA polymerase for mutagenic primer-directed replication of both plasmid strands with the highest fidelity.

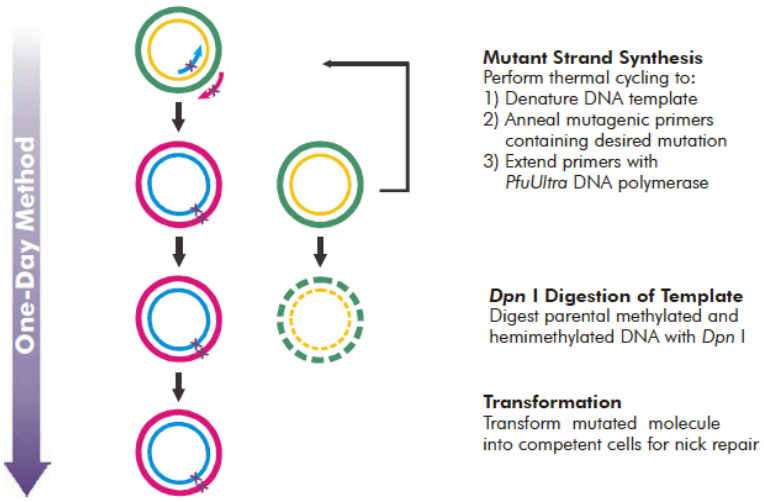

Figure A3. Site directed-muatagenesis. *Overview of the site-directed mutagenesis method.*

The basic procedure utilizes a supercoiled double-stranded DNA (dsDNA) vector with an insert of interest (either mini-prep plasmid DNA or cesium-chloride-purified DNA) and two synthetic oligonucleotide primers, both containing the desired mutation. The oligonucleotide primers, each complementary to opposite strands of the vector, are extended during temperature cycling by *Pfu Ultra* HF DNA polymerase, without primer displacement. Extension of the oligonucleotide primers generates a mutated plasmid containing staggered nicks. Following temperature cycling, the product is treated with *Dpn* I. The *Dpn* I endonuclease (target sequence: 5′-Gm^{6}ATC-3′) is specific for methylated and hemi-methylated DNA and is used to digest the parental DNA template and to select for mutation-containing synthesized DNA (DNA isolated from almost all *E. coli* strains is dam methylated and therefore susceptible to *Dpn* I digestion). The nicked vector DNA containing the desired mutations is then transformed into *E. coli* DH5a super-competent cells. Site-directed mutagenesis is an invaluable technique for characterizing the dynamic, complex relationships between protein structure and function, for studying gene expression elements and for carrying out vector modification.

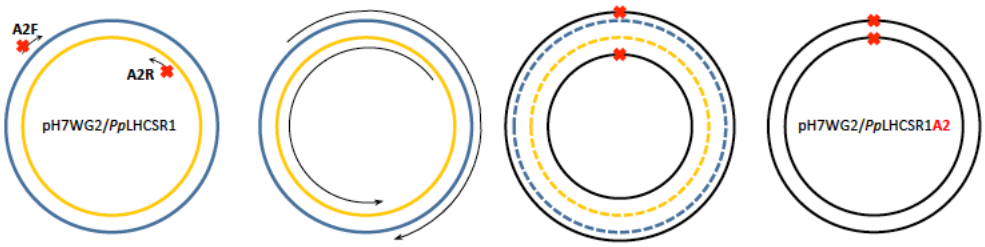

Figure A4. An example of site-directed mutagenesis for the generation of a mutant pH7WG2/LHCSR1 construct. *A set of primers (reverse and forward) introduces the ChlA2 mutation, using as a template the pH7WG2/LHCSR1 construct. After the new mutated vector is generated, DpnI is added in order to eliminate the parental DNA.*

3.1 Site-directed mutagenesis in *A. thaliana psbs* KO

In the case of *A. thaliana*, the QuickChange™ site-directed mutagenesis technology was used in order to create mutant versions of LHCSR1. Having the pH7WG2/LHCSR1 construct as a DNA template, each set of primers was used in a series of PCR reactions in order to obtain pH7WG2 constructs carrying LHCSR1 with modified Chl-binding sites.

Site	Helix	LHCSR1	Mutated to
A2 (Chl612)	A	Asn 212	Phe
A3 (Chl613)	A	Gln 226	Leu
A5 (Chl603)	B	His 99	Phe
B3 (Chl614)	D	His 237	Leu
B5 (Chl609)	C	Glu 159	Val
B6 (Chl606)	C	Glu 149	Gln

Table A.I. Point mutations on LHCSR1 Chl-binding sites. *Six point mutations were introduced for six different residues coordinating Chl-binding sites, mutating them to apolar residues with similar steric hindrance. The Chl-binding site, LHCSR1 helix and mutation are presented.*

The codons for the Chl coordinating residues were muted to apolar residues with similar steric hindrance using specific primers. A total number of six primer pairs were designed in order to alter the codons responsible for Chl-binding with each pair introducing a specific mutation to an individual residue responsible for chlorophyll binding in LHCSR1 (Table A.II).

Site	Forward primer (5'-3')	Reverse primer (5'-3')
A2 (Chl612)	AAAGAGCTCAACTTCGGGCGT CTTGCCATG	CATGGCAAGACGCCCGAAGT TGAGCTCTTT
A3 (Chl613)	GCTGCCTTCGTTGCGCTGGAG TTGGTCTCG	GCAGACCAACTCCAGCGCAA CGAAGGCAGC
A5 (Chl603)	GAGTCTGAGATTACCTTCGGC CGTGTGGCC	GGCCACACGGCCGAAGGTA ATCTCAGACTC
B3 (Chl614)	GAG ATC TTC GTG CTT TTG TTC AAG AGA TTG GGC	GCC CAA TCT CTT GAA CAA AAG CAC GAA GAT
B5 (Chl609)	GCC ATC GCT CTT TGC GTG GCC TAC AGA GTT	AAC TCT GTA GGC CAC GCA AAG AGC GAT GGC

Table A.II. DNA primer sets for the generation of single-point mutations in *LHCSR1* gene. *Six DNA primer sets were specifically designed in order to alter Chl coordinating codons into apolar residues unable to bind pigments. The Chl-binding site, as well as the forward and reverse primers (5'-3' direction) for the introduction of each individual mutation are presented.*

The primers pairs were used in individual PCR reactions directly on the pH7WG2/LHCSR1 construct (DNA template) in order to obtain pH7WG2 constructs carrying LHCSR1 with modified Chl-binding sites. After each reaction methylated and semi-methylated parental DNA was removed from the PCR product by digestion with DpnI and the generated mutated pH7WG2/LHCSR1* construct was used to transform *E. coli* DH5a competent cells. After incubation for 1h in 37^{o}C, transformed *E. coli* was

plated in petri dishes containing Kanamycin-complemented LB agar medium and left to grow overnight. The next day, DNA from resistant colonies was extracted and amplified by colony PCR in order to verify the presence of *lhcsr1**. Isolated DNA from selected colonies was then used to transform *A. tumefaciens* GV3101 competent cells following a standard transformation protocol. Transformed *agrobacterium* was plated in petri dishes containing LB agar medium supplemented with spectinomycin, streptomycin, rifampicin and gentamycin. Petri dishes were left in 28^{o}C for 2 days in order to grow, followed by DNA extraction and amplification by colony PCR. After the final verification of the *lhcsr1** presence, transformed GV3101 *A. tumefaciens* cells were used for the in vivo transformation of *A. thaliana npq4* plants (agrobacterium-mediated transformation method, see below).

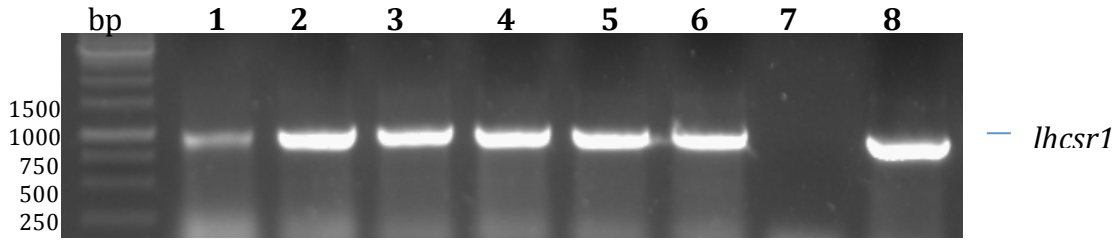

Figure A5. Mutated *lhcsr1 amplification from transformed GV3101 *A. tumefaciens* cells by colony PCR.** *DNA from resistant A. tumefaciens GV3101 colonies transformed with pH7WG2/LHCSR1* constructs was extracted and amplified by PCR using lhcr1 specific primers. The amplified lhcr1 locus (966bp) is shown in all lanes. Lane 1-6: pH7WG2/LHCSR1*, 7: negative control (no vector), 8: positive control (pH7WG2/LHCSR1 without mutation).*

These constructs were later used in order to transform *A. thaliana npq4* plants. After transformation, T0 seeds from each individual Chl mutated plant series were collected, purified and selected for their hygromycin-B resistance, producing T1 generation transgenic plants. In order to verify the presence of the Chl mutation in the T1 plants, DNA from selected LHCSR1-expressing lines was isolated and the *lhcsr1* locus was amplified by PCR using specific primers (Figure A6).

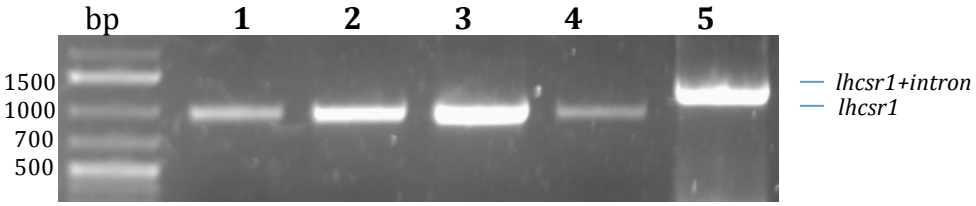

Figure A6. Mutated *lhcsr1 amplification from extracted 35S::LHCSR1*A2 plant DNA .** *DNA from transgenic 35S::LHCSR1* plant lines was extracted and amplified by PCR using lhcr1 specific primers. The amplified lhcr1 locus (966bp) is shown in all lanes. Lane 1-3: pH7WG2/LHCSR1*, 4: control (non-mutated lhcsr1 cDNA), 5: control (lhcsr1 gene).*

The PCR product was purified and sequenced verifying the presence of the whole correct *lhcsr1* sequence altered only in the codon responsible for the binding of Chl (Figure A7).

A

```
ATCGCTATGTCCTCCGTGAGCTGCATCTCAGGTGCTAAGCTCTTCTCAACCCCAGCAGCC
||||||||||||||||||||||||||||||||||||||||||||||||||||||||||||
ATCGCTATGTCCTCCGTGAGCTGCATCTCAGGTGCTAAGCTCTTCTCAACCCCAGCAGCC

TACCAGGTGACTCGCCGCGCCGGCGTTCAGCGGATCAGTGCTGTGGCCGACAAGGTCTCC
||||||||||||||||||||||||||||||||||||||||||||||||||||||||||||
TACCAGGTGACTCGCCGCGCCGGCGTTCAGCGGATCAGTGCTGTGGCCGACAAGGTCTCC

CCCGACCCCGAAGTTGTTCCCCCCAATGTGCTCGAATACGCCAAGGGAATGCCCGGAGTG
||||||||||||||||||||||||||||||||||||||||||||||||||||||||||||
CCCGACCCCGAAGTTGTTCCCCCCAATGTGCTCGAATACGCCAAGGGAATGCCCGGAGTG

TGCGCTCCATTCCCAAACATCTTCGACCCTGCCGATTTGTTGGCTCGTGCTGCCTCTAGC
||||||||||||||||||||||||||||||||||||||||||||||||||||||||||||
TGCGCTCCATTCCCAAACATCTTCGACCCTGCCGATTTGTTGGCTCGTGCTGCCTCTAGC

CCTCGCCCCATCAAGGAATTAAACAGGTGGAGGGAGTCTGAGATTACCCACGGCCGTGTG
||||||||||||||||||||||||||||||||||||||||||||||||||||||||||||
CCTCGCCCCATCAAGGAATTAAACAGGTGGAGGGAGTCTGAGATTACCCACGGCCGTGTG

GCCATGCTTGCTTCCCTTGGATTCATCGTGCAGGAGCAGCTCCAGGACTATTCTCTGTTC
||||||||||||||||||||||||||||||||||||||||||||||||||||||||||||
GCCATGCTTGCTTCCCTTGGATTCATCGTGCAGGAGCAGCTCCAGGACTATTCTCTGTTC

TACAACTTCGACGGGCAGATCTCTGGCCCTGCCATCTACCACTTCCAGCAGGTTGAGGCC
||||||||||||||||||||||||||||||||||||||||||||||||||||||||||||
TACAACTTCGACGGGCAGATCTCTGGCCCTGCCATCTACCACTTCCAGCAGGTTGAGGCC

CGCGGTGCCGTGTTCTGGGAGCCCTTGCTGTTCGCCATCGCTCTTTGCGAGGCCTACAGA
||||||||||||||||||||||||||||||||||||||||||||||||||||||||||||
CGCGGTGCCGTGTTCTGGGAGCCCTTGCTGTTCGCCATCGCTCTTTGCGAGGCCTACAGA

GTTGGACTTGGGTGGGCTACTCCCCGCTCCGAGGACTTCAACACCTTGAGGGACGACTAC
||||||||||||||||||||||||||||||||||||||||||||||||||||||||||||
GTTGGACTTGGGTGGGCTACTCCCCGCTCCGAGGACTTCAACACCTTGAGGGACGACTAC

GAGCCCGGCAACTTGGGCTTCGACCCCTTGGGTCTCCTCCCCTCTGACCCCGCCGAAAGG
||||||||||||||||||||||||||||||||||||||||||||||||||||||||||||
GAGCCCGGCAACTTGGGCTTCGACCCCTTGGGTCTCCTCCCCTCTGACCCCGCCGAAAGG

AAGGACATGCAGACCAAAGAGCTCAACTTCGGGCGTCTTGCCATGATTGCCATTGCTGCC
||||||||||||||||||||||||||  ||||||||||||||||||||||||||||||||
AAGGACATGCAGACCAAAGAGCTCAACAACGGGCGTCTTGCCATGATTGCCATTGCTGCC
```

B

```
Query  1    MAIAMSSVSCISGAKLFSTPAAYQVTRRAGVQRISAVADKVSPDPEVVPPNVLEYAKGMP  60
            MAIAMSSVSCISGAKLFSTPAAYQVTRRAGVQRISAVADKVSPDPEVVPPNVLEYAKGMP
Sbjct  1    MAIAMSSVSCISGAKLFSTPAAYQVTRRAGVQRISAVADKVSPDPEVVPPNVLEYAKGMP  60

Query  61   GVCAPFPNIFDPADLLARAASSPRPIKELNRWRESEITHGRVAMLASLGFIVQEQLQDYS  120
            GVCAPFPNIFDPADLLARAASSPRPIKELNRWRESEITHGRVAMLASLGFIVQEQLQDYS
Sbjct  61   GVCAPFPNIFDPADLLARAASSPRPIKELNRWRESEITHGRVAMLASLGFIVQEQLQDYS  120

Query  121  LFYNFDGQISGPAIYHFQQVEARGAVFWEPLLFAIALCEAYRVGLGWATPRSEDFNTLRD  180
            LFYNFDGQISGPAIYHFQQVEARGAVFWEPLLFAIALCEAYRVGLGWATPRSEDFNTLRD
Sbjct  121  LFYNFDGQISGPAIYHFQQVEARGAVFWEPLLFAIALCEAYRVGLGWATPRSEDFNTLRD  180

Query  181  DYEPGNLGFDPLGLLPSDPAERKDMQTKELNNGRLAMIAIAAFVAQELVSGEEIFVHLFK  240
            DYEPGNLGFDPLGLLPSDPAERKDMQTKELN GRLAMIAIAAFVAQELVSGEEIFVHLFK
Sbjct  181  DYEPGNLGFDPLGLLPSDPAERKDMQTKELNFGRLAMIAIAAFVAQELVSGEEIFVHLFK  240

Query  241  RLGL  244
            RLGL
Sbjct  241  RLGL  244
```

Figure A7. DNA sequencing and alignment of *lhcsr1 gene* amplified by PCR from 35S::LHCSR1*A2 plants. *A) The wild-type LHCSR1 (upper line) is aligned with the generated LHCSR1* mutated in Chl A2 (low line). The change of the CTT codon (Asp) into the CAA codon (Phe) is shown. B) Translation and alignment of LHCSR1 (query) vs. LHCSR1*A2 (sbjct). The alteration of Asp212 into apolar Phenylalanine is indicated in yellow.*

4. *Agrobacterium*-mediated transformation of *A. thaliana*

Plant transformation is a process of genetic manipulation by which foreign genes are introduced into plant cells and stably integrated in the plant genomes, and the transformed cells are regenerated to obtain transgenic plants (Christou, 1996). The conventional transformation method typically includes preparation of transformation-competent plant cells or tissues, delivery into plant cells of foreign genes mainly by *Agrobacterium tumefaciens* or by the biolistic method, selection of transformed cells that have stably incorporated foreign genes, and regeneration of transformed cells into transgenic plants. This transformation method has been widely used to produce transgenic plants, including many agriculturally important crops, whose tissue culture systems are well established (Herrera-Estrella et al., 2005). However, since it involves a tissue culture and plant regeneration step, this approach could be painstaking and time consuming. It also requires skilled labor and relatively expensive laboratory facilities for its execution. Further, this method can result in undesired DNA modification and somaclonal variation during the processes of plant dedifferentiation and differentiation, which is mostly due to the stress imposed by the in vitro cell culture protocol (Labra et al., 2004).

A plant transformation method that excludes the use of tissue culture and plant regeneration would greatly reduce the time required to produce transgenic plants, and such a method was first described as *in planta* transformation almost 30 years ago (Feldmann et al., 1987) popularly referred to as ‘‘the floral dip method’’. In the simplified, yet improved version of it, the steps of uprooting and replanting of infiltrated-plants are omitted. The vacuum-aided infiltration of inflorescences (Bechtold et al., 1993) was replaced by the use of a surfactant (Silwet L-77), which had already been shown, in the formulation of some pesticides, to help chemicals enter the plant tissues (Clough et al., 1998). All these modifications simplified the initial procedure. The *Arabidopsis* flower buds were simply dipped in an *A. tumefaciens* cell suspension containing 5% w/v sucrose and 0.01–0.05% v/v Silwet L-77 to allow uptake of the agrobacteria into female gametes (Desfeux et al., 2000; Bechtold et al., 2003). Compared with traditional transformation methods that require tissue culture and plant regeneration, the floral dip transformation method offers several advantages and opens up new opportunities.

- It requires minimal labor, relatively inexpensive equipment and few specialized reagents, and can be successfully executed even by non-specialists.
- It is easily scalable and therefore allows production of a large number of independent Arabidopsis transgenic lines within a short period. Although the overall transformation efficiency of the floral dip method may not be high, the total number of seed produced by an *Arabidopsis* plant ensures that sufficient transgenic events can be recovered even in a single transformation experiment. An *Arabidopsis* plant produces thousands of seeds by self-pollination, and seeds from one treated plant can be screened on one or two petri dishes.
- The floral dipping procedure can be used not only for introducing specific gene constructs into *Arabidopsis* plants but also for larger-scale transformation projects such as generation of a library of enhancer-trapped lines or of mutant lines tagged by T-DNA.
- The floral dip method easily maintains genomic stability in *A. thaliana* transgenic plants, which can otherwise be harmed by the tissue culture–based transformation.

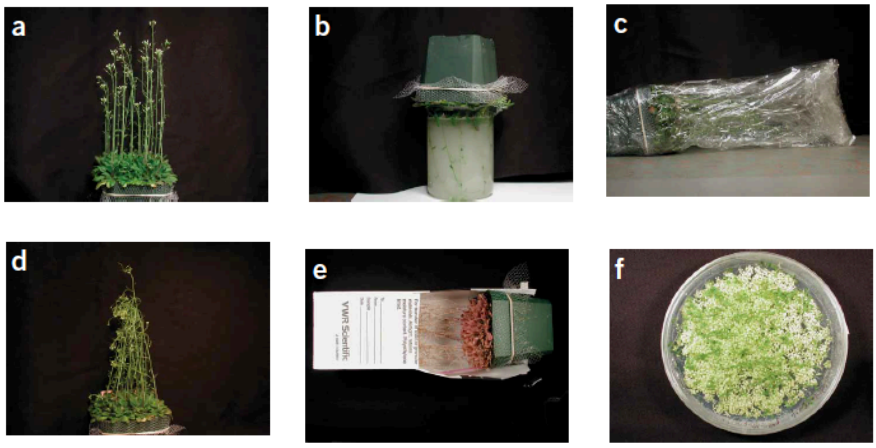

Figure A8. Stages during the floral dip transformation method. *Specific steps are discussed in the text. (a) A good stage for floral dipping is when a pot of healthy plants contain approximately 20–30 inflorescences and some maturing siliques. (b) Invert plants and dip their aerial parts in an Agrobacterium cell suspension for 10 s. (c) Wrap the dipped plants with plastic films to maintain high humidity for 16–24 h. (d) Remove the plastic covers and grow plants in a growth chamber for 3-4 weeks. (e) Dry and harvest seeds with a sample bag. (f) Select primary transformants. Transgenic plantlets are readily distinguished from non-transgenic plants by their green true leaves and roots that penetrate into the selection medium. Primary transformants are selected using hygromycin (+ carbenicillin) and on MS medium selection plates. Note that non-transformed seedlings germinated as well but their cotyledons became chlorotic and bleached soon after germination, whereas true transformants were very healthy, with green cotyledons and true leaves, and developed roots that penetrated into the medium.*

Similar to floral dip, flowering spray also works very well with *Arabidopsis* (Chung et al., 2000). Whereas the floral dip transformation method works well for the majority of *Arabidopsis thaliana* ecotypes, for example, Col-0,Ws-0, Nd-0 and No-0, its efficiency is reduced in the Ler-0 ecotype6. Using a similar protocol, the successful production of transgenic radish (*Raphanus sativus L. longipinnatus*) has been reported with optimum transformation efficiency (Curtis and Nam, 2001). In addition, the floral transformation methods including vacuum infiltration have been successfully used to produce transgenic *Pakchoi Brassica rapa* (Cao et al., 2000), *Arabidopsis lasiocarpa* (Tague, 2001) and rapeseed *Brassica napus* (Wang et al., 2003). These findings extend the utility of the floral dipping method beyond the *Arabidopsis* species, though presently it is still limited to species belonging to the *Brassicaceae* family.

5. Insertion of *PpLHCSR1* in *A. thaliana* using *Agro*-meditated transformation

In this study the *Agrobacterium*-mediated transformation was widely used in order to insert the *LHCSR1* gene in various *A. thaliana* mutants. Competent GV3101 *A. tumefaciens* cells were transformed with the pH7WG2/*PpLHCSR1* construct using a standard *A. tumefaciens* transformation protocol (Figure A9).

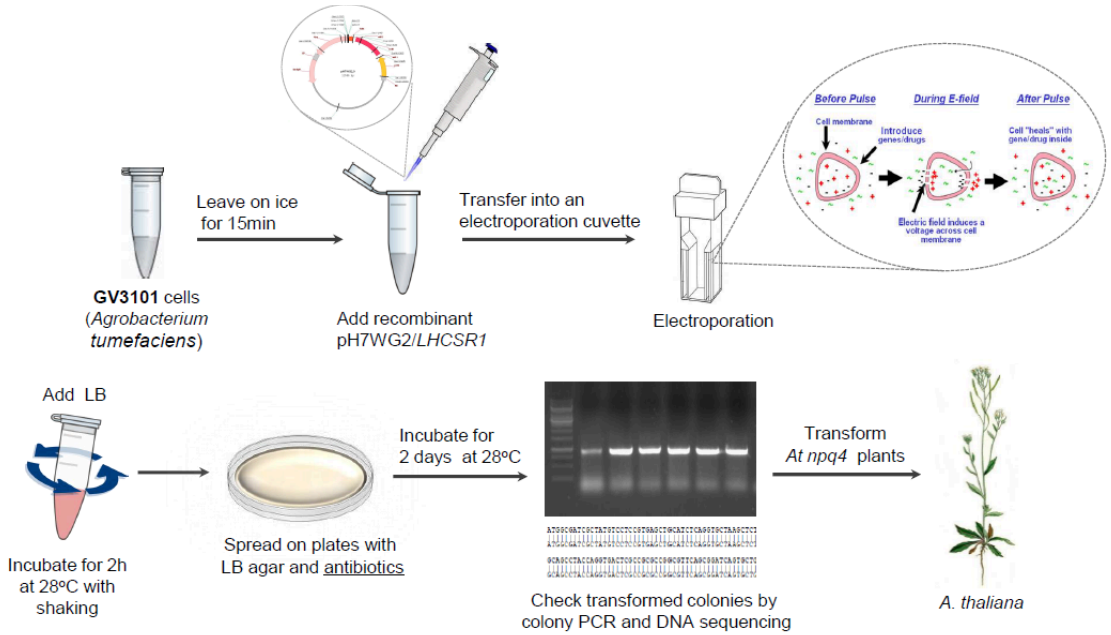

Figure A9. Agrobacterium tumefaciens-mediated in vivo transformation of *A. thaliana* plants

Transformed agrobacterium cells were plated on selection petri dishes containing LB medium enriched with spectinomycin, streptomycin, rifampicin and gentamycin and left in 28^{o}C for 2 days in order to grow. 'Positive' resistant colonies were collected and verified by performing a standard colony PCR and then the purified PCR product was sent for sequencing for further verification (Figure A9).

Next step was the transformation of *A. thaliana* mutant plants following the *Agrobacterium*-mediated method mentioned above. In all cases transformed plants were left to grow for 3-4 weeks and after seeds were collected, sterilized and passed through MS medium petri dishes containing hygromycin as a selection marker (pH7WG2 contains a hygromycin resistance cassette) and carbenicillin (Figure A10). Resistant plants were then screened by western blot analysis (presence of LHCSR1 protein) and fluorescence video-imaging (NPQ activity).

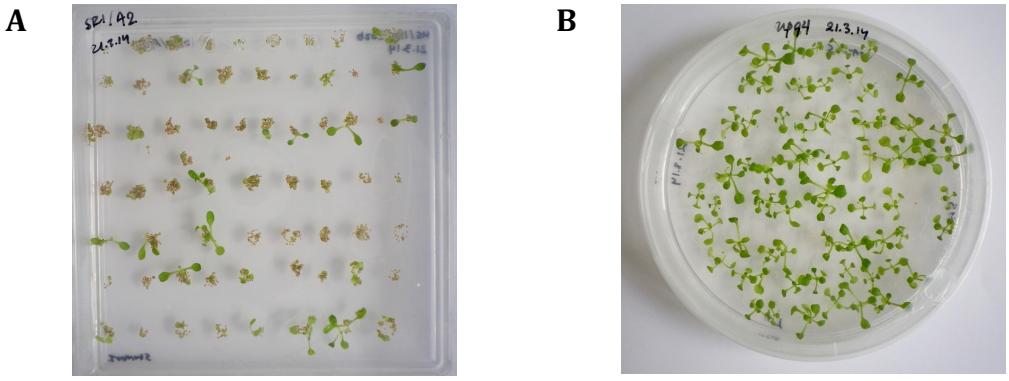

Figure A10. Selection of transformed LHCSR1 plant lines. *After transformation of A. thaliana npq4 plants with the pH7WG2/LHCSR1* construct, transgenic seeds were collected, sterilized and let for 10 days to grow in petri dishes with MS medium, supplemented with hygromycin-B (selection marker). A) Selection of hygromycin-resistant 35S::LHCSR1*A2 plants on MS plate, B) Growth of control A. thaliana npq4 plants on an MS plate without antibiotics.*

6. Moss growth conditions

P. patens can be easily cultivated in laboratory conditions both in solid and liquid medium. Liquid medium allows us the P. patens growth both in small and large-scale cultivation in simple agitated flasks, in batch culture (Wang et al., 1980), in an airlift fermenter (Boyd et al., 1988) or in a stirred bioreactor (Hohe et al., 2002; Decker and Reski, 2004). The solid medium is poured in Petri dishes and overlaid by a cellophane disk to provide mechanical support (A.A. PACKAGING LIMITED, PRESTON, UK). The cellophane prevents plant growth into the medium disk making tissue harvest easier (Grimsley et al., 1977). Cultures are grown in a growth chamber at 24°C, with 16 h light/8 h dark photoperiod and a light intensities of about 40-50 μmol photons m-2 s-1.

The protonemal stage is the most convenient not only for genetic engineering but also biotechnological approaches. The protonema can easily be propagated without the production of persistent spores. Protonemal tissues can grow in a simple medium of inorganic salts without sugars or other organic compounds, and nitrate is the nitrogen source (minimum medium). Growth rates increase by including ammonium as a nitrogen source (rich medium) and adding carbon sources such as tartrate and glucose. Cells from almost any tissue of P. patens, both gametophytic and sporophytic, can regenerate to produce protonemal tissue, although cultures grow faster if started from young protonemal tissue (Cove, 2000). Protonema tissue from 5-6 days-old plants is collected and blended in water by homogenizing moss material with Polytron (IKA T25 Digital Ultra Turrax). The suspension is then spread on new agar plates with medium overlaid with cellophane disks, where it regenerates rapidly as a uniform rug. This propagation protocol works well for short-term cultures. Culture grown on rich medium can be analyzed and sub-cultured in a week; instead culture spread on minimum medium are let grow for about 10-15 days before measurement. Homogenized tissue can be stored for months at 4°C.

P. patens can complete its life cycle under lab conditions: collection of sporangia is the best method for long-term storage. To this aim, homogenized tissue is spread on sterile soil (Jiffy, Jiffy Products International AS, Norway) instead of agar plates. After 5 weeks of growth in standard conditions (16/8 h photoperiod, 24°C) cultures are moved to 16°C and short day photoperiod (8h light/16 h dark) to induced antheridia and archegonia differentiation on gametophore shoot apices and fecundation: after about other 6-8 weeks mature sporangia can be collected. Thus, in about 2-3 months the whole life cycle of *P. patens* is completed. Protocols were adapted from those described at NIBB PHYSCObase (http://moss.nibb.ac.jp) (Ashton et al., 1979).

7. *P. patens* transformation: gene targeting and homologous recombination

P. patens is the only plant model able to perform homologous recombination (HR) with a level of gene targeting comparable to those shown by the yeast Saccharomyces cerevisiae (Kammerer and Cove, 1996; Schaefer and Zrÿd, 1997; Hofmann et al., 1999; Schaefer, 2001; Hohe et al., 2004). HR allows “gene targeting”, an elegant and precise technique that delivers exogenous DNA to a defined location of the recipient genome.

The key feature of such genetic transformation is that the site of DNA integration is predetermined. Gene targeting requires that the exogenously supplied DNA shares sequence homology with the target region (Knight et al., 2009). The technique is powerful because of the range of modifications that can be made to individual genes. It allows the deletion of all, or part of a gene (knock out), the insertion of reporter sequences such as enzymes (b-glucuronidase, luciferase, GFP and other fluorescence derivatives), and affinity- or epitope-tag sequences (His-tags, THR-His-tag, myc-tags, etc.) and the defined alteration of coding sequences by as little as a single base pair, in order to engineer the structure or activity of a specific gene or gene product with surgical precision. The construction of a gene knockout is performed by a targeted insertion of a selectable marker cassette; the selection cassette is inserted into the cloned sequence of the gene to be disrupted. The targeted gene replacement (TGR) occurs as a result of an HR event occurring between the homologous sequences at either end of the targeting construct and its cognate locus.

Many studies report key parameters for a good yield of transformants with a targeted insertion of the transgene. For example, the construct should be delivered in the form of linear DNA: the circular constructs do exhibit gene targeting, but only at low frequency. Indeed, the overall recovery of stable transformants is greatly reduced when circular DNA is delivered, in favor of a predominance of unstable transformants that maintain transgenes only so long as selection is maintained (Kamisugi et al., 2005, 2006). Moreover, the length of homology regions between the transforming DNA and the targeted sequence determines the efficiency of gene targeting.

An homology length of about 600 bp can ensure that 50% of the stable transformants were targeted to the desired locus (Kamisugi et al., 2005). TGR is favored when the two homologous arms of the targeting construct are of approximately equal length (Kamisugi et al., 2005). The optimization of the DNA amount to be used for each transformation (10-20 μg) also improved the efficiency (Hohe et al., 2004; Kamisugi et al., 2005, 2006). Simultaneous transformation with multiple vectors to obtain a multiple targeted KO has also been reported, although the probability of obtaining a multiple KO with a targeted gene replacement in all desired loci with a single transformation is low, being the combination of the frequencies observed for individual constructs (Hohe et al., 2004; Kamisugi et al., 2006).

8. PEG-mediated transformation of *P. patens* protoplasts

Transformations reported in this thesis were performed as in (Schaefer and Zrÿd, 2001) with minor modification. Protoplasts for moss transformation are obtained from 5-6 days old protonema inoculated from a freshly fragmented culture. Protoplasts are isolated from protonema by the digestion (30 min at RT) with 1% (w/v) Driselase (Sigma-Aldrich) dissolved in 8.5% (w/v) mannitol. The digested moss material was then filtered by gravity through a 100µm sieve, left for additional 15 min at RT to continue digestion on the filter and carefully washed with 8.5% mannitol. The protoplasts were collected by centrifuging the filtrate at 200 X g for 5 min at RT, then supernatant was discarded and the pellet was washed twice in 8.5% mannitol. Protoplasts were then re-suspended in MMM solution (8.5% mannitol, 15mM $MgCl_2$, 0.1% MES, pH 5.6) at a concentration of 1.2*106 cells/ml. Afterwards, aliquots of 15-30 µg of linearized DNA was dispensed in falcon tubes and 300µl of protoplast suspension and 300µl of PEG solution (7% mannitol, $Ca(NO_3)_2$ 0.1 M, PEG 4000 35-40%, 10 mM Tris pH 8.0) were added mixing gently. The mixture was heat-shocked 5 min at 45°C and brought to RT for 10 min. Samples were progressively diluted with liquid rich medium (PpNH4 supplemented by 66 g/l mannitol; adding 5x300 µl and 5x1000 µl) and incubate in dark at RT overnight.

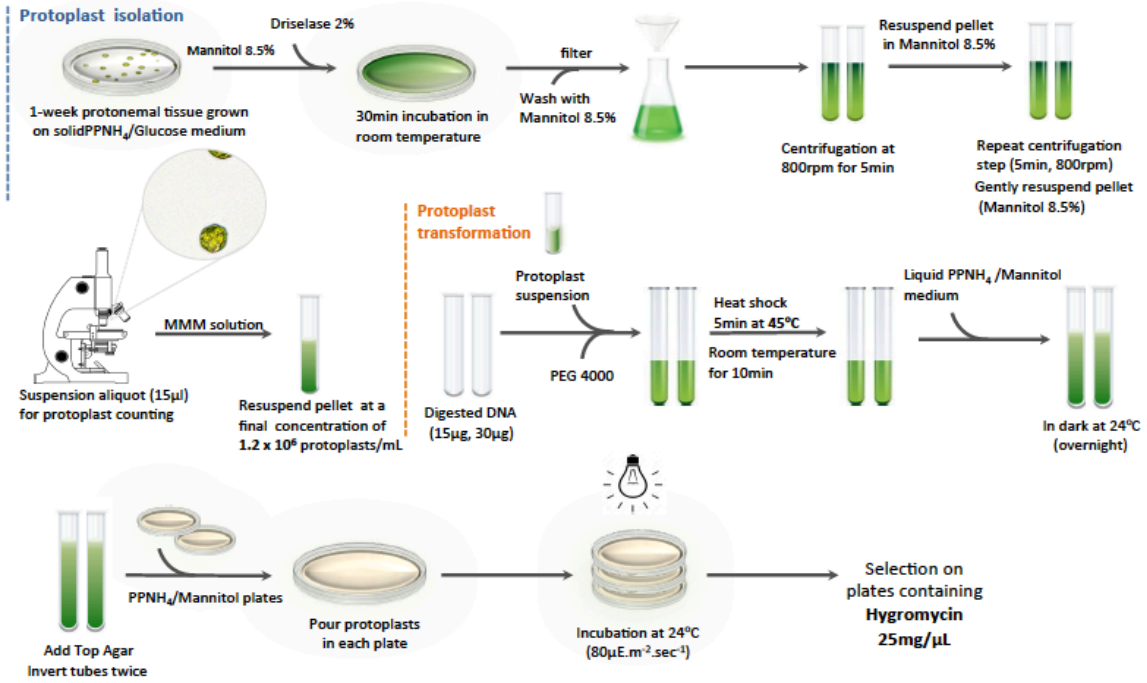

Figure A11. PEG-mediated transformation of *P. patens* protoplasts. *In the figure, the process is divided in two phases: the protoplast isolation and the protoplast transformation.*

The next day, protoplasts were embedded in protoplast top-layer (mannitol 8.5% with 0.84% agar Sigma (A9799); 7 ml of top layer for each tube, thus final agar concentration is 0.42%) and plated on the cellophane covered plate with rich medium ($PPNH_4$) added with 66 g/l mannitol and 0.7% agar. Plates were incubated in a plant growth chamber under standard growth conditions (16/8 h photoperiod, 24°C, light intensity about 40 µE). Selection of transformants started 6 days after transformation by transferring top layer to a new Petri dish with $PPNH_4$ medium supplemented with the appropriate antibiotic (50 µg/ml G418, 30 µg/ml hygromycin or 50 µg/ml zeocin) for about 10 days.

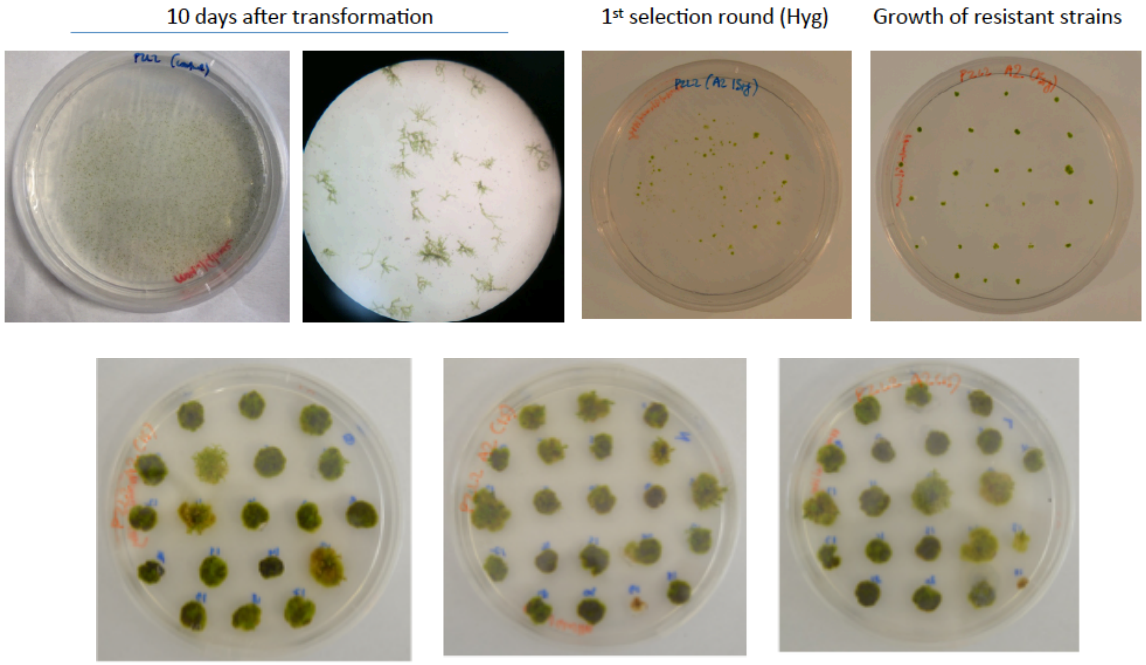

Figure A12. ***P. patens* transformed protoplasts.** *After protoplast isolation and transformation, selection of transformants is made on $PPHN_4$ medium supplemented with antibiotics (50 µg/ml G418, 30 µg/ml hygromycin or 50 µg/ml zeocin) for about 10 days. Resistant mosses are transferred in new antibiotic-supplemented dishes for a second round of selection. Finally true resistant mosses are grown on $PPHN_4$ medium.*

Resistant colonies are then transferred to non-selective $PPNH_4$ medium for additional 10 days and then again on selective media to isolate only stable transformants, which integrated the transgene in their genome. In fact, *P. patens* is also able to episomally replicate exogenous circularized DNA. This can be the original vector if transformation was performed with the circular plasmid, or mainly a circularized concatemer of transgene fragments in the case of transformation with linearized DNA (Ashton et al., 2000; Murén et al., 2009). These lines represent "transient transformants", as the extra-chromosomal elements are then likely lost during growth in non-selective media (Ashton et al., 2000; Murén et al., 2009) and thus these lines are not able to survive to the second selection.

9. Site-directed mutagenesis in *P. patens lhcsr2 psbs* KO

For *P. patens*, LHCSR1 mutational analysis was performed following the same strategy. Pairs of primers introducing Chl-binding site mutations were used together with a parental DNA template (BHRf vector with the *lhcsr1* gene already integrated, Figure A.8) creating mutated BHRf/LHCSR1* by the QuickChange ™ site-directed mutagenesis kit. The transformation procedure performed using the *P. patens lhcsr2 psbs* KO genetic background, a moss expressing only LHCSR1. Use of this background would allow the visualization of LHCSR1 in NPQ without any interference by LHCSR2 or PSBS.

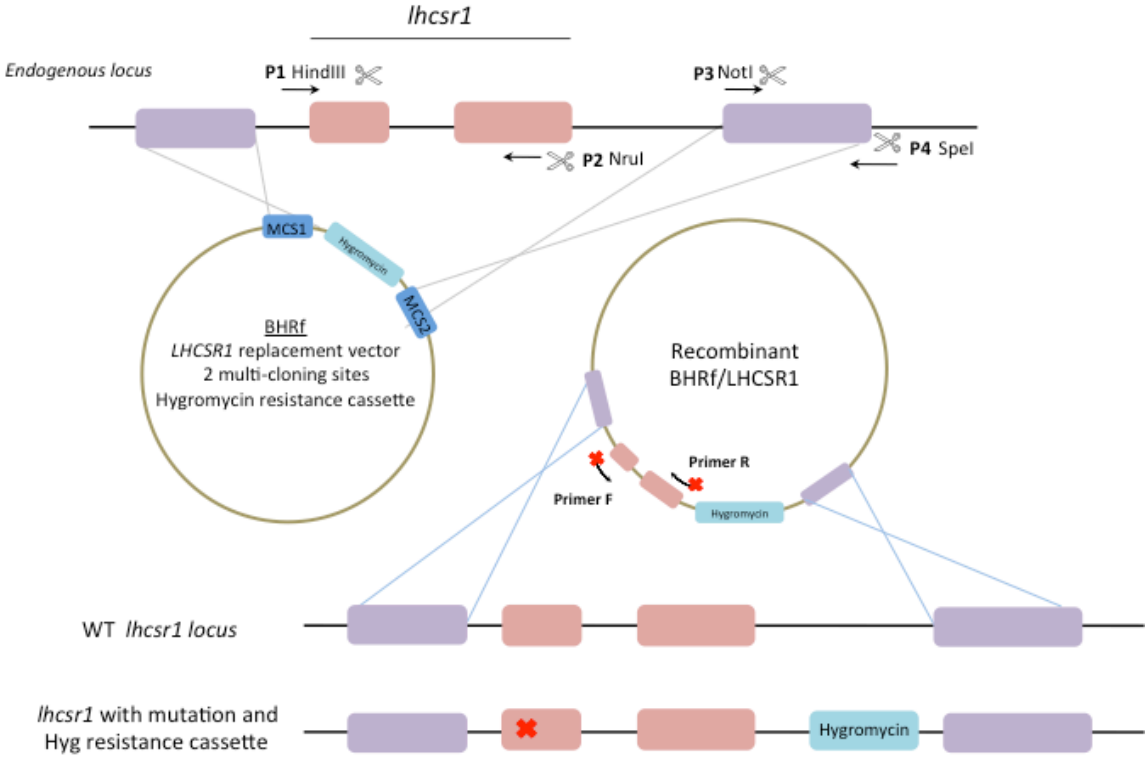

Figure A13. Cloning of *lhcsr1* in BHRf and homologous recombination in Physcomitrella patens. *A plasmid construct (BHRf) carrying a modified version of lhcsr1 gene and a specific antibiotic resistance cassette is used together with a downstream region in order to 'exchange' DNA regions with the same homology (target gene) in the genome of P. patens, creating a LHCSR1-mutant, resistant in hygromycin. Genomic region of lhcsr1 with exons is shown in pink. Purple boxes represent the genomic regions used for homologous recombination. Primers 1 and 2 insert two restriction sites for endonucleases HindIII and NruI while primers 3 and 4 create two restriction sites for the endonucleases NotI and SpeI used for cloning in the two multi-cloning sites (MCS1, MCS2) of BHRf vector. After the generation of BHRf/LHCSR1 a pair of primers introduces a mutation of a specific codon in lhcsr1, in a direct mutagenesis procedure, using BHRf/LHCSR1 construct as parental DNA. The new BHRf/LHCSR1* carrying the mutation is then used for the transformation of P. patens protoplasts, where homologous recombination will occur, exchanging the original lhcsr1 locus with the mutated one and also adding a hygromycin resistance cassette.*

Also in this case, after mutagenesis, constructs were carefully checked with DNA digestion and DNA sequencing in order to ensure that the whole *lhcsr1* locus was present (ATG to STOP codon) together with the correct mutation and without any additional alteration.

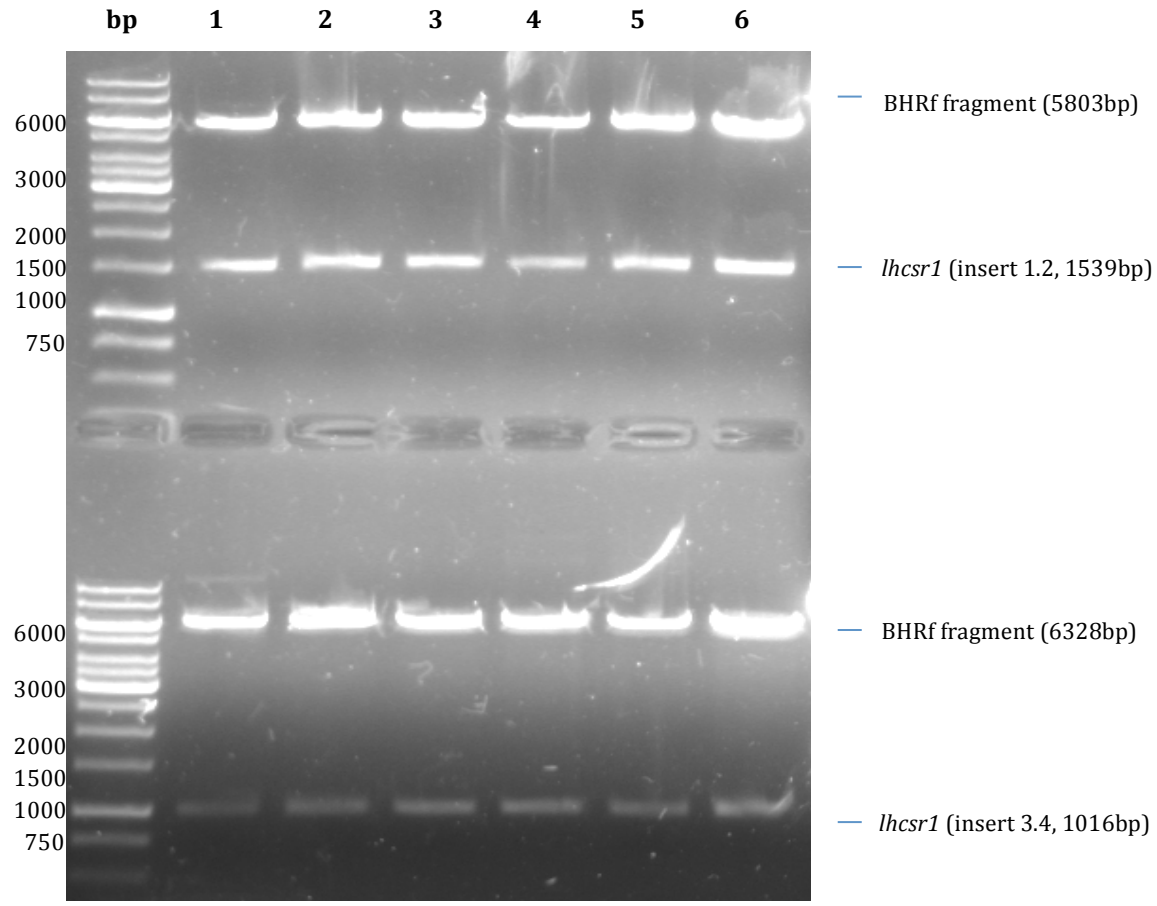

Figure A14. Verification of *lhcsr1* insert in BHRf/LHCSR1* plasmid constructs by double digestion. *Generated BHRf/LHCSR1 carrying Chl-binding sites mutations were checked by double-digestion analysis with different restrictions endonucleases for the lhcsr1 insert. A) Double digestion check of all generated BHRf/LHCSR1 with HindIII and NruI restriction endonucleases. These two restriction endonucleases cut the lhcsr1 insert (left border insert 1.2, 1539bp). B) Double digestion of BHRF/LHCSR1 constructs with NotI and SpeI restrictions endonucleases. This pair of enzymes cuts the lhcsr1 downstream region used for homologous recombination (right border insert 3.4, 1016bp) . BHRf/LHCSR1* constructs (from left to right): Chl A2, ChlA3, ChlA5, ChlB5, LHCSR1 STOP, non-mutated LHCSR1 (control).*

Next, DNA sequencing results for some of the BHRf/LHCSR1* constructs are presented (BHRf/LHCSR1*A2, A3 and A5). Upper line (in grey) is the non-mutated *lhcsr1* while lower line (in black) is the mutated *lhcsr1**. Mutations are highlighted in yellow:

>BHRf A2_PRIMER_forward

CATGGCGATCGCT**ATG**TCCTCCGTGAGCTGCATCTCAGGTGCTAAGCTCTTCTCAACCCCAGCAGCCTACCAGGTGACTC
CATGGCGATCGCT**ATG**TCCTCCGTGAGCTGCATCTCAGGTGCTAAGCTCTTCTCAACCCCAGCAGCCTACCAGGTGACTC

GCCGCGCCGGCGTTCAGCGGATCAGTGCTGTGGCCGACAAGGTCTCCCCCGACCCCGAAGTTGTTCCCCCCAATGTGCTC
GCCGCGCCGGCGTTCAGCGGATCAGTGCTGTGGCCGACAAGGTCTCCCCCGACCCCGAAGTTGTTCCCCCCAATGTGCTC

GAATGTAAGCCCTCACCTCTCGAGCCTATCGTTTTTTAGTTTATCTTACGCATCATACTTTTCCGTGTCCGTTCAAGTGA
GAATGTAAGCCCTCACCTCTCGAGCCTATCGTTTTTTAGTTTATCTTACGCATCATACTTTTCCGTGTCCGTTCAAGTGA

ACCATCACATTACCATGGAGGCAATGTGATTAGTCGTGACATCAATGTCTGAGGTTTATAGTATGAACACCGCCTGGAGC
ACCATCACATTACCATGGAGGCAATGTGATTAGTCGTGACATCAATGTCTGAGGTTTATAGTATGAACACCGCCTGGAGC

TTCTAGTTCGTGACTGTCAATGAGTGAACCATCGAAGATGTGTTCTTCAGTGGAGCTGCGTCGTAAGTCGGTATCTTCCA
TTCTAGTTCGTGACTGTCAATGAGTGAACCATCGAAGATGTGTTCTTCAGTGGAGCTGCGTCGTAAGTCGGTATCTTCCA

CTGGCTCTGTGTTGATCAATCTCTGTATGTTTATTCCAGACGCCAAGGGAATGCCCGGAGTGTGCGCTCCATTCCCAAAC
CTGGCTCTGTGTTGATCAATCTCTGTATGTTTATTCCAGACGCCAAGGGAATGCCCGGAGTGTGCGCTCCATTCCCAAAC

ATCTTCGACCCTGCAGATTTGTTGGCTCGTGCTGCCTCTAGCCCTCGCCCCATCAAGGAATTAAACAGGTGGAGGGAGTC
ATCTTCGACCCTGCAGATTTGTTGGCTCGTGCTGCCTCTAGCCCTCGCCCCATCAAGGAATTAAACAGGTGGAGGGAGTC

TGAGATTACCCACGGCCGTGTGGCCATGCTTGCTTCCCTTGGATTCATCGTGCAGGAGCAGCTCCAGGACTATTCTCTG
TGAGATTACCCACGGCCGTGTGGCCATGCTTGCTTCCCTTGGATTCATCGTGCAGGAGCAGCTCCAGGACTATTCTCTG

TTCTACAACTTCGACGGGCAGATCTCTGGCCCTGCCATCTACCACTTCCAGCAGGTTGAGGCCCGCGGTGCCGTGTTCT
TTCTACAACTTCGACGGGCAGATCTCTGGCCCTGCCATCTACCACTTCCAGCAGGTTGAGGCCCGCGGTGCCGTGTTCT

GGGAGCCCTTGCTGTTCGCCATCGCTCTTTGCGAGGCCTACAGAGTTGGACTTGGGTGGGCTACTCCCCGCTCCGAGGA
GGGAGCCCTTGCTGTTCGCCATCGCTCTTTGCGAGGCCTACAGAGTTGGACTTGGGTGGGCTACTCCCCGCTCCGAGGA

CTTCAACACCTTGAGGGACGACTACGAGCCCGGCAACTTGGGCTTCGACCCCTTGGGTCTCCTCCCCTCTGACCCCGCC
CTTCAACACCTTGAGGGACGACTACGAGCCCGGCAACTTGGGCTTCGACCCCTTGGGTCTCCTCCCCTCTGACCCCGCC

GAAAGGAAGGACATGCAGACCAAAGAGCTCAACAACGGGCGTCTTGCCATGATTGCCATTGCTGCCTTCGTTGCGCAGG
GAAAGGAAGGACATGCAGACCAAAGAGCTCAACTTCGGGCGTCTTGCCATGATTGCCATTGCTGCCTTCGTTGCGCAGG

AGTTGGTCTCGGGTGAAGAGAT
AGTTGGTCTCGGGTGAAGAGAT

>BHRf A3_PRIMER_forward

TGGCGATCGCT**ATG**TCCTCCGTGAGCTGCATCTCAGGTGCTAAGCTCTTCTCAACCCCAGCAGCCTACCAGGTGACTCG
TGGCGATCGCT**ATG**TCCTCCGTGAGCTGCATCTCAGGTGCTAAGCTCTTCTCAACCCCAGCAGCCTACCAGGTGACTCG

CCGCGCCGGCGTTCAGCGGATCAGTGCTGTGGCCGACAAGGTCTCCCCCGACCCCGAAGTTGTTCCCCCCAATGTGCTC
CCGCGCCGGCGTTCAGCGGATCAGTGCTGTGGCCGACAAGGTCTCCCCCGACCCCGAAGTTGTTCCCCCCAATGTGCTC

GAATGTAAGCCCTCACCTCTCGAGCCTATCGTTTTTTAGTTTATCTTACGCATCATACTTTTCCGTGTCCGTTCAAGTG
GAATGTAAGCCCTCACCTCTCGAGCCTATCGTTTTTTAGTTTATCTTACGCATCATACTTTTCCGTGTCCGTTCAAGTG

AACCATCACATTACCATGGAGGCAATGTGATTAGTCGTGACATCAATGTCTGAGGTTTATAGTATGAACACCGCCTGGA
AACCATCACATTACCATGGAGGCAATGTGATTAGTCGTGACATCAATGTCTGAGGTTTATAGTATGAACACCGCCTGGA

GCTTCTAGTTCGTGACTGTCAATGAGTGAACCATCGAAGATGTGTTCTTCAGTGGAGCTGCGTCGTAAGTCGGTATCTT
GCTTCTAGTTCGTGACTGTCAATGAGTGAACCATCGAAGATGTGTTCTTCAGTGGAGCTGCGTCGTAAGTCGGTATCTT

CCACTGGCTCTGTGTTGATCAATCTCTGTATGTTTATTCCAGACGCCAAGGGAATGCCCGGAGTGTGCGCTCCATTCCC
CCACTGGCTCTGTGTTGATCAATCTCTGTATGTTTATTCCAGACGCCAAGGGAATGCCCGGAGTGTGCGCTCCATTCCC

AAACATCTTCGACCCTGCAGATTTGTTGGCTCGTGCTGCCTCTAGCCCTCGCCCCATCAAGGAATTAAACAGGTGGAGG
AAACATCTTCGACCCTGCAGATTTGTTGGCTCGTGCTGCCTCTAGCCCTCGCCCCATCAAGGAATTAAACAGGTGGAGG

GAGTCTGAGATTACCCACGGCCGTGTGGCCATGCTTGCTTCCCTTGGATTCATCGTGCAGGAGCAGCTCCAGGACTATT
GAGTCTGAGATTACCCACGGCCGTGTGGCCATGCTTGCTTCCCTTGGATTCATCGTGCAGGAGCAGCTCCAGGACTATT

CTCTGTTCTACAACTTCGACGGGCAGATCTCTGGCCCTGCCATCTACCACTTCCAGCAGGTTGAGGCCCGCGGTGCCGT
CTCTGTTCTACAACTTCGACGGGCAGATCTCTGGCCCTGCCATCTACCACTTCCAGCAGGTTGAGGCCCGCGGTGCCGT

GTTCTGGGAGCCCTTGCTGTTCGCCATCGCTCTTTGCGAGGCCTACAGAGTTGGACTTGGGTGGGCTACTCCCCGCTCC
GTTCTGGGAGCCCTTGCTGTTCGCCATCGCTCTTTGCGAGGCCTACAGAGTTGGACTTGGGTGGGCTACTCCCCGCTCC

GAGGACTTCAACACCTTGAGGGACGACTACGAGCCCGGCAACTTGGGCTTCGACCCCTTGGGTCTCCTCCCCTCTGACC
GAGGACTTCAACACCTTGAGGGACGACTACGAGCCCGGCAACTTGGGCTTCGACCCCTTGGGTCTCCTCCCCTCTGACC

CCGCCGAAAGGAAGGACATGCAGACCAAAGAGCTCAACAACGGGCGTCTTGCCATGATTGCCATTGCTGCCTTCGTTGC
CCGCCGAAAGGAAGGACATGCAGACCAAAGAGCTCAACAACGGGCGTCTTGCCATGATTGCCATTGCTGCCTTCGTTGC

GCAGGAGTTGGTCTCGGGTGAAGAGATCTTCGT
GCTGGAGTTGGTCTCGGGTGAAGAGATCTTCGT

>BHRf A5_PRIMER_forward
ATGGCGATCGCT**ATG**TCCTCCGTGAGCTGCATCTCAGGTGCTAAGCTCTTCTCAACCCCAGCAGCCTACCAGGTGACTC
ATGGCGATCGCT**ATG**TCCTCCGTGAGCTGCATCTCAGGTGCTAAGCTCTTCTCAACCCCAGCAGCCTACCAGGTGACTC

GCCGCGCCGGCGTTCAGCGGATCAGTGCTGTGGCCGACAAGGTCTCCCCCGACCCCGAAGTTGTTCCCCCCAATGTGCT
GCCGCGCCGGCGTTCAGCGGATCAGTGCTGTGGCCGACAAGGTCTCCCCCGACCCCGAAGTTGTTCCCCCCAATGTGCT

CGAATGTAAGCCCTCACCTCTCGAGCCTATCGTTTTTTAGTTTATCTTACGCATCATACTTTTCCGTGTCCGTTCAAGT
CGAATGTAAGCCCTCACCTCTCGAGCCTATCGTTTTTTAGTTTATCTTACGCATCATACTTTTCCGTGTCCGTTCAAGT

GAACCATCACATTACCATGGAGGCAATGTGATTAGTCGTGACATCAATGTCTGAGGTTTATAGTATGAACACCGCCTGG
GAACCATCACATTACCATGGAGGCAATGTGATTAGTCGTGACATCAATGTCTGAGGTTTATAGTATGAACACCGCCTGG

AGCTTCTAGTTCGTGACTGTCAATGAGTGAACCATCGAAGATGTGTTCTTCAGTGGAGCTGCGTCGTAAGTCGGTATCT
AGCTTCTAGTTCGTGACTGTCAATGAGTGAACCATCGAAGATGTGTTCTTCAGTGGAGCTGCGTCGTAAGTCGGTATCT

TCCACTGGCTCTGTGTTGATCAATCTCTGTATGTTTATTCCAGACGCCAAGGGAATGCCCGGAGTGTGCGCTCCATTCC
TCCACTGGCTCTGTGTTGATCAATCTCTGTATGTTTATTCCAGACGCCAAGGGAATGCCCGGAGTGTGCGCTCCATTCC

CAAACATCTTCGACCCTGCAGATTTGTTGGCTCGTGCTGCCTCTAGCCCTCGCCCCATCAAGGAATTAAACAGGTGGAG
CAAACATCTTCGACCCTGCAGATTTGTTGGCTCGTGCTGCCTCTAGCCCTCGCCCCATCAAGGAATTAAACAGGTGGAG

GGAGTCTGAGATTACCCACGGCCGTGTGGCCATGCTTGCTTCCCTTGGATTCATCGTGCAGGAGCAGCTCCAGGACTAT
GGAGTCTGAGATTACCTTCGGCCGTGTGGCCATGCTTGCTTCCCTTGGATTCATCGTGCAGGAGCAGCTCCAGGACTAT

TCTCTGTTCTACAACTTCGACGGGCAGATCTCTGGCCCTGCCATCTACCACTTCCAGCAGGTTGAGGCCCGCGGTGCCG
TCTCTGTTCTACAACTTCGACGGGCAGATCTCTGGCCCTGCCATCTACCACTTCCAGCAGGTTGAGGCCCGCGGTGCCG

TGTTCTGGGAGCCCTTGCTGTTCGCCATCGCTCTTTGCGAGGCCTACAGAGTTGGACTTGGGTGGGCTACTCCCCGCTC
TGTTCTGGGAGCCCTTGCTGTTCGCCATCGCTCTTTGCGAGGCCTACAGAGTTGGACTTGGGTGGGCTACTCCCCGCTC

CGAGGACTTCAACACCTTGAGGGACGACTACGAGCCCGGCAACTTGGGCTTCGACCCCTTGGGTCTCCTCCCCTCTGAC
CGAGGACTTCAACACCTTGAGGGACGACTACGAGCCCGGCAACTTGGGCTTCGACCCCTTGGGTCTCCTCCCCTCTGAC

CCCGCCGAAAGGAAGGACATGCAGACCAAAGAGCTCAACAACGGGCGTCTTGCCATGATTGCCATTGCTGCCTTCGTTG
CCCGCCGAAAGGAAGGACATGCAGACCAAAGAGCTCAACAACGGGCGTCTTGCCATGATTGCCATTGCTGCCTTCGTTG

CGCAGGAGTTGGTCTCGGGTGAAGAGAT
CGCAGGAGTTGGTCTCGGGTGAAGAGAT

Constructs were used in the basis of two different DNA concentrations (15 and 30 ug) in order to test the transformation efficiency. Before transformation constructs were checked with double DNA digestion analysis using Hind III and SpeI restriction endonucleases.

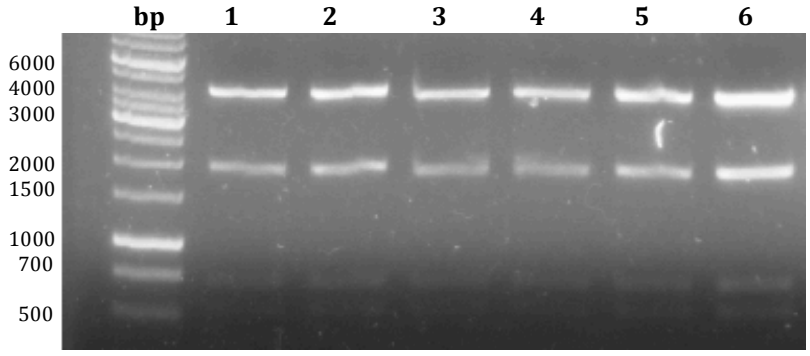

Figure A15. Verification of BHRf/LHCSR1* plasmid constructs by double digestion. *Generated BHRf/LHCSR1 carrying Chl-binding sites mutations were checked by double-digestion analysis with different restrictions endonucleases. A) Double digestion check of all generated BHRf/LHCSR1 with HindIII and PstI restriction endonucleases. Hind III cuts in a region inside lhcsr1 locus while PstI cuts the in a total of 3 regions, one inside lhcsr1 and two on the BHRf plasmid. Expected fragments: 4145, 1969, 697 and 531bp. BHRF/LHCSR1 constructs (from left to right): Chl A2, ChlA3, ChlA5, ChlB5, LHCSR1 STOP, non-mutated LHCSR1 (control).*

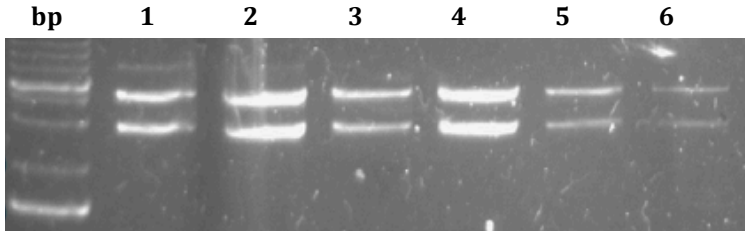

Figure A16. Verification of BHRf/LHCSR1* plasmid constructs by double digestion before protoplast isolation. *Generated BHRf/LHCSR1 carrying ChlA2, ChlA5 and LHCSR1 STOP were checked with double-digestion before proceeding with P. patens lhcsr2 psbs KO protoplast transformation. Restriction enzymes HindIII and SpeI ucut the plasmid construct into two regions, one inside lhcsr1 locus and one outside, creating two separate fragments of 4415 and 2909bp respectively. All samples were incubated for 2 hours in 37°C. BHRf/LHCSR1 samples (from left to right: Chl A2 (15 and 30ug DNA), Chl A5 (15 and 30ug DNA), LHCSR1 A3 (15 and 30ug).*

After isolation and transformation of *P. patens lhcsr2psbs* KO protoplasts with the BHRf/LHCSR1*, stable resistant mosses were grown in rich $PPHN_4$ medium and screened by western blot analysis and in vivo fluorescence video-imaging for the LHCSR1 expression and NPQ activity respectively.

10. Screening tools for transformed mosses

10.1 Facilitating *P. patens* screening: Mutation PstI

During transformation of P. patens multiple insertions might occur at the same time (Schaefer and Zrÿd, 1997; Kasimugi et al., 2006). In order to allow the fast screening of single-insert mutant *P. patens* mosses after protoplast transformation, a PstI restriction site was created in the BHRf plasmid with the LHCSR1 genetic sequence already integrated (BHRf/LHCSR1 construct). Addition of PstI was inserted as a silent mutation in position Ala73 (PstI_F: 5'- TCTTCGACCCTGCAGATTTGTTGGC -3', PstI_R: 5'- GCCAACAAATCTGCAGGGTCGAAGA -3') thus avoiding any effect in the structure of the LHCSR1 protein (Figure A.16, A). Insertion of the PstI mutation was inserted by site-directed mutagenesis procedure and verified by DNA sequencing. After moss transformation and isolation of DNA, single-insertion transformed mosses can be discriminated from the ones having at the same time a mutated and a non-mutated *lhcsr1* gene by DNA extraction, amplification of an *lhcsr1* fragment with a pair of specific screening primers (P1, P2 see table A.III) and digestion with PstI (Figure A.16, B).

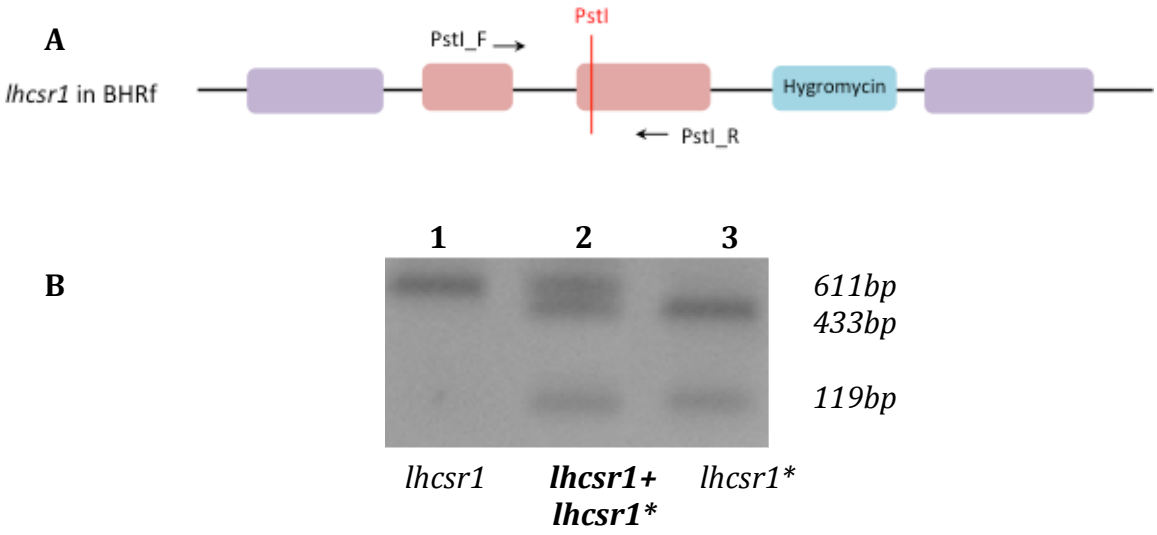

Figure A17. Insertion of PstI restriction site. *A) A PstI restriction site is created (silent mutation, Ala73) using a pair of primers on the BHRf/LHCSR1 construct. B) After P. patens lhcsr2 psbs KO protoplast transformation 'true' single-insertion mosses can be discriminated from multiple-insertion mosses carrying at the same time the mutated and non-mutated version of LHCSR1 by digestion with PstI restriction endonuclease. In the case of single insertion, after digestion PstI will cut only the genetic sequences of the mutated lhcsr1 generating two fragments (lane 3; 433 and 119bp). If there is a multiple insertion in the same moss the non-mutated lhcsr1 co-exists with the mutated sequence giving three bands after PstI digestion instead of two (lane 2; 611, 433 and 119bp). lhcsr1: non-mutated gene, lhcsr1*: gene with PstI mutation.*

10.2 Proof of concept: Mutation STOP

Before starting *P. patens* protoplast transformation with the Chl mutations, we decided to verify the possibility of integrating point mutations in planta as well as the efficiency of homologous recombination. This preliminary work included the integration of a 'STOP' codon in *lhcsr1* that would lead to a truncated, non-functional LHCSR1 protein, observing the corresponding genotype (mutant mosses with low or no NPQ response) after protoplast transformation. Using BHRf – the destination vector for P. patens – the mutated *lhcsr1* sequence would go exactly at the same position as the non-mutated *lhcsr1* allele under the control of the endogenous promoter via homologous recombination. The STOP mutation as in the case of the other Chl mutations was introduced using the QuickChange™ mutagenesis kit. A pair of specific DNA primers (*Pp*LHCSR1$_{STOP}$F: 5'-ACCTTGAGGGACGACTAGGAGCCCGGCAAC-3', *Pp*LHCSR1$_{STOP}$R: 5'-GTTGCC GGGCTCCTAGTCGTCCCTCAAGGT-3' was used together with the BHRf/LHCSR1 plasmid construct (parental DNA template) generating a new BHRf/LHCSR1*STOP vector by PCR. BHRf/LHCSR1* constructs were later used for the transformation of isolated *P. patens* protoplasts.

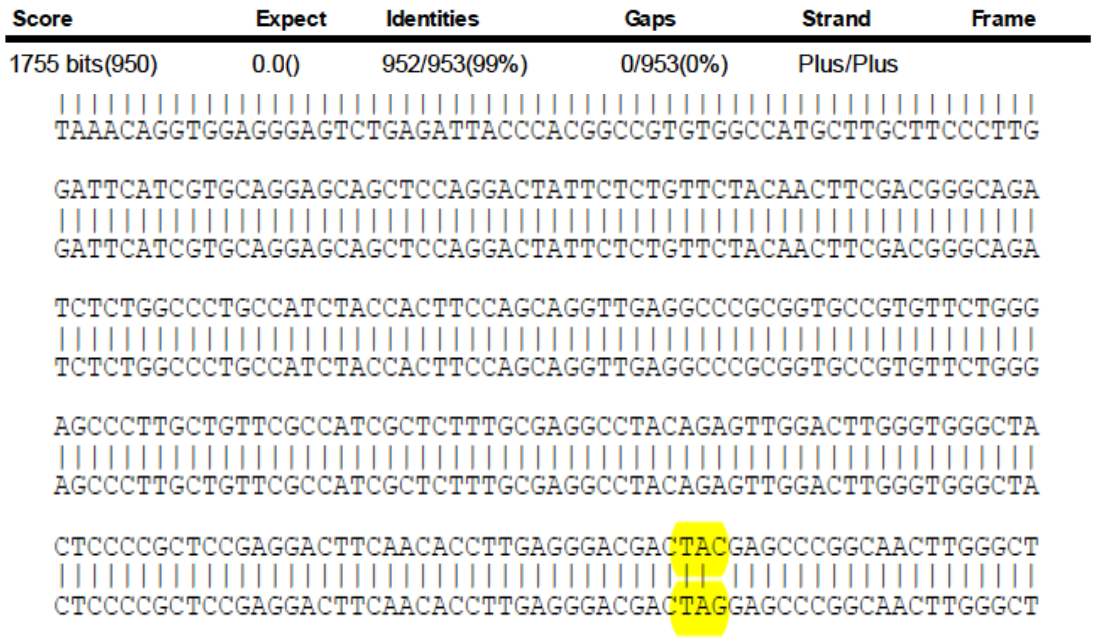

Figure A18. Verification of STOP mutation by DNA sequencing. *The lhcsr1 gene carrying the STOP mutation (TAC altered into TAG), was amplified after single point site-directed mutagenesis and sent for DNA sequencing against non-mutated control lhcsr1. Part of the sequence is presented here, showing the alteration of the Y182 (Tyr) codon into a termination codon, thus leading to a truncated, non-functional LHCSR1 protein.*

10.3 Control of screening strategies

Before starting with the Chl-binding site mutational analysis, both of the screening mutations generated were controlled for their impact on the *lhcsr1* locus. More specifically, after transforming *P. patens lhcsr2psbs* KO with both BHRf/LHCSR1*STOP and BHRf/LHCSR1*PstI constructs, resistant transformants were grown and screened by PCR western blot analysis and fluorescence video-imaging. This was made in order to make sure that the mutations that were inserted on the protein, as controls would not have any effect on its expression. The only expected alteration is the one of the truncated LHCSR1 protein coming from the STOP mutation and leading to a reduced NPQ. Western blot analysis on non-mutated *P. patens lhcsr2psbs* KO, STOP-mutant and PstI-mutant mosses showed that there is no alteration in the amount of the expressed protein, showing that integration of the ' screening control' mutations do not have any effect on the *lhcsr1* content (Figure A19)

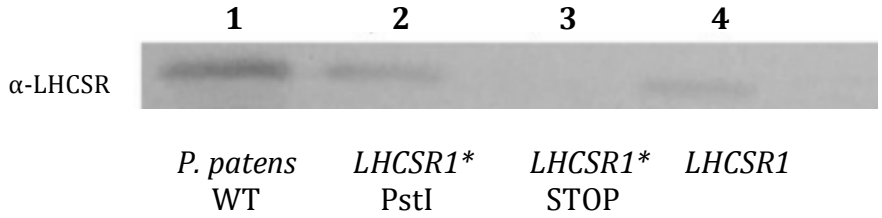

Figure A19. Effect of STOP and PstI mutations on LHCSR1 accumulation. *After transformation of P. patens lhcsr2 psbs KO with BHRf/LHCSR1*PstI and BHRf/LHCSR1*PstI constructs, total protein extracts from resistant transformants were analyzed with western blot analysis against α-LHCSR antibody. Extracts from P. patens wild-type (lane 1) and non-transformed psbs lhcsr2 KO (lane 4) were loaded as positive controls. Genotypes analyzed: Lane 1: P. patens wild-type; lane 2: lhcsr2psbs KO + BHRf/LHCSR1*PstI; lane 3: lhcsr2psbs KO + BHRf/LHCSR1*STOP; lane 4: lhcsr2psbs KO.*

Primer name	Forward primer (5'-3')	Reverse primer (5'-3')	Target
LHCSR1_STOP	ACCTTGAGGGACGACTAGGAGCCCGGCAAC	GTTGCCGGGCTCCTAGTCGTCCCTCAAG	Mutation STOP (Y182 to STOP codon TAG)
LHCSR1_PstI	TCTTCGACCCTGCAGATTTGTTGGC	GCCAACAAATCTGCAGGGTCGAAGA	Adds PstI restriction site
LHCSR1_Check	AGCAGCCTACCAGGTGACTC	CACGATGAATCCAAGGGAAG	Used for *lhcsr1* screening

Table A.III. DNA primers used for single-point mutations by site-directed mutagenesis. *Primer sets for the insertion of STOP mutation (Y182 changed into a STOP codon) in lhcsr1 (LHCSR1_STOP), the addition of a PstI restriction site (LHCSR1_PstI) and the screening of mutant mosses (LHCSR1_Check) are presented.*

Finally the NPQ activity of the same mutant mosses was measured by fluorescence video imaging, on dark-adapted samples. As expected in the case of PstI mutation there is no significant difference between *lhcsr2psb*s KO and PstI-complemented *lhcsr2psbs* KO lines, showing that the mutation has no effect on the activity of LHCSR1. However in the case of STOP mutation, the lines having the truncated LHCSR1 version show loss of NPQ activity with respect to the non-mutated line, something which was also expected (Figure A20).

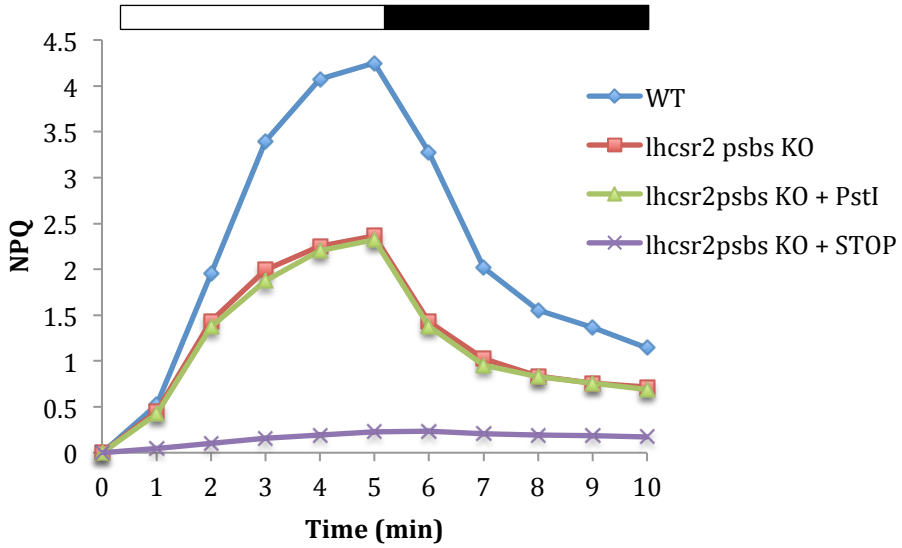

Figure A20. Effect of STOP and PstI mutations in NPQ induction of *lhcsr2psbs* KO. *NPQ kinetics of P. patens dark-adapted plants generated from the transformation of lhcsr2psbs KO with BHRf/LHCSR1*STOP and BHRf/LHCSR1*PstI constructs were measured by applying a standard NPQ protocol (5-min light treatment followed by 5min of dark recovery). Each mutant line is indicated with a different colour (see figure).*

11. *In vivo* chlorophyll fluorescence to measure NPQ

Pigments bound to LHC antenna proteins harvest solar light. Light absorption results in singlet-excited state of Chla molecules ($_1$Chl*). The energy of $_1$Chl* can return to the ground state by different pathways: photochemistry, Chl fluorescence or thermal dissipation processes (NPQ). As a consequence, monitoring Chl fluorescence can give information about NPQ and photochemical quenching. In fact, Chl fluorescence analysis has become an indispensable method for photosynthetic studies because it is a non-intrusive tool and it can give useful information on the PSII very quickly (Krause and Weis, 1991). At room temperature, Chl fluorescence originates mainly from PSII. This is monitored using instruments for chlorophyll fluorescence measurements, called

fluorometers; they utilize the “Saturation Pulse Method” which applies saturating pulses of light in order to rapidly reduce the RCs of the PSII. Different phases can be distinguished for this measurement.

Phase I: Samples are dark adapted at least 20 minutes before measurement in order to ensure full oxidation of all electron transporters. After this dark period all PSII reaction centers are “open” and ready to collect a photon for photochemical reduction of Q_A. Exposure of a dark-adapted leaf to a weak modulated measuring beam (0.1 μmol photons m−2s−1) results in the minimal level of fluorescence (F_0). The intensity of the measuring beam has to ensure that Q_A remains maximally oxidized.

Phase II: A saturating flash of light is then applied, allowing the measurement of maximal fluorescence (Fm). Saturating light is a short pulse with very high intensity, which reduces all Q_A sites; as a consequence all PSII reaction centers are “closed” and fluorescence reaches its maximal value. It has very short time length and thus its contribution to photochemistry is negligible.

Phase III: The leaf is subjected to a short period of dark adaptation (usually 30-60 seconds, according to the species) to allow re-oxidation of electron transporters. Actinic light is switched ON to analyze Chl fluorescence during illumination. Actinic light is the light absorbed by the photosynthetic apparatus and drives electron transport. Its intensity has to be optimized for each species. Usually, to analyze NPQ, actinic light intensity is adjusted in order to almost saturate photochemical capacity of the sample, to achieve also the maximal NPQ induction. In fact, plants are able to maintain a low steady-state fluorescence yield and $_3$Chl* yield due to a combination of photochemical quenching (qP) and NPQ. During the application of actinic light at appropriate intervals, further saturating pulses are applied. These pulses allow determining the different contribution of qP and NPQ, thanks to the determination of local maximum of fluorescence (Fm’) (Maxwell, 2000; Baker, 2008). A saturating pulse is a brief (<1 s) pulse of light that completely saturates photochemistry so that there is no quenching anymore due to qP and so the quenching due solely to NPQ, can be determined. Fluorescence quenching is due to both photochemistry and thermal dissipation. To distinguish between these two contributions the usual approach is to “switch off” one of the two contributions,

specifically photochemical quenching, so that the fluorescence yield in the presence only of the other (NPQ) can be estimated: the saturating light transiently closes all reaction centers and during the flash the fluorescence yield reaches a value equivalent to that which would be attained in the absence of any photochemical quenching (Maxwell, 2000; Baker, 2008).

Phase IV: The period of actinic light is usually followed by a period of dark recovery, during which the relaxation kinetics of the processes previously induced by light exposure can be analyzed. Also in this phase, repetitive saturating pulses are applied. Using different measurement, different parameters can be analyzed. One of the main parameter derived from fluorescence analysis is the F_v/F_m ratio [$F_v/F_m = (F_m-F_0)/F_m$], calculated as the ratio between variable fluorescence and maximal fluorescence of dark adapted sample, which is used to estimate the maximum quantum yield of PSII. This value is usually about 0.8 for plants; a decrease in this parameter is usually related to stress conditions and radiation damage to PSII, thus F_v/F_m is also a simple and rapid way of monitoring stress. The overall NPQ of Chl fluorescence can be determined as: NPQ = $(F_m - F_m')/F_m'$. Figure A21 shows the typical fluorescence induction curve of *A. thaliana* leaf (A21, A) and the NPQ curve obtained using the formula above (A21, B). This simple and fast measurement has been very useful for the screening of NPQ mutant. This simple and fast measurement has been very useful for the screening of NPQ mutant since they have phenotype detectable by fluorescence video-imaging.

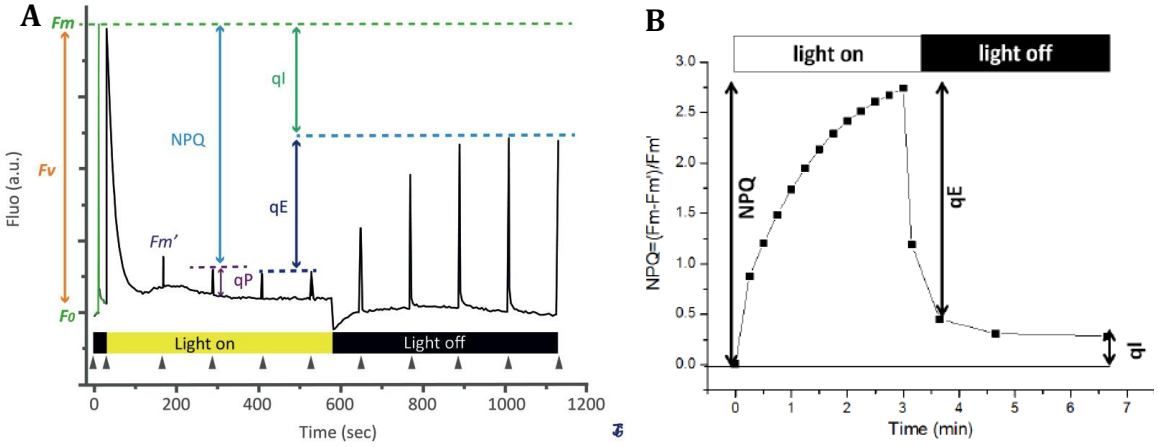

Figure A21. Measuring NPQ. A) *Chl fluorescence measurement from an A. thaliana leaf. NPQ (qE + qT + qI) can be seen as the difference between Fm and the measured maximal fluorescence after a saturating light pulse during illumination (Fm'). After switching off the light, recovery of Fm' within a few minutes reflects relaxation of the qE component of NPQ. Image from* (Müller et al., 2001). *B) NPQ kinetics obtained using the following formula: NPQ=(Fm–Fm')/Fm'.*

Bibliography

Ashton, N., Champagne, C., Weilere, T., Verkoczy, L., and . (2000). The bryophyte *Physcomitrella patens* replicate extrachromosomal transgenic elements. New Phytologist 146: 391–402.

Ashton, N.W., Grimsley, N.H., and Cove, D.J. (1979). Analysis of gametophytic development in the moss, *Physcomitrella patens*, using auxin and cytokinin resistant mutants. Planta 144: 427–35.

Baker, N.R. (2008). Chlorophyll fluorescence: a probe of photosynthesis in vivo. Annual review of plant biology 59: 89–113.

Bechtold, N., Jolivet, S., Voisin, R. & Pelletier, G. The endosperm and the embryo of *Arabidopsis thaliana* are independently transformed through infiltration by *Agrobacterium tumefaciens*. Transgenic Res. 12, 509–517 (2003).

Bechtold, N., Ellis, J. & Pelletier, G. *In planta Agrobacterium*-mediated gene transfer by infiltration of adult *Arabidopsis thaliana* plants. C. R. Acad. Sci. Ser. III Sci. Vie Life Sci. 316, 1194–1199 (1993).

Berteotti S., Ballottari M., Bassi R. Increased biomass productivity in green algae by tuning non-photochemical quenching. Sci Rep. 2016 Feb 18;6:21339. doi: 10.1038/srep21339

Boyd, P., Hall, J., and Cove, D. (1988). An airlift fermenter for the culture of the moss *Physcomitrella patens*. In Methods in Bryology. Proc. Bryol. Meth. Workshop Mainz, ed. JM Glime, pp. 41–45. Nichinan: Hattori Bot. Lab.

Cao, M.Q. et al. Transformation of Pakchoi (*Brassica rapa L. ssp. chinensis*) by *Agrobacterium* infiltration. Mol. Breeding 6, 67–72 (2000).

Christou, P. Transformation technology. Trends Plant Sci. 1, 423–431 (1996).

Chung, M.H., Chen, M.K. & Pan, S.M. Floral spray transformation can efficiently generate *Arabidopsis* transgenic plants. Transgenic Res. 9, 471–476 (2000).

Clough, S.J. & Bent, A.F. Floral dip: a simplified method for *Agrobacterium*-mediated transformation of *Arabidopsis thaliana*. Plant J. 16, 735–743 (1998).

Cove, D. (2000). The Moss, *Physcomitrella patens*. J Plant Growth Regul: 275–283.

Curtis, I.S. & Nam, H.G. Transgenic radish (*Raphanus sativus L. longipinnatus* Bailey) by floral-dip method—plant development and surfactant are important in optimizing transformation efficiency. Transgenic Res. 10, 363–371 (2001).

Decker, E.L. and Reski, R. (2004). The moss bioreactor. Current opinion in plant biology 7: 166–70.

Desfeux, C., Clough, S.J. & Bent, A.F. Female reproductive tissues are the primary target

of *Agrobacterium*-mediated transformation by the *Arabidopsis* floral-dip method. Plant Physiol. 123, 895–904 (2000).

Engel, P. (1968). The induction of biochemical and morphological mutants in the moss *Physcomitrella patens*. Am. J. Bot.: 438–46.

Feldmann, K.A. & Marks, M.D. *Agrobacterium*-mediated transformation of germinating seeds of *Arabidopsis thaliana*: a non-tissue culture approach. Mol. Gen. Genet. 208, 1–9 (1987).

Grimsley, N., Ashton, N., and Cove, D. (1977). The production of somatic hybrids by protoplast fusion in the moss, *Physcomitrella patens*. Mol. Gen. Genet.: 97– 100.

Grimsley, N. and Withers, L. (1983). Cryopreservation of cultures of the moss *Physcomitrella patens*. Cryoletters 4:251–58. Cryoletters: 251–258.

Herrera-Estrella, L., Simpson, J. & Martinez-Trujillo, M. Transgenic plants: an historical perspective. Methods Mol. Biol. 286, 3–32 (2005).

Hofmann, A.H., Codón, A.C., Ivascu, C., Russo, V.E., Knight, C., Cove, D., Schaefer, D.G., Chakhparonian, M., and Zrÿd, J.P. (1999). A specific member of the Cab multigene family can be efficiently targeted and disrupted in the moss *Physcomitrella patens*. Molecular & general genetics : MGG 261: 92–9.

Hohe, A., Decker, E., Gorr, G., Schween, G., and Reski, R. (2002). Tight control of growth and cell differentiation in photoautotrophically growing moss (*Physcomitrella patens*) bioreactor cultures. Plant Cell Rep: 1135–1140.

Hohe, A., Egener, T., Lucht, J.M., Holtorf, H., Reinhard, C., Schween, G., and Reski, R. (2004). An improved and highly standardised transformation procedure allows efficient production of single and multiple targeted gene-knockouts in a moss, *Physcomitrella patens*. Current genetics 44: 339–47.

Kamisugi, Y., Cuming, A.C., and Cove, D.J. (2005). Parameters determining the efficiency of gene targeting in the moss *Physcomitrella patens*. Nucleic acids research 33: e173.

Kamisugi, Y., Schlink, K., Rensing, S.A., Schween, G., von Stackelberg, M., Cuming, A.C., Reski, R., and Cove, D.J. (2006). The mechanism of gene targeting in *Physcomitrella patens*: homologous recombination, concatenation and multiple integration. Nucleic acids research 34: 6205–14.

Kammerer, W. and Cove, D.J. (1996). Genetic analysis of the effects of retransformation of transgenic lines of the moss *Physcomitrella patens*. Molecular & general genetics : MGG 250: 380–2.

Karimi M, De Meyer B and Hilson P (2005) Modular cloning in plant cells. Trends In Plant Science 10(3): 103-105.

Karimi M, Inze D and Depicker A (2002) Gateway vectors for *Agrobacterium*-mediated

plant transformation. Trends In Plant Science 7(5): 193-195.

Kromdijk J, Głowacka K, Leonelli L, Gabilly ST, Iwai M, Niyogi KK, Long SP. Improving photosynthesis and crop productivity by accelerating recovery from photoprotection. Science. 2016 Nov 18;354(6314):857-861.

Knight, C., Perroud, P., and D, C. eds. (2009). The Moss *Physcomitrella patens* (Wiley-Blackwell).

Krause, G.H. and Weis, E. (1991). Chlorophyll Fluorescence and Photosynthesis: The Basics. Annual Review of Plant Physiology and Plant Molecular Biology 42: 313–349.

Labra, M. et al. Genomic stability in *Arabidopsis thaliana* transgenic plants obtained by floral dip. Theor. Appl. Genet. 109, 1512–1518 (2004).

Maxwell, K. (2000). Chlorophyll fluorescence--a practical guide. Journal of Experimental Botany 51: 659–668.

Murén, E., Nilsson, A., Ulfstedt, M., Johansson, M., and Ronne, H. (2009). Rescue and characterization of episomally replicating DNA from the moss *Physcomitrella*. Proceedings of the National Academy of Sciences of the United States of America 106: 19444–9.

Müller, P., Li, X.P., and Niyogi, K.K. (2001). Non-photochemical quenching. A response to excess light energy. Plant physiology 125: 1558–66.

Prigge, M.J. and Bezanilla, M. (2010). Evolutionary crossroads in developmental biology: *Physcomitrella patens*. Development (Cambridge, England) 137: 3535– 43.

Schaefer, D.G. (2001). Gene targeting in *Physcomitrella patens*. Current opinion in plant biology 4: 143–50. Schaefer, D.G. and Zrÿd, J.P. (1997). Efficient gene targeting in the moss *Physcomitrella patens*. The Plant journal : for cell and molecular biology 11: 1195–206.

Schaefer, D.G. and Zrÿd, J.P. (2001). The moss *Physcomitrella patens*, now and then. Plant physiology 127: 1430–8. Schultz, J. and Reski, R. (2004). High-throughput cryopreservation of 140000 *Physcomitrella patens* mutants. Plant biology: 119–127.

Tague, B.W. Germ-line transformation of *Arabidopsis lasiocarpa*. Transgenic Res. 10, 259–267 (2001).

Wang, T., Cove, D., Beutelmann, P., and Hartmann, E. (1980). Isopentenyladenine from mutants of the moss, *Physcomitrella patens*. Phytochemistry: 1103–1105.

Wang, W.C., Menon, G. & Hansen, G. Development of a novel *Agrobacterium*-mediated transformation method to recover transgenic Brassica napus plants. Plant Cell Rep. 22, 274–281 (2003).

ABBREVIATIONS

$_1$Chl*: chlorophyll singlet excited state
$_1$O2*: singlet oxygen
$_3$Chl*: triplet chlorophyll
$_3$P680*: triplet P680
***A. thaliana*:** *Arabidopsis thaliana*
ATP: adenosine triphosphate
ATPase: ATP synthase
bp: base pair
***C. reinhardtii*:** *Chlamydomonas reinhardtii*
CAO: Chlorophyllide a oxygenase
Car: carotenoid
Chl: chlorophyll
CO_2: carbon dioxide
Cys: cysteine
Cyt-*b6f*: cytochrome b_6f complex
DCCD: N, N'-Dicyclohexylcarbodiimide
***E. coli*:** Escherichia coli
F_0: minimal fluorescence of dark adapted sample
Fd: ferredoxin
Fm: maximal fluorescence of dark adapted sample
Fm': maximal fluorescence of light exposed sample
FNR: Ferredoxin $NADP^+$ oxidoreductase
Fv/Fm: The ratio between variable fluorescence and maximal fluorescence of dark-adapted samples
GAP: glyceraldehyde-3-Phosphate
H_2O_2: hydrogen peroxide
HR: homologous recombination
kDa: kilodalton
KO: knock-out
LHC: Light Harvesting Complex
LHCI: antenna system of Photosystem I
LHCII: major antenna complex of Photosystem II
LHCSR: Light Harvesting Complex Stress-Related
Lut: Lutein
MCS: Multi-Cloning Site
Mg: magnesium
Mn: manganese
MS medium: Murashige and Skoog medium
ms: millisecond
MW: Molecular Weight
N. tabacum: *Nicotiana tabacum*
NaCl: Sodium chloride
$NADP^+$/ NADPH: Nicotinamide adenine dinucleotide phosphate
NPQ: Non-Photochemical Quenching
ns: nanosecond
O_2: molecular oxygen
OE: over-expression
OEC: oxygen-evolving complex
OH•: hydroxyl radical
P. patens: Physcomitrella patens
P680: Primary electron donor absorbing at 680 nm
P700: Primary electron donor absorbing at 700 nm
PC: Plastocyanin
PEG: polyethylene glycol
PG: phosphatidylglycerol
Pheo: pheophytin
PQ/PQH2: plastoquinone/plastoquinol
ps: picosecond
PSBS: photosystem II subunit S
PSI: Photosystem I
PSII: Photosystem II
qE: energy-dependent component of NPQ
qI: photo-Inhibitory quenching, component of NPQ
qM: component of NPQ related to chloroplast photorelocation
qP: photochemical quenching
qT: component of NPQ related to State transition
RC: Reaction Center
ROS: Reactive Oxygen Species
RT: Room Temperature
Ru5P: Ribulose-5-phosphate
RuBisCo: Ribulose-1,5-bisphosphate carboxylase/oxygenase
S_0: electronic ground state
S_1: first electronic excited state
S_2: second electronic excited state of electrons
Sup: supernatant
Thr: threonine
Thyl: thylakoids
Tyr: Tyrosine
VDE: violaxanthin deepoxidase
Viola: violaxanthin
ZE: zeaxanthin epoxidase
Zea: zeaxanthin
WT: wild-type
α-DM: n-Dodecyl-a-D-maltopyranoside
β-Car: β-carotene
ΔpH: pH gradient

GLOSSARY

Antenna system: component of photosystems responsible for light harvesting and energy transfer to the reaction centre. For both PSI and PSII two antenna systems are present: an inner antenna system located in the core complex and a peripheral antenna system composed by LHC proteins. In particular the peripheral antenna systems are formed by Lhca and Lhcb proteins for PSI and PSII respectively. Antenna systems are responsible for light harvesting and photoprotection.

ATP: Adenosine 5'-triphosphate. It is a multifunctional nucleotide that is most important in intracellular energy transfer. In this role, ATP transports chemical energy within cells for metabolism.
It is produced as an energy source during the processes of photosynthesis and cellular respiration and consumed by many enzymes and a multitude of cellular processes including biosynthetic reactions, motility and cell division

ATP-ase: a multimeric complex involved in the light phase of photosynthesis: this complex is responsible for ATP production, coupling ATP synthesis with transmembrane proton movement. During photosynthetic electron transport, protons are pumped in the lumen compartment: the transmembrane ΔpH formed constitutes a proton motive force used by ATPase to produce ATP. ATP-ase is characterized by stromal and transmembrane regions that are known as CF1 and CF0, respectively, and represents a molecular motor that is driven by proton movement across the membrane. Proton movement through CF0 is coupled to ATP synthesis/hydrolysis.

PSII-C2S2: the basic unit of PSII supercomplex composed by a PSII dimer, and the subunits CP26, CP29 and a trimeric LHCII bound to each PSII core.

Calvin-Benson cycle: the series of reactions in which atmospheric CO2 is reduced to carbohydrates, using the chemical free energy (ATP and NADPH) produced during the light reactions. These reactions occur in the stroma compartment of the chloroplast.

Car●+: carotenoid radical cation. The formation of this species, and in particular zeaxanthin radical cation, has been correlated to qE induction and belongs to a charge separation in a heterodimer composed by a chlorophyll a and a carotenoid. The subsequent charge recombination allows the thermal dissipation of the energy used for charge separation, in a mechanism called Charge Transfer quenching. Carotenoid radical cation is characterized by absorption in the NIR at ~1000nm.

***Ch1*:** mutant of *Arabidopsis* thaliana lacking the Chl a oxygenase, resulting in absence of Chl b production. Absence of Chl b leads to impairment in the assembly of Chl b containing Lhcs.

$_1$Chl*: singlet chlorophyll excited states. This specie is formed upon light absorption or excitonic energy transfer; singlet chlorophyll excited states can decay to the ground states through several pathways: fluorescence emission, heat production, intersystem crossing or photosynthetic reactions.

$_3$Chl*: triplet chlorophyll excited states. This specie is formed through intersystem crossing from singlet chlorophyll excited states. Triplet Chl excited state is a long-lived state (~ms time scale) and thus can react with triplet oxygen, converting it to singlet oxygen (1 O2), a highly reactive oxygen specie. Carotenoid have a determinant role in 3 Chl* quenching.

Core complex: the inner part of the photosystems binding the reaction centre and the co-factors involved in electron transport. Core complexes are composed by the products of the genes denominated Psa and Psb respectively for PSI and PSII. Among them there are both nuclear and chloroplast encoded polypeptides. At the reaction centre level a chlorophyll special pair undergo charge separation after being excited by the excitonic energy. Core complexes have also an inner antenna system responsible for light harvesting and energy transfer to the reaction centre.

CP24: Lhc antenna protein, named also Lhcb6. This protein is one of the PSII antenna minor complexes and it's found in monomeric form in Photosystem II.

CP26: Lhc antenna protein, named also Lhcb5. This protein is one of the PSII antenna minor complexes and it's found in monomeric form in Photosystem II.

CP29: Lhc antenna protein, named also Lhcb4. This protein is one of the PSII antenna minor complexes and it's found in monomeric form in Photosystem II.

CP43: PSII core complex subunit encoded by the plastidial gene psbC. This subunit binds 14 chlorophylls a and forms with CP47 the inner antenna of photosystem II.

CP47: PSII subunit encoded by the plastidial gene psbB. This subunit binds 14 chlorophylls a and forms with CP47 the inner antenna of photosystem II.

CT quenching: mechanism of thermal dissipation of absorbed light energy by chlorophylls trough carotenoid radical formation. When this mechanism is activated the absorbed energy is used for charge separation in a heterodimer composed by a chlorophyll a and carotenoid heterodimer. The subsequent charge recombination allows the thermal dissipation of the energy.

Cyclic electron transport: electrons from ferredoxin are transferred (via plastoquinone) to a proton pump, cytochrome b6f . They are then returned (via plastocyanin) to P700. This cycle does not produce reducing power, NADPH, but ATP.

Cytochrome-b6*f*: a multiproteic complex involved in the light phase of the photosynthesis. Cytochrome b6f is a plastoquinol—plastocyanin reductase located in the thylakoids. It transfers electrons between the two reaction center complexes of oxygenic photosynthetic membranes, photosystem I and photosystem II, and participates in formation of the transmembrane electrochemical proton gradient by transferring protons from the stromal to the internal lumen compartment. It is minimally composed of four subunits: cytochrome b6, carrying a low- and a high-potential heme groups (bL and bH); cytochrome *f* with one covalently bound heme c ; Rieske iron-sulfur protein (ISP) containing a single [Fe2 S2] cluster; and subunit IV (17 kDa protein).

D1: PSII subunit forming dimers with D2 subunit. D1 and D2 subunits bind the PSII reaction centre P680. D1 subunit is encoded by the plastidial psbA gene.

D2: PSII subunit forming dimers with D1 subunit. D1 and D2 subunits bind the PSII reaction centre P680. D1 subunit is encoded by the plastidial psbD gene.

Dark phase: the photosynthesis phase in which the ATP and NADPH produced during light phase are used in order to produce biomass trough CO_2 fixation. The reactions constituting the dark phase are indicated as the Calvin-Benson cycle.

Ferredoxin: iron-sulfur protein that mediates electron transfer during light phase of photosynthesis. The chloroplast ferredoxin is involved in both cyclic and non-cyclic photophosphorylation reactions of photosynthesis. In non-cyclic photophosphorylation, ferredoxin is the last electron acceptor, being reduced by PSI, and reduces the enzyme NADP+ reductase, which finally produces NADPH. Ferredoxins are small proteins containing iron and sulfur atoms organized as iron-sulfur clusters. These biological "capacitors" can accept or discharge electrons, the effect being change in the oxidation states (+2 or +3) of the iron atoms.

Ferredoxin-$NADP^+$ reductase: enzyme that catalyzes the reduction of NADP+ to NADPH. This enzyme is present in the stroma compartment and it's reduced by ferredoxin.

Grana: the stacked structures formed by thylakoids

Homologous recombination: a type of genetic recombination in which nucleotide sequences are exchanged between two similar or identical molecules of DNA. Homologous recombination (HR) is essential to cell division in eukaryotes. The moss Physcomitrella patens owns this unique abitilty thus it is used widely as a model organism. In this study homologous recombination was expoilted for the mutational

analysis of LHCSR1

L1: carotenoid binding site, located in the inner part of antenna proteins close to helix A. L1 site is prevalently filled by lutein in all plant species and in all LHC proteins.

L2: carotenoid binding site, located in the inner part of antenna proteins close to helix B. L2 sites is prevalently filled by lutein in LHCII trimers, while in monomeric antenna proteins L2 can be occupied by lutein, violaxanthin, neoxanthin and zeaxanthin, depending by several factors, as environmental condition, plant species, protein properties. L2 in LHCI and Lhcb minor complexes binds the product of the xanthophyll cycle.

LHC proteins: antenna proteins of photosystem I and II. These proteins are responsible for light harvesting and photoprotection; LHC proteins bind chlorophyll a, chlorophyll b and xanthophylls. Lhc proteins are encoded by nuclear genes forming a multigenic family. The structure of Lhc proteins is similar.

Lhca proteins: members of the Lhc antenna proteins family associated to Photosystem I. Lhca1, 2, 3, 4 proteins form the LHCI antenna complex which is bound to PSI core, while Lhca5 and Lhca6 are rarely expressed and their role is still uncertain.

Lhca1: Lhc antenna protein associated to PSI. It is a subunit of the LHCI antenna complex. Lhca1 forms heterodimer with Lhca4 subunit.

Lhca2: Lhc antenna protein associated to PSI. It is a subunit of the LHCI antenna complex. Lhca1 forms heterodimer with Lhca3 subunit.

Lhca3: Lhc antenna protein associated to PSI. It is a subunit of the LHCI antenna complex. Lhca3 forms heterodimer with Lhca2 subunit. Lhca3 and Lhca4 are the sites of the red forms in LHCI complex.

Lhca4: Lhc antenna protein associated to PSI. It is a subunit of the LHCI antenna complex. Lhca3 forms heterodimer with Lhca1 subunit. Lhca3 and Lhca4 are the sites of the red forms in LHCI complex.

Lhca5: rarely expressed antenna protein similar to the Lhca1-4 subunit of LHCI complex.

Lhca6: rarely expressed antenna protein similar to the Lhca1-4 subunit of LHCI complex.

Lhcb proteins: members of the Lhc antenna proteins family associated to Photosystem II. Lhcb proteins are divided into two classes: the more abundant LHCII trimers, constituted by Lhcb1, 2, 3 subunits and the monomeric minor complexes constituted by Lhcb4, 5, 6 subunit. The amount of Lhcb protein associated to PSII depends from environmental conditions and the plant species. The subunit Lhcb7 and Lhcb8 are only rarely expressed and their role is still uncertain.

Lhcb1: Lhc antenna protein associated to PSII. It is a subunit of the heterotrimeric antenna complex LHCII.

Lhcb2: Lhc antenna protein associated to PSII. It is a subunit of the heterotrimeric antenna complex LHCII.

Lhcb3: Lhc antenna protein associated to PSII. It is a subunit of the heterotrimeric antenna complex LHCII.

Lhcb4: Lhc antenna protein, named also CP29. This protein is one of the PSII antenna minor complexes and it's found in monomeric form in Photosystem II.

Lhcb5: Lhc antenna protein, named also CP26. This protein is one of the PSII antenna minor complexes and it's found in monomeric form in Photosystem II.

Lhcb6: Lhc antenna protein, named also CP24. This protein is one of the PSII antenna minor complexes and it is found in monomeric form in Photosystem II.

Lhcb7: rarely expressed antenna protein similar to the Lhcb4-6 subunit associated to PSII.

Lhcb8: rarely expressed antenna protein similar to the Lhcb4-6 subunit associated to PSII.

LHCI: antenna complex associated to PSI. It is composed by Lhca1, 2, 3 and 4 subunits and it is positioned in a half-moon shape at one side of PSI.

LHCII: the trimeric more abundant antenna complex associated to PSII. Each trimmer is a heterotrimer with different levels of Lhcb1, 2, 3 subunits. The structure of each monomer is constituted by three transmembrane and one amphypathic helices, indicated respectively as A-C and D. Each monomer binds 14 chlorophylls and 4 carotenoids.

LHCII-L: LHCII trimers forming the outer layer of antennae protein bound to PSII core. LHCII-L amount per PSII core depend from environmental condition.

LHCII-S: LHCII trimers bound to the basic unit of PSII, the C2S2 particle. LHCII-S amount per PSII core does not depend from environmental condition.

LHCSR: members of the LHC family, found in green algae and bryophytes and associated with light-harvesting and energy quenching. LHCSR play a crucial role in the activation of non-photochemical quenching photoprotection mechanism.

LHCSR1: a three transmemberane pigment-binding protein, member of LHC family and responsible for the activation of non-photochemical quenching (NPQ) in *Physcomitrella patens*.

Light phase: the photosynthesis phase in which sunlight is absorbed by photosynthetic pigments (chlorophylls and carotenoids); absorbed energy is subsequently transferred to the reaction centre where charge separation occurs, thus converting light energy into chemical energy. Photosystems I and II, Cytochrome b6f and ATP-ase are the proteic complexes involved in the light phase. During light phase a water molecule is consumed in order to produce O_2, ATP and NADPH.

Lumen: the soluble compartment in the chloroplast delimited by thylakoids: in the lumen protons are pumped during photosynthetic light phase, forming a transmembrane ΔpH which constitutes the force used by ATP-ase to produce ATP.

***Lut2*:** mutant of *Arabidopsis thaliana* lacking the ε-cyclase enzyme. This mutant does not produce the α-branch carotenoids, and in particular does not accumulate lutein.

***Lut2npq4*:** mutant of *Arabidopsis thaliana* lacking both PSBS subunit and ε-cylase enzyme. This mutant doesn't accumulate the α -branch carotenoids, in particular lutein; moreover this sample is impaired in NPQ induction, since PSBS is missing.

Minor complexes: monomeric antenna proteins associated to PSII. Minor complexes are composed by CP24, CP26 and CP29 antenna proteins and bind 2-3 carotenoids per molecule. They are located between PSII core and the peripheral LHCII trimers.

N1: carotenoid binding site, located close to helix C of antenna proteins. N1 site is present in LHCII and it is specific for neoxanthin, even if violaxanthin or lutein binding was found therein. N1 site is stabilized by a Tyrosine residue which can form hydrogen bounds with the carotenoid therein. N1 site is also stabilized in LHCII by the chlorophylls located near Helix C and D.

NADPH: Nicotinamide adenine dinucleotide phosphate. This specie is used in anabolic reactions, such as lipid and nucleic acid synthesis, as a reducing agent. NADPH is the reduced form of NADP+, and NADP+

is the oxidized form of NADPH. In chloroplasts, NADP+ is reduced by ferredoxin-NADP+ reductase in last step of the electron chain of the light reactions of photosynthesis. The NADPH produced is then used as reducing power for the biosynthetic reactions in the Calvin cycle of photosynthesis.

***NoM*:** mutant of *Arabidopsis thaliana* lacking minor antennae CP24, CP26 and CP29

***NoMnpq4*:** mutant of *Arabidopsis thaliana* lacking minor antennae CP24, CP26 and CP29 and PSBS protein. This mutant is constitutively impaired on NPQ induction.

NPQ: Non Photochemical Quenching. It's a lightinduced photoprotective process by which plants are able to rapidly dissipate the excess absorbed energy as heat. When light is absorbed in excess the photosynthetic electron transport establish a low lumenal pH, which activate the mechanisms inducing NPQ. NPQ is detectable monitoring the decrease of leaf fluorescence during illumination. NPQ is characterized by a fast component called qE with relaxation time within minutes, and a slower component called qI, correlated to photoinhibition, which has relaxation time of hours.

***Npq1npq4*:** mutant of *Arabidopsis thaliana* lacking the Violaxanthin de-epoxidase enzyme and PSBS protein. This mutant is impaired in xanthophyll cycle and cannot convert violaxanthin to zeaxanthin. It is also constitutively impaired on NPQ induction.

***Npq2npq4*:** mutant of *Arabidopsis thaliana* lacking the zeaxanthin epoxidase enzyme and PSBS protein. This mutant constitutively accumulates zeaxanthin but not violaxanthin and neoxanthin. It is constitutively impaired on NPQ induction.

***Npq4*:** mutant of *Arabidopsis thaliana* lacking the PSBS protein. This mutant is constitutively impaired on NPQ induction.

OEC: Oxygen Evolving Complex. It's a multiproteic complex characterized by the presence of four manganese ions cluster. This complex it's associated to PSII and extracts electrons from water producing O2 and H^+ , through redox reactions with the manganese cluster. Electrons extracted from water reduce the oxidized P680+ . On the lumenal side of the complex, three extrinsic proteins of 33, 23 and 17 KDa (OEC1-3) compose the oxygen evolving complex and have a calcium ion, a chloride ion and a bicarbonate ion as necessary cofactors.

P680: the chlorophyll special pair constituting the reaction centre of PSII. These chlorophylls are characterized by absorption at 680nm and upon excitation undergo charge transfer, transferring one electron to the electron acceptors located in PSII. The oxidized P680+ is reduced by a Tyrosine residue named TyrZ, which was previously reduced by the Oxygen Evolving Complex (OEC).

P700: the chlorophyll special pair constituting the reaction centre of PSI. These chlorophylls are characterized by absorption at 700nm and upon excitation undergo charge transfer, transferring one electron to the electron acceptors located in PSI. The oxidized P700+ is reduced by a plastocyanin, which was previously reduced at the cytochrome b6*f* level.

Photoinhibition: reduction of photosynthetic efficiency in plants due to damages deriving from light energy absorbed in excess. When light is absorbed in excess and photosynthetic pathway become saturated, the energy can diverted to produce ROS, which causes damage through oxidation of lipids, proteins and pigments, reducing the photosynthetic efficiency.

Photoprotection: the whole mechanisms developed by photosynthetic organisms in order to avoid photoinhibition. Photoprotective mechanisms can be divided into two different classes, depending on the time-scale of action: a) short-term photoprotective mechanisms and b) long-term photoprotective mechanisms.

Photorespiration: an alternate pathway for production of glyceraldehyde 3-phosphate, an intermediate of the Calvin-Benson cycle, by RuBisCO. Although RuBisCO favors carbon dioxide to oxygen, oxygenation of RuBisCO occurs frequently, producing a glycolate and a glycerate. This usually occurs

when oxygen levels are high; for example, when the stomata are closed to prevent water loss on dry days. It involves three cellular organelles: chloroplasts, peroxisomes, and mitochondria. Photorespiration produces no ATP, but consumes ATP and NADPH: it may function as a "safety valve", preventing excess NADPH and ATP from reacting with oxygen and producing free radicals.

Photosystems: multiproteic complexes involved in the light phase of photosynthesis. Photosystems are responsible for light absorption and its conversion into chemical energy trough charge separation at the reaction centre level. In higher plants are present two photosystems: photosystem I (PSI) and photosystem II (PSII). Both photosystem are composed by a core complex where is located the reaction center and an antenna system.

Plastocyanin: a monomeric copper-containing protein involved in photosynthetic electron-transfer. Plastocyanin functions as an electron transfer agent between cytochrome *f* of the cytochrome b6*f* complex from photosystem II and P700+ from photosystem I.

PSBS: an integral membrane protein component and member of the Lhc-protein superfamily, even if it does not bind pigments. Its presence is fundamental for NPQ induction, and in particular for the qE component. PSBS has two conserved glutamic acid exposed to the lumen (Li, X. P. et al. 2002) which substitution results is PSBS inactivation.

PSI: Photosystem I. It's one of the multiproteic complexes responsible for the light phase of the photosynthesis and it is mainly located in the unstacked stroma lamellae membranes. PSI is a light-dependent plastocyanin-ferredoxin oxidoreductase. PSI is composed by a core complex and a peripheral antenna system. The core complex is constituted by 12 about subunits, encoded by the *psa* genes and binds the reaction center P700 and the primary electron acceptors A0 (chlorophyll-a), A1 (phylloquinone) and FX (a Fe4 – S4 cluster). The oxidized P680+ is reduced by the plastocyanin at the lumen-exposed side, while ferrodoxin is reduced at the stroma-exposed side. The inner antenna system of PSI is constituted of 97 chlorophylls a while the outer antenna system, the LHCI complex, is constitutes of 56 Chls bound by Lhca1-4 subunits. 9 "gap" chlorophylls are present at the interface between LHCI and PSI core. PSI is characterized by the presence of the "red forms".

PSII: Photosystem II. PSII is water–plastoquinone oxidoreductase. It's one of the multiproteic complexes responsible for the light phase of photosynthesis and it is mainly located in the stacked grana membranes. PSII is composed by a core complex and a peripheral antenna system. The core complex is constituted by 16 subunits, encoded by the psb genes and binds the reaction center P680 and the primary electron acceptors: pheophytin and the quinones Q_A and Q_B. The oxidized P680+ is reduced by a TyrZ residue, which is reduced by electrons extracted from water by the Oxygen Evolving Complex. The final electron acceptor of PSII is the plastoquinone pool. Reduced plastoquinones (plastoquinols) migrates to cytochrome b6*f*. The inner antenna system of PSII is constituted by CP43 and CP47 subunits, while the outer antenna system is composed by the Lhcb proteins. The amount of Lhcb proteins bound to PSII core depends from environmental conditions and plant species.

qE: the faster component of leaf fluorescence decrease due to NPQ induction; it's associated to the reduction of lumenal pH upon extreme electron transport reactions as a consequence of light absorption in excess. qE depends from the presence of the PSII associated protein PsbS and from zeaxanthin accumulation. qE component of NPQ has relaxation time of few minutes.

qI: the slower component of NPQ. When leaves are placed to dark, after being illuminated to activate NPQ, their fluorescence level is lower than the initial level: this difference represents the qI component of NPQ, which has a relaxation time of hours. qI is associated to photoinhibition events and to zeaxanthin accumulation, which takes hour to be re-converted to violaxanthin and activates some long-term photoprotective mechanisms.

Red forms: low-energy absorption forms associated to photosystem I. Photosystem I, respect to Photosystem II, is characterized by absorption forms at long-wavelengths, over 700 nm. This absorption forms are called "red forms" and are mainly located in the antenna system LHCI. "Red forms" originate from an excitonic interaction between chlorophylls located in A5 and B5 chlorophyll binding sites. In

particular Lhca3 and Lhca4 show the red-most shifted absorptions, determined by the modulation of the A5-B5 excitonic interaction given by the presence of an asparagine residue in A5 chlorophyll binding sites.

ROS: Reactive Oxygen Species. These reactive species are byproduct of photosynthesis and their products is increased during abiotic stresses, which impair the photosynthetic reactions. The main classes of ROS present in the chloroplast are: singlet oxygen, superoxide anion, hydrogen peroxide or hydroxyl radical. ROS production has mainly three different sites in the thylakoids: LHC proteins of PSII, PSII reaction centre and PSI acceptor side. Singlet oxygen is produced mainly at LHC proteins level when light is absorbed in excess and cannot be transferred to the reaction centre: in this case $^3Chl^*$ is formed, which can convert O_2 to singlet oxygen. Singlet oxygen can be produced also at P_{680^+} level, since it can become a triplet P_{680} ($^3P_{680}$) due to charge recombination and other back-reactions of PSII. Superoxide anion, hydrogen peroxide or hydroxyl- radical are mainly produced at PSI acceptor side. ROS accumulation causes damages to the photosynthetic apparatus though oxidation of lipids, proteins and pigments. Their accumulation induce a situation known as oxidative stress.

RuBisCO: Ribulose-1,5-bisphosphate carboxylase/ oxygenase. It is an enzyme that is used in the Calvin-Benson cycle to catalyze the first major step of carbon fixation, a process by which the atoms of atmospheric carbon dioxide are made available to organisms in the form of energy-rich molecules such as sucrose. RuBisCO catalyzes either the carboxylation or oxygenation of ribulose-1,5-bisphosphate (also known as RuBP) with carbon dioxide or oxygen.

State transitions: migration of Lhcb proteins from PSII to PSI, in order to balance the PSI and PSII excitation here LHCII can transfer the energy absorbed to PSI, rather than PSII. The state transition takes several minutes to be activated, since it involves also the migration of LHCII from grana to stroma lamellae.

Stroma lamellae: the interconnecting regions of thylakoids between grana.

Stroma: the soluble compartment of the chloroplast. In the stroma are present the enzymes involved in the dark phase of photosynthesis, that use the ATP and NADPH produced during light phase in order to produce biomass.

Thylakoids: the inner membranes of the chloroplast. The complexes involved into the light phase of the photosynthesis (PSI, PSII, ATP-ase, Cytochrome b6f) are located in the thylakoids membranes. Thylakoids are organized into two membrane domains: 1) cylindrical stacked structures called grana, and 2) interconnecting regions, the stroma lamellae. Thylakoids confine a compartment called lumen: in the lumen protons are pumped during photosynthetic light phase, forming a transmembrane ΔpH which constitutes the force used by ATP-ase to produce ATP.

TyrD: Tyrosine residue located on D2 polypeptide of PSII supercomplex homologous to Y_Z. Y_D forms a dark stable radical $Y_{D\bullet}$ influencing the PSII reaction centre P_{680} oxidation.

Tyrz: Tyrosine residue located on D1 polypeptide of PSII supercomplex responsible for PSII oxidized reaction centre P_{680^+} reduction. In this way P_{680} specie is formed, which can receive further excitons to undergo charge separation.

V1: carotenoid-binding site, located at the peripheral part of antenna proteins LHCII. V1 site is a specific site for violaxanthin and it's involved in xanthophyll cycles product binding in LHCII.

VDE: Violaxanthin de-epoxidase enzyme. This enzyme catalyzes the xanthophyll cycle reactions: it de-epoxidates violaxanthin to antheraxanthin and finally to zeaxanthin. VDE has a maximum active at low pH (~5.2 pH): in this way the xanthophyll cycles and the photoprotection mechanisms correlated, are activated only when photosynthesis reaction are saturated, inducing a strong reduction of the luminal pH, the compartment where VDE enzyme is localized.

Xanthophyll cycle: a series of enzymatic reactions by which the carotenoid violaxanthin is de-epoxidated to zeaxanthin, through the intermediate antheraxanthin. These reactions are catalyzed by the

Violaxanthin deepoxidase enzyme (VDE), which is activated at acid pH around 5.2. When photosynthetic reactions are saturated the lumenal pH is reduced by proton pumping: this event activates VDE enzyme which induces the xanthophyll cycle. Accumulation of zeaxanthin is responsible for activation of several photoprotective mechanism as NPQ, $^3Chl^*$ quenching and ROS scavenging.

$Z^{\bullet+}$: zeaxanthin radical cation. The formation of this species has been correlated to qE induction and belongs from charge separation in a heterodimer composed by a chlorophyll a and zeaxanthin heterodimer. The subsequent charge recombination allows the thermal dissipation of the energy used for charge separation, in a mechanism called Charge Transfer quenching. Zeaxanthin radical cation is characterized by absorption in the NIR at ~1000nm.

ZE: Zeaxanthin epoxidase enzyme. This enzyme catalyzes the zeaxanthin epoxidation to produce violaxanthin through antheraxanthin intermediate.

FIGURE INDEX

Introduction

Chapter 1 - Expression of *Pp*LHCSR1 in *Arabidopsis thaliana npq4* mutant

Chapter 2: An *in vivo* analysis of factors controlling LHCSR1 activity through heterologous expression in *Arabidopsis thaliana*

Chapter 3: Towards LHCSR1 mutational analysis *in vivo*

Appendix

ACKNOWLEDGMENTS

Here I would like to thank and express my gratitude to all the people who were with me during these last three years.

First of all, I would like to thank my supervisor Professor Roberto Bassi, for giving me the chance to work in his laboratory along with a scientific team of high quality and expertise and for trusting me with a challenging research project.

Next, I would like to thank all the members of the photosynthesis laboratory in Verona for their collaboration, support and precious advice but also for their help during my stay in Italy. Thanks to each and every one of you.

All the people from the AccliPhot Consortium for the collaboration, as well as Marie Curie Actions for the funding of the project. Meetings, workshops and conferences all around the world – It was a truly great journey.

Dr. Alessandro Alboresi for his scientific advice, guidance and support.

The members of the committee for providing useful comments and suggestions in order to improve this thesis manuscript.

My family for their tireless support and understanding. Violetta, Foteini, Yiannis, Mattia and all my dear friends.

Thank you.

Μα περισσότερο απ'όλους θα ήθελα να ευχαριστήσω την οικογένειά μου για την αγάπη, την κατανόηση και την αμέριστη υποστήριξή τους, όχι μόνο γι' αυτά τα τελευταία τρία δύσκολα χρόνια αλλά και για πάντα. Έτσι λοιπόν, αφιερώνω αυτή τη διδακτορική διατριβή στην μητέρα μου Μαρία, τον πατέρα μου Αλέξανδρο και την αδερφή μου Κωνσταντίνα. Δεν θα τα είχα καταφέρει χωρίς εσάς.

Σας ευχαριστώ

Music during the writing of the PhD thesis:
Lena Platonos – 'Sun Masks'
Aphrodite's Child – '666' (The Apocalypse of John, 13/18)
Brian Eno – 'Another Green World'
Jean-Luc Ponty – 'Civilized Evil'
Kate Bush – 'The Dreaming'
Works of Alexander Scriabin and Vladimir Horowitz

The research leading to these results has received funding from the European Union's Seventh Framework Programme for research, technological development and demonstration under grant agreement PITN-GA-2012-316427.